

وزارة التعليم العالي والبحث العلمي

BADJI MOKHTAR-ANNABA UNIVERSITY  
UNIVERSITÉ BADJI MOKHTAR-ANNABA



جامعة باجي مختار - عنابة

FACULTY OF EARTH SCIENCES  
DEPARTMENT OF GEOLOGY  
LABORATORY : Laboratoire de Recherche de Géologie (LRG)

## THESIS

Presented to obtain the diploma of

Doctorate 3<sup>rd</sup> Cycle (LMD)

Discipline : Geology

Option : Geodynamics of sedimentary basins

### Title

**The biostratigraphic characteristics of the Coniacian and Santonian in  
the Eastern Saharan Atlas**

**Les caractéristiques biostratigraphiques du Coniacien et du Santonien dans  
l'Atlas saharien oriental**

by

**Nemouchi Sakina**

**SUPERVISOR :**

Pr. SALMI- LAOUAR Sihem

**Professor**

Badji Mokhtar University- Annaba

**CO-SUPERVISOR :**

Dr. Youcef Brahim Elhadj

**MCA**

Batna 2 University

**PRESIDENT:**

Ms. HALIMI Fahima

**MCA**

Badji Mokhtar University- Annaba

**EXAMINATEURS:**

Mr. TLILI Mohamed

**MCA**

Badji Mokhtar University- Annaba

Mr. AOUISSI Riadh

**MCA**

Larbi Ben M'hidi University - Oum El bouaghi

Ms. MAHBOUBI Salamet

**MCA**

Abou Bekr Belkaid University -Tlemcen

**Year: 2026**

## Acknowledgment

First of all, thanks to **ALWWAHID ALAHAD** who created me, protected me, who is always with me and who never leaves me alone. Praise be to **ALLAH**.

I would like to take this opportunity to express my deep gratitude to all the people who supported and contributed to the completion of my doctoral thesis.

First and foremost, I would like to express my deepest gratitude to **Pr. Salmi– Laouar Sihem**, my supervisor for their invaluable guidance, continuous support, and encouragement throughout the course of this research. Their insightful feedback and unwavering patience have been fundamental to the completion of this thesis.

I extend my sincere thanks, appreciation, and gratitude to co-supervisor **Dr. Youcef Brahim Elhadj** for motivation, his sound guidance, for accompanying me on the field. I have the utmost respect and gratitude for him.

I am sincerely thankful to the members of my doctoral committee, for their constructive criticism, helpful suggestions, and the time they have dedicated to reviewing my work. Their expertise has greatly enriched this research.

I extend my sincere thanks to Ecole of the Mines at Badji Mokhtar University of Annaba and the Tunisian Petroleum Activities Company (ETAP) for providing the facilities and resources necessary for scanning electron microscopy (SEM).

I also extend my sincere thanks to my colleagues and friends, **Kherchouch Adila, Maared Manal, Moud Fatma Zohra, Khanfer Somia, Garah Abd Elmoumen, Chemcham Abdelali, Diab Ibtissam, Amrane Thiziri, Doghmane Rahima, Abdelmoumen Ouafa, Saci Rayen, Laagab Adel, Benlaala Naima, Torchi Rania, Youcef Brahim Khaoula, Hamhoum Imen and Aouda Djouhaina**, to sincerely thank you for accompanying me in the field and for your cooperation.

Finally, I would also like to express my gratitude to my family for their unconditional support, understanding, and encouragement during the ups and downs of this adventure. Their love, confidence in my abilities, and constant encouragement have been a vital source of motivation.

In conclusion, I am deeply grateful to all the individuals and institutions who played a role in the success of my thesis. Your contributions, guidance, and support have been essential in helping me reach this important milestone in my academic journey.

## **Dedication**

To my dear family,

To my father, **Mostefa**, and my mother, **Hasrour Beldia**, for their unconditional love and valuable support throughout my journey.

To my brothers, **Islam, Moussa, and Ayoub**, for their support and encouragement.

To my sisters, **Lilia, Chaima, and Rihab**, for their love and trust in me.

To my distinguished teachers who have never held back their knowledge and guidance.

To every loyal friend who has shared my moments of fatigue and sleeplessness and been a source of comfort and support.

This work is the fruit of your sacrifices, love, and constant support.

With my sincere gratitude and love.

## Abstract

The study of Coniacian and Santonian deposits in the Eastern Saharan Atlas (northeastern Algeria) spans two areas: the Tébessa Mountains (Essen section) and the Bellezma-Batna Mountains (Boukezez section). Despite their geological interest, these sedimentary series have not been the subject of any detailed study until now. This contribution offers a first integrated biostratigraphic and paleoenvironmental analysis, based on the joint study of macro- and microfossils, including macroinvertebrates, planktonic foraminifera, and ostracods. The dating of the formations is based on the identification of 26 species of planktonic foraminifera divided into 11 genera. Thus, the Coniacian is characterized by the *Dicarinella primitiva* and *Marginotruncana sinuosa* Zones, while the Santonian is defined by the *Sigalia carpatica*, *Dicarinella asymetrica* and *Globotruncanita elevata* Zones. Despite the paucispecificity of the Coniacian and Santonian marls in macroinvertebrates, a total of 23 species of bivalves, 4 species of gastropods, 1 species of cephalopod and 5 species of irregular echinoids were identified. The quantitative analysis of this macrofauna allowed to distinguish several characteristic assemblages: (1) *Agelasina plenodonta*, *Cucullaea*, *Oscillopho-*  
*Plicatula* and *Hemiaster fourneli*– *Paraesa faba* Assemblages for the Coniacian; (2) *Nuculana* cf. *mariae* Assemblage for the Santonian. These marls also contain a microfauna rich in ostracods, with 55 species identified from a total of 10194 individuals. Statistical analyses (NMDS and PERMANOVA) allowed us to distinguish four distinct assemblages: (1) *Cytherella* aff. *austinensis*– *Cytherella* aff. *contracta* Assemblage and *Cytherella ovata*–  
*Spinolebris yotvatensis* Assemblage, in the Coniacian, (2) *Cytherella* aff. *austinensis*–  
*Cytherella* aff. *elongata* Assemblage and *Paracypris* aff. *posteriusacuminatus*– *Ovocytheridea triangularis* Assemblage, in the Santonian. All the quantitative data reveal a marked contrast between the Coniacian and Santonian stages. The Coniacian and early Santonian are characterized by low diversity, a predominance of smooth-shelled ostracods, and an abundance of globose and keeled planktonic foraminifera. The upper Santonian, on the other hand, is characterized by a decrease in diversity and an increased dominance of ornamented species, suggesting an ecological imbalance. An inverse relationship was observed between the abundance of ostracods and that of planktonic foraminifera. Furthermore, the complete absence of ostracods at the Coniacian– Santonian boundary coincides with a dominance of planktonic foraminifera and opportunistic benthic forms. Interpretation of the integrated results from both sections shows that the region underwent a progressive environmental

evolution: from a shallow, warm, well-oxygenated, and nutrient-rich marine environment characterized by a hard bottom and stable substrates, but also by isolated environments, restricted faunal exchange, and a significant reduction in benthic habitats during the Coniacian, to a deeper, euhaline, nutrient-enriched environment with more compact and consolidated marly substrates, reflecting a shift toward more favorable climatic and environmental conditions during the Santonian. The observed decline in diversity in the Late Santonian could be attributed to climatic cooling. The transition between the two stages appears to be marked by a punctual environmental disturbance, reflecting moderate dysoxic conditions, without clear evidence of a global anoxic event (OAE3). The Essen and Boukezez sections exhibit comparable sea-level fluctuations and paleoenvironmental evolutions, influenced mainly by local tectonics. Furthermore, the opening of the Trans-Saharan route facilitated faunal connections between the eastern Tethys and the South Atlantic, promoting extensive biotic exchanges along the marine margins. This connectivity explains the similarities observed between the faunas of northeastern Algeria and those of adjacent regions of North and West Africa.

**Keywords :** Coniacian- Santonian- Eastern Saharan Atlas- Batna- Tebessa- Biostratigraphy- Essen- Boukezez- Biozones- Paleoenvironmental.

## Résumé

Les dépôts du Coniacien et Santonien dans l'Atlas saharien oriental (nord-est de l'Algérie) s'étendent sur deux zones ; notamment les montagnes de Tébessa (section d'Essen) et celles de Bellezma-Batna (section de Boukezez). Malgré leur intérêt géologique, ces séries sédimentaires n'avaient, jusqu'à présent, fait l'objet d'aucune étude détaillée. La présente contribution propose une première analyse biostratigraphique et paléoenvironnementale intégrée, fondée sur l'étude conjointe de macro- et microfossiles, incluant les macroinvertébrés, les foraminifères planctoniques et les ostracodes. La datation des formations repose sur l'identification de 26 espèces de foraminifères planctoniques réparties en 11 genres. Ainsi, le Coniacien est caractérisé par les Zones de *Dicarinella primitiva* et *Marginotruncana sinuosa*, tandis que le Santonien est défini par les Zones de *Sigalia carpatica*, *Dicarinella asymetrica* et *Globotruncanita elevata*. Malgré la paucispécificité des marnes coniaciennes et santoniennes en macroinvertébrés, un total de 37 espèces de bivalves, 12 espèces de gastéropodes, 1 espèce de céphalopode, 37 espèces d'oursins irréguliers et 10 espèces d'oursins réguliers a été identifiées. L'analyse quantitative de cette macrofaune a permis de distinguer plusieurs assemblages caractéristiques : (1) *Agelasina plenodonta*, *Cucullaea*, *Oscillopho*–*Plicatula* et *Hemiaster fourneli*–*Paraesa faba* Assemblages pour le Coniacien ; (2) *Nuculana cf. mariae* Assemblage pour le Santonien. Ces marnes renferment également une microfaune riche en ostracodes, avec 55 espèces identifiées sur un total de 10194 individus. Les analyses statistiques (NMDS et PERMANOVA) ont permis de distinguer quatre assemblages distincts: (1) *Cytherella aff. austinensis*– *Cytherella aff. contracta* Assemblage et *Cytherella ovata*–*Spinolebris yotvatensis* Assemblage, au Coniacien, (2) *Cytherella aff. austinensis*– *Cytherella aff. elongata* Assemblage et *Paracypris aff. posteriusacuminatus*– *Ovocytheridea triangularis* Assemblage, au Santonien. L'ensemble des données quantitatives révèle un contraste marqué entre les étages coniacien et santonien. Le Coniacien et le début du Santonien se distinguent par : une faible diversité, une prédominance d'ostracodes à coquille lisse, ainsi qu'une abondance de foraminifères planctoniques globuleux et carénés. La partie supérieure du Santonien, en revanche, se caractérise par une baisse de la diversité et une domination accrue d'espèces ornementées, suggérant un déséquilibre écologique. Une relation inverse a été observée entre l'abondance des ostracodes et celle des foraminifères planctoniques. En outre, l'absence totale d'ostracodes à la limite

Coniacien et Santonien coïncide avec une dominance des foraminifères planctoniques et des formes benthiques opportunistes. L'interprétation des résultats intégrés des deux sections montrent que la région a connu une évolution environnementale progressive : d'un milieu marin peu profond, chaud, bien oxygéné et riche en nutriments au Coniacien caractérisé par un fond dur et des substrats stables, mais aussi par des environnements isolés, un échange faunique restreint et une réduction significative des habitats benthiques à un environnement plus profond et plus riche en nutriments au Santonien reflétant à la fois d'une élévation régionale du niveau marin et d'une transition vers des conditions climatiques et environnementales plus favorables, caractérisée par un refroidissement plus marqué des eaux superficielles par rapport aux eaux profondes, des substrats marneux plus compacts et consolidés, ainsi que des conditions pleinement marines et euhalines. Le déclin de la diversité observé dans la partie supérieure du Santonien pourrait être attribué à un refroidissement climatique. La transition entre les deux étages semble marquée par une perturbation environnementale ponctuelle, traduisant des conditions dysoxiques modérées sans preuve manifeste d'un événement anoxique global (OAE3). Les sections d'Essen et de Boukezez présentent des fluctuations du niveau marin et des évolutions paléoenvironnementales comparables, influencées principalement par la tectonique locale. Par ailleurs, l'ouverture de la voie transsaharienne a facilité les connexions fauniques entre la Téthys orientale et l'Atlantique Sud, favorisant des échanges biotiques étendus le long des marges marines. Cette connectivité explique les similitudes observées entre les faunes du nord-est de l'Algérie et celles des régions adjacentes d'Afrique du Nord et de l'Ouest.

**Mots clé :** Coniacien- Santonien- Atlas saharien oriental- Batna- Tébessa- Essen- Boukezez- Biostratigraphie- Biozones- Paléoenvironnementale.

## ملخص

تشمل دراسة رواسب الكونيك والسانتونيان في أطلس الصحراء الشرقية (شمال شرق الجزائر) منطقتين: جبال تبسة (مقطع إيسن) وجبال بلزمة-باتنة (مقطع بوكزان). ورغم أهميتها الجيولوجية، لم تخضع هذه السلاسل الرسوبية لأي دراسة مفصلة حتى الآن. تقدم هذه المساهمة أول تحليل متكامل للطبقات الحيوية والبيئية القديمة، استنادًا إلى دراسة مشتركة للأحافير الكبيرة والصغيرة، بما في ذلك اللافقاريات الكبيرة، والمنخربات العوالية، والصدفيات. ويستند تأريخ التكوينات إلى تحديد 26 نوعًا من المنخربات العوالية، مقسمة إلى 11 جنسًا. وهكذا، يتميز الكونياسيا بمنطقتي ديكارينيليا بريميتيفا ومارجينوترينكانا سينوزا، بينما يُعرّف السانتوني بمنطقتي سيقالبا كارباتيكا وديكارينيليا اسيميتريكا وقلوبوترينكانا الفاتا. وعلى الرغم من ندرة تحديد صخور الكونيك والسانتوني في اللافقاريات الكبيرة، فقد تم تحديد ما مجموعه 37 نوعًا من ذوات الصدفتين، و12 نوعًا من بطنيات القدم، ونوع واحد من رأسيات الأرجل، و37 نوعًا من قنافظ البحر غير المنتظمة، و10 أنواع من قنافظ البحر المنتظمة. سمح التحليل الكمي لهذه الحيوانات الكبيرة بتمييز العديد من التجمعات المميزة: (1) تجمعات اجلزينا بلوندوتا وكوكوليا واوسيلوفا-بليكاتيليا و ايماستر فورنلي-باراييزا فبا للكونيك؛ (2) تجمعات نيكولانا ماريا للسانتوني. تحتوي هذه الرواسب الطينية أيضًا على مجموعة حيوانية دقيقة غنية بالصدفيات، حيث تم تحديد 55 نوعًا من أصل 10194 فردًا. سمحت لنا التحليلات الإحصائية (تحجيم متعدد الأبعاد غير المتري و تحليل التباين متعدد المتغيرات باستخدام إعادة الترتيب العشوائي) بالتمييز بين أربع مجموعات مميزة: (1) مجموعة سيتيريليا اوتنسيس - سيتيريليا كونتراكتا ومجموعة سيتيريليا اوفاتا - سيبينولوبيريس يوتفانتسيس. في الكونياسيا؛ (2) مجموعة سيتيريليا اوتنسيس - سيتيريليا اوفاتا ومجموعة باراسيبيريس بوسنريوسكيميناتيس - اوفوسيتيريد تريونفيلاريس، في السانتونيا. تُظهر جميع البيانات الكمية تباينًا ملحوظًا بين المرحلتين الكونيك والسانتونية. يتميز الكونيك والسانتونية المبكرة بانخفاض التنوع، وهيمنة الصدفيات لمساء الصدف، ووفرة من الفورامينيفيرا العوالية الكروية والمحدبة. من ناحية أخرى، يتميز السانتوني العلوي بانخفاض التنوع وزيادة هيمنة الأنواع المزخرفة، مما يشير إلى اختلال التوازن البيئي. ولوحظت علاقة عكسية بين وفرة الصدفيات ووفرة الفورامينيفيرا العوالية. علاوة على ذلك، يتزامن الغياب التام للصدفيات عند حدود الكونيك والسانتونية مع هيمنة الفورامينيفيرا العوالية والأشكال القاعية الانتهازية. يُظهر تفسير النتائج المتكاملة من كلا القسمين أن المنطقة شهدت تطورًا بيئيًا تدريجيًا: من بيئة بحرية ضحلة ودافئة وغنية بالأكسجين وغنية بالمغذيات، تتميز بقاع صلب وركائز مستقرة، بالإضافة إلى بيئات معزولة وتبادل حيواني محدود وانخفاض كبير في الموائل القاعية خلال العصر الكونيك، إلى بيئة أعمق وأكثر ملحية وغنية بالمغذيات مع ركائز طينية أكثر تماسكًا وتماسكًا، مما يعكس تحولًا نحو ظروف مناخية وبيئية أكثر ملاءمة خلال العصر السانتوني. يمكن أن يُعزى الانخفاض الملحوظ في التنوع في العصر السانتوني العلوي إلى التبريد المناخي. يبدو أن الانتقال بين المرحلتين يتميز باضطراب بيئي متقطع، يعكس ظروفًا معتدلة من نقص الأكسجين، دون وجود دليل واضح على حدوث نقص أكسجين عالمي (OAE3). يُظهر قسما إيسن وبوكزان تقلبات مماثلة في مستوى سطح البحر وتطورات بيئية قديمة، متأثرة بشكل رئيسي بالتكتونيات المحلية. علاوة على ذلك، سهّل فتح الطريق عبر الصحراء الكبرى التواصل بين الكائنات الحية بين شرق تيثيس وجنوب المحيط الأطلسي، مما عزز التبادلات الحيوية واسعة النطاق على طول الهوامش البحرية. يُفسر هذا الترابط أوجه التشابه الملحوظة بين حيوانات شمال شرق الجزائر وحيوانات المناطق المجاورة في شمال وغرب أفريقيا.

الكلمات المفتاحية: الكونياسيان- السانتوني- أطلس الصحراوي الشرقي- باتنة- تبسة- إيسن- بوكزاز- الطبقات الحيوية-  
المناطق الحيوية- البيئة القديمة.

## **Acknowledgment**

**Dedication**

**Abstract**

**Résumé**

**.....ملخص**

**Table of Contents**

**Liste of figures**

**Liste of table**

**Liste of plates**

<b>GENERAL INTRODUCTION .....</b>	<b>1</b>
<b>CHAPTER I OVERVIEW.....</b>	<b>9</b>
<b>1. Introduction.....</b>	<b>9</b>
<b>2. Presentation and objectives :.....</b>	<b>10</b>
<b>3- Geographic setting.....</b>	<b>10</b>
<b>4. Geological setting .....</b>	<b>11</b>
<b>4.1. The Tébessa region .....</b>	<b>13</b>
<b>4.2. The Batna region .....</b>	<b>15</b>
<b>4. Materials and Methods .....</b>	<b>19</b>
<b>5. Previous works.....</b>	<b>23</b>
<b>Conclusion.....</b>	<b>25</b>
<b>CHAPTER II LITHOLOGICAL AND PALEONTOLOGICAL CHARACTERISTICS.....</b>	<b>30</b>
<b>1. Introduction.....</b>	<b>30</b>
<b>2. Description of the Dj. Essen section (Tébessa) .....</b>	<b>30</b>
<b>3. Description of the Djebel Boukezez section (Batna) .....</b>	<b>37</b>
<b>4. Conclusion.....</b>	<b>49</b>
<b>CHAPTER III SYSTEMATIC.....</b>	<b>53</b>
<b>1. Introduction .....</b>	<b>52</b>
<b>2. Results .....</b>	<b>52</b>
<b>2.1. Macrofauna .....</b>	<b>52</b>
<b>Ammonite .....</b>	<b>54</b>
<b>Echinoids :.....</b>	<b>55</b>
<b>Bivalves.....</b>	<b>58</b>

Gastropods :.....	74
2.2. Microfauna.....	88
Ostracods.....	90
Planktonic Foraminifera.....	135
Benthic Foraminifera.....	163
<b>CHAPTER IV BIOSTRATIGRAPHIC.....</b>	<b>166</b>
1. Introduction.....	168
2. Results.....	171
2.1. Ammonites Zones.....	171
2.2. Inocerames Zones.....	171
2.3. Foraminifera Zones.....	172
Conclusion.....	177
<b>CHAPTER V RESULTS, INTERPRETATION AND DISCUSSION.....</b>	<b>178</b>
1. Introduction.....	179
2. Results.....	179
2.1. Macrofaunal assemblages.....	179
2.1. 1. Essen section.....	179
2.1.2. Boukezez section.....	184
2.2. Ostracods and foraminifera assemblage.....	187
2.2.1. Essen section.....	187
2.2.2. Boukezez section.....	190
3. Paleoenvironmental discussion and interpretation.....	193
3.1. Paleooxygenation.....	194
3.2. Paleotemperature.....	200
3.3. Sea level.....	202
3.4. Paleoenergy.....	206
3.5. Paleosalinity.....	209
3.6. Substrate.....	212
4. Coniacian- Santonian transition.....	215
5. Paleobiogeography.....	218
6. Regional correlation.....	222
7. Conclusion.....	224
<b>GENERAL CONCLUSION.....</b>	<b>226</b>
<b>REFERENCES.....</b>	<b>236</b>



## List of figures

### Chapter I

**Figure. I. 1:** Geographical position of the two sections surveyed ; the Essen section of Tébessa and Boukezez section of Batna

**Figure I. 2 :** Structural map showing the position of the Bellezma and Mellegue mountains. Location map of Tébessa region within the main structural units of eastern Algeria (Herkat, 2007).

**Figure I. 3:** Geological map of the Eastern Saharan Atlas study area (red star). (modified after Vila, 1980).

**Figure I. 4:** Macrofaunal step.

**Figure. I. 5 :** Microfaunal step.

### Chapter II

**Figure. II. 1:** Litho-stratigraphic column of the Essen section and with field photograph. A) The Turonian/Coniacian boundary at the study section. B-D) Yellowish marly facies of the Essen Formation. C) The topmost carbonate part of the Essen Formation.

**Figure. II. 2:** Litho-stratigraphic column of the Essen section with distribution of Macrofauna and microfauna

**Figure.II. 3a :** Limestones generally of mudstone to wackestone texture with planktonic foraminifera.

**Figure. II. 3b:** Bioclastic limestone.

**Figure. II. 4:** Litho-stratigraphic column of the Boukezez section with field photograph.

**Figure. II. 5 :** Litho-stratigraphic column of the Boukezez section with the distribution of macrofauna and microfauna.

**Figure. II. 6 :** Limestone mudstone with rare large bioclastic fragments and echinoid radiole.

**Figure. II. 7:** Wackestone to packstone limestone with miliolids and other benthic foraminifera

**Figure. II. 8:** Wackestone to packstone limestone with large fragments of invertebrates and miliolae.

**Figure. II. 9:** laminated limestone with calcispheres and planktonic foraminifera.

**Figure. II. 10:** limestone with fragments of lamellibranchs and pelletoids.

**Figure. II. 11:** packstone to grainstone limestone with bivalves, mililoids and bryozoans

**Figure. II.12:** Bioclastic limestones with bryozoans and mililoids.

**Figure. II. 13:** dolomitic limestone with large fragments of gastropods and lamellibranchs

#### **Chapter IV**

**Figure. IV. 1 :** Spindle diagram shows the stratigraphic range chart and abundance of the identified foraminifera.

**Figure. IV. 2:** Stratigraphic framework and the planktic foraminiferal biozones identified in the study section at Djebel Essen.

#### **Chapter V**

**Figure. V. 1 :** UPGMA cluster analysis using Bray-Curtis method. This analysis produced three clusters of sample groups based on relative abundances of the macrofossils. Essen Coniacian

**Figure. V. 2 :** UPGMA cluster analysis using Bray-Curtis method. This analysis produced three clusters of sample groups based on relative abundances of the macrofossils. Essen Santonian

**Figure. V. 3 :** 2D-NMDS (Bray-Curtis similarity) plot shows the identified association in Coniacian Essen.

**Figure. V. 4 :** 2D-NMDS (Bray-Curtis similarity) plot shows the identified association in Santonian Essen

**Figure. V. 5 :** UPGMA cluster analysis using Bray-Curtis method. This analysis produced three clusters of sample groups based on relative abundances of the macrofossils of Boukezez section

**Figure. V. 6 :** 2D-NMDS (Bray-Curtis similarity) plot shows the identified association in Boukezez section.

**Figure. V. 7:** PCA plots of the faunal assemblages categorized based on their ages; A-B) Ostracods; C-D) Foraminifera. Note the little overlap among the Coniacian and the Santonian assemblages, suggesting marked fauna changes. Green crosses: Santonian samples, yellow circles: Coniacian samples.

**Figure. V. 8.** 2D-NMDS plot visualize the relationship among the proposed clusters (assemblages).

**Figure. V. 9.** Box plots show marked differentiation between the ostracods/foraminifera of Coniacian and the Santonian assemblages.

**Figure. V. 10:** Stratigraphic framework of the Boukezez section. Shaded area denotes the Coniacian- Santonian transition

**Figure. 11a :** Geographic distribution of the identified macrofaunal species in the study section.

**Figure. 11b :** Geographic distribution of the ostracods taxa identified in the study section. 1: Egypt, 2:Tunisia, 3: Algeria, 4: Morocco, 5: France.

## **List of tables**

### **Chapter IV**

**Table.IV. 01 :** Stratigraphic framework and the Ammonit biozones identified in the study section at Djebel Essen.

**Table.IV. 02 :** Stratigraphic framework and the Inoceramids biozones identified in the study section at Djebel Essen.

**Table.IV. 03 :** Stratigraphic correlation of the identified biozones to previous zones in adjacent areas.

**Table.IV. 04 :** Stratigraphic framework and the planktic foraminiferal biozones identified in the study section at Djebel Essen.

### **Chapitr V**

**Table.V.01 :** Summary of the NPMANOVA test among the identified associations of Coniacian in Essen section.

**Table.V.02 :** Summary of the NPMANOVA test among the identified associations of Santonian in Essen section.

**Table.V.03 :** Summary of the characteristics of the identified associations of Essen section.

**Table.V.04 :** Summary of the NPMANOVA test among the identified associations of Boukezez section.

**Table.V. 5 :** Trophic nucleus (>80 %) composition of the identified assemblages of Essen section.

**Table.V. 6:** Summary of the differences between the two identified ostracod assemblages of Essen section.

**Table.V. 7 :** Summary of the differences between the two identified ostracod assemblages of Boukezez section.

**Table.V.8 :** The geographic distribution of the identified macrofaunal species in the Essen Formation.

**Table.V.9 :** Geographic distribution of ostracods recorded at Boukezez section

## List of plates

### Plates Macrofaunals

Plate 1 : Ammonites

Plate 2 to 3 : Echinoids

Plate 4 to 9 : Bivalves

Plate 10: Inocerames

Plate 11: Gasteropods

### Plates Microfaunals

Plate 1 to 6 : Ostracods

Plate 1 to 5 : Planktonic Foraminifera

Plate 6: Benthic Foraminifera.

## Legende

Lithology		Macrofauna			
	Marl		Ammonite		gasteropod
	Limestone		Echinode		Rudist
	Laminated limestone		Bivalve		Inocerame

***GENERAL  
INTRODUCTION***

## GENERAL INTRODUCTION

The Coniacian and Santonian is the third and fourth of the six stages of the Upper Cretaceous. The Coniacian extends from -89.3 Ma to -85.8 Ma and the Santonian from 85.7 Ma to -83.5 Ma. They represent a warm period with an average global surface temperature of over 20°C compared with around 15°C today (Salome 2015) and an ocean temperature in tropical areas of around 37°C compared with 28°C today in the tropical western Atlantic (Salome 2015). During these two stages, sea levels fell by 25 to 40 metres and environments became much shallower (Yahiaoui 1990).

In the Tethys, the Coniacian and Santonian outcrops are well known thanks to numerous studies (France: Troughetti- Gaspard, 1983- Babinot, 1983- Andrieu et al., 2019 - Leleu et al., 2009 - Guiliano et al, 2006– Simo, 1986- Bilotte, 1985- Razin, 1989- Lasseur, 2009- Pomerol et al., 1983 ; Spain : Wilmesen et al., 1996, Wiese et Wilmesen, 1999 ; Morocco : Farah et al., 2021 - Haddomi et al., 2015- Hadach et al., 2015 ; Algeria : Yahiaoui, 1990 - Laffite, 1939 – Billion, 1973- Cheriet– Dubourdiou, 1956, Bentaher et al. , 2023 , Benzerouel et al., 2024, Nemouchi et al., 2024 ; Tunisia : Perthuisot, 1979- Billot et al., 2005- Fournié 1978; Egypt: Bauer et al., 2001, Abdelhady et al., 2023). Generally, the results of these works reveal the carbonate nature of deposition.

These works also reveal the fossiliferous character of these deposits and emphasize their rate the diversity in: Ammonite (France: Bilotte, 1983- Pomerol et al., 1983; Pomerol et al., 1983; Troughetti, 1983- Deramond et al., 1993, Fabre-Taxy, 1961, 1963; Collignon et al., 1979, Spain : Wiese, 2000, Wiese, Wilmsen et al., 1996, Karrenberg, 1936, Wiedmann, 1960-1964, Martinez, 1982, Santamaria, 1992-1995, Mengand, 1920, Wilmesen, 1997, Wilmesen et al., 1996, Kauffman et al., 1996, Morocco: Agouti et al., 1999 - Haddach et al, 2015- Agouti et al., 1998, Algeria: Yahiaoui, 1990– Laffitte, 1939- Billion, 1973; Tunisia : Jacob, 1939- Gélard, 1969- Billot, 1985- Pellisier et al., 1988- Billot et al., 2005- Jacob, 1939- Gélard, 1969- Billot, 1985- Pellisier et al., 1988- Billot et al., 2005- Rami, 1998- El Amri and Zeghib-Turki, 2004- Robaszynski et al., 2000- Delbiez, 1956- Salaj, 1980- Bellier, 1983, Egypt: Bauer et al., 2001, Abdelhady et al., 2023). Bivalves; (Algeria; Cheriet et al., 2016 ,El Manai, 2009, Bentaher et al., 2023, Nemouchi et al., 2024). From Rudistes; (France; Guiliano et al., 2006, Bilotte. 1983- Pomerol et al., 1983– Algeria : Laffitte, 1939; Egypt : Bauer et al., 2001). Of brachiopods; (France; Aspard, 198). In echinoderms; (Algeria; M. Cheriet et al., 2016 - Laffitte 1939, Billion 1973); inoceram; (Germany; Voigt, 1954- Ernst 1963a. 1978-

## GENERAL INTRODUCTION

Schulz, 1978, Schulz et al., 1984– Ernst, 1963a, 1966– Ernst and Schulz, 1974, France; Deramond et al., 1993, Algeria; Cheriet-Laffite, 1939– Dubourdiu, 1956, Blès and Fleury, 1970, Billion, 1973, Tunisia : Jacob, 1939– Gélard, 1969– Billot, 1985– Pellisier et al., 1988– Billot et al., 2005– Rami, 1998– El Amri and Zeghib-Turki, 2004– Robaszynski et al., 2000– Delbiez, 1956– Salaj, 1980– Bellier, 1983– Iraq; Walaszczyk, William Cobban, 2007) benthic and planktonic foraminifera; (France: Bilotte, 1983; Pomerol et al., 1983; Troughetti, 1983; Babinot, 1983–Malatre, Grosheny, 2005– Deramond et al., 1993, Morocco; Haddomi et al., 2015– Agouti et al., 1999; Haddach et al., 2015– Agouti et al., 1998, Algeria; Yahiaoui, 1990 – Djaballah and Defalía– Dubourdiu 1956– Sigal, 1967; Caron, 1966; Cheriet, Benzeroual et al., 2023, Bentahar et al., 2024, Nemouchi et al., 2025; Tunisia: Caron, 1966 – Perthuisot, 1979– Rami et al., 1997– Rami, 1998– El Amri and Zeghib-Turki, 1987– Zeghib-Turki, 2004– Robaszynski et al., 2000– Robaszynski et al., 1984– Delbiez, 1956– Salaj, 1980– Bellier, 1983– Jacob, 1939– Gélard, 1969– Billot, 1985– Pellisier et al., 1988– Billot et al., 2005– Robaszynski and Caron, 1979– Weiss, 1983– Loeblich and Tappan, 1987– Nederbragt, 1990– Ayad et al., 1996– Matimati et al., 1991, Egypt: Bauer et al., 2001 , Iraq: Bakir and Kahtany, 2020, Ukraine; Korchagin, et al., 2011) and ostracods; (France; Malatre, Grosheny 2005, Troughetti 1983, Babinot, 1983, Morocco; Andreu et al., 2004, Haddomi et al., 2015– Agouti et al., 1999; Haddach et al., 2015– Agouti et al., 1998, Algeria; Cheriet et al., 2016, Billion, 1973, Egypt; Bauer et al., 2001; Abdelhady et al., 2023). The Coniacian and Santonian macroinvertebrates of the Middle East and North Africa are generally rare and show low faunal diversity paucispecific, largely influenced by ecological or taphonomic factors. In the Hawashia Formation (Eastern Desert, Egypt) (Abdelhady et al., 2023), a relatively poor assemblage has been documented, comprising five bivalves, seven gastropods, two ammonites, and a single echinoid taxon. The poor preservation of shells heavily encrusted, bioeroded, and fragmented indicates prolonged exposure within the Taphonomic Active Zone, reflecting a shallow, low-energy, tide-influenced subtidal environment with low sedimentation under arid conditions. Ammonites confirm the Coniacian and Santonian age and display a cosmopolitan distribution across several continents, whereas most benthic taxa exhibit restricted geographic ranges, suggesting relatively low sea levels. Whereas the Coniacian deposits of Djebel Essen (Tébessa Mountains, northern Algeria) reveal a low-diversity macrofaunal assemblage dominated by bivalves, with fewer gastropods, cephalopods, and irregular echinoids. Quantitative analysis identified three benthic assemblages *Agelasina plenodonta*, *Cucullaea*, and *Oscillopho*–*Plicatula*. While the first two are infaunal, the *Cucullaea* assemblage is composed exclusively of suspension feeders, reflecting oligotrophic conditions and reduced

## GENERAL INTRODUCTION

diversity, whereas epifauna dominate the Oscillopho– Plicatula group. All assemblage are paucispecific, and their limited diversity is attributed to sea-level retreat and the restriction of shallow marine habitats. The absence of evidence for the Coniacian anoxic event (OAE-3) supports its restricted development in the region. Nevertheless, the occurrence of taxa with regional and cosmopolitan affinities points to episodic connections with the Tethyan Ocean (Nemouchi et al., 2024).

The results of these works demonstrate the value of studying this macrofauna and microfauna, particularly in the stratigraphic and biostratigraphic division of the interval in question and the establishment of standard biozonations. The dating of the Coniacian and Santonian stages of the Upper Cretaceous is mainly based on biostratigraphic criteria based on Ammonites, inoceramids, and planktonic foraminifera, which are widely used worldwide. The lower boundary of the Coniacian is characterized by the first occurrence (FO) of ammonites of the subgenus *Texanites* (*Texanites*), while the lower boundary of the Santonian is defined by the FO of the inoceramid *Cladoceramus undulatoplicatus* (= *Platyceramus undulatoplicatus*), which is the main biostratigraphic criterion recognized at the first symposium on Cretaceous stage boundaries (Birkelund et al., 1984). Ammonites, although excellent for dating in the Tethyan and Atlantic regions, are sometimes absent from boreal environments or restricted platforms, which justifies the use of inocerams, notably the species *Cremnoceramus deformis erectus* and *Cremnoceramus rotundatus*, which mark the Coniacian. At the same time, planktonic foraminifera play a crucial role, particularly in oceanic environments; the Coniacian is marked by species such as *Dicarinella concavata*, while the Santonian begins with the extinction of *D. concavata* and the appearance of *Dicarinella asymerica* (Gradstein et al., 2020). These combined criteria allow for precise correlations between different paleogeographic domains (Kennedy et al., 1996).

The Global boundary stratotype section and point (GSSP) defines the base of Coniacian and comes in the carriage of Salzgitter-Salder, in Basse-Saxe (Allemagne). This new product, approved by the International Commission of Stratigraphy in 2005, corresponds to the initial application (FO) of the ammonite *Forresteria (Fagesia) petrocoriensis*, which consists of the main fossil reptile of this locality. This apparition is the correct correlative with the presence of the inocerame *Cremnoceramus deformis erectus*, which enables it to have a valid biostratigraphical and allow interconnected fossil correlations. The selection of the Salzgitter-Salder section reposes on the continuation of the device (Kauffman et al., 2005).

## GENERAL INTRODUCTION

At the Brussels symposium (1996), the Coniacian working group proposed a subdivision into three substages based mainly on inocerames and ammonites. Thus, the Lower Coniacian is defined by the first appearance of *Cremnoceramus rotundatus* (sensu Tröger, non Fiege), accompanied in Europe by the ammonite *Forresteria (Harleites)*, while in North America *Forresteria peruana* and *Forresteria brancoi* appear. The Middle Coniacian begins with the first occurrence of the inoceramus *Volvicceramus koeneni* (Müller), and, when ammonites are present, it is correlated with the appearance of *Peroniceras (Peroniceras) tridorsatum*. Finally, the Upper Coniacian is characterized by the first appearance of *Magadiceramus subquadratus* (Schlüter), which constitutes its main reference fossil.

In the report of the Santonian Working Group at the Second Symposium on Cretaceous Stage Boundaries (Lamolda and Hancock, 1996), the (FO) of *Platyceramus undulatoplicatus* was confirmed as the primary marker of the base of the Santonian stage. The FO of *Texanites (Texanites)* was rejected because it appeared below the lower boundary of *Platyceramus undulatoplicatus* and had been cited in assemblages with inocerames normally considered coniacian (Lamolda and Hancock 1996). The FO of the planktonic foraminifer *Sigalia carpatica* was accepted as a secondary marker of the basal Santonian. It is widespread in the Mediterranean region of the Tethys, was associated with *Inoceramu ssiccensis* and *Texanites* in Tunisia, and in northern Spain (Navarre) its FO is very close to the lowest occurrence of *Platyceramus undulatoplicatus*. Three sections were approved as candidate GSSPs; Olazagutia Quarry (Navarra, Spain), Sea ford Head (Sussex, England) and Ten Mile Creek (Dallas, Texas). The results were published in a special issue of Cretaceous Research “Stratigraphy of the Coniacian–Santonian transition” (vol. 28 no. 1, 2007; Gallemei et al., Howe et al., Lamolda and Paul, Lamolda et al., Peryt and Lamolda), and another paper in Acta Geologica Polonica (Gale et al., 2007).

The Olazagutia section was selected as the GSSP by the Santonian Working Group in November 2007 and was approved by the International Subcommittee on Cretaceous Stratigraphy in September 2010. This decision was finally approved by the International Commission on Stratigraphy in April 2012 and ratified by the International Union of Geological Sciences in January 2013.

According to the GSSP definition, the base of the Santonian Stage is placed in the lower part of the *Dicarinella asymetrica* Zone and corresponds to nannofossil Zone CC16 (Lamolda et al., 2014). At the GSSP reference section in northern Spain and at the Gubbio section in

## GENERAL INTRODUCTION

Italy, the *D. asymetrica* Zone is positioned slightly lower, within the upper Coniacian (Lamolda et al., 2014; Coccioni & Premoli Silva, 2015). Lamolda et al. (2014) proposed that, in paleotropical regions, the boundary can be broadly recognized by the (FO) of *D. asymetrica*. Conversely, in other Neo-Tethyan regions, particularly the Middle East, the (LO) of *D. asymetrica* has also been widely used to approximate the base of the Santonian (Caron, 1985; Premoli Silva & Sliter, 1995; Robaszynski et al., 2000; Petrizzo, 2000, 2002; Sari, 2006; Farouk & Faris, 2012; Gradstein et al., 2012; Farouk et al., 2016). However, Meilijson et al. (2014) suggested placing this boundary slightly higher in the stratigraphic record.

The Coniacian– Santonian boundary CSB is formally defined at the Cantera de Margas section Spain, where the first occurrence of *Platyceramus undulatopticatus* provides the primary marker. Additional reliable bioevents include the FO of *Lucianorhabdus cayeuxii*, *Platyceramus cycloides*, and the LO of *P. undulatopticatus*, while the FO of *Sigalia carpatica* occurs slightly below the boundary, the *D. asymetrica* Zone is taken lower down in the upper Coniacian (Lamolda et al. 2014; Coccioni and Premoli Silva 2015). However, Lamolda et al. (2014) used the first common occurrence of *D. asymetrica* to define broadly the base Santonian in the paleotropics. Calcareous nannofossils, such as *Lucianorhabdus inflatus*, further refine biostratigraphic resolution. Stable carbon isotopes show no major excursion but record a gradual decline, with the CSB lying just above a minimum bracketed by the Peak 3 and Michel Dean events (Lamolda et al., 2014). Integration of these biostratigraphic and isotopic signals provides a robust framework for regional and interregional correlation, linking Olazagutia with both temperate and Tethyan provinces.

The Coniacian and Santonian interval marks a critical phase in the Late Cretaceous, representing the cessation of the Oceanic Anoxic Events (OAEs), specifically OAE 3 (Jenkyns, 1980; Arthur et al., 1990; Hofmann et al., 2003). This event is generally considered a regional Atlantic phenomenon, predominantly shaped by variations in the climate ocean system (Wagreich, 2009) and further modulated by eustatic sea-level changes (Slipper, 2005). During this time, significant paleoenvironmental and paleoecological transitions occurred, which are traceable through fossil assemblages, particularly microfossils such as foraminifera and ostracods. Ostracods, owing to their sensitivity to environmental changes and excellent preservation potential, have long been employed as robust proxies in reconstructing past marine environments (Bismuth et al., 1995; Boomer et al., 2003; Whatley et al., 2003; Gebhardt and Zorn, 2008; Andreu et al., 2013; Trabelsi et al., 2015; Jomaa-Salmouna et al., 2017; Piovesan et al., 2020; Sayed et al., 2022). Importantly, a major planktonic foraminiferal

## GENERAL INTRODUCTION

turnover at the end of the Santonian has been linked to tectonically induced circulation changes (Ando et al., 2013), brief cooling episodes (Huber et al., 1995; O'Brien et al., 2017), ecological competition, and the ecological reorganization following OAE3 (Petruzzo et al., 2022; Schlanger and Jenkyns, 1976; Wagreich, 2009, 2012).

Although Coniacian and Santonian outcrops are widespread and readily accessible in eastern Algeria, these stages have received limited scientific attention to date. Apart from the foundational works of Pervinquière (1902), Dubourdieu (1956) and Kazi-Tani (1970), the deposits of this interval have been described only in broad terms, without the establishment of a high-resolution biostratigraphic framework or a detailed characterization of the Coniacian and Santonian transition. The stratigraphic succession for this interval thus remain poorly constrained, primarily due to the scarcity of detailed paleontological investigations and a reliance on macrofaunal markers, particularly ammonites (Dubourdieu, 1956; Nemouchi et al., 2024). The presence of genera such as *Muniericeras*, *Peroniceras*, and *Forresteria* provides only broadage constraints and fails to precisely define the Coniacian–Santonian boundary. This challenge is further compounded by the absence of radio metrically calibrated data and the occurrence of Turonian taxa intermingled with in Coniacian strata, complicating regional correlations. Dubourdieu (1956) was among the first to provide a preliminary description of the macrofaunal assemblage in the southern Constantine province, basing his subdivision mainly on inoceramid bivalves (Chriet, 2016). In this context, the Lower Santonian of the Constantinois and the Mellegue Mountains is typically dated by the occurrence of *Platyceramus undulatoaplicatus*, as endorsed by the Brussels symposium (1996), while the Middle Santonian is characterized by *Platyceramus* aff. *ahsenensis*, no inoceramids have been reported from the Upper Santonian. Given these limitations, microfossil based approaches, particularly those relying on planktonic foraminifera, provide a refined tool for both age determination and palaeoenvironmental reconstruction. However, previous studies conducted on these deposits in the Bellezma–Batna Mountains (Savornin, 1920; Laffitte, 1935, 1939; Coquand, 1862; Kazi-Tani, 1970; Billion, 1972, 1973; Guiraud, 1973; Villa, 1977; Péron, 1883, 1986; Yahiaoui, 1990; Harkat and Delfaud, 2000) and in the Mellegue Mountains of Tébessa (Dubourdieu, 1956; Pervinquière, 1902; Kazi-Tani, 1970) have largely focused on lithostratigraphic and macrofossil descriptions. These contributions, while valuable, do not establish a high-resolution biostratigraphic framework for the Coniacian and Santonian interval, nor do they clarify the critical palaeoenvironmental and faunal events that mark the transition between these two stages. Moreover, since the work of Laffitte (1939), the

## GENERAL INTRODUCTION

limited and the passage between the two stages remains difficult to distinguish. He places it either at the disappearance of the Coniacian faunas, or at the appearance of the Santonian faunas, and he explains certain understandings by lack of sediments and stratigraphic gaps. The only notable contribution dates back to Yahiaoui (1990), who described six ostracod species from the lower Coniacian of the Boukezez region. Subsequent intervals, particularly the late Coniacian to Santonian, have yet to be systematically explored.

In recent years, numerous studies have proposed biozonations for Late Cretaceous calcareous planktic foraminifera (e.g., Roth, 1973; Sissingh, 1977; Caron, 1985; Robaszynski and Caron, 1995; Robaszynski et al., 2000; Sari, 2006; Farouk and Faris, 2012a, 2012b; Elamri et al., 2014; Farouk, 2014a, 2014b; Farouk et al., 2016a, 2016b; Jaff et al., 2015; Farouk et al., 2017a, 2017b; Petrizzo, 2019; Faris et al., 2019a, 2019b; Fang et al., 2020a, 2020b). Similarly, ostracod-based paleoenvironmental reconstructions have been extensively conducted in North and West Africa (e.g., Bismuth et al., 1978; Carbonel and Colin, 1982; Peypouquet et al., 1983; Carbonel and Colin, 1982; Bassiouni and Luger, 1990; El Waer, 1992; Elewa et al., 1998, Elewa et al., 1999; Bassiouni et al., 2000; Morsi and Speijer, 2003; Elewa, 2004, 2005, Elewa, 2007; Elewa and Morsi, 2004; Ismail and Ied, 2005a, 2005b; Morsi et al., 2008; Amami-Hamdi and Ben Ismail-Lattrache, 2013; Amami-Hamdi et al., 2014, 2016; Sayed et al., 2022), demonstrating their utility in reconstructing paleoenvironments and paleowater depths (Southward et al., 2004; Morsi et al., 2016; Youssef et al., 2017; El Baz and Khalil, 2019; Elewa and Abdelhady, 2020).

Within this context, the present study undertakes an integrated biostratigraphic and palaeoenvironmental analysis of the Essen Formation (Tébessa) and Boukezez Formation (Batna) NE Algeria, areas where previous research has largely focused on the Cenomanian–Turonian interval (e.g., Naili et al., 1995; Salmi-Laouar et al., 2018). The Coniacian and Santonian succession in these regions, historically described as a thick marly-limestone series (Durozoy, 1956, Benzeroual et al., 2023, Bentaher et al., 2024, Nemouchi et al., 2024 and 2025), remains largely unexplored in terms of its microfossil content.

This study provides the first detailed palaeontological and lithological data from the Coniacian and Santonian deposits of the Essen Formation in Tébessa and the Boukezez Formation in Batna (northeastern Algeria). It aims to fill existing stratigraphic gaps and reconstruct the palaeoenvironment during these two geological periods.

***CHAPTER I***  
***OVERVIEW***

## CHAPTER I OVERVIEW

### 1. Introduction

In the Eastern Saharan Atlas, the Coniacian and Santonian deposits exhibit continuous, well-exposed outcrops with an average thickness of approximately 2000 meters (Dubourdieu, 1956; Kazi-Tani, 1970; Guiraud, 1973; Ben Mansour, 2009, Bentaher, 2024). This segment of the Upper Cretaceous is predominantly composed of fossiliferous carbonate rocks, notably rich in inoceramid bivalves and ammonites, which serve as key biostratigraphic markers (Laffite, 1939 ; Yahiaoui, 1990, El Manai, 2009, Bentaher, 2024). Despite numerous studies conducted in the Bellezma–Batna (Laffite, 1939 ; Yahiaoui, 1990) and the Mellegue (Tébessa) ranges (Dubourdieu, 1956; Kazi-Tani, 1970; Guiraud, 1973; Ben Mansour, 2009), most have not provided a high-resolution biostratigraphic frame work or clarified the events marking the Coniacian and Santonian transition. A Batna, The dating of these successions is primarily based on ammonite studies conducted by Yahiaoui (1990). The lower Coniacian is identified by the first appearance of *Barroisiceras haberfellneri* (Hauer, 1866), while the early Coniacian is marked by the presence of *Tissotia* sp., The Santonian stage is characterized by the occurrence of *Mortoniceras texanum* Roemer, 1852, at its base and *Placenticeras syrtale* Morton, 1834, at its top. To our knowledge, no additional biostratigraphic markers indicating the Coniacian/Santonian boundary have been observed in the Bellezma-Batna Mountains. Since Laffitte’s (1939) work, the boundary between these stages has remained ambiguous, being variably defined by the disappearance of Coniacian faunas or the emergence of Santonian assemblages, a situation likely compounded by sedimentary gaps. In Tébessa, Durozoy (1956) described a thick, monotonous sequence of dark marls (250 m), with the lower two-thirds (Coniacian) characterized by fossiliferous ochre lumachelles, and the upper part (Santonian) comprising more calcareous levels. The benthic fauna is abundant and diverse, including species such as *Hemiaster furneli*, *Plicatula ferryi*, *Ostrea maresi*, and *Pgenodonta vesicularis*. Furthermore, micropaleontological evidence suggests that portions of strata previously assigned to the Coniacian may, in fact, belong to the Turonian. This interval corresponds to a phase of global sea-level highstand, which triggered widespread shallow-marine transgressions across the North African margin of the Tethys Ocean, resulting in the deposition of thick, fossil-rich marly-limestone sequences in a warm, shallow epicontinental sea.

## CHAPTER I OVERVIEW

### 2. Presentation and objectives :

In our study area, we are particularly interested in the Coniacian and Santonian stratigraphic interval in the Bellezma–Batna Mountains and the Tébessa Mountains (Mellegue) regions, located in northeastern Algeria. Several multidisciplinary studies were applied, including:

- A detailed lithological description and analysis of the deposits traversed by the sections studied;
- The identification of the main biostratigraphic markers (foraminifera, inoceramides, ammonites) with a view to establishing a precise chronological frame work accompanied by detailed biozonations;
- Analysis of the stratigraphic distribution of the various taxa identified, comparing them with their related taxa along the southern margin of the Tethys Sea;
- A descriptive and systematic study of all identified species;
- Interpretation of their paleoecological significance and life adaptation;
- The study of dispersal patterns, diversification dynamics, and the composition of faunal assemblages;
- The analysis of the response of ostracods to environmental changes and ecological fluctuations;
- The reconstruction of the biogeographic distribution of faunas between the Mellegue and Bellezma–Batna basins, and more broadly within the southern bank of the Tethys;
- Finally, the reconstruction of the paleoenvironmental conditions that prevailed during this Late Cretaceous interval in northeastern Algeria.

### 3- Geographical settings

The study region is part of the Eastern Saharan Atlas, and more specifically the Batna Mountains (Boukezez section) and the Mellegue Mountains of Tébessa (Essen section). (Figure.1)

The Essen section studied belongs to the commune of Bir Mokadam, approximately 40 km west of the town of Tébessa near the RN 83, bordered by Djbele Essen to the north and Djbel Gaagaa to the south. The base of the section studied has coordinates (35°25'10.0"N 7°53'42.8"E / N35°24'59" 7°53'29"E). It runs NE-SW.

The Boukezez section with geographical coordinates (35°30'43.6"N 6°00'55.1"E/ 35°30'41.5"N 6°01'08.4"E) exposed in Batna in the Bellezma-Batna mountains in NE Algeria;

## CHAPTER I OVERVIEW

on the right bank of the CW161 road, approximately 6.5 km east of the town of Chebat Ouled Chelih. It runs NW-SE.

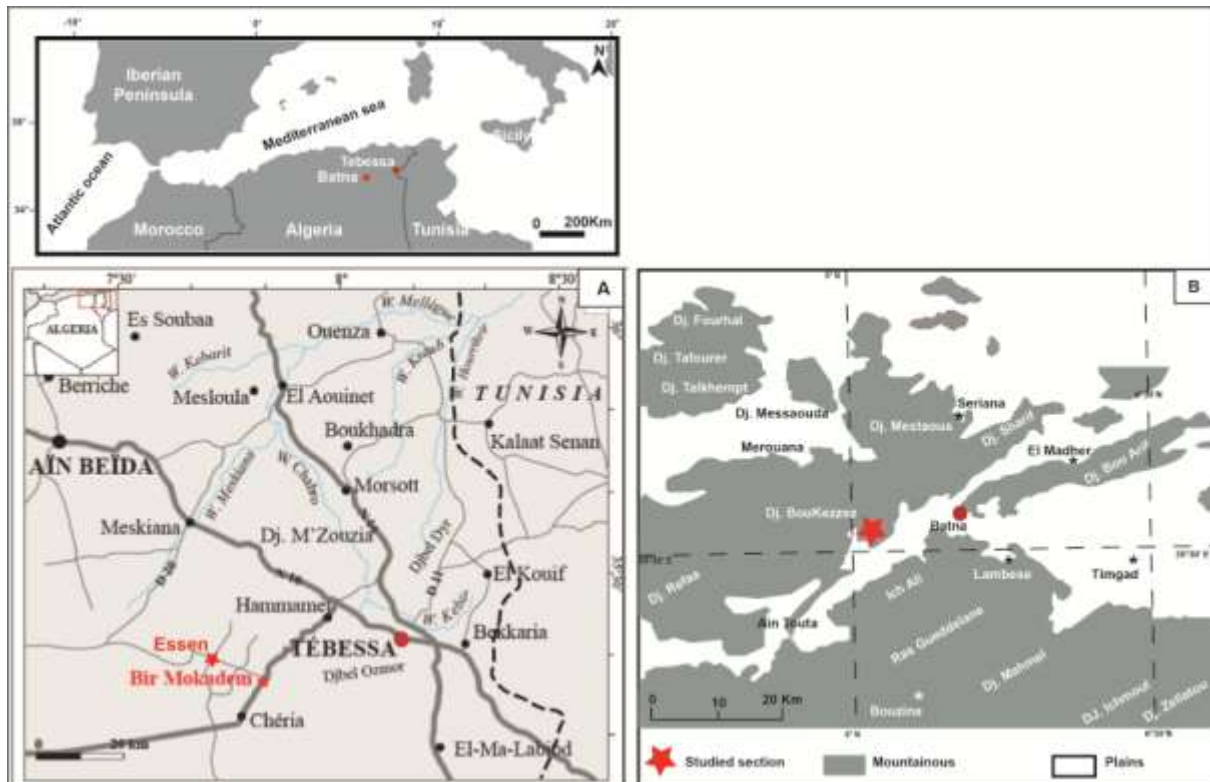


**Figure. 01:** Geographical position of the two sections surveyed; the Essen section of Tébessa and the Boukezze section of Batna.

### 4. Geological setting

The study area belongs to the Eastern Saharan Atlas, which extends to the Tunisian border. This eastern part of the range is characterized by the presence of the Mellegue Mountains as well as the Aurès, Batna and Nementcha massifs (KaziTani, 1986, cited in Bettahar, 2003). These reliefs are part of a subsiding basin of Mesozoic age, located between the Saharan plateau to the south and the pre-Atlas zone to the north (Figure. 2). This study focuses specifically on the sectors of Tébessa, corresponding to the Mellegue Mountains, and Batna, associated with the Bellezma–Batna Mountains (Figure. 3).

CHAPTER I OVERVIEW

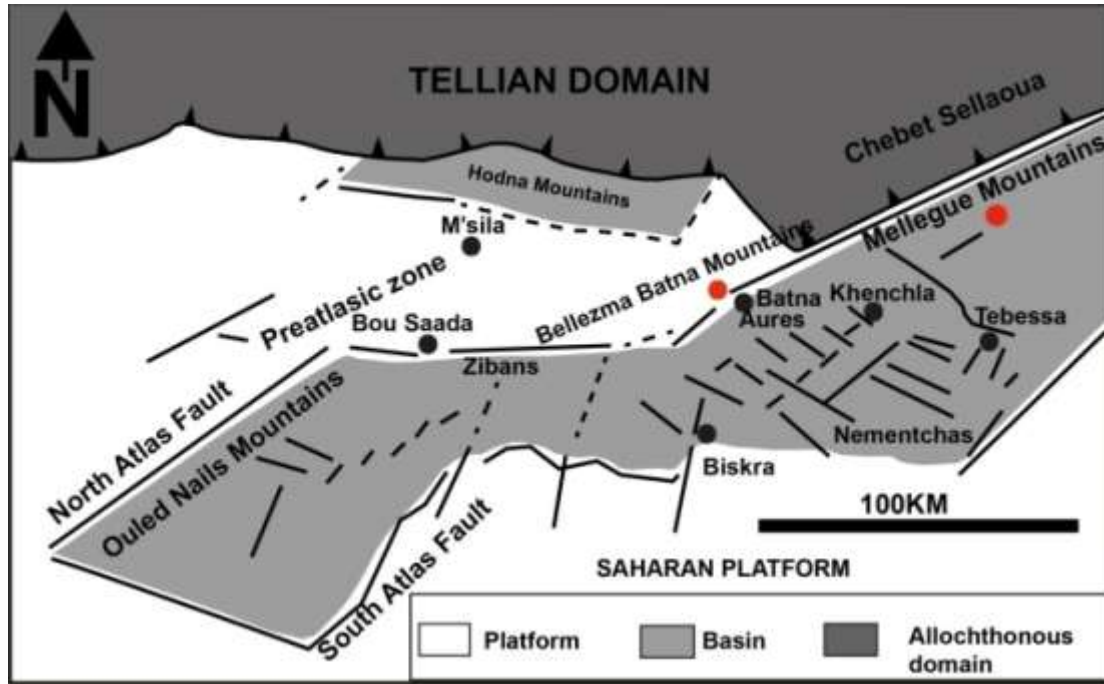


Figure. 2 : Structural map showing the position of the Bellezma and Mellegue mountains (Herkat, 2007).

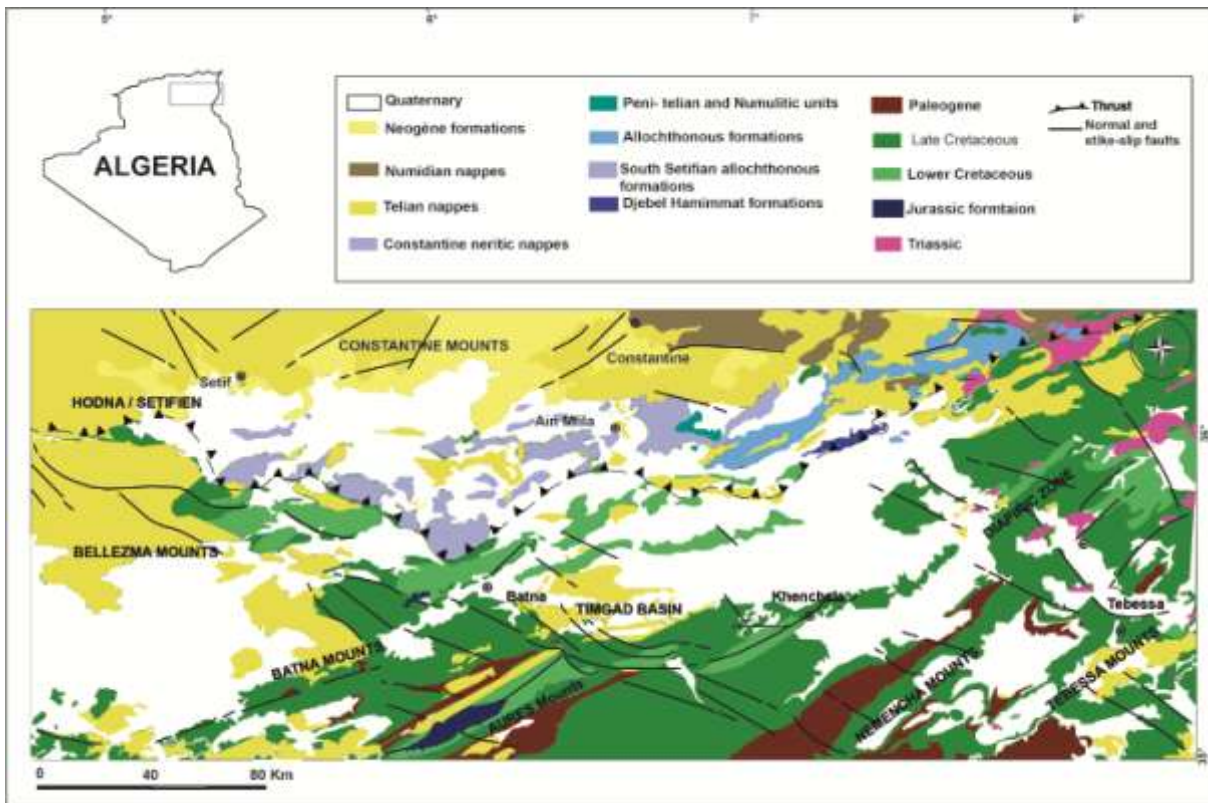


Figure. 3 : Geological map of the Eastern Saharan Atlas Modified from Vila (1980) and Haddouche et al. (2014)

## CHAPTER I OVERVIEW

### 4.1. The Tébessa region

North of Tébessa, the Mellegue mountains form a transition zone between the Tell to the north, the Aurès and the Saharan plateau to the south, the Bellezma-Batna mountains to the west and the Tunisian Atlas to the east.

Its palaeogeographic context necessarily inherits the tectonic-sedimentary past of these different areas. It is covered by the 1:50,000 geological maps of Morsott and Tébessa. This region lies between the major relief chains of the Mellegue mountains to the north and the Tébessa mountains to the south.

The broad outlines of the geology of the Tébessa region are well known thanks to the many geological studies and notes already published. These are mainly Meso-Cenozoic deposits and various Quaternary epicontinental and continental overlays (Othmanine, 1987, Dubourdieu & Durozoy, 1950; Dubourdieu, 1956; Laffitte (1939) and Glangeaud (1932) Belhai et al. (1990); Castany, 1951; David, 1956; Kazi-Tani, 1986). Thibiéroz & Madre, (1976); Rouvier et al. (1985); Ohmanine, (1987); Perthuisot et al. (1987); Aoudjehane et al. (1992); Bouzenoune (1993); Bouzenoune et al. (1995) and Kowalski & Hamimed (2000), All these formations are pierced by Triassic formations with lagoonal facies. The absence of Jurassic and Lower Cretaceous formations prior to the Barremian in the region is explained by the existence of pre-Aptian diapiric movements which caused bulges (Othmanine, 1987; Beghoul, 1974). The Lower and Upper Cretaceous outcrops are widespread in the Tébessa region and extend over vast areas. The only outcrops attributed to the Barremian are found and dated NE of the Ouenza region, at Djebel Herraba, on the southern flank of the Sidi Emmbarka anticline and in its immediate vicinity (the SW flank of the Mesloulou anticline, along the Oued Batma and NW of Dehar-Mesloulou) (Dubourdieu, 1956). The Aptian occupies vast areas in the Tébessa region. In fact, the imposing and curiously isolated reliefs that are the most characteristic feature of the landscape of the Mellegue and Tébessa mountains are due to the large masses of Aptian reef limestone. The Albian is widespread in the region and is represented by very thick formations up to 100m thick. The Cenomanian in the Tébessa region (Essouabaa, Ouenza, Mzouzia, Ouasta, Boukhadra, El Guelb, Hameimat Nord, Hameimat Sud, Tenoukla, Aïn Chenia, ...) is represented almost entirely by greenish clay marls with thickness of 750 to 1100 m thick (Dubourdieu, 1956). The Cenomanian facies of the Tébessa region, rich in fibrous calcite and varied macrofauna (bivalves, gastropods,

## CHAPTER I OVERVIEW

cephalopods, echinoids), are distinguished by regular limestone intercalations facilitating stratigraphy. They constitute the thickest and most extensive Cretaceous formation in the region. The Turonian forms most of the flanks of the major anticlines and synclines in the region. It is very marked by its very hard compact limestone facies, which give rise to pronounced relief. The formation is mainly composed of compact limestone alternating at the base with inoceramic marls and then with clay marls rich in ammonites and other lamellibranchs (Dubourdieu, 1956 and 1959). Its thickness can reach 300 m south of Boukhadra (Dubourdieu, 1956). The Coniacian-Santonian, which cannot be separated for lack of characteristic fauna, are located at the edge of anticlines and synclines throughout the Tébessa region (Degaichia, 2014). They consist mainly of grey, greenish or yellowish-grey marls with fibrous calcite platelets, sometimes interspersed with clayey limestones. The thickness varies from 200 to 300 metres at Ouenza and from 490 to 600 metres at Boukhadra (Dubourdieu, 1956). The Santonian and the Coniacian deposits are a thick (250 m) and monotonous series of black or green marls (yellow in alteration), admitting in the upper part more calcareous levels and, in the lower 2/3 (Coniacian), (Durozoy, 1956), the Santonian is essentially made up of 300 m of very blue-grey clayey marl with, however, some calcareous intercalations with Inocerames (in particular, *Inoceramus siccaensis* PERV.) (G. Dubourdieu, 1956; J.L. Blès and J.J. Fleury, 1970). The upper limit is clearly marked by the disappearance of foraminifera *Globotruncana carinata* and *Sigalia deflaensis* and the appearance of Campanian forms. The lower limit remains poorly known due to a lack of dating data. The Coniacian-Santonian is located within the boundaries of anticlines and synclines throughout the region. The Campanian consists of an accumulation of dark marls at the base, chalky limestones and yellowish marls at the top, alternating with whitish limestones in the middle and upper part. It varies in height from 300 to 500 metres. The Maastrichtian extends the depositional conditions of the Campanian, demonstrating a marked sedimentary continuity. It consists of well-bedded white limestone banks (around 60 m thick), which become more compact towards the centre of the formation, and is interspersed with argillite. It is overlain by grey to black clay marl. Its total thickness is estimated at between 250 and 300 m (Dubourdieu, 1956).

The Paleocene has very similar facies, beginning with a thick series of black or yellowish marls (around 300 m), followed by levels of marl and flinty marly limestone, including phosphate horizons. The Eocene is represented by thick banks of flinty limestone (50 to 60 m) containing nummulites, resting on a 5m base of white marly flinty limestone. These deposits are mainly located in the south of the region and in the Monts du Mellegue

## CHAPTER I OVERVIEW

area. The Miocene formations lie unconformably on the older series (Albian to Senonian, or even Triassic), marking a transgressive phase. They are most extensive in the Oulad Soukiès basin, where they are up to 1,000 m thick (Dubourdieu, 1956; Kowalski and Hamimed, 2000; Salmi-Laouar, 2004; Chaabane, 2015). The Lower and Middle Miocene are characterised by conglomerates rich in various elements (limestone, flint, ferruginous pebbles, Triassic fragments), reflecting diapiric activity (Bouzenoune, 1993). The Upper Miocene is made up of sandstone, sandstone limestone and clay layers, reflecting a period of regression (Salmi-Laouar, 2004). The average thickness of these deposits in the region is around 150 m. The Quaternary, of continental origin, occupies the lower relief areas (plains and valleys), where it is subdivided into an ancient Quaternary (slope deposits, foothill formations, alluvium) and a recent Quaternary (filling of collapse ditches). The facies encountered consist of limestone crusts, silts, scree, pebbles and pudding, with a thickness of between 10 and 30 m (Dubourdieu, 1956).

This region is made up of a series of massifs oriented NE-SW. The main structural features of the region are the accumulation of thick sedimentary series, subsidence, the appearance of Triassic formations, folding and the creation of collapse troughs. They are the result of tectonic movements (distension and compression) accompanied by episodes of breakthrough and ascent of Triassic formations from the Aptian to the present day. These features have thus determined the geological, palaeogeographical and structural evolution of the region in question.

### **4.2. The Batna region**

The Bellezma-Batna Mountains are located in a convergence zone between the Tell Atlas domain to the north and the Saharan Atlas domain to the south (Bellion, 1972). They are limited to the northwest by the Hodna Mountains (Guiraud, 1973) and to the southeast by the Batna-Aïn Touta syncline.

The Batna study area covers the Merouana 1:50,000 and Ain El Ksar (1:50,000) sheets. It belongs to the pre-atlasic domain, the Bellezma-Batna mountains, to the north and the atlasic domain, the Aurès mountains, to the south. Extensive NE-SW anticlinal folds and NW-SE, NE-SW and E-W faults are the main structural features of the region. The sedimentary deposits known in the region range from the Triassic to the Quaternary. The Cretaceous is the most developed geological unit in the region. It is widespread in the Bellezma-Batna Mountains, where it forms a concordant stratigraphic series that includes all the stages. A clear distinction can be made between two successive series (Laffite, 1939; Burolet, 1956; Bellion, 1972; Guiraud, 1973; Vila, 1980; Bureau, 1986; Yahoui, 1990).

## CHAPTER I OVERVIEW

The Lower Cretaceous is widely exposed in the anticlines of the Bellezma-Batna mountains (Djebel Rfaâ, Djebel Tuggurt, Ravin Bleu, Djebel Sarif). It begins with a predominantly clayey basal formation, with local layers of sandstone and quartzite, while limestone represents only about 15% of the total thickness. The latter reaches almost 1,000 m. Most of this terrain is Valanginian, although the base has been dated as Berriasian (Bureau, 1975c).

The Upper Cretaceous outcrops at Ktef Akhal, Dj. Tuggurt, Dj. Aïn Drihem, Hamla, Théniet El Manchar...). It has been the subject of several stratigraphic studies (Yahiaoui, 1990; Herkat, 1999) and recently the work of Djeffal (2014), Slami (2014) and Slami et al, (2018) and Bentahar et al, (2023) and Benzeroual et al, (2024). The sedimentation of these deposits took place in a platform environment characterised by shallower facies and less subsident series (Herkat, 1999). In the Aurès, the Upper Cretaceous outcrops at Dj. Metlili, Bou Arif, El Kantara, Dj. Chentouf, Ras Iggèdlène, Dj. Akhal, Ras-El-Mers, Tadjera and Foum-Toub. It has been the subject of several stratigraphic studies (Laffite, 1939; Yahiaoui, 1990; Herkat, 1999, Herkat, 2004; Maandi, 2011; Djeffal, 2014 et Benmansour, 2016. These deposits were deposited in a subsident intracratonic basin bounded to the north by the pre-atlasic high zone and to the south by the Saharan platform (Herkat, 2004).

The series corresponding to the Upper Cretaceous, with a thickness of 3,000 m, begins in the Cenomanian. Contrary to the Lower Cretaceous, there are no sandstones (Laffite, 1939).

The Cenomanian is well represented in the Bellezma-Batna mountains and comprises two distinct lithological units: a marly base and a limestone top. Its maximum thickness, observed at Djebel Chafez (SW of the Oued Chaâbat), is about 600 m, of which 260 m corresponds to the calcareous Cenomanian.

The Turonian formations display lithological characteristics typical of Upper Cretaceous marine sedimentation. The succession is mainly composed of alternating massive and bedded limestones, which are at times enriched with rudists and other marine macrofauna indicative of subtidal settings associated with carbonate platform environments. These limestones are predominantly light-colored to whitish, occasionally chalky, and are notable for their high calcium carbonate content.

## CHAPTER I OVERVIEW

The lower part of the Turonian sequence is frequently distinguished by marly horizons or intercalations of marly layers within the limestone, representing episodes of increased clay input during the initial phase of transgression. Upsection, the deposits are increasingly dominated by compact, less marly limestones, signaling a transition to a more stable marine setting characterized by primarily carbonate sedimentation under warm climatic conditions in a well-oxygenated epicontinental sea.

The Santonian is generally characterised by a marly formation which outcrops between the southern foothills of the Bellezma-Batna mountains and the Djebel Metlili. It is composed of a very thick succession of alternating marls and limestones. This formation is surmounted by a layer of compact limestone, beginning with a marly series containing numerous sea urchins and lamellibranchs, and ammonites of the *Tissotia* genus (fossils from areas at the base of the Coniacian), followed by alternations of flinty limestone and Inocerames, marl with sea urchins and lamellibranchs, gypsum banks and a rare glauconitic level (Bellion, 1972). The Sedimentation is essentially marly in most basins. In the central zone of the Algerian-Tunisian basin, basin facies are replaced by deposits with pelagic and benthic microfauna in the platform/basin transition. A net decrease in depth has thus occurred in this basin, corresponding to a decrease in tectonic subsidence and eustatic rises in sea level.

In this region of Batna, the Upper Cretaceous occupies the most outcropping part, where the Coniacian-Santonian shows significant accumulations. These formations are characterised by the association of types of facies; very thick deposits of marno- carbannate (alternating marl and limestone) This formation is surmounted by a bed of compact limestone. It begins with a marly series containing numerous sea urchins and lamellibranchs, and ammonites of the *Tissotia* genus (fossils from the base of the Coniacian), followed by alternating flinty limestones and Inocerams, marl with sea urchins and lamellibranchs, gypseous banks and a rare glauconitic level (Bellion, 1972). The Campanian is a marly formation, in which calcareous beds are rare, and which also contains oyster lumachelles and sea urchins. The Maastrichtian is a neritic limestone, very rich in bryozoans at the base and in laffitte at the top, with algae, polyps and inocerames.

The Tertiary outcrops in the foothills of the eastern Algerian Alpine are relatively sparse compared to the Secondary. The most recent terrains often rework microfaunal associations related to eroded formations (Marmi, 1995).

## CHAPTER I OVERVIEW

The Danian is characterised by a heterogeneous sedimentation, very different from the previous series, although concordant. They have a more or less pronounced detrital or continental character (sandstones, ferruginous concentrations and red beds, bone debris and driftwood) (Bellion et al. 1973).

The Miocene formations, predominantly continental and occasionally lagoonal, are generally red in colour and rest unconformably - sometimes markedly - on Eocene or older Mesozoic units (Guiraud, 1973). The oldest Miocene deposits consist of conglomerates, sandstones, marls and red clays and are well developed west of Ras Moulay Yahia and at Kef Sefiane. In the Middle Miocene, the sedimentary sequence includes two distinct marl beds of unequal thickness: Bed I, the most complete, extends between the Bellezma Mountains and Jebel Metlili in the Oued Berriche valley, while Assise II, further west, consists of gypsiferous marls devoid of macrofauna and is often overlain by Quaternary deposits (Bellion, 1972).

The Pliocene is developed in the western part of the Bellezma- Batna mountains and is characterised by a detrital formation with three subgroups that are in harmony with each other and with the marl formation, which is mainly sandstone. The most recent deposits are conglomeratic, probably deltaic. (Bellion, 1972).

The Quaternary is well represented at the western end of the Bellezma-Batna Mountains by two distinct types of deposits. The first consists of glaciais, which are detrital accumulations forming a generally thin cover, varying in pebble content. The second type includes four travertine levels, characterized by superimposed carbonate horizons with relatively few clastic elements. These travertine formations are closely associated with the activity of ancient spring systems (Bellion, 1972).

The **Bellezma-Batna region** in northeastern Algeria exhibits a complex geological structure shaped predominantly by the Alpine orogeny (Bellion, 1972; Bureau, 1973). This area forms a transitional zone between the High Plains and the surrounding mountainous relief and constitutes the southeastern extension of the Atlassic domain within the Aurès Mountains. The landscape is marked by a rugged topography, composed of a series of **folds, thrusts, and faults**, with dominant orientations ENE-WSW and NW-SE (Yahiaoui, 1990), reflecting significant crustal shortening during Alpine compressional phases (Fabre, 1961; Beaugé, 1962; Vila, 1980).

## CHAPTER I OVERVIEW

At its core, the **Bellezma Massif** is defined by a major anticline with a Triassic core, bordered by Mesozoic formations primarily Jurassic and Cretaceous that are disrupted by reverse faults and major structural discontinuities. The tectonic architecture is typified by **imbricated thrust sheets and fault-propagation folds**, influenced by deep-seated fault systems inherited from Tethyan tectonics and reactivated Hercynian structures. Regionally, the Bellezma represents a tilted block of the internal Tellian zone, delineated from the Saharan platform by the Bordj Bou Arreridj Tolga structural corridor (Vila, 1980; Bessedik et al., 2002).

The superficial formations rest upon a heterogeneous substratum, ranging from **Triassic evaporites** which locally served as the main detachment horizon to extensive **Cretaceous limestones** that form prominent ridges and escarpments. The structural complexity is further accentuated by active fault systems, which account for the moderate seismicity recorded in the region (Yelles-Chaouche et al., 2006).

### 4. Materials and Methods

To achieve the above objectives, two sections covering the Coniacian and Santonian were selected and surveyed southwest of Djebel Essen in Tébessa and Djebel Boukezez in Batna.

The following steps summarize all the methods adopted and the steps taken in this study:

#### Literature Research

A fairly extensive bibliographical documentation concerning the study of the Coniacian and Santonian throughout the world, particularly in the Tethyan domain, was conducted to fill the information gaps resulting from previous research results in the study area.

#### The field

Geological fieldwork was conducted over four years (2021, 2023, 2024 and 2025) in Bellezma-Batna and Bir Mokadam, with a specific section chosen in Djebel Boukezez and Djebel Essen. In the field, the main tasks performed were: surveying two sections over one from Djebel Essen to Tébessa, a thickness of 533 m, and for the second section from Djebel Boukezez to Batna, a thickness of 160 m, the recognition and description of facies, systematic sampling, and fossil samples were meticulously collected from each stratum. A total of 242

## CHAPTER I OVERVIEW

samples were collected from the Essen Formation, with sampling intervals ranging between 2 and 3 m in the soft marls. A total of 72 samples were collected include 40 limestones and 32 marl samples from the Boukezez Formation. The petrography of the limestone facies was studied using thin section observations.

### The laboratory

**Macrofauna:** fossil material was prepared and identified down to the species level. For better identification of the collected macrofauna, all specimens were thoroughly washed, cleaned, photographed, and measured. These steps enabled the identification of the main taxa existing in the region and the establishment of their systematics. Many taxa that have an originally aragonitic shell were preserved in calcite, or as internal molds. All samples that contain fossils were used for multivariate analysis. The data have been normalized to percent abundance for the comparison of guild proportions.



**Figure 4:** Macrofauna work steps ; **a** : collected macrofauna; **b** : washed, cleaned and photographed **c** : measured for identification.

## CHAPTER I OVERVIEW

**Microfauna** : They were processed using the standard technique for ostracods and foraminifera extraction that consists of washing about 500 g subsample using hydrogen peroxide (H<sub>2</sub>O<sub>2</sub>). The samples, then, underwent a series of sieving procedures, with mesh sizes set at 255, 200, 100, and 63 micrometers. The residues were dried in an oven at 60°C. Representative ostracods and foraminifera specimens of different taxonomic entities were selected for scanning electron microscopy (SEM) at the “Entreprise Tunisienne d'Activités Pétrolières (ETAP)” in Tunisia and the Ecole des Mines in Annaba.



**Figure 5:** Microfauna work steps (Washing of marls) ; **a** : Soaking ; **b** : Wash with wat ;  
**c** : Draying of the residue; **d** : Soting and identification ; **e** : SEM

### **Statistique :**

**Macrofauna:** All samples that contain fossils were used for multivariate analysis.

The data have been normalized to percent abundance for the comparison of guild proportions. The Unweighted Pair Group Method with Arithmetic Mean (UPGMA) clustering was used to group the samples into associations (Legendre and Legendre, 1998; Hammer and

## CHAPTER I OVERVIEW

Harper, 2006). The Permutational analysis of variance (PERMANOVA) test was applied to test the null hypothesis that similarities between associations are smaller or equal to similarities within associations (Zelditch et al., 2012).

***Microfauna*** : The identified planktic foraminifera were used to establish the biozonation. The ostracods occurrence matrix was converted into relative abundance and analyzed statistically. Principal Component Analysis (PCA) was applied to visualize the relationships between the identified assemblages. The matrix was then subjected to a Non-Parametric Multivariate Analysis of Variance (NPMANOVA) to assess the significance of these relationships. A Sequential Bonferroni-corrected  $p$ -value ( $p = 0.001$ ) was used to determine significant differences. A Reduced Major Axis (RMA) linear model was applied to evaluate the relationship between ostracods and foraminifer distributions. Box plots were used to compare the biotic attributes of the ostracods assemblages. All analyses were performed using PAST version 4.16c (Hammer et al., 2001a, 2001b).

The ostracods occurrence matrix (presence/absence) was statistically analyzed. Unweighted Pair Group Method with Arithmetic Mean (UPGMA) hierarchical clustering based on the Jaccard similarity index was used to divide the succession into ecozones. Constrained method was used to save the stratigraphic distribution (q-mode cluster), aiming to highlight the vertical variation of the ostracods distribution. We categorized the samples by age to compare environmental variables across these intervals. The main hypothesis was to determine whether significant vertical environmental changes occurred, as inferred from variations in ostracod assemblages within the study section. A marked variation in the ecological attributes of the recognized assemblages will be interpreted to reconstruct the paleoenvironmental changes (Elewa and Abdelhady, 2020). The Canonical Correlation Coefficient (CCC) was used to evaluate the quality of the fit, where a value close to 1 is the more accurate clustering solution (Sokal and Rohlf, 1962; Abdelhady and Fürsich, 2015).

Moreover, non-metric Multidimensional scaling (NMDS) was used to plot the relationships visualizes the relationships among the identified associations (Hammer and Harper, 2006). The stress value was used to assess the quality of the fit, where 0.2 or less is a good fit (Kruskal, 1964; Abdelhady et al., 2019). Furthermore, the non-parametric Permutational MANOVA (PERMANOVA) test based on Jaccard similarity coefficient was also applied to assess significant compositional differences among the identified ostracod assemblages. Clustering was used also for biogeographic analyses based on species country

## CHAPTER I OVERVIEW

matrix. Reduced Major Axes (RMA) regression was applied to evaluate the relationships. The significance of all correlations was tested at a significance level ( $p < 0.001$ ) using a one-tailed t-test and the Sequential Bonferroni correction.

Shannon Index, Simpson Index, and Dominance Index were used to characterize the diversity, where the Dominance Index is not perfectly correlated to the Shannon index (as the Simpson Index), in addition, it varies from 0 to 1, and thus, it is easier to evaluate (Hammer and Harper, 2006). All of the analyses were carried out on PAST version 2.17 (Hammer et al., 2001).

The methods adopted as well as the results obtained during these studies were represented in Six (06) chapters:

- First chapter devoted to overview and deals with the study area in its general and local geological framework.

- Second chapter deals with the litological and paleontological characteristics of two sections studied, where aims to provide a comprehensive and detailed description of the lithological layers and fossil content within the analyzed sections, with the objective of situating the studied series within its stratigraphic framework.

- Third chapter evokes the systematics of all the collected species which could be determined

- Fourth chapter represents the results of biostratigraphic synthesis and correlations

- Fifth chapter and finished with a Results, Interpretation and discussion.

The manuscript ends with a general conclusion

### 5. Previous works

Research on the Coniacian and Santonian stages in the Eastern Saharan Atlas has historically been limited due to poor exposure and restricted outcrop availability. However, significant contributions have been made in various domains over the decades, allowing for a gradual reconstruction of the stratigraphy, sedimentology, paleontology, and tectonics of the region.

#### A. Stratigraphic and Lithostratigraphic Studies

- **R. Laffitte (1939)** conducted the first comprehensive stratigraphic study of the Aurès region, establishing a foundational reference for subsequent work on the Upper Cretaceous succession and paleogeography.

## CHAPTER I OVERVIEW

- **G. Durozoy (1956)** produced the 1:50,000 geological map of Tébessa and outlined the local stratigraphy in the associated explanatory notes.
- **F. Bentaher (2023)** carried out a detailed litho-biostratigraphic study in the Aurès Mountains, subdividing the Coniacian and Santonian succession into two units: a fossiliferous lower Coniacian marl-limestone unit (with *Peroniceras*) and an upper Santonian marl unit (*Palcenticeras polyopsis*). Three foraminiferal biozones were identified: *Dicarinella primitiva*, *D. concavata*, and *D. asymetrica*.
- **L. Benzeroual (2024)** provided the first detailed description of Upper Cenomanian–Lower Coniacian carbonate stratigraphy in the northern Aurès. Four formations and three depositional environments were identified, with three depositional sequences grouped into two megasequences.
- **S. Nemouchi (2025)** analyzed the Essen Formation in the Bir Mokadam Mountains, west of Tébessa. Based on 318 samples, he identified six biozones spanning the Coniacian (*D. primitiva*, *Marginotruncana sinuosa*) to Santonian (*Sigalia carpatica*, *D. asymetrica*, *Globotruncanita elevata*). The study also documented a decline in foraminiferal diversity in the upper Santonian.

### B. Sedimentological and Tectono-Sedimentary Research

- **D. Bureau (1967–1986)** developed the concept of "prismatic sedimentary wedges" in the northern Aurès and Belezma Mountains, challenging earlier allochthonous models (e.g., J.M. Vila). In 1986, he emphasized tilted-block tectonics and sedimentation dynamics in the Aurès and northern Saharan margin.
- **A. Yahiaoui (1990)**, in his doctoral thesis, investigated the sedimentology of Upper Cenomanian to Lower Coniacian marl-limestone deposits between Batna and El-Kantara. His findings enriched knowledge of depositional settings in the southern Belezma and northern Aurès.
- **S. Benmansour (2008–2009)** revisited Late Cretaceous tectono-sedimentary evolution in the Eastern Saharan Atlas. Her 2016 work integrated sedimentological and micropaleontological data, refining facies models and environmental interpretations in the Aurès and Gaâga basins.

### C. Paleontological and Micropaleontological Contributions

## CHAPTER I OVERVIEW

- **S. Benmansour (2016)** analyzed a broad array of microfossil material, enabling the reconstruction of foraminiferal and ostracod assemblages and paleoecological preferences through qualitative and quantitative approaches.
- **S. Nemouchi et al., (2024)** investigated Coniacian macrofauna at Djebel Essen. Low-diversity assemblages dominated by bivalves and echinoids reflected marginal marine environments under oligotrophic conditions, with no evidence of the OAE-3 anoxic event.
- **S. Nemouchi et al., (2025)**, in addition to biozonation, found an inverse relationship between ostracod and planktonic foraminiferal abundances, suggesting environmental stress (e.g., climate cooling or bottom-water dysoxia) during the upper Santonian.

### D. Tectonic and Structural Studies

- **G. Dubourdieu (1956)** highlighted the role of deep-seated tectonic movements in shaping the Ouenza region based on petrographic and geomorphological evidence.
- **D. Bureau (1986)** emphasized tectonic/sedimentation interactions and proposed tilted-block tectonics affecting the Aurès and Bellezma Mountains.

### Conclusion

The sedimentary deposits forming this vast area are Meso-Cenozoic in age, ranging from the Triassic to the Miocene, and are covered, in places, by Quaternary continental and epicontinental formations. The Triassic, always diapiric and in an anomalous position, corresponds to the oldest formation. The Cretaceous, with its upper terms, outcrops widely in the Tébessa region and extends over vast areas. As for the upper terms, these are formed of more or less powerful formations of the Cenomanian, Turonian and Senonian (Coniacian-Santonian; Campanian-Maastrichtian).

The current structure of the Tébessa region is the result of multiple phases of deformation as well as polyphase diapirism ; and in the Batna region, it is one of the results of the Alpine phase.

In the Tébessa region, the Coniacian and Santonian are predominantly marly; in the Batna region, the Coniacian and Santonian are predominantly carbonate (alternating marl and limestone).

## **CHAPTER I OVERVIEW**

The Coniacian and Santonian formations are located within the boundaries of anticlines and synclines throughout the Batna region. These two stages are represented by gray, greenish, and yellowish-gray clayey marls with fibrous calcite plates and intercalated lumachelle marls. Their thickness varies from 200 to 500 m.

The Coniacian and Santonian deposits, Formations are located along the boundaries of anticlines and synclines throughout the Tébessa region (Degaichia, 2014). These deposits are mainly composed of grey, greenish, or yellowish-grey marls containing plates of fibrous calcite, occasionally interbedded with argillaceous limestones. Their thickness ranges from 200 to 300 meters in the Ouenza area and from 490 to 600 meters in Boukhadra (Dubourdiou, 1956).

***CHAPTER II***  
***LITHOLOGICAL AND***  
***PALEONTOLOGICAL***  
***CHARACTERISTICS***

## CHAPTER II LITHOLOGICAL AND PALEONTOLOGICAL CHARACTERISTICS

### 1. Introduction

In the Tébessa and Batna regions, very little is known about the Coniacian and Santonian due to a lack of lithological markers, paleontological evidence and scientific research. Where are deposits attributed to the Coniacian and Santonian intervals are characterized by well-exposed outcrops of relatively significant thickness. Lithologically, these series are mainly composed of carbonate rocks. Especially as previous work (Dubourdieu, 1956 ; Laffitte, 1939 and Yahiaoui, 1990) did not provide a detailed biostratigraphic framework for these intervals, and did not clarify the events associated with the Coniacian-Santonian transition. Since the observations of Dubourdieu, (1956), the boundary with the Coniacian is not determined and the two stages are undifferentiated; the observations of Laffitte (1939) where the definition of the boundary between these two stages remains imprecise. This author places it either at the disappearance of the Coniacian faunas or at the emergence of the Santonian faunas, attributing the difficulties of interpretation to the presence of sedimentary gaps and stratigraphic discontinuities. Yahiaoui (1990) describes a Coniacian succession dominated by marls, interstratified at the base by decimetric limestone beds rich in ammonites and sea urchins, topped by an alternation of lumachellic marls and limestones containing bryozoans and sea urchins. As for the Santonian, it begins with marls containing Hemipneustes at its base, evolving towards upper limestones where *Inoceramus regularis* and occasionally rudists appear.

In this chapter we will provide a lithological and paleontological study detailed of the Coniacian and Santonian series of Djebel Essen (Tébessa) and Djebel Boukezez (Batna), in an attempt to determine the lithological and paleontological characteristics of the series.

### 2. Description of the Dj. Essen section (Tébessa)

The section at Tébessa is represented by the Essen Formation (Nemouchi et al. 2024, 2025). It covers deposits of Coniacian and Santonian stage (Dubourdieu, 1956, Nemouchi et al. 2025). It has an apparent thickness of 533m. It is essentially formed by marl mainly composed of marls with benthic macro-invertebrates, notably bivalves and echinoids, with a limited presence of gastropods (Figure. 1). The Coniacian represented by 300m is separated from the Santonian (200m) by a 3m limestone bench of bioconstructed. The lower limit of the section marked by the rudist limestone bar with a reef-like character of Turonian stage (Dubourdieu, 1956). The upper limit of the cut remains unlimited in marls.

CHAPTER II LITHOLOGICAL AND PALEONTOLOGICAL CHARACTERISTICS

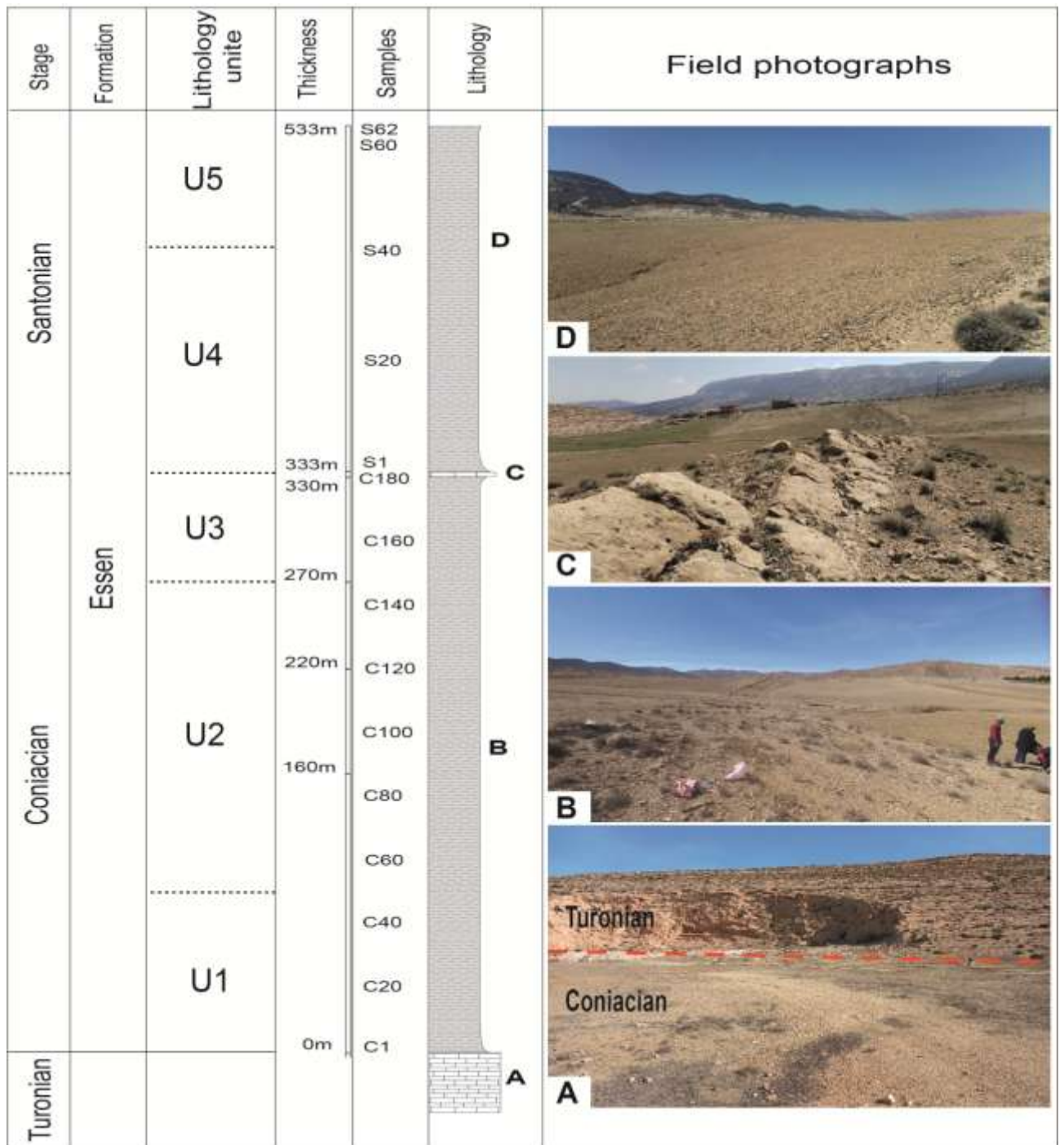


**Figure II. 1:** Litho-stratigraphic column of the Essen section andwith field photograph. **A)** The Turonian/Coniacian boundary at the study section. **B-D)** Yellowish marly facies of the Essen Formation. **C)** The topmost carbonate part of the Essen Formation.

## CHAPTER II LITHOLOGICAL AND PALEONTOLOGICAL CHARACTERISTICS

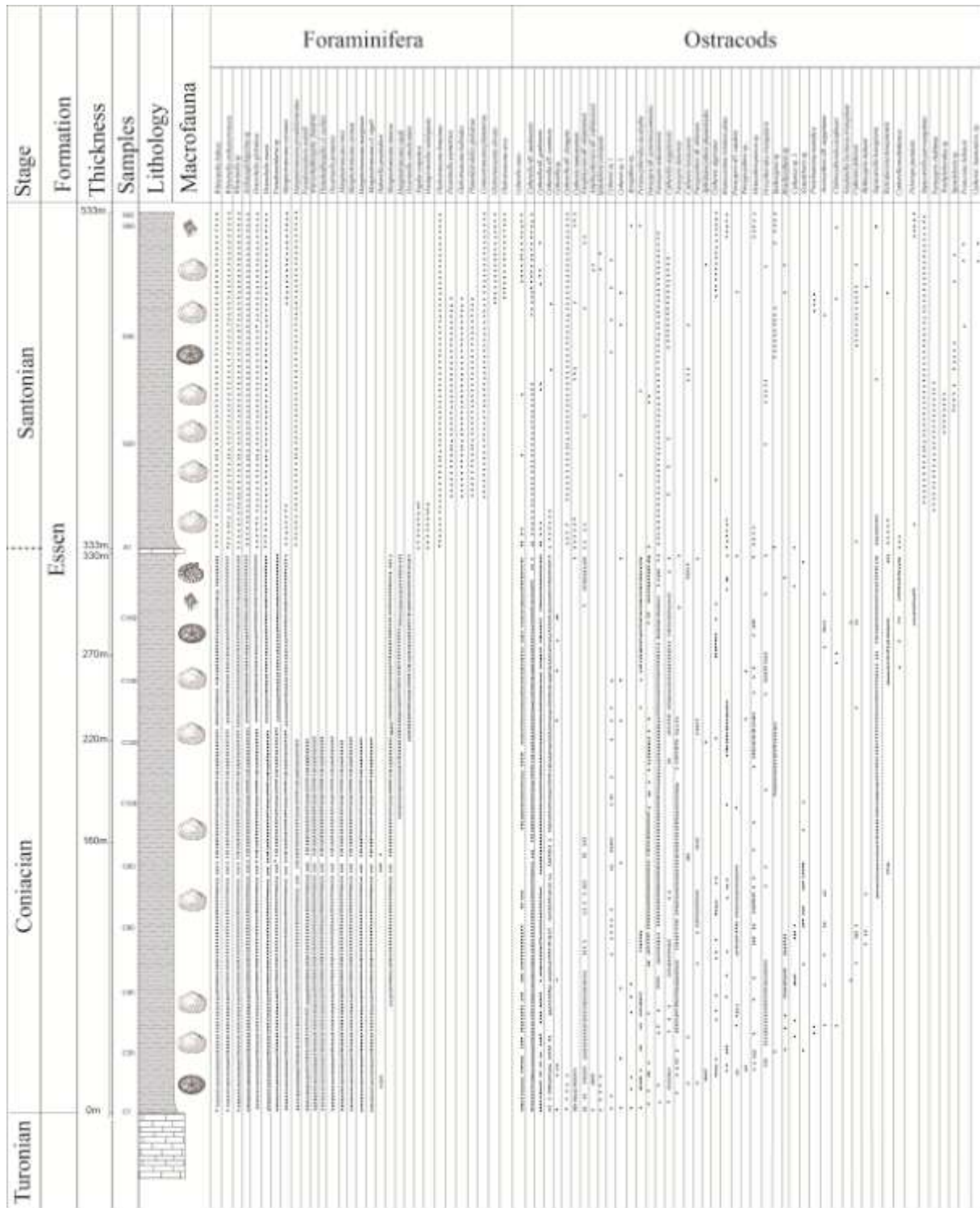


**Figure II. 2:** Litho-stratigraphic column of the Essen section with distribution of macrofauna and microfossils

The homogeneity of the facies in the Dj Essen section precludes any lithological subdivision. The analysis, on the other hand, of the distribution of the macrofauna and

## CHAPTER II LITHOLOGICAL AND PALEONTOLOGICAL CHARACTERISTICS

microfauna along the 533m allows us to distinguish informal lithological units and separate the Coniacian from the Santonian. From bottom to top, five distinct units were detected.

### 2.1. Unit 1: Marls with *Agelasina plenodonta*

They represent the base of the section studied from sample C1 to sample C50 over an apparent thickness of 91.60m. It is a yellowish marly unit with a homogeneous facies. It contains mainly macrofauna; bivalves and echinoids and microfauna of planktonic and benthic foraminifera and ostracods. Echinoids are generally *Mecaster batnensis*. The bivalves are represented by: *Agelasina plenodonta* constitutes 43% of the association, while *Pycnodonte (Phygraea) vesicularis vesicularis* represents 16 %. *Mecaster batnensis* accounts for less than 13 %. In general, the diversity is low. The dominant planktic species are : *Dicarinella primitiva*, *Heterohelix globulosa*, *H. reussi*, *Pseudotextularia nuttalli*, *Pseudotextularia* sp., *Whiteinella baltica*, *W. archaeocretacea*, *W.sp.*, *Archaeoglobigerina* sp., *Hastigerinoides subdigitata*, *Marginotruncana marginata*, *M. rensi*, *M. caronae*, *M. coronata*, *M. pseudolinneiana*, *M. cf. sigali*, *Globotruncana linneiana*, *Muricohedbergella flandrini*, *Planohedbergella cf. escheri* and *Marginotruncana sinuosa*. Associate with ostracods; *Cytherella ovata*, *Cytherella* aff. *austinensis*, *Cytherella* aff. *gambiensis*, *Cytherella* sp., *Cytherella* aff. *contracta*, *Cytherella* aff. *elongata*, *Cytherella aegyptiensis*, *Peloriops pustulata*, *Cythereis namousensis*, *Cythereis* sp. 1 *Cythereis* sp. 2, *Paraplatycosta* aff. *talayninensis*, *Amphicytherura* aff. *yakhiniensis*, *Spinoleberis yotvatensis*, *Aysegulina* sp., *Perissocytheridea ascalopha*, *Paracypris* aff. *posteriusacuminatus*, *Paracypris* aff. *caudata*, *Paracypris chekhai*, *Sapucariella honigsteini*, *Trachyleberidea* sp., *Bythocypris mohani*, *Clithrocytheridea kaufmani*, *Asciocythere* aff. *aegyptiana*, *Protobuntonia numidica*,

### 2.2. Unit 2 : Marls with *Cucullaea*

This association dominates the middle part of the Essen Formation from the sample C70 to C150, over an apparent thickness of 146.66m. Only, four bivalve species represent this association: *Cucullaea thevestensis*, *Cucullaea diceras*, *Oscillopsa dichotoma*, and *C. trigona*. Each of these three species represents more than 25 % of the association, while *C. trigona* accounts for about 23 %. This association is dominated by the infaunal suspension-feeder *Cucullaea*, constituting 75 %. The dominant planktic species are : *Marginotruncana sinuosa*; *Heterohelix globulosa*, *H. reussi*, *Pseudotextularia nuttalli*, *Pseudotextularia* sp., *Whiteinella baltica*, *W. archaeocretacea*, *W. sp.*, *Archaeoglobigerina* sp., *Hastigerinoides subdigitata*, *Dicarinella canliculata*, *Marginotruncana coronata*, *M. sigali*, *M. pseudolinneian*, *Muricohedbergella flandrini*. With ostracods; *Reticulocosta kenaanensis*, *Sapucariella honigsteini*, *Asciocythere* aff. *aegyptiana*, *Peloriops pustulata*, *Clithrocytheridea*

## CHAPTER II LITHOLOGICAL AND PALEONTOLOGICAL CHARACTERISTICS

*kaufman*, *Cytherella ovata*, *C. aff. contracta*, *C. aff. gambiensis*, *C. aegyptiensis*, *C. austinensis*, *Cytherella aff. elongata*, *C. sp.*, *Sapucariella parvoangulata*, *Cythereis kosticensis*, *Paracypris mdaouerensis*, *Paracypris aff. posteriusacuminatus*, *Paracypris debertreti*, *Perissocytheridea ascalopha*, *Ovocytheridea triangularis*, *Xestoleberis sp.*, *Brachycythere sp.*, *Bythocypris mohani*, *Cythereis fahrioni*.

### 2.3. Unit 3: Marls with *Oscillopha-Plicatula*

The association dominates the upper part of the Essen Formation from the sample C160 to C180 over an apparent thickness of 36.66m. It comprises a total of twelve species. Notably, *Plicatula ferryi* constitutes 32 %, and *Oscillopha dichotoma* represents 31 %. The overall diversity within this association is low. Between the thickness of (170m-180m).It's occurs through about 268 m on observe abundance d'espèce d'Ammonite *Hemitissotia morreni* and the dominant planktic species are : *Heterohelix globulosa*, *H. reussi*, *Pseudotextularia nuttalli*, *Pseudotextularia sp.*, *Whiteinella baltica*, *W. archaeocretacea*, *W. sp.*, *Archaeoglobigerina sp.*, *Hastigerinoides subdigitata*, *Dicarinella canliculata*, *Marginotruncana coronata*, *M. sigali*, *M. pseudolinneian*, *Muricohedbergella flandrini*. With ostracods; *Peloriops pustulata*, *Clithrocytheridea kaufman*, *Cytherella ovata*, *C. aff. contracta*, *C. aff. gambiensis*, *C. aegyptiensis*, *C. austinensis*, *Cytherella aff. elongata*, *C. sp.*, *Sapucariella parvoangulata*, *Cythereis kosticensis*, *Paracypris mdaouerensis*, *Paracypris aff. posteriusacuminatus*, *Paracypris debertreti*, *Perissocytheridea ascalopha*, *Ovocytheridea triangularis*, *Xestoleberis sp.*

In this Unit, *Cytherella aff. austinensis* is the most abundant species, comprising 33.3% of the assemblage. This is followed by *Cytherella aff. contracta* (8.7%), *Spinoleberis yotvatensis* (7.9%), and *Cytherella gambiensis* (7.2%). These species together dominate the trophic nucleus, which accounts for 80.1% of the Coniacian Assemblage. Additional contributions come from species like *Paracypris mdaouerensis* (4.3%) and *Paracypris aff. posteriusacuminatus* (4.1%), along with minor contributions from others such as *Amphicytherura aff. yakhiniensis* and *Cytherella aegyptiensis*.

The upper limit of this unit is marked by a 3m bioslastic limestone bed. The petrographic study of the limestone revealed the presence of two microfacies:

The first is represented by limestones generally of mudstone to wackestone texture with planktonic foraminifera and ostracod valves (Figure II. 3a). This is a micritic microfacies with a mudstone to wackestone texture; the figured elements represent approximately 40% of the total volume of the microfacies with a poor classification, the sizes are different with a generally elongated shape and rounded supers. Represented by planktonic foraminifera and

## CHAPTER II LITHOLOGICAL AND PALEONTOLOGICAL CHARACTERISTICS

ostracods, rare lamellibranchs and benthic foraminifera are also found. The diagenetic phenomena observed are represented by: recrystallisation and micritisation.



**Figure II. 3a :** mudstone to wackestone limestones with planktonic foraminifera (PF), globular (GPF) and carinated (CPF) planktonic foraminifera.

The second microfacies is that of packstone limestones with large fragments of bioclasts, plates and echinoid radiodes (Figure II. 3b). This is a micritic microfacies with a Packstone texture; the figured elements represent 70% of the total volume with a mediocre classification, their size is medium to large represented essentially by lamellibranchs,

## CHAPTER II LITHOLOGICAL AND PALEONTOLOGICAL CHARACTERISTICS

echinoderms, annelids, filaments, planktonic foraminifera (Figure 3). The diagenetic phenomena observed are represented by ferruginisation, filling by a mosaic calcitic sparitic cement and micritisation.



**Figure II. 3b:** Packstone limestone with large fragments of bioclasts with plates and echinoid radiodes (RE), lamellibranchs (Lam), echinoderms (E), annelids (An), filaments (fs), planktonic foraminifera (GPF, CPF).

## CHAPTER II LITHOLOGICAL AND PALEONTOLOGICAL CHARACTERISTICS

### 2.4. Unit 4: Marls with *Nuculana cf. mariae*

These marls are around 200 metres thick and yellowish in colour sample S1 to sample S62. They are characterised a less biodiverse a macrofaunal assemblage composed mainly of bivalves associated with numerous echinoids and rare gastropods, generally of the same species. In order of abundance, we note the presence of: *Nuculana cf. mariae* (D'Orbigny, 1844), *Arctica cordata* (Sharpe 1850), *Rostrocardia papieri* (Coquand, 1862), *Astare gigantea* deshayes, 1842, *Plicatula fourneli* (Coquand, 1862), *Plagiostoma subsimplex* (Thomas & Peron 1891), *Granocardium desvauxi* coquand 1862, *Plicatula ferryi* (coquand 1862) *Plicatula fourneli* (Coquand, 1862) and *Hemiaster cf. bibansensis* Péron & Gauthier, 1881 and the gastropod: *Aporrhais fourneli* (Coquand, 1862). The dominant planktic species are: *Sigalia carpatica*, *Dicarinella asymetrica*, *Heterohelix globulosa*, *H. reussi*, *Whiteinella baltica*, *W. archaeocretacea*, *Hastigerinoides subdigitata*, *Archaeoglobigerina* sp., *Globotruncana linneiana*, *Marginotruncana coronata*, *M. pseudolinneiana*, *Globotruncanita elevata*, *Globotruncana arca*, *Marginotruncana coronata* Bolli and *Globotruncana linneiana* d'Orbigny. With ostracods; *Cytherella ovata*, *C. aff. contracta*, *C. aff. gambiensis*, *C. aegyptiensis*, *Cytherella aff. austinensis*, *Cytherella aff. elongata*, *Sapucariella parvoangulata*, *Trachyleberidea* sp., *Spinoleberis* sp., *Protocosta babinoti*, *Cythereis kosticensis*, *Cythereis algeriana*, *Cythereis namousensis*, *Paracypris mdaouerensis*, *Paracypris aff. posteriusacuminatus*, *Paracypris aff. caudata*, *Paracypris chekhmai*, *Perissocytheridea ascalopha*, *Paraplatycosta aff. talayninensis*, *Spinoleberis* sp., *Protocosta babinoti*, *Peloriops pustulata*, *Bythocypris mohani*, *Clithrocytheridea kaufmani*, *Asciocythere aff. aegyptiana*, *Protobuntonia numidica*, *Brachycythere* sp, *Monoceratina trituberculata*, *Aphrikanecythere phumatoides*, *Perissocytheridea ascalopha*, *Aysegulina* sp., *Amphicytherura aff. yakhiniensis*, *Paraplatycosta aff. talayninensis*.

In this Assemblage features *Cytherella aff. austinensis* as the dominant species, accounting for 24.5% of the trophic nucleus. Other significant contributors include *Cytherella aff. elongata* (16.9%) and *Paracypris mdaouerensis* (15.5%), highlighting a shift in dominance compared to the unites 1,2 et 3. The contribution of *Cytherella ovata* decreases markedly to 6.2% in the unite 4, while species such as *Spinoleberis yotvatensis* (4.1%) and *Cythereis algeriana* (3.4%) play smaller roles.

### 3. Description of the Djebel Boukezez section (Batna)

In the Batna region, the studied section corresponds to the Boukezez Formation, which encompasses deposits from the Coniacian and Santonian stages (Yahiaoui, 1990; Laffitte,

## CHAPTER II LITHOLOGICAL AND PALEONTOLOGICAL CHARACTERISTICS

1939). In this particular section, the continental cover only allows the outcropping of upper Coniacian to Santonian strata. These deposits consist of a 160-meter-thick alternation of marls and limestones. The marl-limestone succession contains a fossil assemblage that includes bivalves, gastropods, and echinoderms. Notably, all the limestone beds, although fossiliferous, predominantly display a bioclastic texture (Figure II.4)

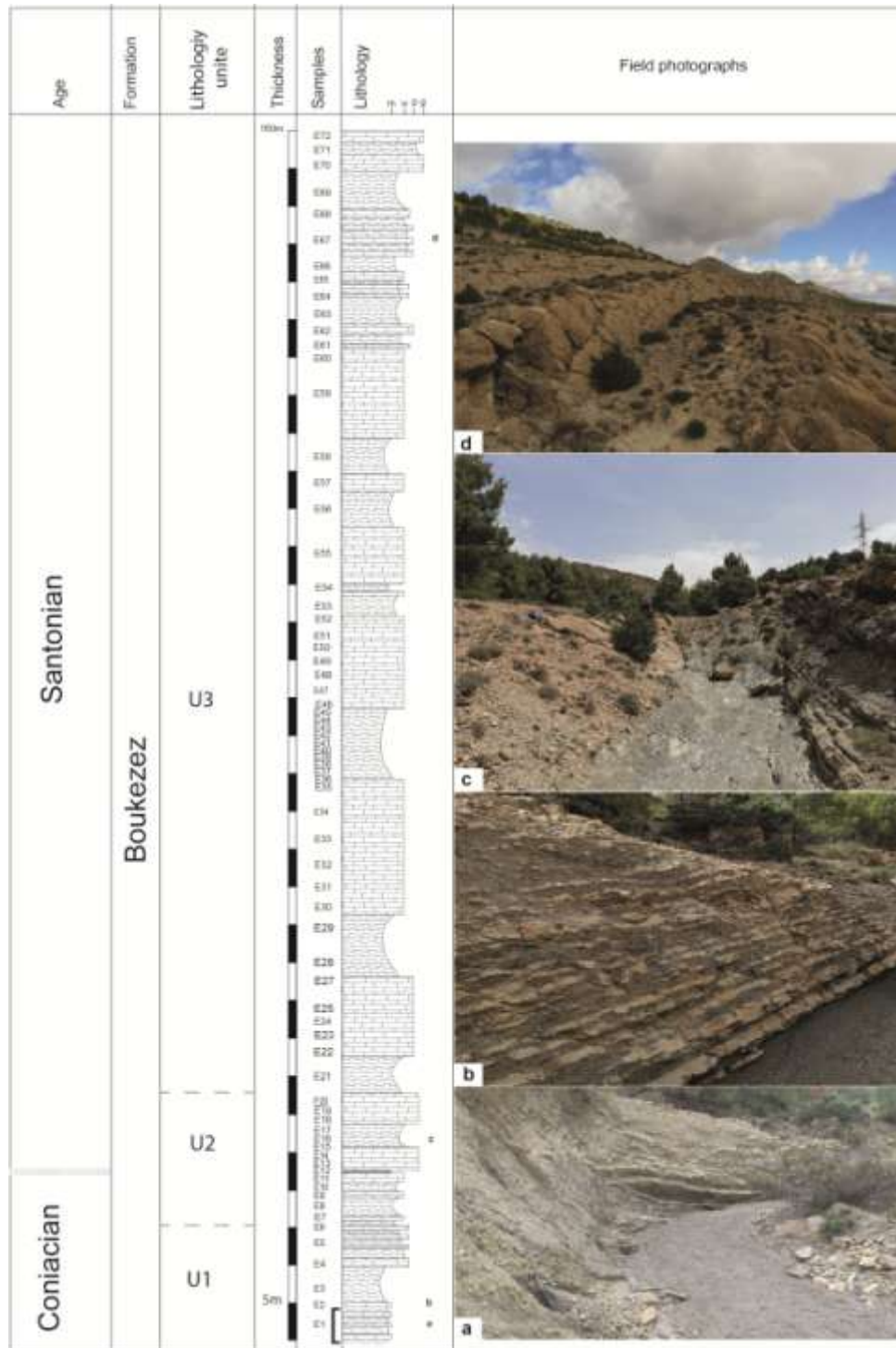


**Figure II. 4:** Litho-stratigraphic column of the Boukezez section with field photograph.

# CHAPTER II LITHOLOGICAL AND PALEONTOLOGICAL CHARACTERISTICS

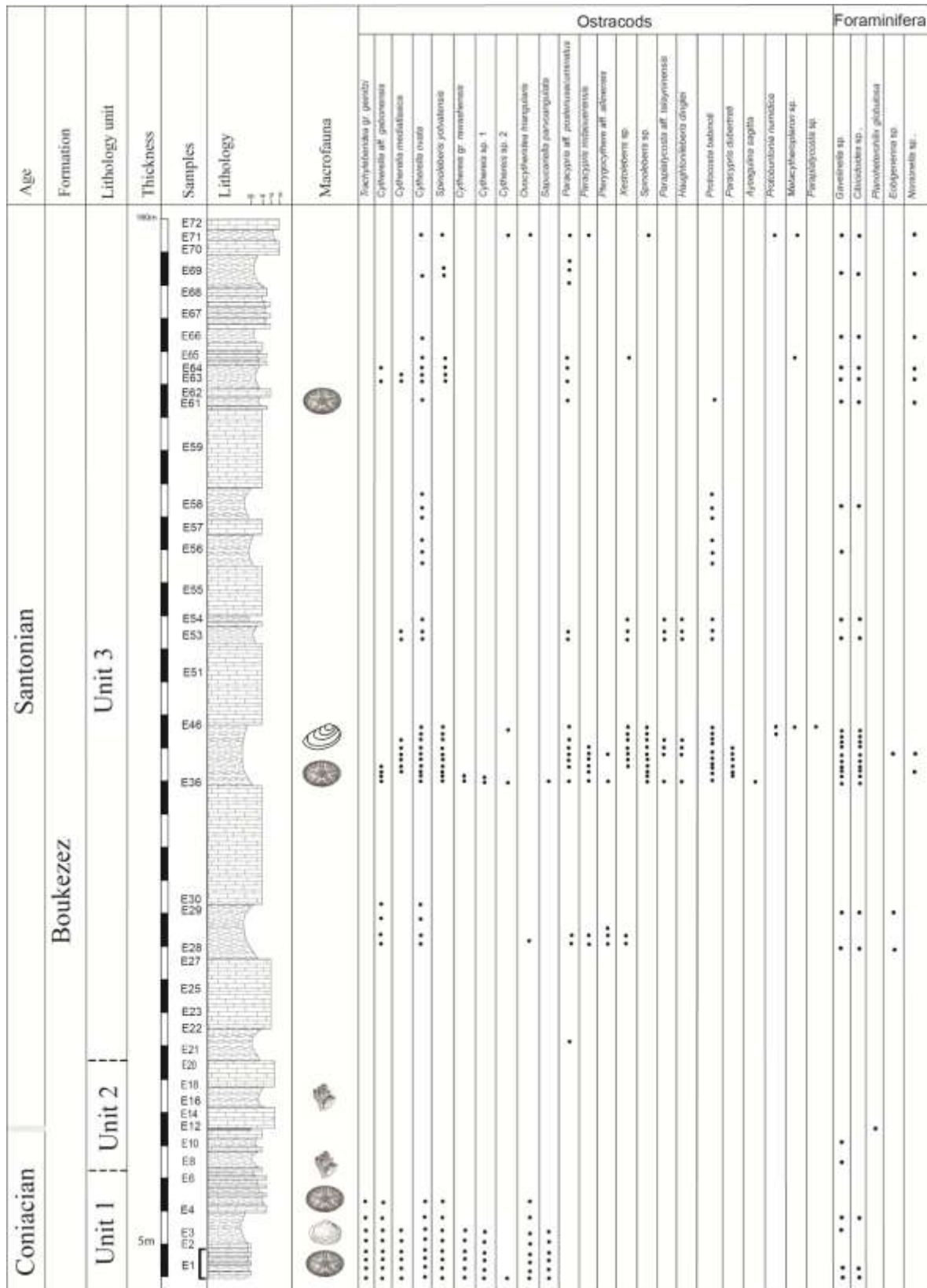


**Figure II. 5 :** Litho-stratigraphic column of the Boukezez section with the distribution of macrofauna and microfauna.

## CHAPTER II LITHOLOGICAL AND PALEONTOLOGICAL CHARACTERISTICS

Three informal lithological units have been delineated in this Formation :

**3.1. Unit 1 (U1)** Marl and limestone with hosting modestly diverse benthic fauna and ostracods

This unit is represented by marls and limestone hosting modestly diverse benthic fauna and ostracods. It has an apparent thickness of 13.5m. These levels (sample E1 to sample E6) are of late Coniacian (see Yahiaoui, 1990). They consist of:

4 meters of alternating marls and limestone (E1 and E2) (Figure II. 4a, b). The marls, bearing a compacted grayish carbonates with well-preserved small irregular echinoids (*Hemiasterourneli* Agassiz and Dessor, 1847), regular echinoids (*Phymosoma thevestense* Péron and Gauthier, 1880), bivalves (*Paraesafaba* sp., *Plicatula ventilabrum* Coquand, 1880), and gastropods (*Cimolithium* sp.), This microfacies contains a large fragment of invertebrates, rare echinoid radioles and lamellibranchs. The dominant cement is micritic with rare traces of stylolitisation and ferruginisation. This microfacies has microfissures with a sparitic filling. The mudstone texture of this microfacies highlights a quiet low-energy environment, deep enough to be placed in the distal platform. (Figure II.6), as well as abundant and moderately diverse ostracods (*Cytherella ovata* Roemer, 1841, *C. aff. gabonensis* Neufville, 1973, *C. mediatlasica* Andreu, 1996, *Trachyleberidea* gr. *geinitzi* Reuss, 1874, *Spinoloberis yotvataensis*, *Cythereis* gr. *rawashensis* Van den Bold, 1964, *Cythereis* sp. 1 and sp.2, *Ovocytheridea triangularis* Piovesan, Cabral and Colin, 2014, *Sapucariella parvoangulata* Andreu and Puckett, 2016). Ostracods are mostly present as articulated carapaces with few isolated valves. These marls also yield benthic foraminifera, including *Gavelinella* sp. In thin sections, the accompanying limestones, intercalated within these marls, exhibit a mudstone texture marked by echinoid spines.

4 meters layer of compacted grayish marls (E3) characterizes this section. These marls feature very small, unidentifiable irregular echinoids, bivalves (*Paraesa faba Plicatula ventilabrum*), and gastropods, including *Nerinea* sp. The ostracods assemblage mirrors that of the underlying level except *Cythereis* sp. 2, co-occurring with numerous small gastropods and foraminifera (*Gavelinella* sp.).

5.5 meters layer of alternating marl and limestone. The limestones (E4) are 1 meter 176 thick, yellowish, and display a wackestone to packstone texture. They contain miliolids and other benthic foraminifera, bioclasts of gastropods. The marls (E5) contain abundant, well-preserved echinoids (*Hemiasterourneli*, *Phymosoma sulcatum* Desor, 1858), bivalves (*Rachiosoma rectilineatum* Péron and Gauthier, 1881). Ostracods exhibiting lower diversity

## CHAPTER II LITHOLOGICAL AND PALEONTOLOGICAL CHARACTERISTICS

than the lower levels (*Cytherella ovata*, *C. aff. gabonensis*, *Trachyliberidea gr. geinitzi*, *Spinoloberis yotvataensis*, *Ovocytheridea triangularis*). The final limestone bed (E6) contains bryozoans and echinoid spines (Figure II. 7).

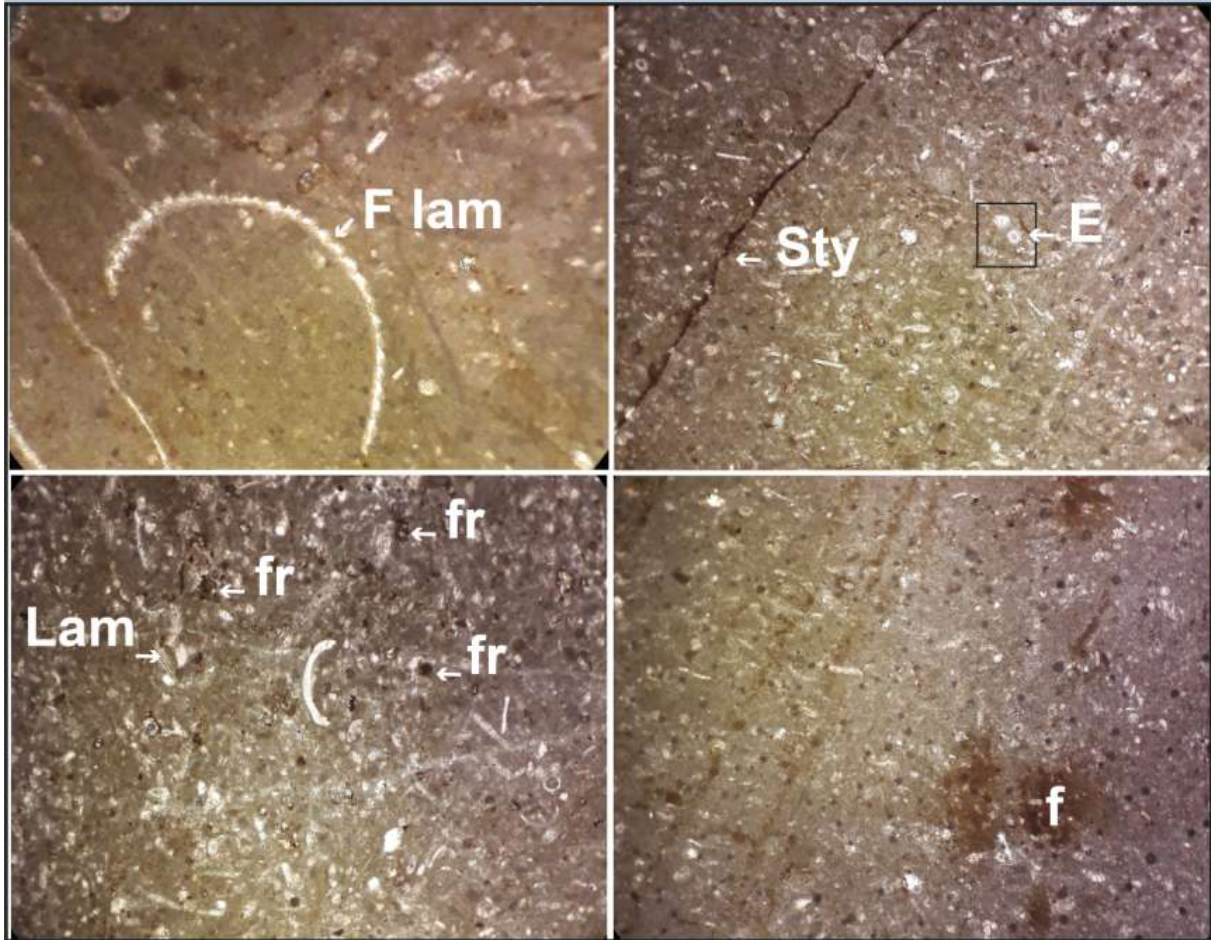


**Figure II. 6:** Limestone mudstone with rare large bioclastic fragments (F lam) and echinoid radiole (RE).

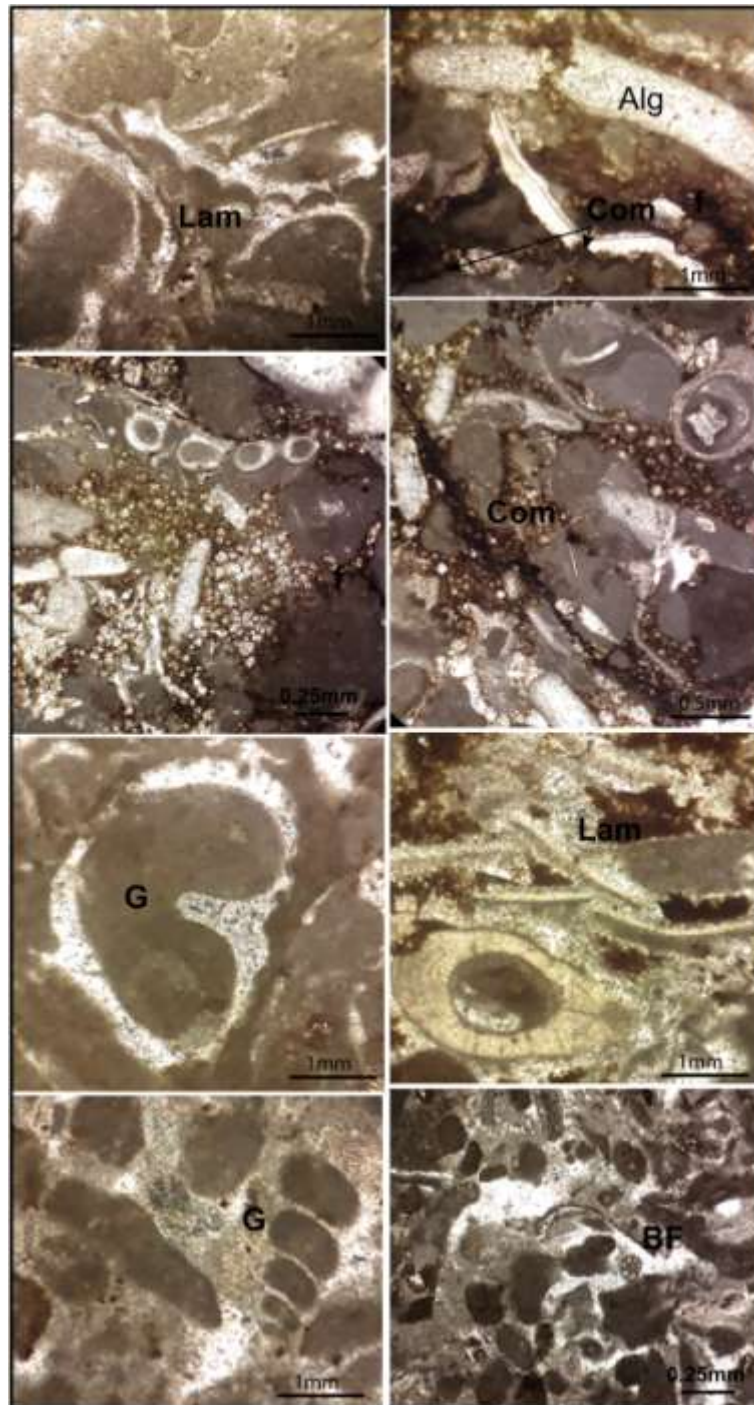


**Figure II. 7:** limestone with miliolids and other benthic foraminifera(BF), Gasteropods (G), lamellibranch (Lam) and Algae (Alg).

**3.2. Unit 2 (U2) Marl and bioclastic limestone devoid of ostracods**

These levels (E7- E20) are composed of marls and bioclastic limestone over an apparent thickness of 30.5m devoid of echinoid fragments and ostracods and are of latest Coniacian–lower Santonian age (Laffitte, 1939). They consist of:

## CHAPTER II LITHOLOGICAL AND PALEONTOLOGICAL CHARACTERISTICS

15 meters of alternating gray marls and yellowish nodular limestone (E7-E11). The marls yielded echinoid fragments and *Gavelinella* sp., but ostracods are absent. The limestone beds feature a wackestone texture with large bioclastic fragments, echinoid plates, miliolids, and other benthic foraminifera. This microfacies represents the laminae (7, 20). These limestones are greyish in colour. It contains mainly large fragments of gastropods, miliolids, radioles and plates of echinoids and rare planktonic foraminifera and bryozoans. The dominant cement is micritic. The texture of this microfacies reveals a medium-energy environment that can be placed in the subtidal zone. (Figure II.8)



**Figure II. 8:** Wackestone to packstone limestone with large fragments of invertebrates and miliolae (M) rare planktonic foraminifera (PF) and bryozoans (Bry).

## CHAPTER II LITHOLOGICAL AND PALEONTOLOGICAL CHARACTERISTICS

2 meters (E12) of laminated limestone with calcispheres and planktonic foraminifera (*Heterohelix globulosa* Ehrenberg, 1840). This microfacies represents layer 12. This limestone is blackish in colour, with a laminated appearance. It contains mainly calcispheres and planktonic foraminifera. (Figure II.9)

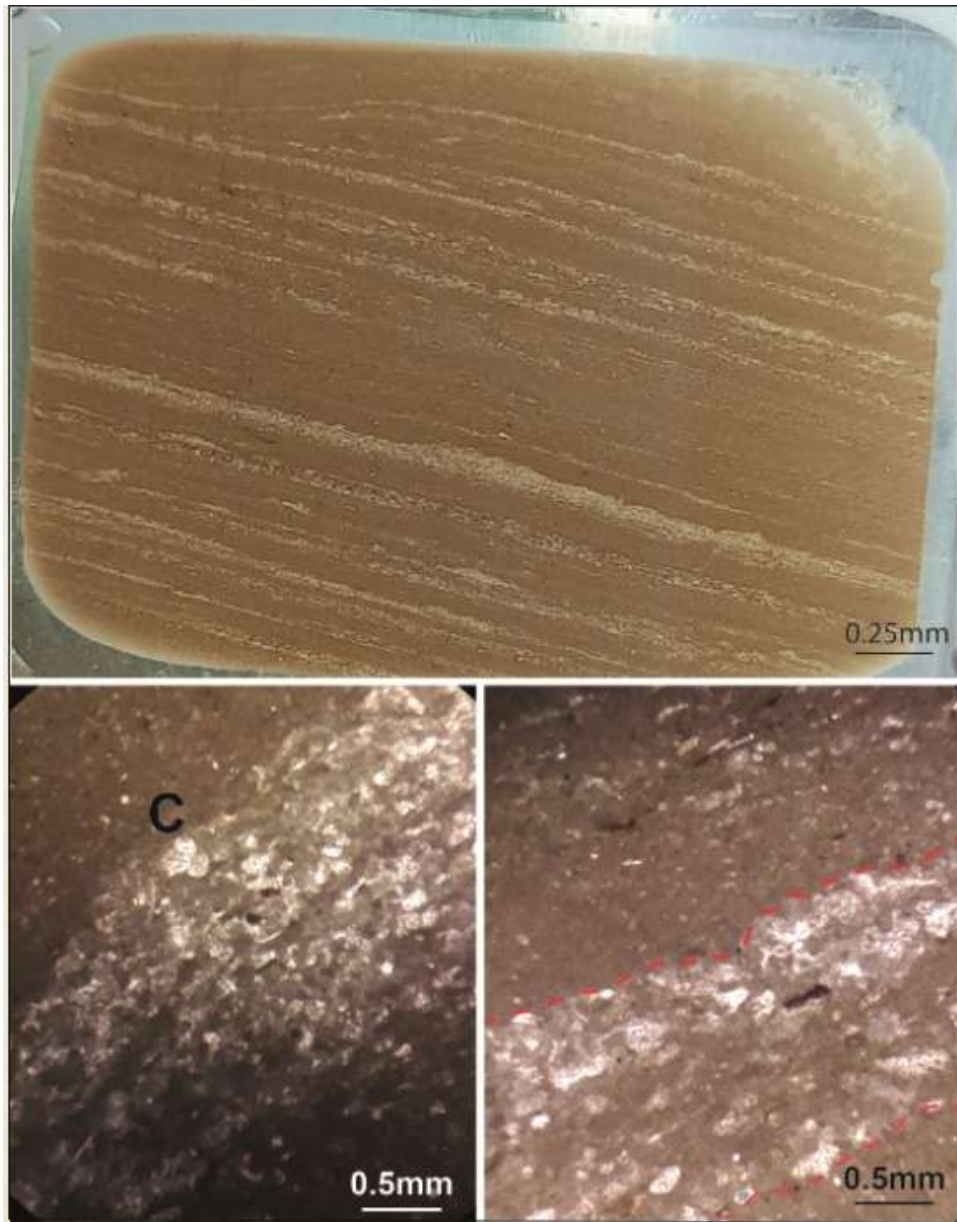


**Figure II. 9:** laminated limestone with calcispheres ( C) and planktonic foraminifera  
5 meters (E13-E15) of bioclastic limestone with a packstone to grainstone texture, with pelletoid structures, bivalves, gastropod fragments, and echinoid plates and spines. The texture of the upper part of this horizon changed vertically to dolomitic limestone with a grainstone texture, which is underlined by a hardground (E15) (Figure II. 4c); représenté par Grainstone limestone with large lamellibranch fragments. This microfacies is represented by

## CHAPTER II LITHOLOGICAL AND PALEONTOLOGICAL CHARACTERISTICS

blades (13 14 and 15). Greyish in colour. It contains the following elements: fragments of lamellibranchs, pelletoids, bryozoans, gastropods, ostracods, echinoid radioles and sections of algae. The texture of this microfacies reveals a shallow, high-energy environment, which can be classified in the middle platform zone. (Figure II.10)

5 meters (E16-E17) of lithified marls and marly limestone with gastropods (*Campanile* sp., *Aporrhais* sp.);

3.5meters (E18-E20) of limestone with a packstone to grainstone texture, possibly evolving towards a wackestone type. These layers contain bivalves, mililoids, bryozoans, echinoids spines, and benthic foraminifera. (Figure II.11)

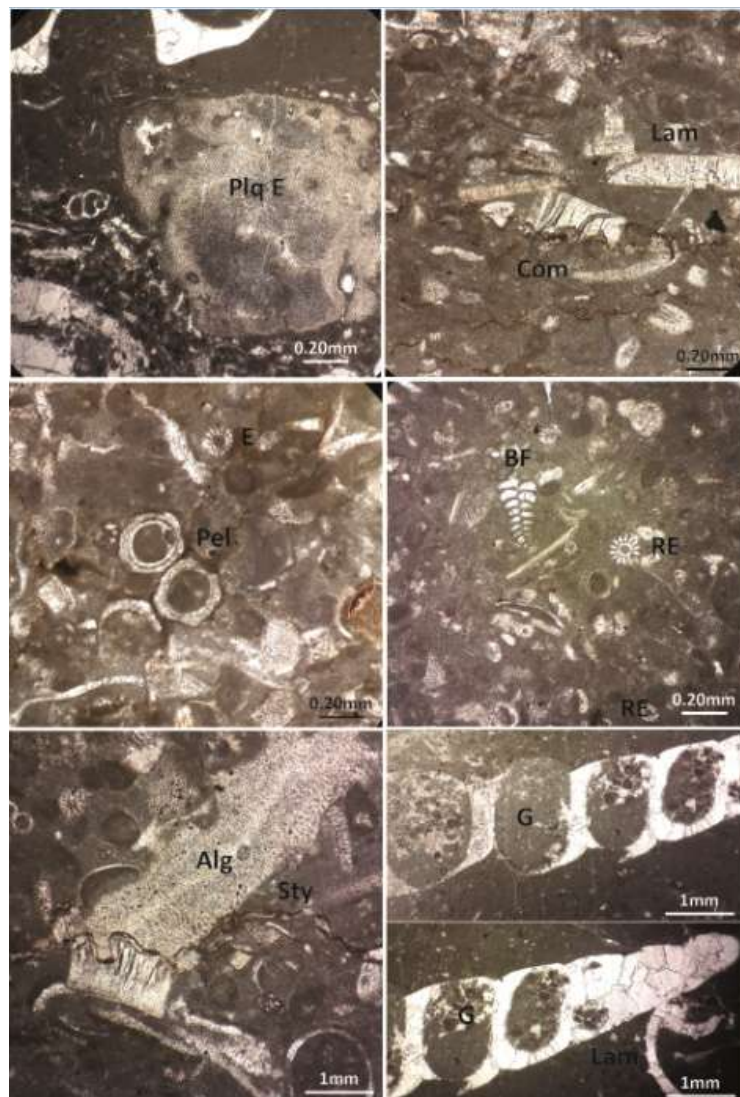


**Figure II.10:** limestone with fragments of lamellibranchs (Lam) and pelletoids (Pel) ; bivalves, gastropod fragments(G), and echinoid plates and spines (Plq E, RE), Algae (Alg) and Benthic foraminifera (BF).

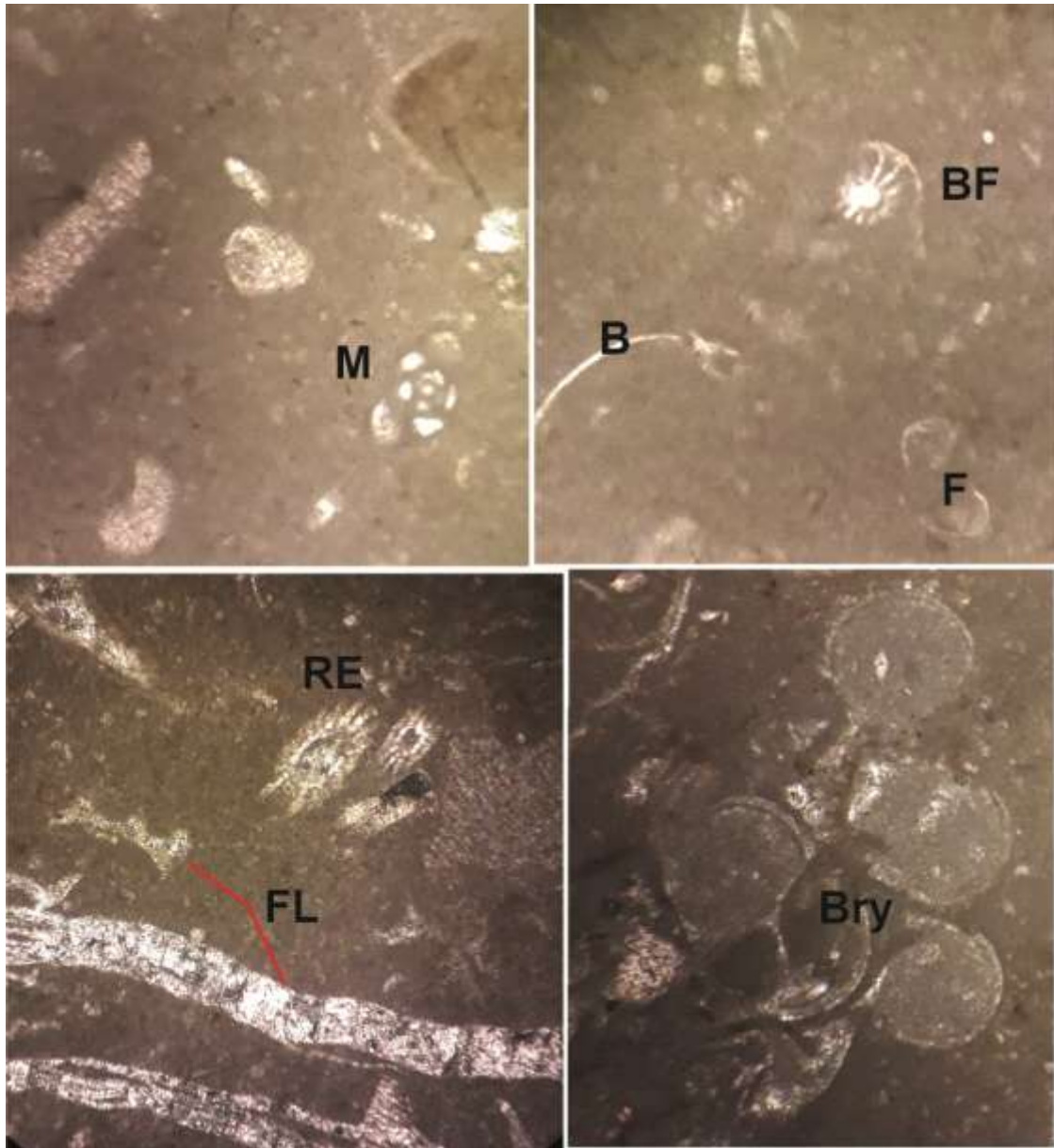


**Figure II. 11:** packstone to grainstone limestone with bivalves (B), mililoids (M) and bryozoans (Bry), echinoids spines (RE), and benthic foraminifera (BF).

**3.3. Unit 3 (U3) Marl and limestone with abundant ostracods**

These levels (E21-E72) represented by marls and limestone over an apparent thickness of 120m (Figure II. 4d) with abundant echinoids and ostracods and are of Santonian (Yahiaoui, 1990, Laffitte, 1939). They consist of:

5 meters (E21) of greenish marls, featuring rare ostracods (*Paracypris* aff. *posteriussacuminatus* Andreu, 1996) and echinoids. Additionally, traces of oxidized pyrite are noted;

## CHAPTER II LITHOLOGICAL AND PALEONTOLOGICAL CHARACTERISTICS

12 meters (E22-E27) of limestone with a packstone texture, containing bryozoans and miliolids, as well as echinoid plates and spines that grades up-section into limestone with a grainstone texture in the upper segment;

3 meters (E28) of greenish marls hosting echinoids and ostracods (*Cytherella ovata*, *C. aff. gabonensis*, *Paracypris aff. posteriusacuminatus*, *Paracypris mdaouerensis* Bassoullet and Damotte, 1969, *Ovocytheridea triangularis*, *Pterygocythere aff. allinensis* Grekoff and Deroo, 1956, *Xestoleberis* sp., *Planoheterohelix globulosa*), alongside foraminifera (*Eobigenerina* sp., *Cibicidoides* sp., and *Gavelinella* sp.). The ostracod assemblage is predominantly smooth, composed by articulate and small specimens.

93 meters (E29-E69) of alternating hard yellow to gray marls and gray bioclastic limestones. These limestones, displaying a wackestone to packstone texture (evolving into grainstone type), contain bryozoans, miliolids, bioclasts, echinoid spines, and other benthic foraminifera, lamellibranchs with millioles and bryozoans; pelletoids with ostracods, fragments of gastropods and fragments of macroinvertebrates where we can also see some rare ferruginisation. The texture of this microfacies reveals a very shallow environment, probably the upper part of the intertidal zone, of medium energy. (Figure II.12). The marls yield irregular echinoids (*Mecaster fourneli* Agassiz, 1847), Inoceramed (*Inoceramus siccensis* Pervinquière, 1912) and an abundantly diversified ostracod assemblage (*Cytherella ovata*, *C. aff. gabonensis*, *C. mediatlasica*, *Spinoloberis yotvatensis*, *Cythereis* gr. *rawashensis*, *Paracypris aff. posteriusacuminatus*, *P. mdaouerensis*, *P. dubertreti* Damotte and Saint-Marc, 1972, *Aysegulina sagitta* (Puckett and Colin, 2012), *Cythereis* sp., 1, *Cythereis* sp., 2, *Protobuntonia numidica*, *Paraplatycosta aff. talayninensis* Andreu, 1995, *Haughtonileberis dinglei* Piovesan, Cabral and Colin, 2014, *Pterygocythere aff. allinensis*, *Paraplatycosta* sp., *Protocosta babinoti* Piovesan et al., 2014, *Sapucariella parvoangulata*, *Metacytheropteron* sp., *Xestoleberis* sp.), alongside foraminifera (*Eobigenerina* sp., *Cibicidoides* sp., *Gavelinella* sp., and *Nonionella* sp.). Many of these ostracods display significant size, ornamented features, and an associated carapace.

The remaining part of the section (7 meters) consists of dolomitic limestone (E70) and lumachelic limestone (E72). These limestone types alternate with greenish marls. This microfacies is represented in slide (70). It is a limestone with a dolomitic packstone texture in places where it shows rhombohedrons of dolomites with ferruginous outlines. It contains large fragments of gastropods and lamellibranchs. The texture of this microfacies highlights a high-energy environment with a tendency to emersion; it can be placed squarely in the intertidal zone (Figure II. 13). rich in ostracods (*Cytherella* sp., *C. ovata*, *Spinoloberis*

## CHAPTER II LITHOLOGICAL AND PALEONTOLOGICAL CHARACTERISTICS

*yotvataensis*, *Spinoloberis* sp., *Cythereis* sp. 2, *Paracypris* aff. *posteriusacuminatus*, *P. mdaouerensis*, *Ovocysteridea triangularis*, *Protobuntonia numidica*, *Metacytheropteron* sp.,

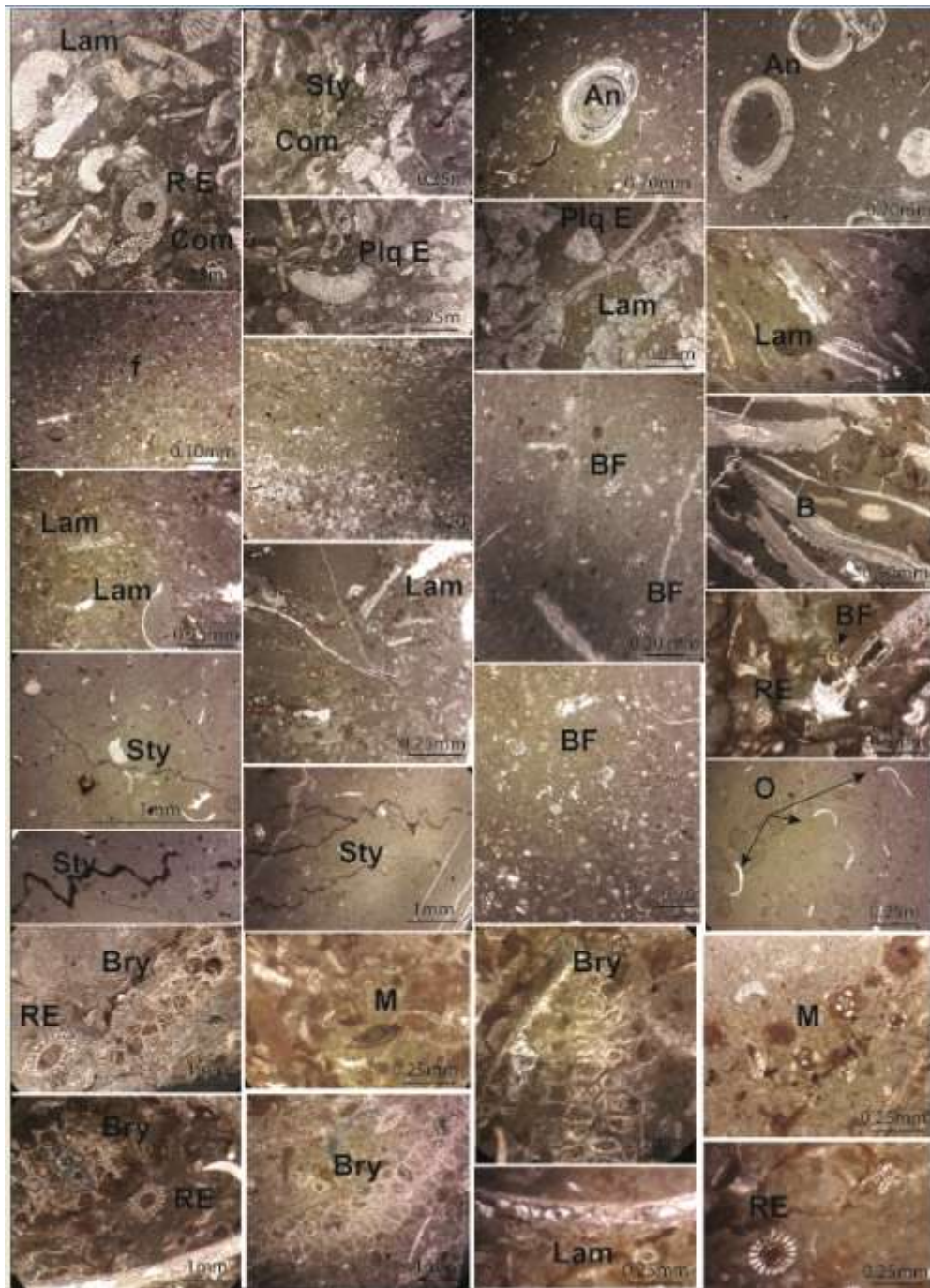


**Figure II.12:** Bioclastic limestones with bryozoans and mililoids; contain bryozoans(Bry), mililoids (M), bioclasts, echinoid spines (RE), and other benthic foraminifera(BF), lamellibranchs (Lam); pelletoids (Pel) with ostracods (O) and fragments of macroinvertebrates (B).

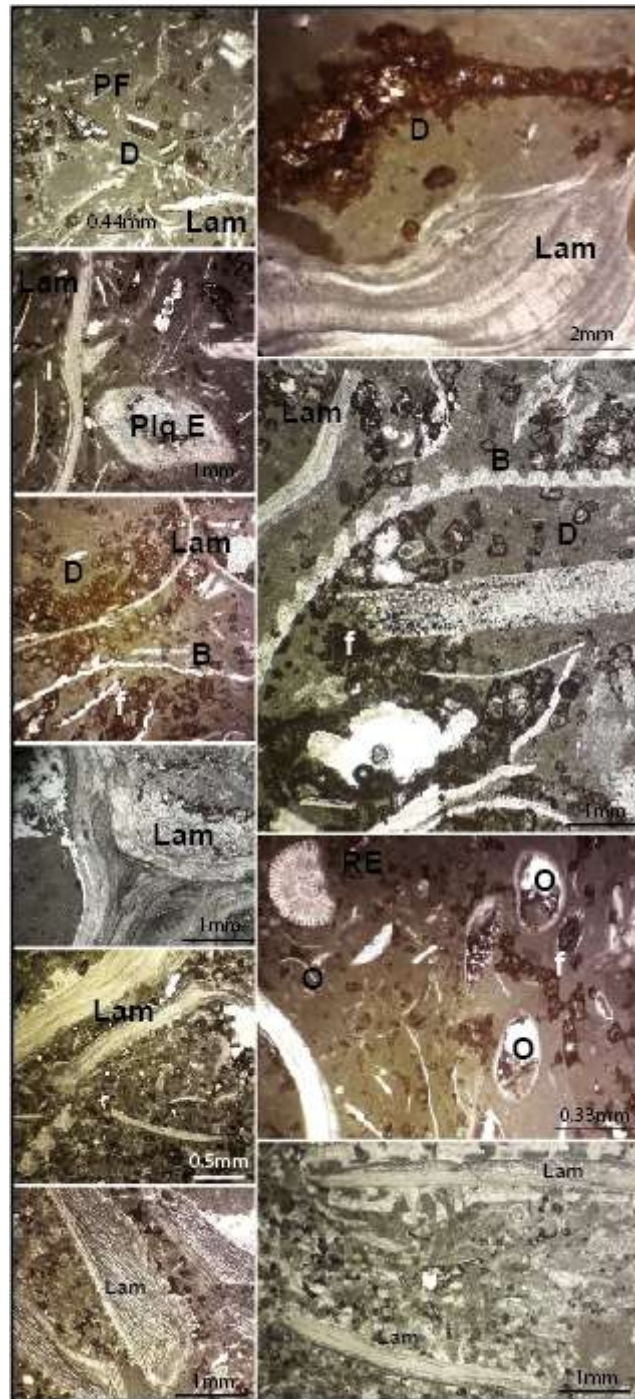


**Figure II.13:** Dolomitic limestone with large fragments of gastropods and lamellibranchs (Lam), rhombohedrons of dolomites (D) with ferruginous outlines (f) ; large fragments of lamellibranchs (Lam); Ostracod (O), Bivalves (B), Plate echiniods (Plq E).

#### 4. Conclusion

The two sedimentary sequences studied, Jebel Essen (Tébessa) and Jebel Boukezez (Batna), were characterised by distinct lithological and paleontological developments during

## CHAPTER II LITHOLOGICAL AND PALEONTOLOGICAL CHARACTERISTICS

the Coniacian and Santonian periods, with marked differences in thickness, lithological style and fossil content composition.

The Coniacian and the Santonian are represented in Tébessa by the 'Essen' Formation, while in Batna by the 'Boukezez' Formation.

At Essen section, the sedimentary sequence covers a considerable thickness of around 533 metres. In contrast, the Boukezez section, although representing the same period, has a much thinner apparent thickness (only around 160 metres).

In the Essen section the deposits are dominated by marly, whereas in the Boukezez section they are more calcareous.

At Essen section the deposits are with specific biogenic units characterized by various fossil assemblages of bivalves, sea urchins and cephalopods, supported by a rich distribution of foraminifera and ostracods. On the other hand, in Boukezez section with a relatively lower fossil diversity than that of Jebel Essen, particularly in terms of ostracods and foraminifera.

The transition between the Coniacian and Santonian periods is better clearly visible in a 3 metre thick layer of bioclastic limestone at Essen section. The distinction between the Coniacian and Santonian is less clear-cut due to the absence of clear biogenic markers and the prevalence of sedimentary lacunae.

In general, this comparison reflects local differences in sedimentary and environmental dynamics during the Coniacian-Santonian between the two regions: Tébessa (Jebel Essen) shows a thicker, more marly and more fossil-rich record reflecting a more stable and fossil-rich depositional environment, whereas the record from Batna (Jebel Boukezez) suggests more erratic and relatively more energetic depositional environments with distinct sedimentary discontinuities.

*CHAPTER III*  
*SYSTEMATIC*

## **CHAPTER III SYSTEMATIC**

### **1. Introduction**

The taxa collected from the Coniacian and Santonian deposits in the eastern part of the Saharan Atlas, specifically from two studied sections Djebel Boukezez (Batna) and Djebel Essen (Tébessa) exhibit a moderately poor macrofauna in terms of macroinvertebrate diversity, but a rich and diverse microfauna, primarily composed of foraminifera and ostracods.

The classification of ammonites follows Wright et al. (1996), echinoids are identified according to Moore (1996), bivalves are classified following Carter et al. (2011), inoceramids according to Harries et al. (1996), and gastropods according to Bouchet & Rocroi (2005). All linear measurements were taken using a digital caliper and are expressed in millimeters. The following abbreviations are used in species descriptions: L (length), H (height), W (width), and C (carapace). Selected species from these groups are illustrated on [11] plates.

The classification of ostracods follows Horne (2005), while planktonic foraminifera are identified based on Loeblich & Tappan (1964, 1988), and benthic foraminifera on Kaminski (2004). Some species from these groups are illustrated on [12] plates as well.

For each taxon, a synonymy list is provided in order to update the biostratigraphic and palaeogeographic distribution data.

The systematic study focuses primarily on planktonic and benthic foraminiferal species identified in the residues of Coniacian and Santonian sediments. The relative abundances of ostracods, planktonic, and benthic foraminifera were calculated based on 100 grams of dry sediment.

All studied specimens are housed in the Department of Geology, Badji Mokhtar University, Annaba (Algeria), under the following registration codes: (E) for the Boukezez locality and (C–S) for the Essen locality.

### **2. Results**

#### **2.1. Macrofauna**

## CHAPTER III SYSTEMATIC

97 macroinvertebrates specimens were recolted in the study area mainly in Essen locality. Of these, 33 species were identified belonging to the 21 families and 26 genera (Table 1).

Groups	Species
<b>Ammonite</b>	- <i>Hemitissotia morreni</i> (Coquand, 1862)
<b>Echinoids</b>	- <i>Mecaster fourneli</i> (Deshayes, dans Agassiz et Desor 1847) - <i>Mecaster turonensis</i> (Bayle, 1878) - <i>Mecaster batnensis</i> Coquand, 1862 - <i>Mecaster texanus</i> (Roemer, 1849) - <i>Hemiaster cf. bibansensis</i> Péron & Gauthier, 1881
<b>Bivalves</b>	- <i>Agelasina plenodonta</i> Riedel, 1933 - <i>Paraesa faba</i> (J. de C. Sowerby, 1827) - <i>Pholadomya</i> sp. - <i>Arctica picteti</i> (Coquand, 1862) - <i>Meretrix desvauxi</i> (Coquand, 1862) - <i>Aphrodinadutrugi</i> (Coquand, 1862) - <i>Protocardia hillana</i> (J. Sowerby, 1813) - <i>Idonearca thevestensis</i> (Coquand, 1862) - <i>Cucullaea (Idonearca) trigona</i> (Seguenza, 1882) - <i>Cucullaea (Idonearca) diceras</i> Seguenza 1882 - <i>Oscillopha dichotoma</i> (Bayle, 1849) - <i>Pycnodonte (Phygraea) vesicularis vesicularis</i> Lamarck 1806 - <i>Amphidonte conica</i> (Sowerby, 1813) - <i>Plicatula ferryi</i> Coquand, 1862 - <i>Arctica cordata</i> (Sharpe 1850) - <i>Nuculana cf. mariae</i> (D'Orbigny, 1844) - <i>Rostrocardia papieri</i> (Coquand, 1862) - <i>Astare gigantea</i> deshayes, 1842 - <i>Plicatula fourneli</i> (Coquand, 1862) - <i>Plagiostoma subsimplex</i> (Thomas & Peron 1891) - <i>Granocardium desvauxi</i> coquand 1862
<b>Inocerames</b>	- <i>Inoceramus pictus?</i> J. de C. Sowerby 1814 - <i>Inoceramus ssiccensis</i> Pervinquièrre 1912

## CHAPTER III SYSTEMATIC

**Gasteropods**

- *Volutomorpha* sp.,
- *Gyrodes* sp.,
- *Leptomaria* sp.,
- *Aporrhais fourneli* (Coquand, 1862)

### Ammonite

Class Cephalopoda

Subclass Ammonoidea

Order Ammonitida Zillel, 1884

Superfamily Acanthoceratoidea

Family Scoceratidae

Genus *Hemitissotia*

***Hemitissotia morreni* (Coquand, 1862)**

**Pl. 1. Figure 1-3 a-c**

1862 *Ammonites morreni* Coquand, p. 173, Pl. Moi, figure 3, 4.

1880 *Cérilites morreni* Coquand, p. 372.

1885 *Buchiceias morreni* Zittel, p. 79.

1889 *Buchiceras* cf. *morreni* Perón, p. 79.

1896 *Hemitissotia morreni* Coquand-Péron. pl. XV, Figure 6 et pl. XVIII, figure 11-14.

**Material :** 5 complete specimens from the upper part of the Coniacian Formation

**Remarks:** The material studied herein resembles to some extent *Hemitissotia batnensis* Peron. Coquand's *Ammonites morreni* is difficult to identify precisely and discrepancies exist in its description, figuration and classification. Although Coquand used Haan's *Ceratites* genus to classify the Algerian ammonites with rounded saddles, he did not include the species in question within this genus, but in the *Ammonites*. Moreover, in describing *Ceratites fourneli*, which external form resembles that of *Ammonites morreni*, he stated that these fossils differ in that the former has the remarkable characteristics of *Ceratites*, unlike the latter. Pervinquierie (1907) and Chancellor et al. (1994) regarded *Hemitissotia batnensis* Peron (1897) and *H. czini* Peron (1897) as synonyms of *H. morreni*. It was recorded from the lower Senonian of Refana, near Tebessa, Algeria (Peron 1896), upper Turonian of Tunisia (Coquand, 1862; Chancellor et al., 1994).

**Ecology:** Aragonitic mobile nektonic carnivore.

**Occurrence :** Late Coniacian of Essen section

**Distribution:** North Africa (Tunisia and Algeria; Chancellor et al., 1994), and the Middle East (Palestine; Parnes, 1964).

## CHAPTER III SYSTEMATIC

### Echinoids :

Embranchement Echinodermata BRUGUIÈRE, 1791

Class Echinoidea LESKE, 1778

Cohort Irregularia LATREILLE, 1825

Superorder Atelostomata VON ZITTEL, 1879

Order Spatangoida CLAUS, 1876

Suborder Hemiasterina FISCHER in MOORE, 1966

Family Hemiasteridae H.L. CLARK, 1917

Genus *Mecaster* POMEL, 1883

**Type species:** *Hemiasterourneli* Deshayes a Agassiz et Desor 1847

***Mecasterourneli* (Deshayes, dans Agassiz et Desor 1847)**

**Pl. 2- 3. Figure 1-2 a-e – Figure 2a-e, (4-5a-d)**

1847 *Hemiasterourneli* Deshayes dans Agassiz et Desor, p. 123.

1991 *Mecasterourneli* (Deshayes à Agassiz et Desor) ; Smith et Bengtson, p. 61, pl. 14.

2002 *Hemiasterourneli* Deshaye : Kora et al. : pl. 4, Figure 13.

2004 *Hemiaster (Mecaster)ourneli* Deshayes : Abdel: Gawad et al. : pl. 10, Figure 12h- 13.

2006 *Hemiaster (Mecaster)ourneli* Deshayes : El Qot: 152. pl. 34, Figure 2 : 3.

2007 *Hemiaster (Mecaster)ourneli* Deshayes : Abdel: Gawad et al. : pl. 4, Figure 9h- 10.

2009 *Hemiaster (Mecaster)ourneli* (Deshayes, 1847): EL QOT et al., p. 82, Pl. 5, Figure 3, 4

2013 *Mecasterourneli* (Deshayes à Agassiz et Desor); Oliveira et coll., p. 6, Figure 4A : C, 6A : I.

2015 *Mecasterourneli* (Deshayes, dans Agassiz et Desor 1847): Abdelhamid, p.190 Figs. 12- 13.

**Material:** 5 complete specimens from the bottom/ top part of the Essen Coniacian Formation and 28 specimens from the upper part of the Boukezez Formation.

**Remarks:** Our material is distinguished by a more elongated test and a higher posterior interambulacrum. *Mecasterourneli* differs from *M. pseudourneli* (Peron & Gauthier, 1878) in that its paired petals are shorter and shallower. In addition, *M. pseudourneli* is older (Cenomanian).

**Ecology:** Mobile infauna with high Mg content: calcite deposit: feeder.

**Occurrence:** Coniacian of Essen and Boukezez section

**Distribution:** *M.ourneli* has been recorded in the Turonian-Campanian interval of North Africa, Nigeria and the Middle East and has also been recorded in Brazil.

## CHAPTER III SYSTEMATIC

### *Mecaster turonensis* (Bayle, 1878)

#### Pl. 2. Figure 3 a-e

1878 *Spatangus turonensis* Bayle, pl. 156, Figure 3e4.

1895 *Micraster turonensis* Lambert, p. 212.

1975 *Micraster turonensis* Stokes, p. 80, Figure 30, pl. XI, Figure 7, 8, pl. XII, Figure 1e3.

1921 *Hemiaster heberti mutatio turonensis* Fourtau, p. 89, pl. 11, Figure 1e10.

2012 *Mecaster turonensis* (Fourtau) ; Abdelhamid et Azab, p.604, Figure 15 IeK, 17 B, C.

2015 *Mecaster turonensis* (Fourtau, 1921), Abdelhamid, p.193 Figure 12FeH, 19

**Material:** One complete, well preserved specimen and 2 incomplete specimens from the lower part of the Coniacian Formation of Essen section.

**Remarks:** *Mecaster turonensis* can be distinguished from *M. fourneli* (Deshayes) by a higher test, wider paired petals and longer posterior paired petals with more pairs of pores (Abdelhamid, 2015).

**Ecology:** Mobile endofaunal deposit with high mg-calcite content: feeder.

**Distribution:** Coniacian to Santonian of France and Egypt.

**Occurrence:** Lower Coniacian of Essen section

### *Mecaster batnensis* Coquand, 1862

#### Pl. 3. Figure 1a-e

1862 *Hemiaster batnensis* Coquand, p. 248, pl. 26, figures 6–8.

1991 *Mecaster batnensis* (Coquand): Smith et Bengtson, p. 56, pl. 12, 13.

1999. *Mecaster batnensis* (Coquand, 1862): Seeling, pl. 7, figures 3 à 8.

2008 *Mecaster batnensis* (Coquand): Manso et Andrade, p. 322, pl. 1, Figure G-H.

2015 *Mecaster batnensis* (Coquand); Abd El-Hamid, p. 168, Figure 27F, 28.

2015 *Mecaster cf. batnensis* (Coquand): Ali, p. 580, Figure 14e16, 17AeH.

**Material:** 4 complete, well-preserved specimens and one incomplete specimen from the lower part of the Coniacian Formation of Essen section.

**Remarks:** *Mecaster batnensis* resembles *Mecaster pseudofourneli* (Peron et Gauthier), but has much longer petals, a higher test and the peristome is situated relatively further back than in *Mecaster pseudofourneli* (Abdelhamid, 2015).

**Ecology:** Mobile infauna with high mg content: calcite deposits: feeder.

**Occurrence:** Lower Coniacian of Essen section

**Distribution:** *Mecaster batnensis* is known from the United States (Arizona, New Mexico and Texas), Mexico, Venezuela and Brazil. It is common in various regions of the Tethys.

## CHAPTER III SYSTEMATIC

Algeria, Tunisia, Egypt, Jordan, Palestine and Portugal (see de Loriol, 1888; Roney, 2013; Zaghib: Turki, 1975; Smith, 1992; Smith and Bengtson, 1991; Manso and Andrade, 2008; Gallemi and Abdallah, 2010).

### *Mecaster texanus* (Roemer, 1849)

#### Pl. 3. Figure 2a-d

1849 *Hemiaster texanus* Roemer, p. 77, 393.

1852 *Hemiaster texanus* Roemer : Roemer, p. 78, 85, Pl. 10, figure 4 a: c.

1915 *Hemiaster texanus* Roemer : Clark & Twitchell, p. 94, Pl. 49, figure 1a : j.

1953 *Hemiaster texanus* Roemer : Cooke, p. 33, Pl. 13, figure 1 : 4.

1955 *Hemiaster texanus* Roemer : Cooke, p. 109, Pl. 29, figure 5: 10.

2003 *Mecaster texanum* Roemer, 1852 - Cassab, p.76.

2013 *Mecaster texanum* (Roemer, 1852) : Oliveira et al., p. 11, figure 7 A : C, 9 A : I.

**Material:** 5 complete specimens from the upper part of the Coniacian formation of Essen section.

**Remarks:** It differs from *M.ourneli* by having a larger and more elongated shell than that observed in *M.ourneli*. It differs from *Hemiaster wayensis* by having a larger and narrower test, with a narrower angle between petals I and V. *H. wayensis* also has shallower and smaller petals.

**Ecology:** Mobile infaunal feeding on calcite-rich deposits.

**Occurrence:** Upper coniacian of Essen section

**Distribution:** it has been recorded in the Cenomanian-Santonian strata of Egypt, Nigeria, Peru, the United States (Texas) and Brazil.

### *Hemiaster cf. bibansensis* Péron & Gauthier, 1881

#### Pl. 3. Figure 3a-d

cf.1881 *Heminster bibansensis* Péron & Gauthier in Cotteau, Péron & Gauthier, p. 68, pl. 3, figure 6-7.

cf.1889 *Hémiastre cf. bibansensis* - Gauthier, p. 16.

cf.1975 *Hemiaster bibansensis*- Zaghib-Turki, p. 57, pl.3, figure 7-9 ; texte figure 40a-c.

cf. 2015 *Hemiaster bibansensis*- Abdelhamid, p.153, figure7 (3).

**Matériel:**7 complete specimens from the lower parte of Santonian formation of Essen section and 5 complete specimens from the lower parte of Santonian formation of Boukezez section.

**Description:** This species was recorded in the Santonian rock of Algeria and later recorded in Tunisia. Here it is recorded for the first time from Egypt. The present material differs from the Egyptian individuals by having a slightly shorter bivium (in *H. bibansensis*, the bivium is

## CHAPTER III SYSTEMATIC

slightly longer than the paired anterior petals). It more closely resembles the Tunisian material in which the paired petals are equal. The present species can be distinguished from *H. pseudofourneli* Péron & Gauthier and *H. obliquetruncatus* Péron & Gauthier by its more eccentric apical disc towards the front, its longer posterior petals and its relatively narrower test.

**Occurrence:** Lower Santonian of Essen section

**Distribution:** Coniacian-Santonian of Wadi Sudr, Egypt.

### Bivalves

BIVALVIA Linnaeus class, 1758

Mega-order Cardiata Férussac, 1822

Superorder Cardiiiformii Férussac, 1822

Order Megalodontida Starobogatov, 1992

Superfamily Megalodontoidea Morris & Lycett, 1853

Family Dicerocardiidae Kutassy, 1934

Genus *Agelasina* Riedel, 1933

**Type Species:** *Agelasina plenodonta* Riedel, 1933.

***Agelasina plenodonta* Riedel, 1933**

#### Pl. 4. Figure 1a-c

1933. *Agelasina plenodonta* n. gen. n. sp.– Riedel, p. 58, pl. 4, figure 1 ; pl. 12, figure 1, 3: 5.

1955. *Agelasina plenodonta* Riedel : Reyment, p. 142, pl. 4, figure 1.

1957. *Agelasina plenodonta* Riedel : Darteville & Freneix, p. 155, pl. 26, figure 3; pl. 27, figure 1 : 3.

2015. *Agelasina plenodonta* Riedel : Moussavou, p. 316, figs 4/F, H, L, P.

2019 *Agelasina plenodonta* Riedel, Ayoub : Hannaa, p. 173, pl. III, figs Q : T ; pl. IV.

2023 *Agelasina plenodonta* Riedel : Benmansour, p. 8, figure 6. 2a : 2d

**Material:** 6 complete and 18 incomplete specimens from the lower/upper part of the Essen Coniacian Formation.

**Remarks:** *A. plenodonta* is similar to *Cyprinabarroisi* Coquand (from the Santonian of Tunisia) in general outline, umbilical curvature and swelling. However, *A. plenodonta* differs in having more pointed and less curled beaks, a narrower umbo and a higher shell. *Agelasina* differs from *Glossus* Poli in that it has two large posteriorly elongated cardinal teeth, and the lateral teeth are absent (for more details, see Ayoub: Hannaa et al., 2019).

**Ecology:** Aragonitec infaunal facultative mobile suspension feeder.

**Occurrence:** Coniacian of Essen section

## CHAPTER III SYSTEMATIC

**Distribution:** West Africa (Congo, Cameroon, Gabon and Nigeria).

Superfamily Veneroidea Rafinesque, 1815

Family Veneridae Rafinesque, 1815

Genus *Paraesa* Casey, 1952

Type species: *Venus faba* J. de C. Sowerby, 1827.

***Paraesa faba* (J. de C. Sowerby, 1827)**

### Pl.4. Figure 2a-d

1827. *Venus Faba* J. de C. Sowerby, p. 129, pl. 567, Figure 3

1957. *Paraesa* cf. *faba* (Sowerby) : Darteville & Freneix, p. 184, pl. 31, Figure 4 : 5.

1962. *Meretrix faba* (Sowerby) : Abbass, p. 146, pl. 22, Figure 21.

1972. *Paraesa faba faba* (Sowerby, 1827): Freneix, p. 178, pl. 18, figs 10 : 12.

2004. *Meretrix faba* (Sowerby): Abdel: Gawad et al., pl. 3, Figure 5.

2006. *Paraesa faba faba* (J. de C. Sowerby, 1827): El Qot, p. 88, pl. 18, figures 1, 3

2014. *Paraesa faba*? (Sowerby, 1827): Niebuhr et coll., p. 157, pl. 14d, f. 2015.

2019 *Paraesa faba* (J. de C. Sowerby): Nagm, p. 15, Figure 6K.

2019 *Paraesa faba* (J. de C. Sowerby): Ayoub: Hannaa et al., p. 201, figure 20; Pl. X, figures D : J.

2019 *Paraesa faba* (J. de C. Sowerby): Ghenim et al., p. 35, figure 8F1 G1–2.

**Material:** 3 complete specimens from the lower part of the Coniacian Formation.

**Notes:** They are distinguished by a taller shell, which makes the species name debatable. Freneix (1972) subdivided *Paraesa faba* into two subspecies, *P. faba faba* (J. de C. Sowerby, 1827) and *P. faba subfaba* (d'Orbigny, 1850). *Venus dutrugi* Coquand and *V. reynesi* Coquand closely resemble *Paraesa faba* in form and ornamentation and were considered junior synonyms (Freneix (1972), El Qot (2006), and Ayoub: Hannaa et al. (2014; Ghenim et al., 2019).

**Ecology:** Aragonitec, infauna, feeds on a facultatively mobile suspension.

**Occurrences:** Coniacian of Essen section

**Distribution:** Great Britain, Algeria, Tunisia, Libya, Morocco, and Egypt, conge Cameron and Brazil (J. de C. Sowerby, 1827; Coquand, 1862; Péron, 1890; Pervinquièrre, 1912; Berizzi and Busson, 1971; Freneix, 1972; Wood, 1908; El Qot et al., 2013). Fourtau, 1917; Abbass, 1962; El Qot, 2006; Ayoub: Hannaa et al., 2014; Niebuhr et al., 2014; Riedel, 1933; Trévisan, 1937 (Darteville & Freneix Seeling, 1999).

## CHAPTER III SYSTEMATIC

Order Pholadomyida Newell, 1965

Superfamily Pholadomyoidea King, 1844

Family Pholadomyidae King, 1844

Genus Pholadomya G.B. Sowerby, 1823

**Type Species:** *Pholadomya candida* G.B. Sowerby, 1823, par désignation ultérieure de Gray (1847).

*Pholadomya* sp.,

### Pl.4. Figure 3a-d

**Material:** A complete specimen from the lower part of the Coniacian Formation.

**Remarks.** No ornamentation preserved. Maximum inflation slightly below the umbonal area. Anterodorsal margin strongly concave, posterior end well rounded.

**Ecology:** facultative aragonitic endomorph fauna: mobile suspension: feeder.

**Occurrences :** lower Coniacian of Essen section

**Distributions :** France, Germany, the United Kingdom), North Africa (including Algeria, Tunisia, and Egypt), North and South America (such as the United States, Argentina, and Brazil), as well as in India, Southeast Asia, and Australasia (Damborenea & Mancenido, 1979; Kiel & Bandel, 2002; Skwarko, 1994). (Kiel & Bandel, 2002; Cox et al., 1969 ; Ben Mansour, 2009; Kazi-Tani, 1970).

Subclass Heteroconchia Hertwig, 1895

Superorder Heterodonta Neumayr, 1883

Order Veneroida H. Adams and A. Adams, 1856

Superfamily Arcticoidea Newton, 1891

Family Arctidae Newton, 1891

Genus Arctica Schumacher, 1817

**Type Species:** *Arctica vulgaris* Schumacher, 1817 (= *Venus islandica* Linnaeus, 1767).

*Arctica picteti* (Coquand, 1862)

### Pl.4. Figure 4a-d

1862 *Crassatella Picteti* sp. nov. Coquand, p. 199, pl. 13, figure 10-11.

1890 *Cyprina picteti* Coquand : Thomas et Péron, dans Péron, p. 293.

1912 *Cyprina picteti* Coquand : Pervinquière, p. 223, pl. 16, figure 6a-b, 7a-b, 8a-b.

2006 *Arctica picteti* (Coquand) : El Qot, p. 84, pl. 17, figure 2a-b, 3.

2014 ? *picteti* (Coquand) : Ayoub : Hannaa et al., p. 118, pl. 11, figure 3a-b, 4a-b.

## CHAPTER III SYSTEMATIC

2021 *Arctica picteti* (Coquand) : Mendir et al., p. 33, figure 7 E1–2 F1–2.

**Material:** 2 complete specimens from the lower part of the Coniacian Formation

**Ecology:** facultative Aragonitec endofauna: mobile suspension: feeding.

**Occurrence :** Coniacian of Essen section

**Distribution:** Algeria, Tunisia, Egypt and Italy (Thomas et Péron, 1890; Pervinquière, 1912 El Qot, 2006; Ayoub: Hannaa et al., 2014; Seguenza, 1882).

Subfamily Meretricinae Gray, 1847

Genus *Meretrix* Lamarck, 1799

**Species type :** *Vénus meretrix* Linnaeus, 1758

***Meretrix desvauxi* (Coquand, 1862)**

### Pl.4. Figure 5a-d

1862 *Vénus desvauxi* sp. nov. Coquand, p. 194, pl. 8, Figure 1-2.

1962 *Meretrix desvauxi* (Coquand) : Abbass, p. 145, pl. 23, Figure 2.

2014 *Meretrix desvauxi* (Coquand) : Ayoub : Hannaa et al., p. 123, pl. 12, Figure 2a-b.

2018 *Meretrix desvauxi* (Coquand) : Ghenim et al., p. 16, Figure 8H1, H2, 0.

2019 *Meretrix desvauxi* (Coquand) : Ghenim et al., p. 36, Figure 8 H1-2.

2021 *Meretrix desvauxi* (Coquand) : El : Sabagh et al., Figure 12F : G3b : i

**Material.** 2 complete specimens from the lower/upper part of the Coniacian Formation.

**Ecology:** facultative aragonitic infauna: mobile suspension: feeding.

**Occurrence:** Coniacian of Essen section

**Distribution:** Egypt and Algeria.

Order Cardiida Férussac, 1822

Suborder Cardiidina Férussac, 1822

Superfamily Veneroidea Rafinesque, 1815

Family Veneridae Rafinesque, 1815

Subfamily Venerinae Rafinesque, 1815

Genus *Aphrodina* Conrad, 1869

**Type species:** *Meretrix tippiana* Conrad, 1858

***Aphrodina dutruei* (Coquand, 1862)**

### Pl.4. Figure 6a-c

1862 *Vénus dutruei* Coquand, p. 193, Pl. 7, Figure 5 : 6.

1917 *Vénus dutruei* Coquand : Fourtau, p. 88.

1962 *Meretrix dutruei* (Coquand, 1862) : Abbas, p. 147, pl. 22, Figure 22.

1963 *Vénus dutruei* Coquand : Fawzi, p. 79.

## CHAPTER III SYSTEMATIC

2002 *Aphrodina (Aphrodina) dutrugei* (Coquand) : Berndt, p. 128, pl. 7, Figure 1 : 2.

2005 *Aphrodina dutrugei* (Coquand): Ahmad, p. 191, pl. 1, Figure 1 : 9.

2013 *Aphrodina dutrugei* (Coquand): Musavu Moussavou et al., p. 4, Figure 4 : 5, 6, 11, 13 : 15.

2015 *Aphrodina dutrugei* (Coquand): Musavu Moussavou, p. 319, pl. 4, Figure 1.

2016 *Aphrodina dutrugei* (Coquand): Benzaggagh, p. 24, Figure 18.

2019 *Aphrodina dutrugei* (Coquand): Hoşgör et Yilmaz, p. 424, Figure 3b : i

**Material:** 2 complete specimens from the upper part of the Coniacian Formation.

**Remarks:** The genus *Aphrodina* Conrad, 1869, family Veneridae Rafinesque, 1815, includes several species from the Cretaceous Tethysian, extending from the Cenomanian to the Santonian.

**Ecology:** facultative aragonite infauna: mobile suspension: feeder.

**Occurrence:** Coniacian of Essen section

**Distribution:** North Africa and Middle East and West Africa (see (Hoşgör and Yilmaz, 2019)

Superorder Cardiiformii Férussac, 1822.

Order Cardiida Férussac, 1822

Suborder Cardiidina Férussac, 1822.

Superfamily Cardioidea Lamarck, 1809.

Family Cardiidae Lamarck, 1809.

Subfamily Protocardiinae Keen, 1951

Genus Protocardia Beyrich, 1845

**Type species:** *Cardium hillanum* Sowerby (1814).

***Protocardia hillana* (J. Sowerby, 1813)**

### Pl. 5. Figure 1a-c

1813 *Cardium hillanum* sp. nov. J. Sowerby, p. 41, pl. 14.

1890 *Protocardia hillana* J. Sowerby: Thomas et Péron, dans Péron, p. 276.

1916 *Protocardia hillana* (J. Sowerby): Douvillé, p. 158, pl. 20, Figure 1–3.

1962 *Protocardia hillana* (J. Sowerby): Abbass, p. 123, pl. 21, Figure 1, 3, 13.

2006 *Protocardia hillana* (J. Sowerby): El Qot, p. 78, pl. 16, Figure 4–6.

2014 *Protocardia hillana* (J. Sowerby): Ayoub : Hannaa et al., p. 115, pl. 10, Figure 8, 9a-b.

2016 *Protocardia hillana* (J. Sowerby): Benzaggagh, p. 201, Figure 16 : C–I

2023 *Protocardia hillana* (J. Sowerby): Benmansour, p. 7, Figure 3c.

**Material:** A complete specimen from the lower part of the Coniacian Formation.

### CHAPTER III SYSTEMATIC

**Remarks:** Traces of concentric and radial ribs, but the umbo and posterodorsal margin are poorly preserved. The material present differs from the type species in being less swollen and more rounded in outline. *P. hillana* differs from *P. coquandi* Seguenza in being more inflated with a larger umbo (Sowerby, 1813). The specimen resembles *P. pauli* but differs in being less elongated and also less swollen.

**Ecology:** facultative aragonitic fauna: mobile suspension feeder.

**Occurrence:** Coniacian of Essen section

**Distribution:** it has been observed from the Aptian to the Maastrichtian in the strata of Africa (Algeria, Tunisia Morocco Cameroon, Gabo), Europe and Asia (India), in addition to Brazil (Riedel, 1933; Darteville and Freneix, 1957; Musavu Moussavou, 2015; (Jaitly and Mishra, 2009; (Thomas and Peron, 1890); (Lefranc à Bengtson, 1983; Seeling, 1999; Coquand, 1862 Andrade and Santos, 2011, Benzaggagh, 2016, Ghenim et al., 2021).

Order Arcida Gray, 1854

Family Cucullaeidae Stewart, 1930

Genus *Idonearca* Conrad, 1862

**Type Species:** *Cucullaea tippana* Conrad, 1858

***Idonearca thevestensis* (Coquand, 1862)**

#### Pl. 5. Figure 2a-d

1862 *Arca Tevesthensis* sp. nov Coquand: 212, pl. 15, figs. 9: 10.

1891 *Arca thevestensis* Coquand: Peron: 257.

1912 *Arca (Trigonarca?) thevestensis* Coquand: Pervinquière: 104, pl. 7, figs. 22, 27a, b.

1934 *Arca (Trigonarca?) thevestensis* Coquand: Blanckenhorn: 211.

2006 *Cucullaea (Idonearca) thevestensis* (Coquand): El Qot, p. 25 ; pl. 2, Figure 14–15 ; pl. 3, Figure 1.

2016 *Cucullaea (Idonearca) thevestensis* (Coquand): Benzaggagh, p. 189, figure 7d: g; figure 8a: c,

2017 *Cucullaea (Idonearca) thevestensis* Coquand: Abdelhady and Mohamed, figure 9a: c.

2021 *Cucullaea (Idonearca) thevestensis* Coquand: Mendir et al., figure 3c.

**Material:** 9 complete specimens and 6 incomplete from middle/Upper part of the coniacian formation.

**Remarks:** It differs from *I. diceras* Seguenza in having a less elongated shell and differ from *I. trigona* Seguenza by less inflated shell and less prominent umbones.

**Ecology:** Aragonitec infaunal facultative: mobile suspension-feeder.

**Occurrences :** Coniacian of Essen section

## CHAPTER III SYSTEMATIC

**Distribution:** Egypt, Algeria, Tunisia, Italy, and Syria.

### *Cucullaea (Idonearca) trigona* (Seguenza, 1882)

#### Pl. 5. Figure 3a-d

1882 *Arca trigona* Seguenza, p. 98, pl. 13, Figure 6, 6a.

1972 *Cucullaea (Idonearca) chouberti* Freneix, p. 96 ; pl. 2, Figure 1–4 ; pl. 3, figure 1a–b, 2.

2004 *Cucullaea (Idonearca) trigona* (Seguenza): Abdel–Gawad et al., pl. 5, figure 2a–b.

2006 *Cucullaea (Idonearca) trigona* (Seguenza): El Qot, p. 25, pl. 3, figure 2a–b.

2011 *Cucullaea (Idonearca) trigona* (Seguenza): Ayoub–Hannaa, p. 59, pl. 3, figure 7–8.

2013 *Cucullaea (Idonearca) trigona* (Seguenza): El Qot et al., p. 194, pl. 1, figure 3a–b.

2013 *Cucullaea (Idonearca) trigona* (Seguenza): Benzaggagh, p. 189, Figure 5D-E ; figure 6A-E.

2021 *Cucullaea (Idonearca) trigona* (Seguenza): Mendir et al., p. 4, figs. 3A-C.

2022 *Cucullaea (Idonearca) trigona* (Seguenza): Feriani et al., figure 12a.

**Material:** 9 complete specimens and 6 incomplete from middle/Upper part of the coniacian formation.

**Remarks:** it differs from *I. dicerias* Seguenza by being bigger (more inflated/elongated) and by having more prominent umbo.

**Ecology:** Aragonitec infaunal facultative: mobile suspension-feeder.

**Occurrences :** Coniacian of Essen section

**Distribution:** Algeria, Tunisia, Italy, and Sicily. It was also recorded from Libya (El Qot., and Abdulsamad, 2016). Albian: Santonian of North Africa (Pervinquièrre, 1912; El Qot et al., 2013; Benzaggagh, 2016).

### *Cucullaea (Idonearca) dicerias* Seguenza 1882

#### Pl. 5. Figure 4a-d

1882 *Arca dicerias* sp. nov.: Seguenza, p. 96, pl. 14, figure 1 a: b.

1912 *Arca (Trigonarca?) dicerias* Seguenza: Pervinquièrre, p. 102, pl. 7, figs. 23a: b, 25: 26.

1918 *Arca (Trigonarca) dicerias* Seguenza: Greco, p. 29 (211), pl. 3 (29), figs. 14: 15.

1937 *Arca (Trigonarca) dicerias* Seguenza: Trevisan, p. 48, pl. 2, figs. 12: 13.

1962 *Arca (Idonearca) dicerias* (Seguenza): Abbass: 23, pl. 2, figure 10.

2002 *Trigonarca dicerias* Seguenza: Abdel-Gawad and Gameil, p.81, pl. 1, figure 10.

2006 *Cucullaea (Idonearca) dicerias* (Seguenza): El Qot, p. 24, pl. 2, figs. 6: 8

2016 *Cucullaea (Idonearca) dicerias* (Seguenza, 1882) Benzaggagh, p. 189, figure 7AC.

### CHAPTER III SYSTEMATIC

**Material:** 11 complete specimens and 7 incomplete from middle/Upper part of the coniacian formation.

**Remarks:** This species was first recorded in Algeria, in the Monts des Sour and the Guir Basin.

**Ecology:** Aragonitec infaunal facultative: mobile suspension-feeder.

**Occurrences :** Middle/Upper Coniacian of Essen section

**Distribution:** Egypt, Algeria, Tunisia, Italy, and Sicily.

Genus *Oscillopha* Malchus 1990

*Oscillopha dichotoma* (Bayle, 1849)

#### Pl. 6-7. Figure 1-3a-c, 7-8a-b

1849 *Ostrea dichotoma* sp. nov. Bayle: 365, pl. 18, figs. 17: 18.

1912 *Alectryonia dichotoma* Bayle, Pervinquière: 206, pl. 14, figs. 19: 21.

1917 *Ostrea dichotoma* Bayle, Fourtau, 35, pl. 5, Figure 8.

1917 *Alectryonia dichotoma* Bayle, Greco, 144 (164).

1962 *Lopha dichotoma* Bayle, Abbass: 81, pl. 11, figure 2.

1987 *Oscillopha (Actinostreon) dichotoma* Bayle, Kora and Hamama, pl. 1, figure 5.

1990 *Oscillopha dichotoma* Bayle, Malchus, 103, pl. 1, figs. 5: 9.

2008 *Oscillopha dichotoma* Bayle, El Sabbagh, pl. 11, figure 3/3–6.

2019 *Oscillopha dichotoma* Bayle, Nagm and Boualem, p. 200, figure 4B.

2020 *Oscillopha dichotoma* Bayle, 1849, Hashmie et al., figure 7d. 2023

2023 *Oscillopha dichotoma* Bayle, 1849, Abdelhady et al., figure 8k and l

**Material:** 8 complete specimens and 33 incomplete from Upper part of the coniacian formation.

**Remark:** it has dense ribs, which are uniformly distributed. It differs from *Lopha siphax* by median-position ligament and by transverse muscle scars positioned near the median line Freneix (1972). Furthermore, Mendir et al., (2021) indicated that the stratigraphic range of *O. dichotoma* is much younger (Coniacian–Campanian).

**Ecology:** low-Mg calcite marine to brackish stationary attached epifaunal suspension-feeder.

**Occurrences :** Coniacian of Essen section

**Distribution:** Coniacian- Santonian of Egypt, Tunisia, Algeria, Iran and Madagascar (Pervinquière 1912; Malchus 1990; Dhondt et al., 1999; Nagm and Boualem 2019).

## CHAPTER III SYSTEMATIC

Order Ostreida Férussac 1822

Family: *Gryphaeidae* Vialov 1936

Subfamily *Pycnodonteinae* Stenzel 1959

Genus *Pycnodonte* Fischer de Waldheim 1835

**Type species:** *Pycnodonte radiata* Fischer von Waldheim, 1835

Subgenus *Phygraea* Vialov 1936

***Pycnodonte (Phygraea) vesicularis vesicularis* Lamarck 1806**

### Pl. 6. Figure 5-6a-c

1806 *Ostrea vesicularis* Lamarck: p. 160.

1913 *Ostrea vesicularis* Lamarck: Woods: p. 360, pl. 55, figs. 4: 9.

1918 *Pycnodonta vesicularis* Lamarck: Greco: p. 110 (130), pl. 13 (12), figs. 1: 5.

1977 *Pycnodonte (Phygraea) vesicularis* (Lamarck): Pugaczewska: p. 191, pl. 13, figs. 1–3.

1990 *Pycondonte (Phygraea) vesiculosum* (Sowerby, 1823): Malchus, p. 145, pl. 2, figs. 2–7).

2002 *Pycondonte (Phygraea) vesiculosum* (Sowerby, 1823): Zakhera and Kassab, pl. 2, Figure 5.

2019 *Pycnodonte (Phygraea) vesicularis vesicularis* (Lamarck): Hewiedy et al.: p. 14, figs. e2

**Material:** 2 complete specimens and 7 incomplete from Lower part of the coniacian formation.

**Remarks:** *P. vesicularis* (Lamarck) differs from *P. vesiculosa* (J. de C. Sowerby) in having larger thicker shell and more incurved and less pointed umbo (Wilmsen and Voigt, 2006; El Qot, 2006; Ayoub-Hannaa et al., 2014).

**Ecology:** low-Mg calcitemarine to brackish stationary attached epifaunal suspension-feeder.

**Occurrences :** Coniacian

**Distribution:** a very widespread Cretaceous oyster, being recorded from the Cenomanian: Santonian sediments of Europe, Africa, Middle East, Jordan, Libya, and Egypt, India, and Brazil and it may extend from the Aptian to the Maastrichtian (Stoliczka, 1871 ; Moroni and Ricco, 1968 ; Seeling and Bengtson, 1999 ; Abdel: Gawad, 1995 ; Malchus, 1990; Hewiady et al., 2012 ; Freneix, 1972 ; Aqrabawi, 1993 Dhondt, 1984)

Family *Gryphaeidae* Vialov, 1936

Subfamily *Exogyrinae* Vialov, 1936

Genus *Amphidonte* Fischer de Waldheim, 1829

**Type species:** *Exogyra costata* Say, 1820

***Amphidonte conica* (Sowerby, 1813)**

## CHAPTER III SYSTEMATIC

### Pl. 6. Figure 4-7a-b

1813 *Chama conica* J. de C. Sowerby, p. 69, pl. 26, figure 3.

1869 *Ostrea conica* Sowerby–Coquand, p. 150, pl. 53, figs. 1–7.

1913 *Exogyra conica* (Sowerby) –Woods, p. 407, textfigs. 215–242.

2014 *Exogyra conica* Sowerby: Ayoub-Hannaa et al., p. 78, pl. 3, figs. 4–6.

2015 *Exogyra conica* Sowerby: Ahmad et al., p. 289, pl. 1C–D.

2018 *Exogyra conica* (Sowerby): Aouissi et al., p. 9, figure 4.4.

2014 *Exogyra conica* (Sowerby): Ayoub-Hannaa et al., p. 79, pl. 3, figs. 7 and 8

2016 *Amphidonte conica* (Sowerby): Benzaggagh, p. 192, figure 9-10

2021 *Exogyra conica* (Sowerby), Mandeir et al., p. 7, figure 4j.

2024 *Amphidonte conica* (Sowerby, Benzaggagh et al., figure 10a-b, figure 9A-f.

**Material:** 2 complete specimens from Upper part of the coniacian formation.

**Remarks:** it has afine concentric growth lines with chomata along the entire inner perimeter of the commissure.

**Ecology:** low-Mg calcite marine to brackish stationary attached epifaunal suspension-feeder.

**Occurrences :** Coniacian of Essen section

**Distribution:**Algeria, Egypt, Ethiopia, Jordan, Madagascar, Egypt, Mozambique, UK, Morocco, Algeria, Spain, Syria, Tunisia, New Zealand, Afghanistan, New Zealand (Amard et al., 1981; Boreham, 1959; Dhondt, 1982; Benzaggagh et al., 2024.

Order Pteroida Newell, 1965

Suborder Pteriina Newell, 1965

Superfamily Pectinacea Rafinesque, 1815

Family Plicatulidae Watson, 1930

Genus Plicatula Lamarck, 1801

**Type species:** *Spondylus plicatus* Linnaeus, 1764

***Plicatula ferryi* Coquand, 1862**

### Pl. 7. Figure 1-6a-b

1862 *Plicatula ferryi* Coquand, p. 221, pl. 16, figs 7–9.

1904 *Plicatula ferryi* Coquand; Fourtau, p. 313, pl. 3, figs 2, 3.

2001 *Plicatula ferryi* Coquand:El: Hedeny et al., p. 29, figure 3a–d

2013 *Plicatula ferryi* Coquand: El Qot et al., p. 210, pl. 3, figs. 9–11.

2014 *Plicatula ferryi* Coquand: Ayoub: Hannaa et al., p. 97, pl. 7, figs. 7–9.

### CHAPTER III SYSTEMATIC

2017 *Plicatula ferryi* Coquand: Musavu Moussavou, p. 4, figure 4K

2021 *Plicatula ferryi* Coquand: Mendir et al., figure 6h

**Material:** 13 complete specimens and 19 incomplete from Upper part of the Coniacian formation.

**Remark:** *Plicatula ferryi* similar in outline and ornamentation to *P. batnensis* (Coquand) (El Qot, 2006; El-Hedeny, 2001). It differs from *P. auressensis* in having larger shell with more radial ribs and having.

**Occurrences :** Coniacian of Essen section

**Distribution :** Coniacian–Santonian species in North Africa and the Middle East (Egypt and Algeria,). It was also recorded from other African countries (e.g., Nigeria Congo, Cameroon) and also recorded from New Mexico (Barber, 1958; Moussavou, 2017; Darteville and Freneix, 1957; Dhondt, 1992; El-Hedeny, 2001).

Order Veneroida Adams & Adams, 1856

Family Arctidae Newton, 1891

Genus Arctica Schumacher, 1817

*Arctica cordata* (Sharpe 1850)

#### Pl.8, Figure 1a-d

1850 *Cyprina cordata* Sharpe. p. 182, pl. 15, figure 2.

2006 *Arctica cordata* (Sharpe) – El Qot: p. 81, pl. 16, figs. 10, 11.

2014 *Arctica cordata* (Sharpe) – Hewaidy et al., p. 225, pl. 3, figure 1.

2019 *Arctica cordata* (Sharpe) – Ayoub-Hannaa et al., p. 185, pl. 6, figs. L–M; pl. 7, figure A

2022 *Arctica cordata* Sharpe- Aouissi et al; p264. figure 6, F1-3

**Material:** 5 complete specimens from Santonian Formation

**Description:** The specimens described are medium-sized, oval in shape and longer than they are tall. They are equivalent, moderately swollen, unequilateral and enlarged towards the rear. The umbels are wide, curved and spaced. The lunula is both wide and deep. The hinge line is long and straight, marked by a sinuous line visible in the internal moulds. The anterior edge is very convex, while the posterior edge is rounded. The ventral margin is also long and well rounded. The surface of the specimens studied shows deep muscular and mantle scars, with no trace of ornamentation.

**Occurrence:** Santonian of Essen section

## CHAPTER III SYSTEMATIC

**Distribution:** *Arctica cordata* is reported from the Cenomanian of Portugal (Sharpe, 1850) and Egypt (El Qot, 2006; Hewaidy et al., 2014), and from the Upper Turonian of Brazil (Ayoub-Hannaa et al., 2019).

Family Nuculanidae Adams & Adams, 1858

Genus *Nuculana* Link, 1807

Subgenus *Nuculana* Link, 1807

***Nuculana cf. mariae* (D'Orbigny, 1844)**

**Pl.8, Figure 2a-d**

cf. 1844 *Nucula mariae* sp. nov. – D'Orbigny: 169, pl. 301, figs.4-6.

cf. 1899 *Nuculana mariae* (D'Orbigny) – Woods: 6, pl.1, figs.25-27

2006 *Nuculana cf. mariae* D'Orbigny-El Qot; p 19 .pl.1, figure3-4

**Material:** 8 complete specimens from Santonian Formation

**Description:** The specimens are small, oval-shaped, slightly swollen, with equivalent valves, unequilateral, rounded at the front and pointed at the rear. The umbilicus is pointed and directed backwards. The ventral edge is clearly curved. These are internal moulds with no trace of ornamentation.

**Occurrence:** Santonian of Essen section

**Distribution:** Cenomanian of Egypt (El Qot, 2006)

***Rostrocardia papieri* (Coquand, 1862)**

**Pl.8, Figure 3a-e**

1880 *Isocardia papieri* sp. nov – COQUAND: 114, pl. 4.

1912 *Anisocardia papieri* COQUAND – PERVINQUIÈRE: 235, pl.17, figs. 20-22.

1918 *Anisocardia papieri* COQUAND – GRECO: 46 (228), pl. 5(21), figure 3.

1937 *Anisocardia cf. papieri* COQUAND – TREVISAN: 91, pl. 4, figure 1.

1963 *Anisocardia papieri* COQUAND – FAWZI: 59.

1972 *Rostrocardia papieri* (COQUAND) – FRENEIX: 174, pl. 18, figs. 6-8; text-figs. 43A-B.

1981 *Anisocardia papieri* (COQUAND) – AMARD et al.,: 79, pl.6, figure 4.

2006 *Rostro cardiapapieri* (Coquand) -El Qot; p 67, pl.13, figure9-10

**Description:** Small, oval, moderately swollen specimens, equivalent, unequilateral, rounded anteriorly and pointed posteriorly. Um bones pointed, opisthogyrate. Um bones pointed, opisthogyrate. Ventral margin considerably curved. The specimen consists of internal moulds that show no trace of ornamentation.

**Occurrence:** Santonian of Essen section

**Distribution:** Cenomanian of Egypt (El Qot, 2006)

## CHAPTER III SYSTEMATIC

Family Astartidae D'Orbigny, 1844

Subfamily Astartinae D'Orbigny, 1844

Genus *Astarte* J. Sowerby, 1816

***Astare gigantea* deshayes, 1842**

### **Pl. 8, Figure 4a-c**

1842 *Astarte gigantea* sp. nov. – Deshayes in Leymerie: 5, pl.4, figure 3.

1846 *Astarte gigantea* deshayes – D'Orbigny: 58, pl. 258, figs. 1-6.

1962 *Astarte (Tridonta) gigantea* (Deshayes) – Abbass: 103, pl. 16, figs. 8, 10-12, 15a

2006 *Astare gigantea* deshayes- El Qot ; p 75.Pl.15 ; fig 9

**Description:** The shell is small, subtriangular, moderately swollen, equivalent and inequilateral. The beaks are prominent, proso-gyrate, positioned at the front and slightly curved. The lunula is deep, oval and tapers downwards. The anterior-dorsal margin is concave below the umbo, while the posterior-dorsal margin is straight to slightly convex. Both the anterior and posterior margins are rounded and convex. The ventral margin is broadly rounded. The ornamentation consists of strong commarginal ribs, separated by concave intervals of equal or slightly lesser width.

**Occurrence:** Santonian of Essen section

**Distribution:** Campanian of Egypt (El Qot, 2006)

***Plicatula fourneli* (Coquand, 1862)**

### **Pl. 9, Figure 1**

1862 *Plicatula fourneli* sp. nov. – Coquand: 220, pl. 16, figs.5-6.

1904 *Plicatula fourneli* Coquand – Fourtau: 311.

1912 *Plicatula fourneli* Coquand – Pervinquierie: 153, pl. 10, figs. 2-6.

1917 *Plicatula fourneli* Coquand – Fourtau: 22.

1918 *Plicatula fourneli* Coquand – Greco: 21 (203).

1934 *Plicatula fourneli* Coquand – Blancken Horn: 193.

1937 *Plicatula fourneli* Coquand – Trevisan: 62, pl. 3, figure 11a-c.

1962 *Plicatula fourneli* Coquand – Abbass: 59, pl. 7, figure 15.

1972 *Plicatula fourneli* Coquand – Freneix: 83, pl. 4, figure 11.

1996 *Plicatula fourneli* Coquand – EL-Mahallawy: 87, pl. 2, figure 5.

2002 *Plicatula fourneli* Coquand – Abdel-Gawad & GAMEIL: 84, pl. 1, figure 21.

2006 *Plicatula fourneli* Coquand-El Qot ; p61. pl.12 ; fig 11-13

**Description:** The small to medium-sized shell is pear-shaped and generally taller than it is long. It is inequivalent and inequilateral, with a concave anterior margin and a convex

## CHAPTER III SYSTEMATIC

posterior margin. The dorsal valve is less convex than the ventral valve. The ornamentation consists of fine tuberculated radial ribs, separated by intervals three to five times wider than the ribs, these intervals being occupied by three to five secondary radial ribs crossed by commarginal threads.

**Occurrence:** Santonian of Essen section

**Distribution:** Upper Cenomanian of Egypt (El Qot, 2006)

**Genus** *Plagiostoma* J. Sowerby, 1814

*Plagiostoma subsimplex* (Thomas & Peron 1891)

### Pl. 9, Figure 2a-b

1891 *Lima subsimplex* sp. nov. – Thomas & Peron in Peron:219, pl. 27, figs. 7-10.

1912 *Lima (Plagiostoma) subsimplex* Thomas & Peron –Pervinquière: 148

2006 *Plagiostoma subsimplex* thomas & peron - El Qot; p33. pl.5; fig 1-2

**Description:** The present material shows great similarity to *Lima subsimplex* Thomas & Peron in form and ornamentation. This species was originally described from the Turonian and Santonian in Tunisia. Of the two specimens available, one shows ornamentation similar to that of the specimen from the Santonian of Tunisia illustrated by Peron (1891: pl. 27, Figure 7), with spiny radial ribs on the anterior and posterior sides, while the rest of the shell is mainly covered with commarginal growth lines, except near the umbo where radial ribs are present. The second specimen appears to be similar to those described by Thomas & Peron from the Turonian (Peron 1891: pl. 27, figs. 8-10), with a surface entirely covered by radial ribs, more spiny on the anterior and posterior parts. Pervinquier (1912) noted that this species is common in Tunisia from the Lower Turonian to the Lower Senonian (Coniacian). This mention in Egypt is a first.

**Occurrence:** Santonian of Essen section

**Distribution:** Algeria and Tunisia, where it is reported in the Coniacian and Santonian formations (Thomas & Peron, 1891; Kazi-Tani, 1970; Ben Mansour, 2009).

***Granocardium desvauxi* coquand 1862**

### Pl. 9, Figure 3

1862 *Cardium desvauxi* sp. nov. Coquand, p. 206, pl. 11, figs. 3-4.

1912 *Cardium (Trachycardium) desvauxi* Coquand – Perivinquière, p. 260.

1962 *Granocardium hassani* sp. nov. Abbass, p. 122, pl. 20, figs. 2-3.

2011 *Granocardium (Granocardium) desvauxi* Coquand – Ayoub-Hannaa, p. 131, pl. 12, Figure 4.

## CHAPTER III SYSTEMATIC

2014 *Granocardium (Granocardium) desvauxi* Coquand – Ayoub-Hannaa & Fürsich, p. 114, pl. 10, Figure 4

2018 *Granocardium desvauxi* coquand -Aouissi et al ; p15. fig5 (10)

**Description:** The shell is triangular, swollen and almost unequilateral. It has a short, excavated buccal side and a very oblique, outwardly keeled anal side. A curved hook is present. No ornamentation is visible.

**Occurrence:** Santonian of Essen section

**Distribution:** Cenomanian of Algeria (Benyoucef et al., 2012), Tunisia (Pervinquière, 1912), and Egypt (Abbass, 1962; Ayoub-Hannaa, 2011; Ayoub-Hannaa & Fürsich, 2014); Cenomanian of Batna (Aouissi et al., 2018).

**Inocerames :**

Superorder Eupteriomorphia Boss, 1982

Order Pterioda Newell, 1965

Family Inoceramidae Giebel, 1852

Genus Inoceramus J. Sowerby, 1814

**Type species:** *Inoceramus cuvierii* J. Sowerby, 1814.

***Inoceramus pictus?* J. de C. Sowerby**

**Pl. 5. Figure 5a-c**

1829 *Inoceramus pictus* sp. nov.: J. de C. Sowerby: 215, pl. 604, figure 1. cf.

1910 *Inoceramus* cf. *pictus* Sowerby: Woods: 279, pl. 49, figs. 5: 6; text: figure 36.

1982 *Inoceramus pictus* Sowerby: Keller: 64

2006 *Inoceramus* cf. *Inoceramus pictus* J. de C. Sowerby, El Qot, p. 26, pl. 3, figs. 3: 5.

2011 *Inoceramus* cf. *Inoceramus pictus* J. de C. Sowerby: Nagm et al., p. 96, figure 4a.

**Material:** 3 complete specimens from Upper part of the Coniacian formation.

**Remarks:** Medium: sized to large, equivalve to moderately inequivalve, ovate, trapeziform or suborbicular; posterior wing variably developed; ligamental area concave transversely. But *umbo is not prominent and shell width exceeds height*

**Ecology:** Aragonitic infaunal facultative: mobile suspension-feeder.

**Occurrences :** Coniacian of Essen section

**Distribution:** Egypt.

Genus : *Platyceramus* Pervinquière 1912

**Type species:** *Platyceramus siccensis* Seitz (1961)

## CHAPTER III SYSTEMATIC

### *Platyceramus siccensis* Pervinquière 1912

#### Pl. 10. Figure 1a-c

1912 *Inoceramus siccensis* Pervinquière; Pervinquière, p. 116- 117, pl. 8, figure 2 ,3 et 4.

1951 *Inoceramus cycloides* Wegner (*I. siccensis* Pervinquière), S6, t.1, pl. 1a.

2009 *Inoceramus siccensis* El Manai, p. 136. pl.6, figure 1, 2

**Material:** 1 complete specimen from the lower part of the Santonian section of Boukezez.

**Description:** A relatively large species characterized by a rounded, oval, or somewhat subquadrate shell outline. The valves appear nearly equivalent, though slightly unequilateral. The beak is small, rounded, and positioned anteriorly, not extending above the cardinal line. The shell is generally flat, exhibiting noticeable anterodorsal inflation. Its anterior, posterior, and ventral margins are smoothly rounded. The posterior wing is only mildly developed. In adult specimens, the shell becomes increasingly irregular, with growth lines that are more widely spaced and follow a rounded, subquadrate trajectory.

**Remarks:** In 1912, Pervinquière created the species *Inoceramus siccensis* to designate specimens with a subcircular outline, a shell that is not very swollen or even flat, a rounded anterior margin and concentric ornamentation that is rounded and not very prominent. In 1951, Voûte figured *Inoceramus cycloides* Wegner (*Inoceramus siccensis* Pervinquière) from the Middle Santonian of the Chebka des Sellaoua. This species was attributed by Dhondt (in Robaszynski et al, 1998) to *Platyceramus ahnesensis*, due to its regular and close costulation. In 1961, Seitz considered that the species *Inoceramus siccensis* as figured by Pervinquière represented at least three taxa, two of which were subspecies of *Platyceramus cycloides* (*Platyceramus cycloides* subsp. indet., pl. 8, Figure 2 and *Platyceramus cycloides* cf. *vanuxemiformis*, pl. 8, Figure 4) and one of which corresponded to the species *Platyceramus siccensis* in the strict sense. The latter has also been designated as the lectotype by Seitz.

The forms described in this work are related to *Platyceramus siccensis* s.s. *Platyceramus cycloides* sens large differs from our material in having a straight to slightly curved anterior margin and concentric ribs that are flattened and less prominent along the growth axis, compared with the anterior and posterior margins.

*Platyceramus cycloides* cf. *vanuxemiformis* differs from our specimens in that its costulation is more regular and closer together.

In addition, the species *Platyceramus siccensis* is restricted to the Lower Santonian, whereas *Platyceramus cycloides* s. l. is known from the Santonian to the Lower Campanian and *Platyceramus cycloides* cf. *vanuxemiformis* occurs throughout the Santonian.

## CHAPTER III SYSTEMATIC

**Ecology:** Aragonitic infaunal facultative: mobile suspension-feeder.

**Occurrences:** Coniacian of Boukezez section

**Distribution:** This species was reported in the Coniacian-Santonian interval in the Nementchas (Alérie) by Vivière (1985). It was recorded in the upper Turonian of Dyr el Kef (Tunisia) by Pervinquière (1912). In Algeria, it is known from the Coniacian-Santonian boundary at El Kantara (Aurès). It has also been cited in the same period in Constantinois and the Monts du Mellegue (Dubourdieu, 1956; Van der Fliert, 1955 and Voûte, 1967).

**Gastropods :**

*Volutomorpha* sp.,

**Pl. 11. Figure 1a-c**

**Material:** Two incomplete specimens from the middle part of the Coniacian Formation (C145)

**Remarks:** the material resembles *Volutomorpha baylei* (Coquand, 1862), which cannot be confirmed due to the incompleteness of specimens (spire length, body whorl, and aperture shape).

**Ecology :** Aragonitic mobile epifaunal carnivore

**Occurrences:** Coniacian of Essen section

Family Gyrodidae

Genus *Gyrodes*

**Species *Gyrodes* sp.,**

**Pl. 11. Figure 2a-b**

**Material:** One complete specimen from the middle part of the Coniacian Formation (C155)

**Remarks:** This specimen is very close to *Gyrodes edura* (Stoliczka, 1867) but differs in having a wider body whorl and a shorter spire that consists of four shouldered whorls. The whorls are smooth, evenly convex; last whorl slightly pointed apically. Aperture semilunar.

**Ecology:** Aragonitic infaunal carnivore.

**Occurrences :** Coniacian of Essen section

*Leptomaria* sp.,

**Pl. 11. Figure 3a-b**

**Material:** One complete specimen from the upper part of the Coniacian Formation (C170)

**Remarks:** Our specimen has a broadly conical shell with strongly convex whorls and a flush to slightly concave, midwhorl-situated selenizone. No ornamentation is preserved.

## CHAPTER III SYSTEMATIC

**Ecology:** Aragonitic epifaunal grazer.

**Occurrences :** Coniacian of Essen section

Superfamily Strombidea Rafinesque, 1815.

Family Aporrhaidae Gray, 1850.

Subfamily Aporrhainae Gray, 1850.

Genus Aporrhais Da Costa, 1778

*Aporrhaisourneli* (Coquand, 1862)

### Pl.11. Figure 4a-c

1862 *Pteroceraourneli* sp. nov. Coquand, p. 184, pl. 5, Figure 7.

2000 *Aporrhaisourneli* (Coquand), Abdel-Gawad, p. 1519, pl. 2, Figure 4.

2002 *Aporrhaisourneli* (Coquand), Zakhera, p. 318, Figure 6 (14–16).

2006 *Aporrhaisourneli* (Coquand, 1862), El Qot, p. 100, pl. 20, Figure 9a–b.

2023 *Aporrhaisourneli* (Coquand, 1862), Abdelhady et al., p. 6, Figure 8r.

**Description:** internal mould of a medium-sized gastropod, fusiform, with a moderately high spire. Conical whorl made up of 2 to 4 superimposed convex whorls, separated by moderately deep sutures. The body whorl is large, representing two thirds of the total height of the specimen. The aperture is narrow and long. The outer lip is broken. The ornamentation is not preserved.

**Remarks :** The Aporrhainae include numerous genera, for example Aporrhais Da Costa, 1778, Monocuphus Piette, 1876, and Dicroloma Gabb, 1868, which are easily distinguished by the morphology of their whorl and labellum (Ayoub-Hannaa and Fürsich, 2011). Precise identification of the specimens present is difficult due to the absence of certain diagnostic features such as the adapical and abapical sinuses and ornamentation.

**Occurrence:** Santonian of Essen section and Boukezez section

**Distribution:** Upper Santonian of Egypt (Abdelhadyet al., 2023); Algeria, Tunisia, Madagascar, and Nigeria (see Albanesi and Busson, 1974).

## CHAPTER III SYSTEMATIC

**Legende :** — 1cm

**Plate Ammonite : Plate 1 : 1-3a-c :** *Hemitissotia morreni* (Coquand, 1862).

**Plates Echinoids: Plate 2 : 1-2 :** *Mecasterourneli* (Deshayes, in Agassiz and Desor 1847).  
**3 :** *Mecaster turonensis* (Fourtau, 1921).

**Plate 3 : 1 :** *Mecaster* sp. var *batnensis* (Coquand, 1862). **2, 4, 5 :** *Mecasterourneli* (Deshayes, in Agassiz and Desor 1847). **3 :** *Mecaster texanus* (Roemer, 1849).

**Plates Bivalves: Plate 4 : 1 :** *Agelasina plenodonta* Riedel (1933). **2 :** *Paraesa faba* (J. de C. Sowerby, 1827). **3 :** *Phalodomya* sp. **4 :** *Arctica picteti* (Coquand, 1862). **5 :** *Meretrix desvauxi* (Coquand, 1862). **6 :** *Aphrodina dutrugei* (Coquand, 1862).

**Plate 5 : 1 :** *Protocardia hillana* (J. Sowerby, 1813), traces of concentric and radial ribs but umbo and posterodorsal margin is badly preserved. **2 :** *Cucullaea (Idonearca) thevestensis* (Coquand, 1862). **3 :** *Cucullaea (Idonearca) trigona* (Seguenza, 1882). **4 :** *Cucullaea (Idonearca) diceras* (Seguenza, 1882). **5 :** Heterodont indet., may be *Inoceramus* but umbo is not prominent, and shell width exceeds height.

**Plate 6 : 1-3 :** *Oscillopha dichotoma* (Bayle, 1849).

**Plate 7 : 1-3 :** *Oscillopha dichotoma* (Bayle, 1849). **5-6 :** *Pycnodonte (Phygraea) vesicularis vesicularis* (Lamarck, 1806). **4, 7 :** *Amphidonte conica* (Sowerby, 1813).

**Plate 8 : 1-6 :** *Plicatula ferryi* (Coquand, 1862). **7-8 :** *Oscillopha dichotoma* (Bayle, 1849).

**Plate 9 : 1a-d :** *Arctica cordata*; **2a-b :** *Nuculana cf. mariae* (D'Orbigny, 1844); **3a-b :** *Rostrocardia papieri* (Coquand, 1862); **4a-b :** *Astare gigantea* Deshayes, 1842; **5a-b :** *Plicatula fourneli* (Coquand, 1862); **6a-b :** *Plagiostoma subsimplex* (Thomas & Peron 1891); **7a-b :** *Plicatula ferryi* Coquand 1862; **8a-b :** *Granocardium desvauxi* Coquand 1862;

**Plate Inocerame: Plate 10 : 1a-c :** *Platyceramus siccaensis* Pervinquier 1912.

**Plate Gasteropods: Plate 11: 1 :** *Volutomorpha* sp., **2 :** *Gyrodes* sp., **3 :** *Leptomaria* sp., **4a-c :** *Aporrhaisourneli* (Coquand, 1862)

CHAPTER III SYSTEMATIC

1a



1b



1c



2a



2b



2c



3a



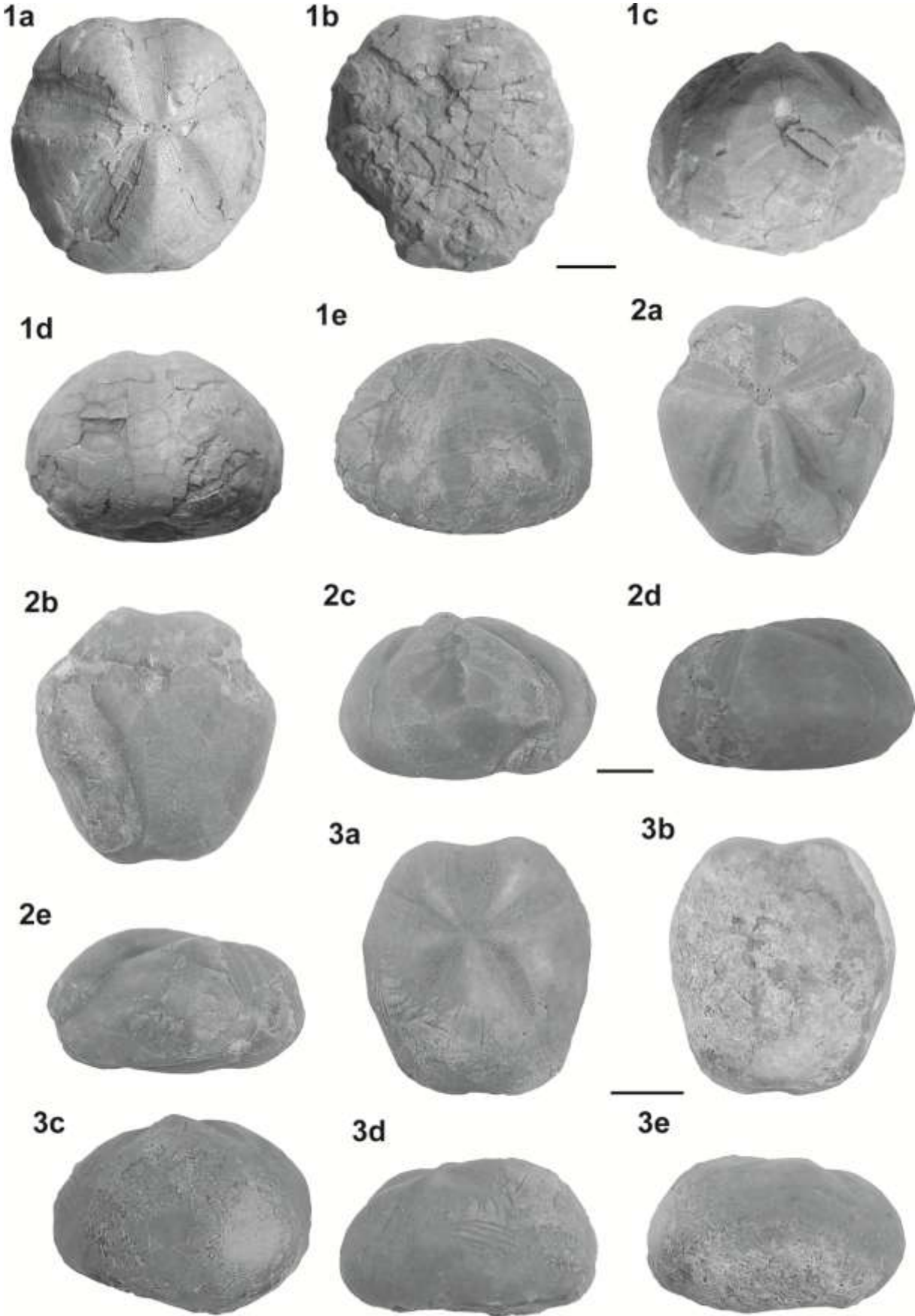
3b



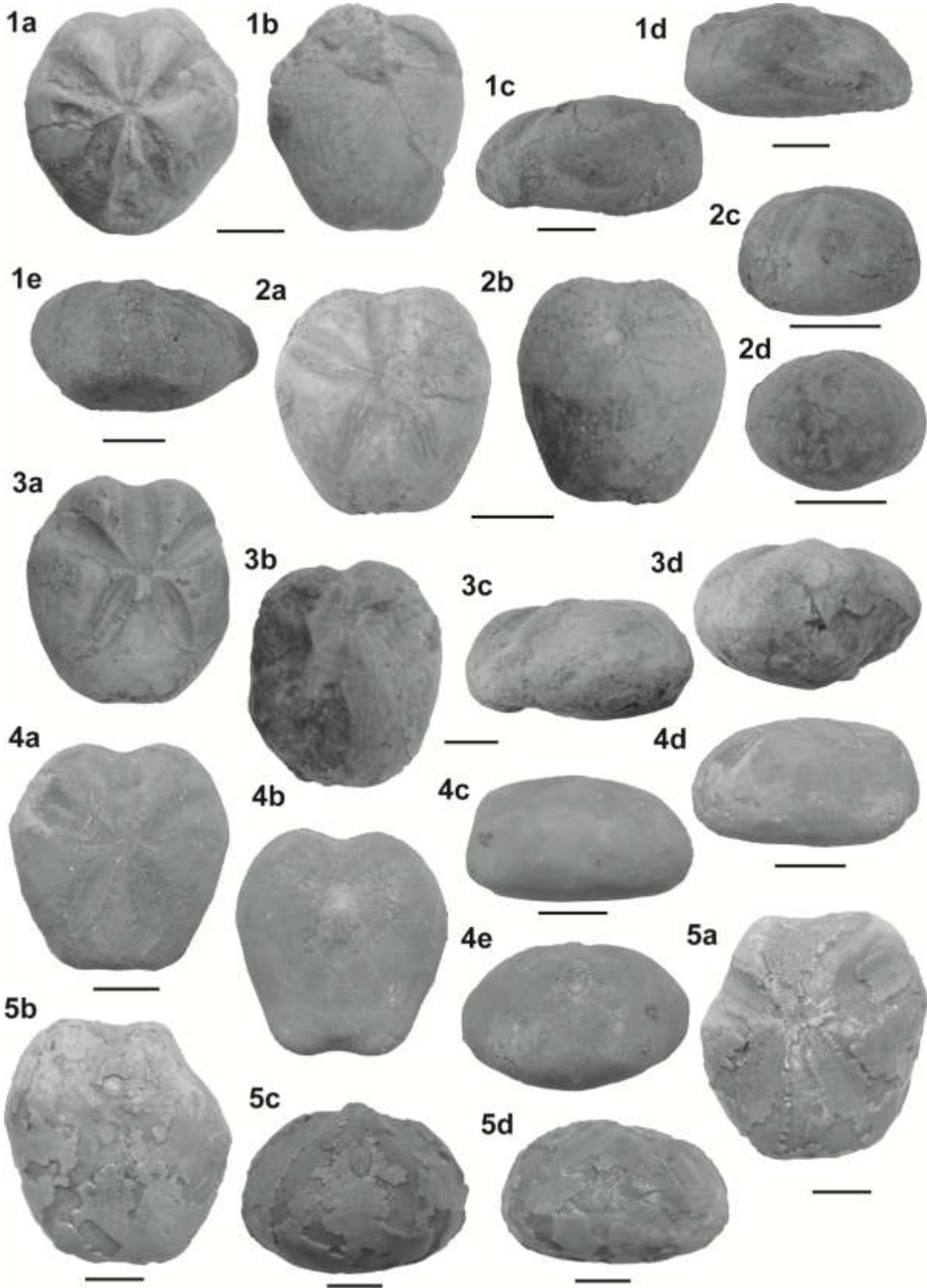
3c



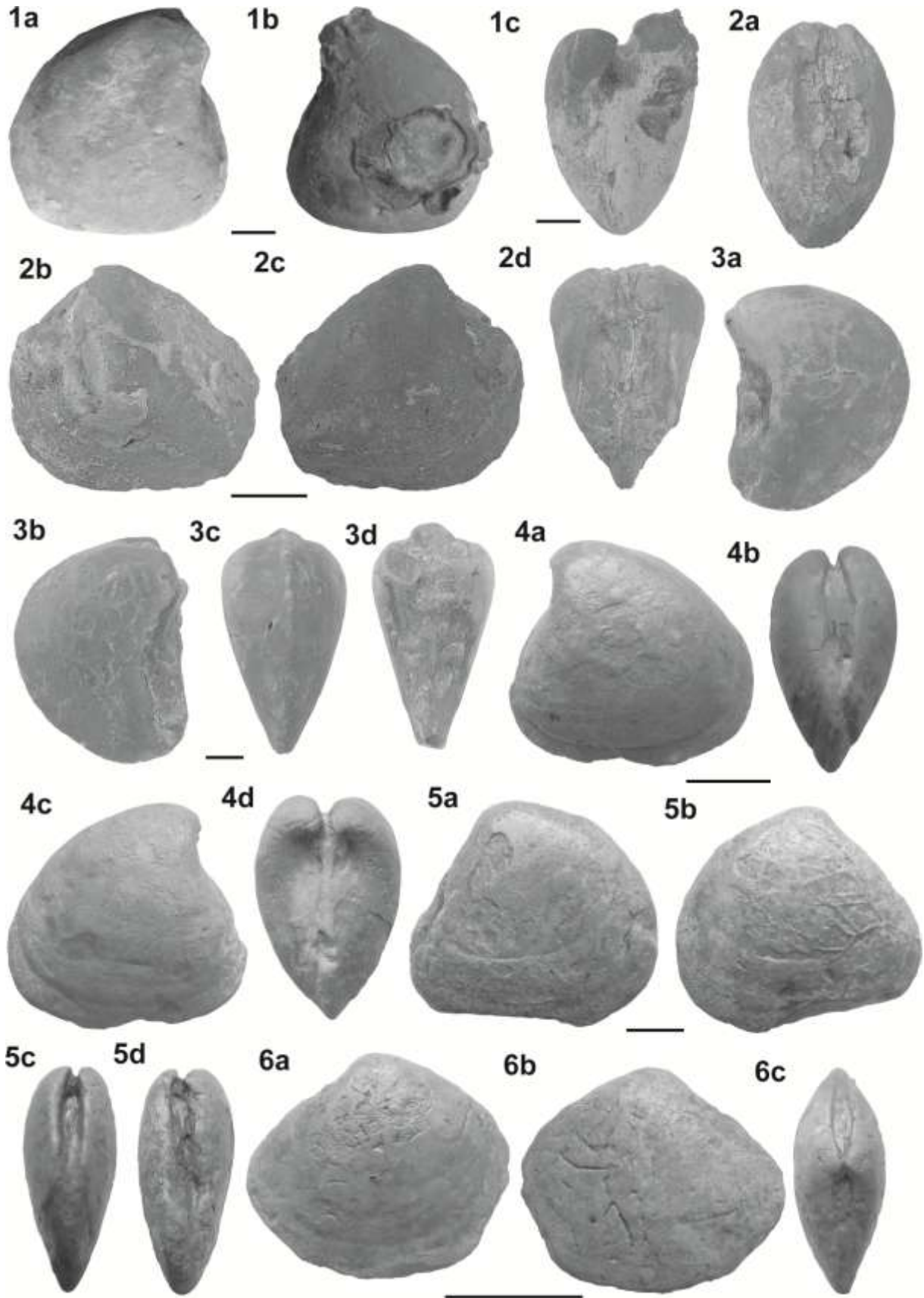
CHAPTER III SYSTEMATIC



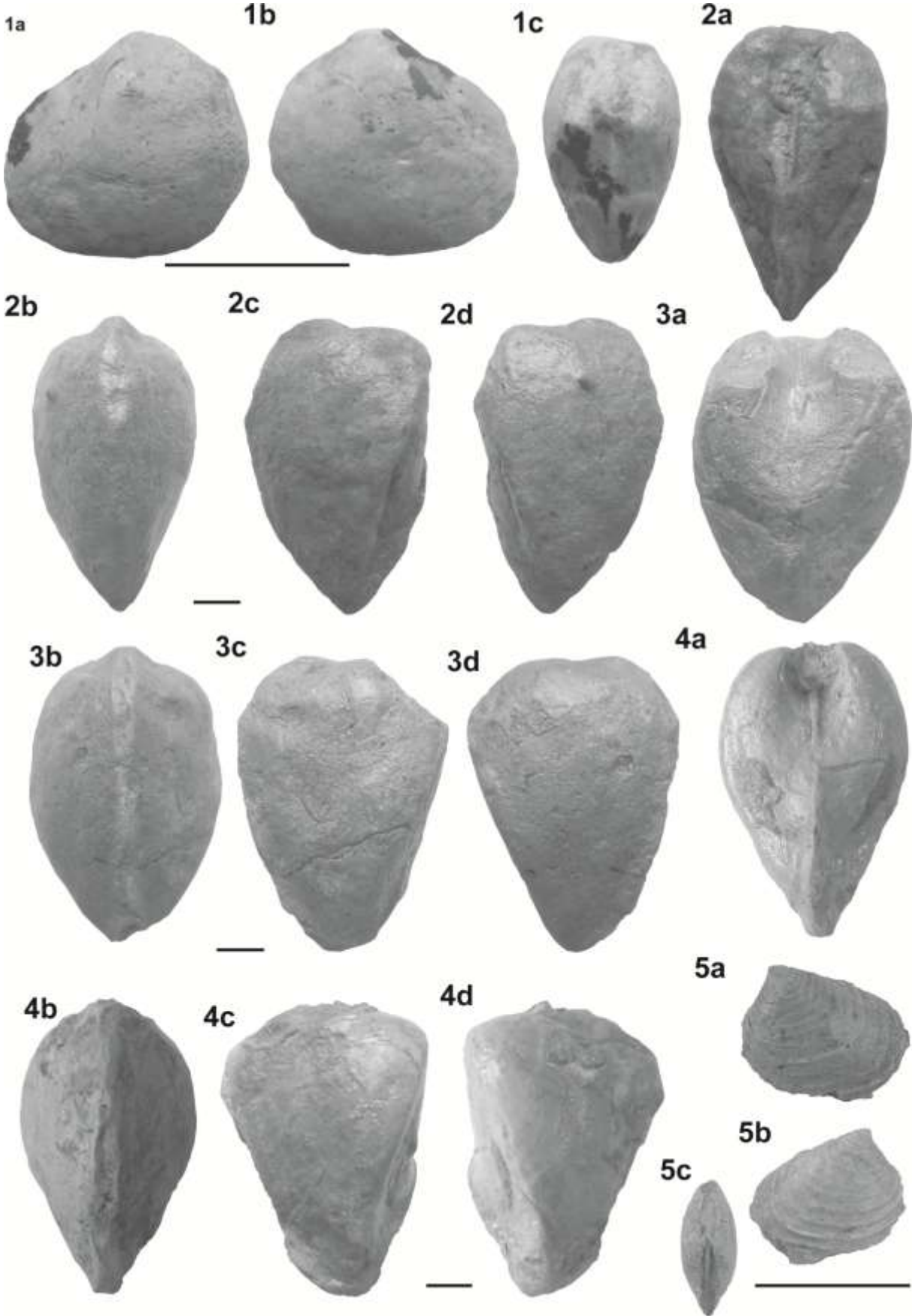
CHAPTER III SYSTEMATIC



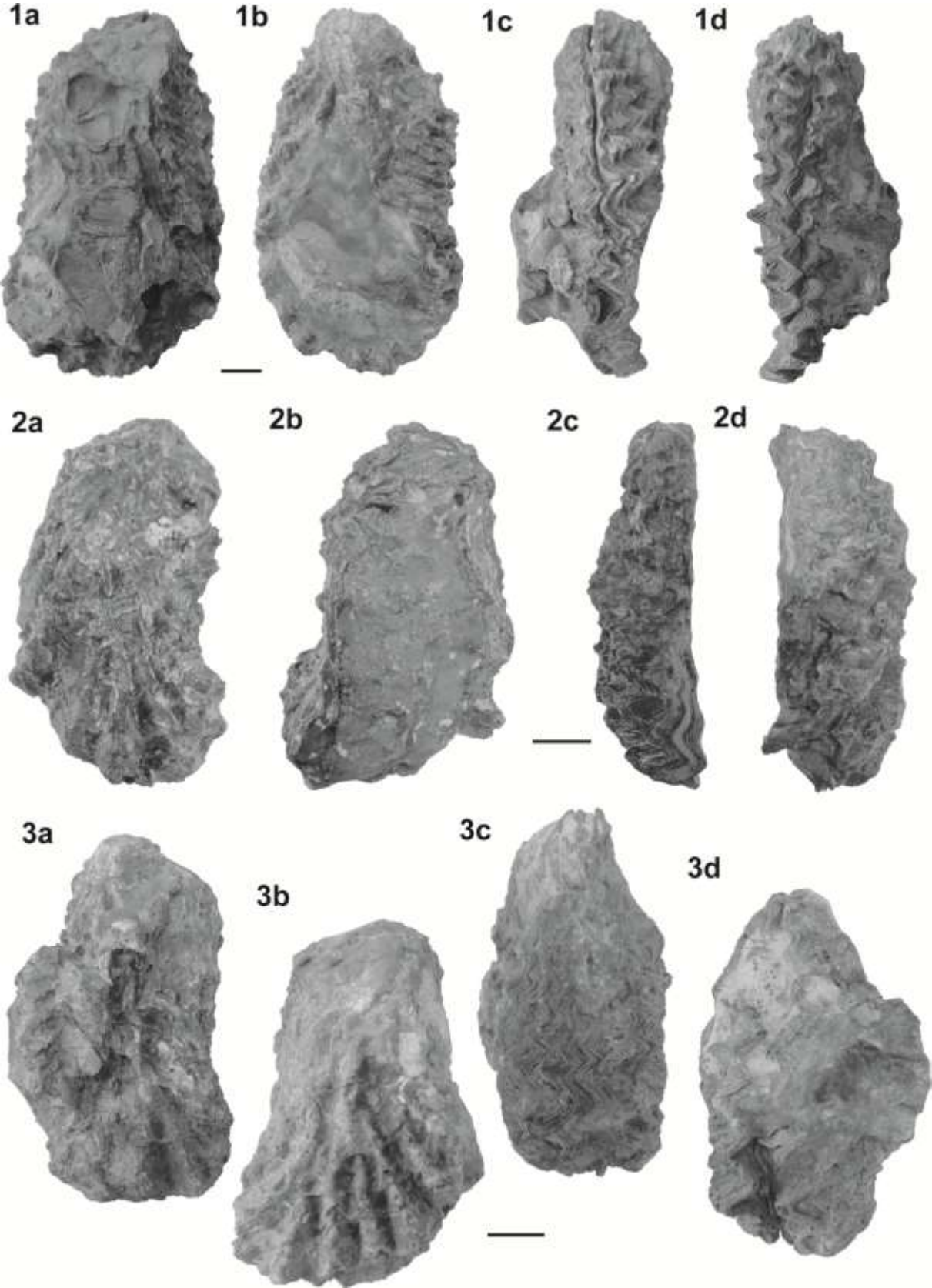
CHAPTER III SYSTEMATIC



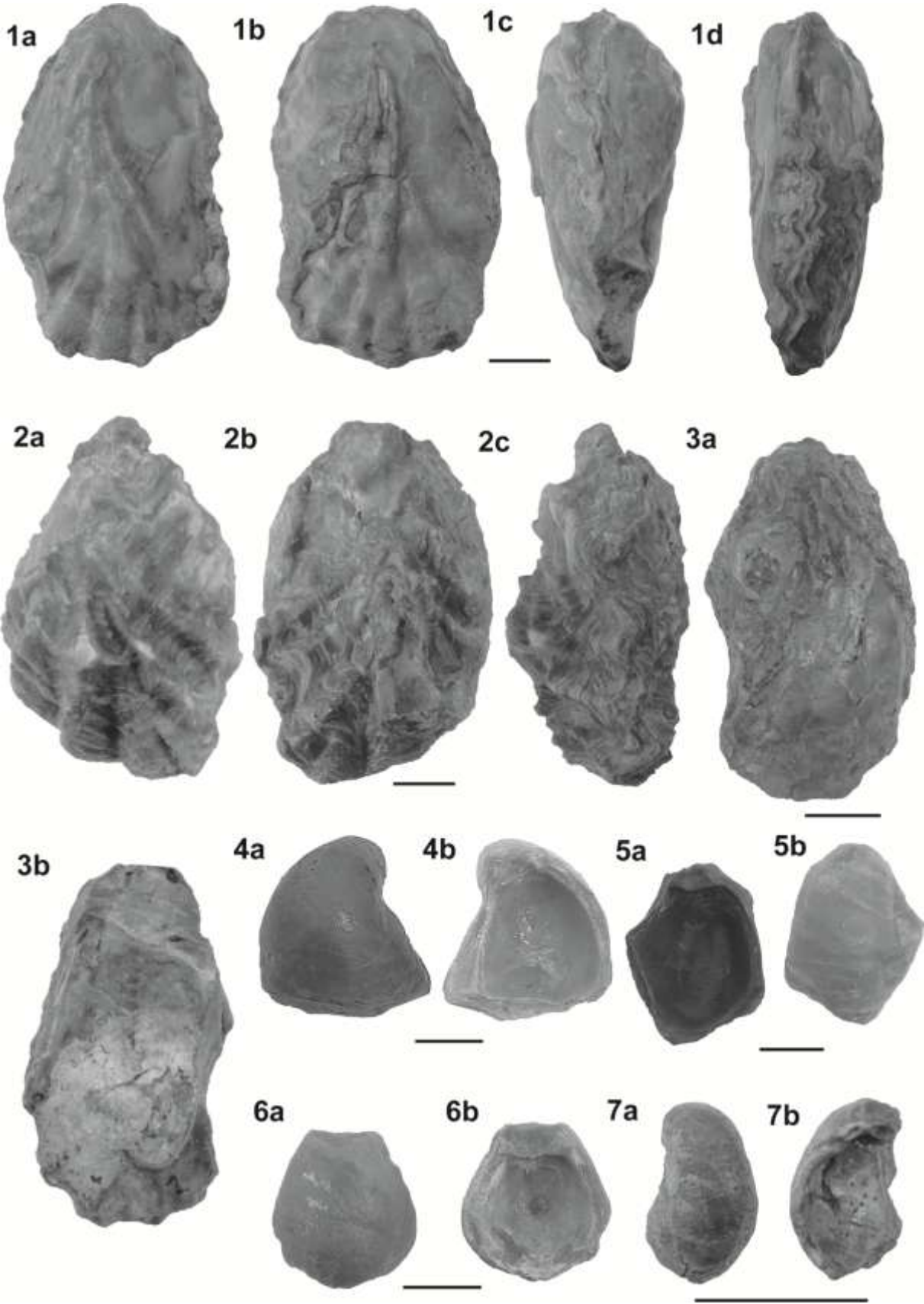
CHAPTER III SYSTEMATIC



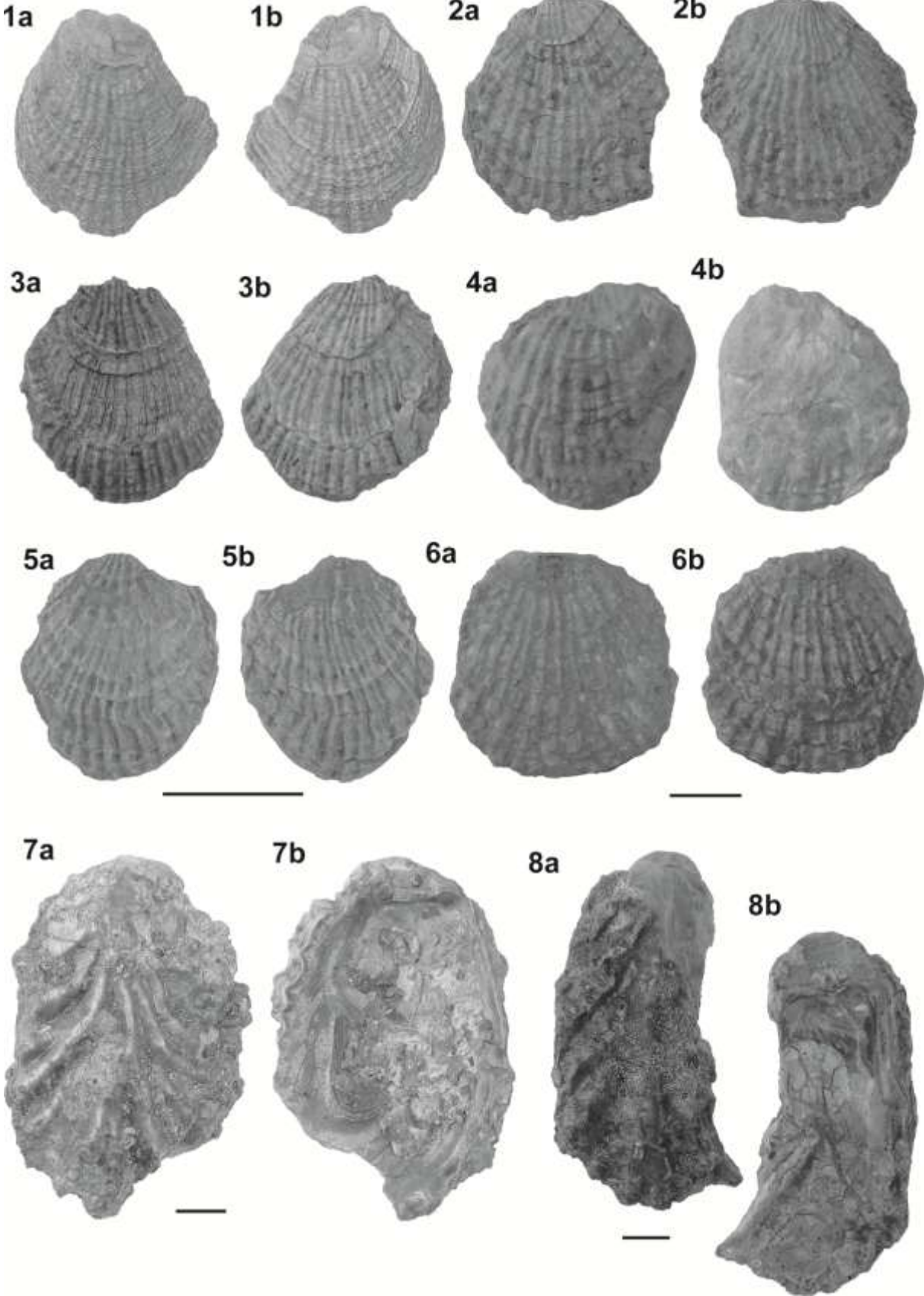
CHAPTER III SYSTEMATIC



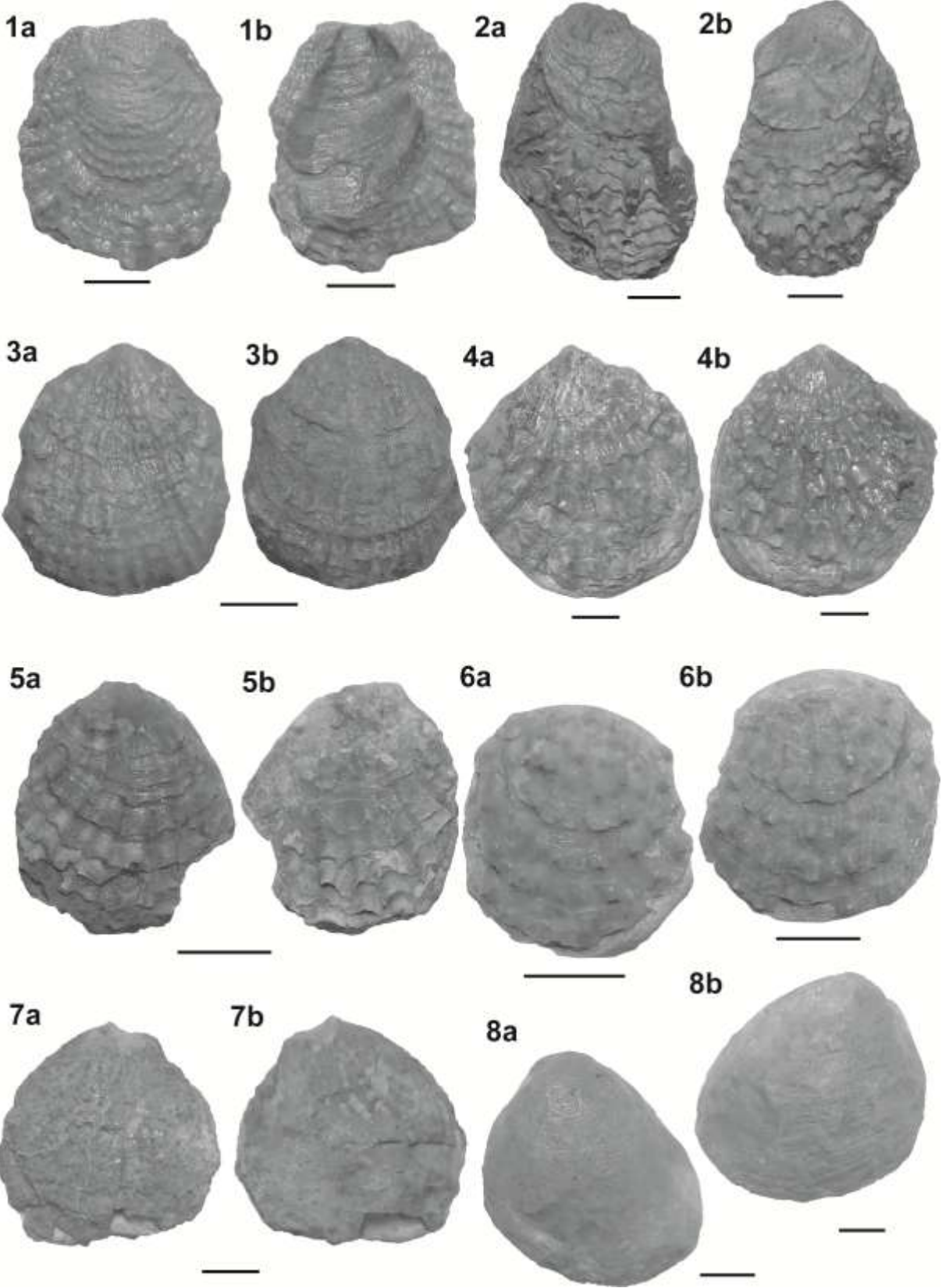
CHAPTER III SYSTEMATIC



CHAPTER III SYSTEMATIC



CHAPTER III SYSTEMATIC



1a



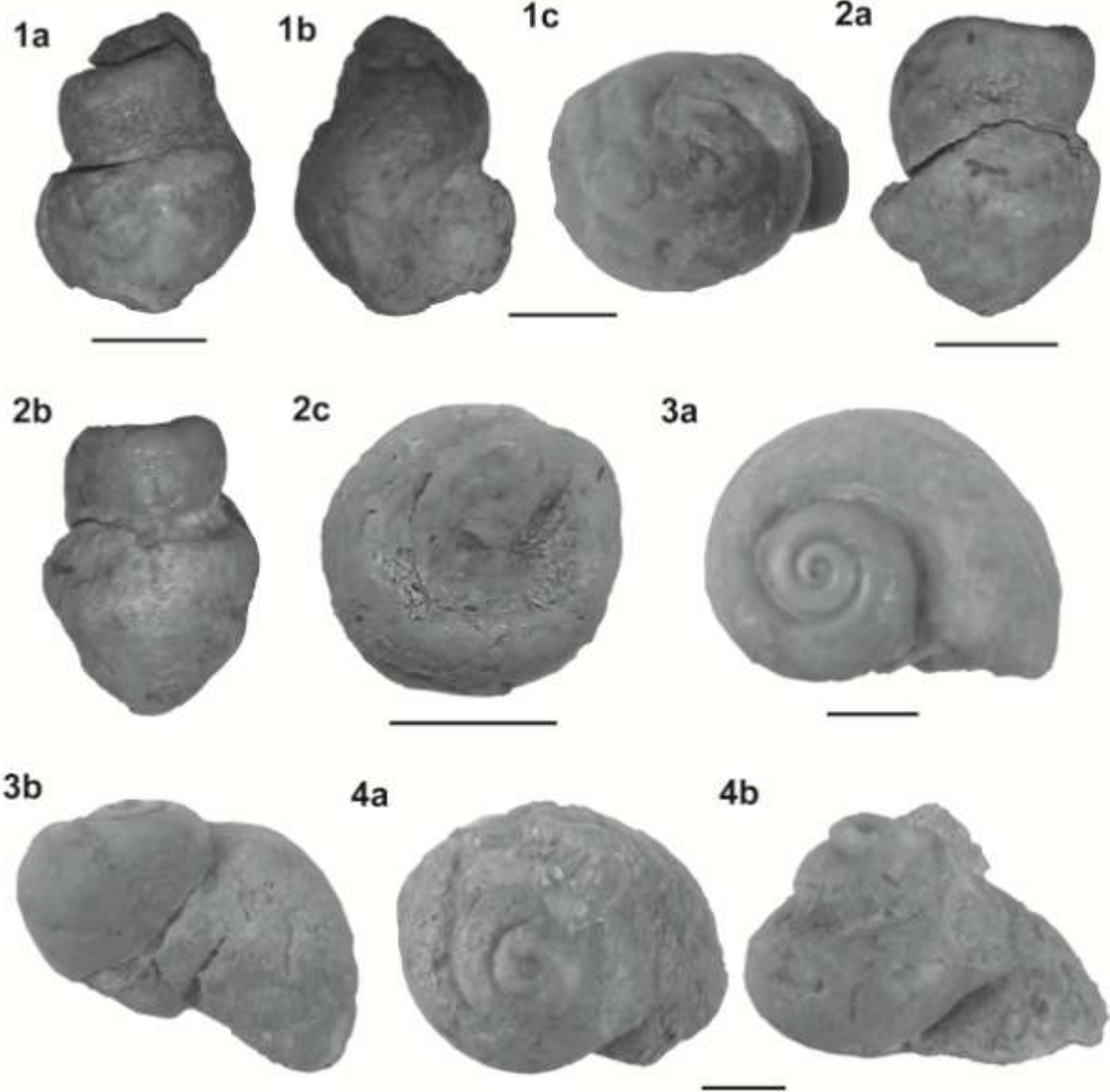
1c



1b



CHAPTER III SYSTEMATIC



## CHAPTER III SYSTEMATIC

### 2.2. Microfauna

10194 ostracods specimens were sorted in the study area ; Essen and Boukezez sections. Of these, 53 species were identified belonging to 10 families and 26 genera (Table 2).

71113 foraminefera specimens were sorted in the study area ; Essen and Boukezez sections. Of these, 31 species were identified belonging to 8 families and 16 genera (cf. Table 2).

Groups	Species
Ostracods	<i>Cytherella ovata</i> Roemer, 1841 <i>Cytherella</i> aff. <i>gabonensis</i> Neufville, 1973 <i>Cytherella mediatlasica</i> Andreu, 1996 <i>Cytherella</i> sp. <i>Cytherella contracta</i> Van Veen; 1932 <i>Cytherella gombienensis</i> Apostolescu, 1963 <i>Cytherella</i> aff. <i>elongata</i> Donze, 1964 <i>Cytherella</i> aff. <i>austinensis</i> Alexander, 1929. <i>Cytherella aegyptiensis</i> Colin & EL Dakkak, 1975. <i>Paracypris mdaouerensis</i> Bassoullet and Damotte, 1969 <i>Paracypris dubertreti</i> Damotte and Saint-Marc, 1972 <i>Paracypris</i> aff. <i>posteriusacuminatus</i> Andreu, 1996 <i>Paracypris</i> aff. <i>caudata</i> (Bold, 1964) <i>Paracypris chekhmai</i> Trabelsi, Sames, Nasri, Piovesan, Elferhi, Skanji, Houla, Soussi, Wagreich, 2020 <i>Ovocytheridea triangularis</i> Piovesan, Cabral and Colin, 2014 <i>Limburgina</i> sp. <i>Aysegulina</i> sp. <i>Sapucariella parvoangulata</i> Andreu and Puckett, 2016 <i>Sapucariella honigsteini</i> Puckett and Andreu 2016 <i>Trachyleberidea</i> gr. <i>geinitzi</i> (Reuss, 1874) <i>Trachyleberididae</i> sp., <i>Spinoleberis yotvataensis</i> Rosenfeld, 1974 <i>Cythereis</i> gr. <i>rawashensis</i> Van den Bold, 1964

## CHAPTER III SYSTEMATIC

	<i>Cythereis</i> sp., 1
	<i>Cythereis</i> sp., 2
	<i>Cythereis</i> sp., 3
	<i>Cythereis fahrioni bigrandis</i> Majoran, 1989
	<i>Cythereis kosticensis</i> Pokorny, 1963;
	<i>Cythereis namousensis</i> Bassoullet & Damotte , 1969
	<i>Cythereis algeriana</i> Bassoullet & Damotte, 1969
	<i>Protocosta babinoti</i> Piovesan, Cabral and Colin, 2014
	<i>Paraplatycosta</i> sp.
	<i>Paraplatycosta</i> aff. <i>talayninensis</i> Andreu, 1995
	<i>Haughtonileberis dinglei</i> Piovesan, Cabral & Colin, 2014
	<i>Protobuntonia numidica</i> Grekoff, 1954
	<i>Pterygocythere</i> aff. <i>allinensis</i> Grekoff and Deroo, 1956
	<i>Pterygocythere</i> sp.
	<i>Taracythere antakaranaensis</i> Jean-François Babinot, Jean-Paul Colin, Auran Randrianasolo 2009
	<i>Peloriops pustulata</i> (Rosenfeld & Raab; 1974)
	<i>Reticulocosta kanaanensis</i> Rosenfeld & Raab (1974)
	<i>Metacytheropteron</i> sp.
	<i>Amphicytherura</i> aff. <i>yakhiniensis</i> Rosenfeld 1974
	<i>Clithrocytheridea kaufmani</i> Hazelannée
	<i>Asciocythere</i> aff. <i>aegyptiana</i> (Morsi 2000)
	<i>Xestoleberis</i> sp.
	<i>Bythocypris</i> sp.
	<i>Bythocypris mohani</i> Singh 1997
	<i>Brachyocyther</i> sp
	<i>Perissocytheridea ascalopha</i> (Van den Bold), 1964
	<i>Soudanella laciniosa triangulata</i> Apostolescu année
	<i>Arculicythere semilunata</i> Singh 1997
	<i>Monoceratina trituberculata</i> Rosenfeld (1974)
	<i>Aphrikanocythere phumatoides</i> Damotte et Oertli
<b>Planktonic foraminifera</b>	<i>Marginotruncana renzi</i> (Gandolfi, 1942)
	<i>Marginotruncana caronae</i> Peryt, 1980

## CHAPTER III SYSTEMATIC

	<p><i>Marginotruncana</i> cf. <i>sigali</i> (Reichel, 1950) <i>Marginotruncana sinuosa</i> Porthault, in Donze et al., 1970 <i>Marginotruncana pseudolinneiana</i> Pessagno, 1967 <i>Globotruncana linneiana</i> (D'Orbigny 1839) <i>Globotruncana bulloides</i> Vogler, 1941 <i>Globotruncana</i> sp. <i>Globotruncana arca</i> (Cushman, 1926) <i>Globotruncanita elevata</i> (Brotzen, 1934) <i>Contusotruncana plummerae</i> (Gandolfi, 1955) <i>Dicarinella primitiva</i>, (Dalbiez, 1955) <i>Dicarinella asymetrica</i>, (Sigal, 1952) <i>Dicarinella canaliculata</i> (Reuss, 1854) <i>Archaeoglobigerina</i> sp <i>Whiteinella baltica</i> Douglas and Rankin, 1969 <i>Whiteinella archaeocretacea</i> Pessagno, 1967 <i>Whiteinella</i> sp., <i>Pseudotextularia</i> sp., <i>Pseudotextularia nuttalli</i> (Voorwijk, 1937) <i>Huberella praehuberi</i> Georgescu, 2007 <i>Muricohedbergella flandrini</i> (Porthault, in Donze et al., 1970) <i>Sigalia carpatica</i> Salaj, Samuel, (1963) <i>Planohétérohélix globulosa</i> (Ehrenberg, 1839) <i>Planohedbergella</i> cf. <i>escheri</i> (Kaufmann, 1865) <i>Planohétérohélix reussi</i> (Cushman) 1938</p>
<b>Benthic foraminifera</b>	<p><i>Eobigenerina</i> sp. <i>Cibicidoides</i> sp. <i>Gavelinella</i> sp. <i>Notoplanulina</i> sp. <i>Nonionella</i> sp.</p>

### Ostracods

Class Ostracoda Latreille, 1802

Subclass Podocopa Müller, 1894

## CHAPTER III SYSTEMATIC

Order Platycopida Sars, 1866

Suborder Platycopina Sars, 1866

Superfamily Cytherelloidea Sars, 1866

Family Cytherellidae Sars, 1866

Genus *Cytherella* Jones, 1849

*Cytherella ovata* Roemer, 1841

### Pl. 1, Figure 1a–c

1841 *Cytherella ovata* Roemer, p. 104, pl. 16, Figure 21.

1958 *Cytherella* ex gr. *ovata* Roemer- Oertli, p.61, pl. 1, figs. 1–3.

1977 *Cytherella ovata* Roemer- Boukhary et al., p. 156, pl. 1, Figure 10a–b.

1980 *Cytherella* gr. *ovata* Roemer-Babinot, pl. 1, figs. 12, 13; pl. 2, figs. 1–3

1985 *Cytherella* gr. *ovata* Roemer- Vivière, p. 135, pl. 1, Figure 1.

1991 *Cytherella* gr. *ovata* Roemer- Shahin, p. 133, pl. 1, Figure 5.

1994 *Cytherella ahmadiensis* Al-Abdul- Razzaq- Shahin et al., p. 36, pl. 1, figs. 1–2.

2001 *Cytherella aegyptiensis* Colin and El Dakkak- Morsi and Bauer, p. 383, pl. 1, figs. 1–2.

2006 *Cytherella* aff. *ovata* Roemer- Andreu & Bilotte, p. 59, pl. 1, figs. 1–5.

2008 *Cytherella ovata* Roemer-El-Nady et al., p. 561, pl. I, Figure 6

2016 *Cytherella* gr. *ovata* Roemer- Mebarki et al., p. 262, pl. 1, figs. 1–2.

2017 *Cytherella* gr. *ovata* Roemer- Jomaa-Salmouna et al., p 536, pl. 1, Figure 3a–c

2018 *Cytherella* gr. *ovata* Roemer- Benadla et al., p. 420, Figure 8A–C.

2023 *Cytherella* gr. *ovata* Roemer- Benadla et al., p.11 , Figure 6a.

**Material:** 150 specimens of Boukezez and 520 specimens of Essen (samples: E1, E3, E5, E28, E29, E36, E37, E45, E53, E56, E58, E61, E63, E64, E66, E69, E71, C1- C11, C13-C17, C22-C24, C26-C34, C36-C38, C42-C44, C46-C59, C65, C66, C68- C70, C91- C108, C110-C114, C116-C119, C121-C155, C157- C169, C175, C179-S2, S15, S26, S47-S62).

**Measurements:** sample **E3, C91, S1, C, L:** 0.77; **H:** 0.48; **W:** 0.24.

**Remarks:** *Cytherella ovata* Roemer, 1841, is very similar to those of Jomaa-Salmouna et al. (2014), described in Tunisia, but show a greater peripheral overflow of the right valve onto the left valve, Its similar to *Cytherella aegyptiensis* Colin and El Dakkak-1975 in the Cenomanian of Egypt (Morsi & Bauer 2001), and similar to *Cytherella ahmadiensis* Al-Abdul- Razzaq - 1994 in the Cenomanian of Egypt (Shahin et al., 1994) The dorsal margin is strongly convex in the right valve, much less so on the left valve, but show a greater peripheral overflow of the right valve onto the left valve.

**Occurrence:** Coniacian and Santonian of Essen Formation and Boukezez Formation.

## CHAPTER III SYSTEMATIC

**Distribution** : Senonian of Germany (Roemer, 1841); late Cretaceous of France (Oertli, 1958); Cenomanian of Egypt (Colin and El-Dakkak, 1975; Boukhary et al., 1977 ; Shahin et al., 1994; Morsi and Bauer, 2001; El Nady et al., 2008); Vraconian–Santonian of NE of Algeria (Vivière, 1985); late Cenomanian and Turonian of Southern Corbières, SE France (Andreu and Bilotte, 2006); Turonian–Coniacian of Tunisia (Jomaa-Salmouna et al., 2017); late Cenomanian of Guir Bassin, Algérie (Mebarki et al., 2016), Cenomanian–Turonian of the Western Saharan Atlas, Algeria (Benadla et al., 2018 ; 2023),

*Cytherella aff. gabonensis* Neufville, 1973.

### Pl. 1, Figure 2a–c

1973 *Cytherella gabonensis* Neufville, p. 121, pl. 7.1, figs 1 a-g.

2000 *Cytherella gabonensis* Neufville. - MORSI, p. 50, pl. 1, figs 3-6.

2001 *Cytherella gabonensis* Neufville.- SHAHIN & EL NADY, p. 153, pl. 1, Figure 3.

2005 *Cytherella gabonensis* Neufville- Shahin, p. 773, pl. I, Figure 2

**Material**: 99 specimens (samples: E1, E3, E5, E28, E29, E36- E39, E63, E71)

**Measurements**: sample **E3, C, L**: 0.66; **H**: 0.48; **W**: 0.16.

**Remarks**: Our specimens differs subtle from *C. gabonensis* Neufville, 1973 especially in the more ovoid outline a less conspicuous valves overlap.

**Occurrence**: Coniacian and Santonian (Boukezez, present study).

**Distribution** : Late Cretaceous of Gabon (Neufville, 1973), Coniacian-Santonian of central Sinai (MORSI, 2000), Maastrichtian of northeastern Sinai (Shahin & El nady, 2001). In the present study it occurs in the Late Maastrichtian-Early Paleocene.

*Cytherella mediatlasica* Andreu, 1996

### Pl. 1, Figure 3a–b

1987 *Cytherella* sp. Okosun, p. 25, pl. 13, figs. 5–6.

1992 *Cytherella* sp. Okosun, p. 328, pl. 2, Figure 20.

1996 *Cytherella mediatlasica* Andreu, p. 484–485, 488, pl. 1, figs. 1–10.

2000 *Cytherella* sp. P6 Viviers, Koutsoukos, Silva-Telles and Bengtson, p. 415, figs. 8, 14–15.

2014a *Cytherella mediatlasica* Andreu- Piovesan et al., p. 214, pl. 1, figs. A–D.

2014b *Cytherella mediatlasica* Andreu- Piovesan et al., p. 318, pl. 1, figs. E–I.

2020 *Cytherella mediatlasica* Andreu- Piovesan et al., p. 83, Figure 3B.

**Material**: 37 specimens (samples: E1, E3, E38 -E43, E53, E63)

**Measurements**: sample **E3, C, L**: 0.49; **H**: 0.27; **W**: 0.20.

### CHAPTER III SYSTEMATIC

**Remarks:** Our material corresponds to the "morphotype A" of this species, according to Piovesan et al. (2014b). This morphotype presents surface punctated, with fine ribs parallel to the anterior margin, while "morphotype B", presents surface entirely and regularly punctuated.

**Occurrence:** Coniacian and Santonian of Boukezeze section

**Distribution :** Turonian–Santonian of Nigeria (Okosun, 1987, 1992); Turonian–Campanian of the Potiguar Basin, Brazil (Viviers et al., 2000; Piovesan et al., 2014a, b); Santonian–Campanian of the Potiguar Basin, Brazil (Piovesan et al., 2020);

#### *Cytherella* sp., 3

##### **Pl. 1, Figure 4a–c**

*Cytherella* sp. D – Margerie 1967: 13, 14, pl. 1, figs 8, 9, pl. 3, figs 6, 7, cellule MA 8.

2007 *Cytherella* sp., Andreu, p. 353, pl.1, Figure 1.

**Material:** 44 specimens of Essen section (samples: **C1, C12, C14, C15, C42, C48**).

**Measurements:** sample **C42, C, L: 077; H: 0.45; W: 0.23.**

#### **Description of the specimens:**

**Remarks:** *Cytherella* sp., similler from *Cytherella* sp., 3 Lower Danian of the Pernambuco-Paraiba Basin, Brazil. (G. Fauth et al., 2005) in having obliquely rounded anterior and posterior margins. (G. Fauth et al. 2005); the carapaces of *Cytherella* sp. Margerie are larger than those of *C. ovata*. In dorsal view, *Cytherella* sp., have roughly the same outline: it is therefore possible that all these carapaces are conspecific.

**Occurrences:** Coniacian of Essen Formation

**Distribution :** Ostracods from the *P. Margerie* collection and the age of the layers at Laffitteines of Mont Aime (Paris basin, Franch)

#### *Cytherella* aff. *contracta* Van Veen; 1932

##### **Pl. 1. Figure 5a-b**

1932 *Cytherella contracta* Van Veen, 342 , 343, pl. 8, figs 1-18. Howe & Laurencich 1958: 246.

1966 *Cytherella contracta contracta* – Herrig 709-714, pl. 1, figs 1-3.

1967 *Cytherella* aff. *contracta* – Margerie 14, pl. 1, Figure 7, pl. 3, Figure 8, cellule MA 9.

2017 *Cytherella* cf. *contracta* Van Veen, 1932. p.229.

## CHAPTER III SYSTEMATIC

**Material:** 399 specimens (samples: C3, C4-C6, C8-C10, C17, C19-C23, C25-C26, C33- C42, C44-C58, C61, C62, C65-C70, C72-C74, C76 -C78, C81, C85- C86- C88, C91- C129, C132- C180, S1-S6, S44-S32)

**Measurements:** Sample C25, S1, C, L: 0.60; H: 0.30; W: 0.20.

**Description of the specimens:** narrow as it appears in dorsal view, with narrowing (contraction) in their median part; they present a clear sexual dimorphism. Their contours differ significantly from those of the individuals of *C. contracta* figured by Van Veen, larger

**Remarques :** They are long and correspond to probably immature individuals whose right and left valves have similar contours, unlike the valves of the species of the ovata group. They are narrow as it appears in dorsal view, with narrowing in their median part. Their contours differ significantly from those of the individuals of *C. contracta* figured by Van Veen,

**Occurrence :** Coniacian and Santonian of Essen section

**Distribution :** This species was first reported in the Lower Cenomanian (Van Veen, 1932; Bismuth et al., 1981), the Turonian, and the Coniacian in several basins of the Tethyan domain, notably in North Africa (Tunisia, Algeria, Morocco) and Europe (Vivière, 1985; Donze et al., 1982). The latest known occurrences are recorded in the Santonian (Vivière, 1985).

### *Cytherella gambiensis* APOSTOLESCU, 1963

#### Pl. 2. Figure 1a-b

1963 *Cytherella gambiensis* APOSTOLESCU, p. 1680, Pl. 1, figs. 1-3.

1981 *Cytherella* cf. *gambiensis* APOSTOLESCU - BISMUTH *et al.*, p. 221-222, Pl. 6, figs. 1-2.

1985 *Cytherella* cf. *gambiensis* APOSTOLESCU - VIVIERE, p. 137-138, pl. 1, Figure 7.

2000 *Cytherella gambiensis* APOSTOLESCU - DELICIO *et al.*, p. 331-332, figs. 8.3-8.4.

2000 *Cytherella* aff. *C. gambiensis* VIVIERS *et al.*, p. 415, figs. 8, 5-6 and 9-11.

2014b *Cytherella gambiensis* APOSTOLESCU- PIOVESAN *et al.*, (pl. 1 , figs. A-D)

2017 *Cytherella* aff. *gambiensis* Apostolescu, Benmansour, pl. 16, 22-24.

**Material:** 556 specimens (samples: C1- C10, C12, C13, C15, C16, C18, C19, C22-C25, C29- C32, C34- C38, C42, C44, C46-C58, C60-C71, C76-C85, C87- C129, C132-C139, C146, C141, C148- C156, C159-C175, C177- S2, S26- S28, S46- S48, S53).

**Measurements:** sample C13, C, L: 0.66; H: 0.48; W: 0.16.

## CHAPTER III SYSTEMATIC

**Description :** *Cytherella gambiensis* is pear-shaped in lateral view and has a higher posterior limit than *Cytherella* aff. *gambiensis*. In Piovesan et al., 2014 (and perhaps Delicio et al., 2000), *Cytherella gambiensis* shows almost the same characteristics as our species; the only difference is the presence, or absence, of a strong development (projection) on the posterior limit of the VD, but less developed than in *Cytherella tuberculifera* Alexander, 1929.

**Remarks:** Despite the similarity, *Cytherella paenovata* ALEXANDER, 1932, from the Upper Cretaceous of Texas, USA, has the maximum height at mid-length and has a small posterior projection. The species identified by BOLD (1964) as *Cytherella* aff. *paenovata* in the Cenomanian–Santonian of Egypt is significantly larger and has a less pronounced overlap. BISMUTH et al. (1981) identified *Cytherella* cf. *gambiensis* in the Turonian of Tunisia, but the BISMUTH's species has a much more prominent overlap of the valves.

**Occurrence:** Coniacian- Santonian of Essen Formation

**Distribution:** Turonian of Algeria (Viviere, 1985), Senonian of Gambia (APOSTOLESCU, 1963), Upper Cretaceous of Potiguar Basin (Delicio et al., 2000), Coniacian–Campanian (Viviere et al., 2000) and Santonian–Campanian of Potiguar Basin (Piovesan et al., 2014), Campanian- Maastrichtian of Algeria( Benmansour et al., 2017) .

### *Cytherella* aff. *elongata* Donze, 1964

#### Pl. 2. Figure 2a-c

**Material:** 399 specimens (samples: C1-C7, C9, C10, C13, C16, C15, C19-C24, C27-C37, C40- C66, C68-C72, C74, C75, C77-C84, C86- C89, C91- C102, C127, C140, C142, C144- C158, C166- C168, C177, C179, S1- S4, S9- S62).

**Measurements:** sample C13, C, L: 0.50-0.70; H: 0.45- 0.48; W: 0.10- 0.16.

**Description:** The carapace of *Cytherella* aff. *elongata* is elongate-subrectangular in the lateral view, with slightly convex dorsal and ventral margins. The anterior margin is broadly rounded, while the posterior is narrower and more pointed. The valves are smooth, thin-shelled, and moderately inflated. The hinge is simple, typical of the genus *Cytherella*. The greatest height occurs near the anterior third of the carapace, and the maximum length is slightly more than twice the height.

**Remarks :** the valves of *Cytherella elongata* Donze, 1964 are some 75 % longer and more oval in lateral view. Consequently, according to the International Code of Zoological Nomenclature (1999) *Cytherella elongata* Donze, 1964 from the Lower Cretaceous of France represents a junior primary homonym of *Cytherella elongata* Jones & Kirkby, 1886 from the

## CHAPTER III SYSTEMATIC

Carboniferous limestone series of Scotland. *Cytherella elongata* valva nom. nov. is herewith introduced as a substitutional new name. Etymology: As originally intended, the new name is hinting to the fact that the valves of male specimens are longer than those of female specimens.

**Occurrence:** Coniacian- Santonian of Essen Formation

**Distribution:** Reported from the Cenomanian–Turonian of Tunisia (Bismuth et al., 1981; Ben Youssef, 1980). Found in the Turonian–Coniacian of Algeria (Vivière, 1985). Also present in the Cenomanian of France (Donze, 1964).

### *Cytherella* aff. *austinensis* Alexander, 1929

#### Pl. 2. Figure 3a-b

1929 *Cytherella austinensis* Alexander, p. 51-52, pl. 2, Figure 4, 6.

2014 *Cytherella* aff. *austinensis* Alexander, 1929 - Piovesan, Cabral, Colin, Fauth, Trescastro, p. 320, pl. 1, Figure J-L.

2017 *Cytherella* aff. *austinensis* Alexander\_ Benmansour et al., pl. 16, 19-21.

**Matériel :** 2585 specimens of Boukezez formation 2840 specimens of Essen formation (samples: C1-C79, C81-C168, C172-C173, C175, C179- C180, C177, S1-S28, S41-S62).

**Measurements:** C79, C, L: 0.60; H: 0.48; W: 0.18.

**Description of the specimens:** *Cytherella* aff. *austinensis* is suboval to elongate-oval in lateral view, with moderately convex dorsal and ventral margins. The anterior margin is broadly rounded, while the posterior is narrower and more tapered. Valves are smooth, thin-shelled, and slightly inflated medially. The greatest height is located slightly anterior to the mid-length of the carapace. The hinge is simple and typical of the genus *Cytherella*. Surface ornamentation is absent, giving the carapace a clean, featureless appearance.

**Remarks:** *Cytherella* aff. *austinensis* has a higher posterior limit than the type species. In fact, the posterior limit of the type species is low and noticeably narrower than the anterior limit. Our species is quite similar to *Cytherella* aff. *austinensis* Piovesan et al., 2014; some differences appeared in the lateral view: an external marginal rim on both valves, and a slightly convex ventral margin at mid-length of the left valve.

**Occurrence:** Coniacian- Santonian of Essen Formation

**Distribution :** Originally described from the Austin Chalk (Turonian–Coniacian) of Texas, USA (Alexander, 1929). Reported in the Cenomanian–Turonian of Tunisia (Glantzboeckel &

## CHAPTER III SYSTEMATIC

Magné, 1959; Ben Youcef, 1980; Bismuth et al., 1981). Found in Algeria (Turonian–Coniacian) (Vivrière, 1985). Recorded in the Cenomanian of Morocco (Donze et al., 1982).

### *Cytherella aegyptiensis* COLIN & EL DAKKAK, 1975.

#### Pl. 2. Figure 4a-b

1975. *Cytherella aegyptiensis* COLIN & EL DAKKAK, p. , pl. , Figure

**Material:** 132 specimens (samples: C8, C12-C16, C18, C29, C33, C38, C48-C58, C71, C73, C115, C116, C124,-C130, C132- C168, C175, C179, S10, S15, S20).

**Measurements:** C132, C, L: 0.60; H: 0.40; W: 0.26.

**Description of the specimens:** Characterized by a subrectangular to subovate carapace, with moderately convex dorsal and ventral margins. The anterior margin is broadly rounded and slightly expanded, whereas the posterior margin is narrower and subtly tapered. The valves are smooth, thin-shelled, and moderately inflated, with the greatest height located slightly anterior to the mid-length. The hinge is simple and lacks prominent teeth or sockets, typical of the genus *Cytherella*. This species differs from closely related taxa, such as *C. contracta* and *C. elongata*, by its more rectangular outline, less tapering posterior, and broader anterior region.

**Remarks :** *Cytherella aegyptiensis* Similar to forms described in the Cenomanian of Djebel Nezzazat, Sinai, Egypt.

**Occurrences :** Coniacian and Santonian of Essen Formation

**Distribution :** *Cytherella aegyptiensis* ranges from the Upper Cenomanian to the Lower Turonian. It was first described from Egypt (Colin & El Dakkak, 1975) and has since been reported in Tunisia (Ben Youssef, 1980; Bismuth et al., 1981), Algeria (Vivrière, 1985), and northern Morocco (Donze et al., 1982).

Suborder Cypridocopina Jones, 1901

Superfamily Cypridoidea Baird, 1845

Family Paracyprididae Sars, 1923

Subfamily Paracypridinae Sars, 1923

Genus *Paracypris* Sars, 1866

*Paracypris mdaouerensis* Bassoullet and Damotte, 1969

#### Pl. 2. Figure 5a–c

1969 *Paracypris mdaouerensis* Bassoullet and Damotte, p. 140, pl. 2, figs. 10 a–d.

1985 *Paracypris mdaouerensis* Bassoullet and Damotte- Vivrière, p. 150, pl. 3, Figure 9.

## CHAPTER III SYSTEMATIC

1991 *Paracypris mdaouerensis* Bassoullet and Damotte- Andreu, pp. 486-489, pl. 18, figs. 10–14 ; pl. 19, figs 1, 2, 6–8, 14, 15.

1991 *Paracypris mdaouerensis* Bassoullet and Damotte- Shahin, p. 138, pl. 2, figs. 3, 4.

1999 *Paracypris mdaouerensis* Bassoullet and Damotte- Ismail, p. 310, pl. 3, Figure 18.

2001 *Paracypris mdaouerensis* Bassoullet and Damotte- Morsi and Bauer, p. 386, pl. 2, Figure 6.

2008 *Paracypris mdaouerensis* Bassoullet and Damotte- El Nady et al., p. 545, pl. 2, Figure 13.

2016 *Paracypris mdaouerensis* Bassoullet & Damotte- Mebarki et al., p. 264, pl. II, figs. 13–15.

2017 *Paracypris mdaouerensis* Bassoullet and Damotte- Jomaa-Salmouna et al., p.537, pl 2, Figure 1a–c

2018 *Paracypris mdaouerensis* Bassoullet and Damotte- Benadla et al., p. 420, figs. 8G–H.

2020 *Paracypris mdaouerensis* Damotte and Saint-Marc- Trabelsi et al., p. 20, Figure 8A1–A8.

2022 *Paracypris mdaouerensis* Bassoullet and Damotte- Slami et al., p. 12, figs. 7.1–7.2.

**Material:** 17 specimens of Boukezez section and 334 specimens of Essen section (samples: E28, E36, E38– E42, C11, C12 C14 C16 C17 C19-C27, C29-C35C42- C45, C50-C58, C60-C62, C65, C66, C68-C167, C169- C172, C175- S59).

**Measurements:** sample **E36**, **C**, **L**: 0.69; **H**: 0.33; **W**: 0.17.

**Occurrence:** Coniacian and Santonian

**Distribution:** Aptian–Lower Turonian of Morocco (Andreu, 1991); Albian from Tunisia (Trabelsi et al., 2020); lower Albian–Turonian from Egypt (Shahin, 1991; Ismail, 1999; Morsi and Bauer, 2001; El-Nady et al., 2008); lower Turonian of the Western Saharan Atlas, Algeria (Bassoullet and Damotte, 1969); Cenomanian–Coniacian from NE Algeria (Vivière, 1985); Turonian–Coniacian of Tunisia (Jomaa-Salmouna et al., 2017); Cenomanian–Turonian of the Western Saharan Atlas, Algeria (Benadla et al., 2018); Cenomanian of Djebel Sabaoune, Batna, Algeria (Slami et al., 2022).

### *Paracypris dubertreti* Damotte and Saint-Marc, 1972

#### Pl. 2. Figure 6a–b

1972 *Paracypris dubertreti* Damotte and Saint-Marc, p. 276, pl. 1, Figure 1.

1985 *Paracypris dubertreti* Damotte and Saint-Marc- Vivière, p. 149, pl. 3, figs. 6–7.

1991 *Paracypris dubertreti* Damotte and Saint-Marc- Andreu, p. 485, pl. 18, Figure 9.

## CHAPTER III SYSTEMATIC

2001 *Paracypris dubertreti* Damotte and Saint-Marc- Morsi and Bauer, pp. 385, 386, pl. 2, figs. 4–5.

2002 *Paracypris dubertreti* Damotte and Saint-Marc- Bassiouni, p., pl. 2, figs. 5–9.

2013 *Paracypris dubertreti* Damotte and Saint-Marc- Andreuet al., pl. 4, figs. 18, 19.

2016 *Paracypris dubertreti* Damotte and Saint-Marc-Mebarki et al., p. 263, pl. I, Figure 12.

Non 2017 *Paracypris dubertreti* Damotte and Saint-Marc- Jomaa-Salmouna et al., p.536 ,pl.1, Figure 4a–c

2018 *Paracypris dubertreti* Damotte and Saint-Marc- Benadla et al., p. 201, p. 420, Figure 8F.

2020 *Paracypris dubertreti* Damotte and Saint-Marc- Trabelsi et al., Figure 8 B, B2

2022 *Paracypris dubertreti* Damotte and Saint-Marc- Slami et al., p. 12, figs. 7.6.

**Material:** 61 specimens (samples: E37- E39, E41, E71, C7, C13, C15, C17, C18, C35, C50-C53, C56, C100-C104, C106-C108, C113, C115-C122, C128, C164, C180).

**Measurements:** sample **E37, C, L:** 0.63; **H:** 0.25; **W:** 0.17.

**Occurrence:** Coniacian- Santonian of Boukezez Formation and Essen Formation

**Distribution :** Albian of Tunisia (Trabelsi et al., 2020); Albian–Cenomanian of Egypt (Morsi and Bauer, 2001; Bassiouni, 2002); Cenomanian–lower Turonian of Algeria (Vivière, 1985, Mebarki et al., 2016); Cenomanian–Turonian of Morocco (Andreu, 1991; Andreu et al., 2013); lower and middle Turonian of Tunisia (Damotte and Saint-Marc, 1972); middle Turonian–Coniacian (Jomaa-Salmouna et al., 2017); Cenomanian of Djebel Sabaoune, Batna, Algeria (Slami et al 2022)

### *Paracypris* aff. *posteriusacuminatus* Andreu, 1996

#### Pl. 2. Figure 7a–b

2000 *Paracypris* sp. 1- Delicio et al., p. 334, figs. 8.8-8.10.

2014b *Paracypris* aff. *posteriusacuminatus* Andreu- Piovesan et al., p 223-224, pl. 3, figs. A–C.

**Material:** 215 specimens (samples: E1, E3, E5, E28, E36, E39–E43, E45, E53, E62, E63, E69, E71, C4, C8, C13, C14, C17- C20, C26- C49, C53- C153, C155, C156, C160- S1, S28, S29).

**Measurements:** sample **E36, C, L:** 0.80; **H:** 0.40; **W:** 0.20.

**Remarks:** Despite the similarities with *P. posteriusacuminatus* described by Andreu (1996) in Morocco, the present specimens have a more marked posterior cardinal angle. Additionally, the specimens from Morocco have the dorsal outline more symmetrically convex. These differences could be related with ontogeny.

## CHAPTER III SYSTEMATIC

**Occurrence:** Coniacian and Santonian Boukezez Formation and Essen Formation

**Distribution :** Late Cretaceous of the Potiguar basin, Brazil (Delicio et al., 2000; Piovesan et al., 2014b);

### *Paracypris* aff. *caudata* (Bold, 1964)

#### Pl. 2. Figure 8a-b

aff. 1964 *Ovocytheridea caudata* BOLD, p. 119, Pl. 14, figs. 4a-b.

1973a *Paracypris caudata* (van den BOLD) -NEUFVILLE, p. 125-126, Pl. 7.3, Figure 4.

1985 *Paracypris* sp. 2 VIVIÈRE, p.150-151, Pl. 3, Figure 10.

2014a *Paracypris* aff. *caudata* BOLD- Pioveson, p. 217, pl. 1, figs. L-O).

**Material:** 55 specimens of Essen section (samples: C13, C14, C29-C35, C58-C81, C100, C168, S1, S37)

**Measurements:** samples C13, C168, C, L: 0.79; H: 0.45; W: 0.22.

**Description of the specimens:** The carapace is large, robust, and sub-triangular in lateral view, while appearing suboval in dorsal view. The left valve (LV) overlaps the right valve (RV) along all margins, with the overlap being most pronounced dorsally. The maximum height and width occur at mid-length of the carapace. The dorsal margin is strongly convex, featuring a slight concavity in the anterodorsal area of the RV, whereas the ventral margin is nearly straight in the LV and slightly concave at mid-length in the RV. The anterior margin is obliquely rounded, while the posterior end is distinctly acuminate. The external surface is smooth.

**Remarks:**-This species shows greater height in the posterior third of the carapace compared to *P. caudata* (Bold, 1964). Overall, *P. aff. caudata* differs from other *Paracypris* species found in the Potiguar Basin by being taller, broader, and exhibiting a more distinctly sub-triangular outline.

**Occurrences :** Coniacian of Essen

**Distribution:** Turonian of Egypt (BOLD, 1964), of Gabon (NEUFVILLE, 1973a), Middle Turonian-Santonian of Algeria (VIVIÈRE, 1985) and Turonian of Brazil (Pioveson et al., 2014a).

### *Paracypris chekhai* Trabelsi, Sames, Nasri, Piovesan, Elferhi, Skanji, Houla, Soussi, Wagreich, 2020

#### Pl. 2. Figure 9a-e

2020 *Paracypris chekhai* sp. nov. Trabelsi (Figure 8D1eD10)

### CHAPTER III SYSTEMATIC

**Material:** 18 specimens of Essen section (samples: C4, C74, C105, C135, C168, C180, S51, S20)

**Measurements:** S51, C, L: 0.77; H: 0.43; W: 0.30.

**Description of the specimens:** Diagnosis. A medium to large-sized species of *Paracypris*. Lateral outline of carapace sub-triangular and short in females, lower and more elongated in males. Dorsal margin strongly convex with abrupt downward curvature posteriorly. Ventral margin perfectly straight in LV, and slightly concave in RV. Anterior and posterior regions compressed. Sexual dimorphism pronounced.

**Description of the specimens:** Carapace of medium to large size, sub-triangular in lateral view and suboval in dorsal view. Slightly inequivalve, with LV overlapping and slightly overreaching RV along almost entire margin except of rounded parts of the antero- and postero-ventral margins. Carapace preplete, with maximum height slightly anterior of mid-length. Maximum length at the lower 1/3 of height. Anterior margin broadly infracurvate with long straight dorsal part. Posterior margin narrow, slightly infracurvate with relatively long straight dorsal part. Dorsal margin strongly convex, with a small concavity in the anterodorsal part of the RV, and abruptly inflected downward in the posterodorsal part. Cardinal angles strongly rounded. Ventral margin perfectly straight in the LV and slightly concave at mid-length of the RV. Carapace surface smooth. Internal features not observed.

**Remarks :** Comparison. *Paracypris chekhmai* differs from *P. mdadourensis* in being of somewhat smaller overall size, the more triangular and less elongate lateral outline, and the maximum height being still anteriorly of, but almost at, mid-length. *P. dubertreti* is much more slender and elongate in lateral outline than *P. chekhmai* with slightly convex to straight dorsal margin and outline, and an almost equicurve anterior margin being distinctly infracurvate in the latter. *Paracypris chekhmai* shows some affinity to *Paracypris lusitanicus* described by Damotte et al. (1990) from the upper Aptian of Portugal. However, *P. chekhmai* exhibits a much more pronounced valve overlap than *Paracypris lusitanicus*. In addition, the anterodorsal angle is much more pronounced in *P. lusitanicus* than in *Paracypris chekhmai* is somewhat similar to *P. caudata* (Van den Bold, 1964) from the Upper Cretaceous of Egypt in general shape and external features, although the new Tunisian species is much smaller, narrower, and shows more compressed anterior and posterior regions than the Egyptian species. Particularly, the new species from Tunisia species is characterized by the abrupt posterodorsal downward inflexion, a feature never previously described in the genus *Paracypris*.

**Occurrences :** Coniacian and Santonian of Essen Formation

## CHAPTER III SYSTEMATIC

**Distribution :** Occurrence and stratigraphic range. Unit 2b, Orbata Formation, Eastern Koumine section, Jebel Koumine, Central Tunisian Atlas, Tunisia. Lower Aptian, calibrated by a rich charophyte association (Trabelsi et al., 2016) as well as orbitolines (M'Rabet, 1981).

Suborder Cytherocopina Jones, 1901

Superfamily Cytheroidea Baird, 1850

Family Cytherideidae Sars, 1925

Subfamily Cytherideinae Sars, 1925

Genus *Ovocytheridea* Grekoff, 1951

*Ovocytheridea triangularis* Piovesan, Cabral and Colin, 2014

### Pl. 3. Figure 1a-b

2000 *Ovocytheridea* aff. *O. producta* Grékoff, 1962-Viviers, Koutsoukos, Silva-Telles and Bengtson, p. 423, Figure 13, 21–22.

2014b *Ovocytheridea triangularis* Piovesan, Cabral & Colin, p. 325, pl. 4, figs. N–R.

2017 *Ovocytheridea* sp., B780- Donze-Jomaa-Salmouna et al., p. 537, pl 2, Figure 2a–c.

**Material:** 165 specimens of Boukezez Formation (E) and 77 specimens of Essen Formation (C-S) (samples: E1, E 3, E5, E28, E71, C15-C17, C23- C50, C74, C80, C136,C140-C149, C168, C180, S20, S28-S51).

**Measurements:** sample **E3, C, L: 0.83; H: 0.51; W: 0.32.**

**Description of the specimens:** The subtriangular aspect, as recognized in this work, is marked and elevated than in *Ovocytheridea* sp., B780- Donze, 2017. It similar from *Ovocytheridea* aff. *producta* Grékoff, 1962 by its developed antero-dorsal margin and the overlap on the right valve pronounced and more developed on the dorsal and ventral margins. Our specimen is very similar to that of Jomaa-Salmouna et al., (2017).

**Occurrence:** Coniacian and Santonian of Boukezez Formation.

**Distribution :** Turonian–Coniacian, Tunisia (Jomaa-Salmouna et al., (2017) Santonian–Campanian, Potiguar Basin, Brazil (Vivers et al., 2000; Piovesan et al., 2014b)

Family Hemicytheridae PURI 1953

Genus *Aysegulina* Ozdikmen 2010

*Limburgina* sp.

### Pl. 3. Figure 2a-c

1973 *Limburgina?* sp. M532 Donze–Donze in Bellion, et al., p. 16, Pl. II, figs. 26–30.

## CHAPTER III SYSTEMATIC

2017 *Limburgina?* sp. M532 Donze–Donze in Jomaa-Salmouna et al., p.541,pl. 4, Figure 4a–c.

2012 *Aysegulina sagitta* (Puckett and Colin) - Puckett et al., Plate 14, Figure 1-7

**Material:** 56 specimens (samples: E36– E45)

**Measurements:** sample **E36**, **C**, **L**: 0.58; **H**: 0.32; **W**: 0.41.

**Description of the specimens:** Carapace large, Subrectangular in lateral view, inflated in dorsal view. The dorsal and ventral outlines are straight. The anterior margin is rounded; the posterior part is sub-triangular. Right valve slightly larger than left valve. The ornamentation consists of clear reticulums and covers the lateral surface longitudinally and is in line with the medial tubercles. The greatest height is located near the anterior cardinal angle. In dorsal view, the carapace is compressed anteriorly and posteriorly. Eye tubercle and subcentral tubercles well developed. Lateral surface reticulated in lateral view. Maximum of width located at the posterior third.

**Remarks:** This species most common in the Maastrichtian deposits of Jamaica (Puckett et al., 2012) differs from *Aysegulina ventrocurva* (Puckett and Colin, 2012) in the widely flaring and nearly straight ventro-lateral carinae, forming arrowhead shape in ventral view, and the lack of longitudinal ridges in posterior portion of carapace.

*Aysegulina sagitta* (Puckett and Colin, 2012) very similar to *Limburgina?* sp. M532 (Donze–Donze in Bellion, et al., 1973) and *Limburgina* sp., 4 (Hazel and Kamiya, 1993), show similarity to this species in shape prominent ventro-lateral alae, eye tubercle, subcentral tubercles well developed and uniformly reticulate surface ornamentation.

**Occurrence:** Santonian of Boukezez Formation

*Aysegulina* sp.,

**Pl. 3. Figure 3**

1968 *Limburgina* sp. A – Margerie: 24, pl. 6, figs 2-4, cellule MA 57.

2017 *Aysegulina* sp., Guernet C. & Villier L. p. 242,

Type species: *Cypridina ornata* Bosquet, 1847 by subsequent designation.

**Material:** 15 specimens of Essen section (samples: C2, C3, C38, C42, S60)

**Measurements:** sample **S60**, **C**, **L**: 0.25; **H**: 0.40; **W**: 0.14.

**Remarques :** The genera *Aysegulina* and *Oertliella* Pokorny, 1964 (type species *Cythere reticulata* Kafka, 1886) appear to be closely related. Their type species have a number of common characteristics: dorsal edge of the valves inclined substantially backward and

## CHAPTER III SYSTEMATIC

roughly triangular tip, reticulate surface, numerous and straight marginal pore canals (which is a characteristic of the *Trachyleberididae* and not of the *Hemicytheridae*), amphidont hinge. On the other hand, *Oertliella reticulata* does not have the well-developed central tubercle of *Aysegulina ornata*. The hinge also appears significantly different, with (on the right valve) a slight crenulation of the anterior and posterior teeth and a slender anterior tooth with a base distinctly shorter than tall for *O. reticulata*, an anterior tooth taller than long, a deep, oval posterior alveolus, ventrally septate, and a posterior dental relief longer than tall, trilobed, with a median lobe dominating the other two for *Aysegulina ornata* (according to Pokorny 1964; Deroo 1966; Benson 1972; Liebau 1977). For *P. Margerie*, this species, represented by five valves or carapace in his collection, is "characterized by the great development, in the width direction, of the ventral wing, particularly at its posterior end." In addition, the meshes at the posterior end take the form of elongated alveoli.

**Occurrences :** Coniacian –Santonian of Essen Formation.

Suborder Podocopina Sars, 1866

Superfamily Cytheracea Baird, 1850

Family Trachyleberididae Sylvester- Bradley, 1948

Subfamily Trachyleberidinae Sylvester- Bradley, 1948

Genus *Sapucariella* Puckett, Andreu & Colin 2016

*Sapucariella parvoangulata* Andreu and Puckett, 2016

### Pl. 3, Figure 4a–c

1959 Ostracode T2- Glintzboeckel and Magné, pl. 4, Figure 43 (four images).

1961 *Brachycythere angulata* Grékoff- Apostolescu, p. 798, pl. 8, figs. 146–149.

1964 *Brachycythere* AUR 1478- Grékoff, pls. 1–2.

1973 *Brachycythere* sp. gr. *ekpo* forme *minor* nov. forme- Bellion et al., p. 17, pl. 3, figs. 1–5.

2016 *Sapucariella parvoangulata* Andreu and Puckett, nov. sp. - Puckett et al., p. 53, pl. 12, figs. 1–8.

2017 *Sapucariella parvoangulata* Andreu and Puckett nov. sp. - Jomaa-Salmouna et al., p. 538, pl. 3, Figure 1a–c.

**Material:** 34 specimens 4 Essen (samples: E1, E3, E36, C29, C35, C44)

**Measurements:** sample **E36, C, L: 0.77; H: 0.44; W: 0.64.**

**Remarks :** *Sapucariella parvoangulata* Puckett, Andreu and Colin, nov. sp., is very similar to *Sapucariella angulata* (Grékoff, 1951) in shape particularly in regard to the distinctive

## CHAPTER III SYSTEMATIC

posterodorsal angle, but is considerably smaller. The carapace is also less elongate than in *S. angulata*. Its similar to *Brachycythere angulata* Grékoff Apostolescu, 1961 in Campanian-Maastrichtian of Senegal, Ivory Coast, similar to *Brachycythere* sp. gr. *ekpo* forme *minor* (Bellion et al., 1973) in Late Turonian-Coniacian of Algeria and similar to Ostracode T2 Glintzboeckel and Magné, 1959 in Coniacian-Campanian of Tunisia in distinctive shape subtriangular to subtrapezoidal and without puncta in the median region of carapace. They are conspecific. This species is undoubtedly related to the *S. parvoangulata* complex of species and is descended from the stock.

**Occurrence:** Coniacian- Santonian of Boukezeze and Essen Formation

**Distribution :** Late Turonian–Coniacian of Algeria (Bellion et al., 1973); Coniacian–Campanian of Tunisia (Glintzboeckel and Magné, 1959); Turonian–Campanian of Tunisia (Abdallah et al., 1995, Jomaa-Salmouna et al., 2017); Campanian–Maastrichtian of Senegal and Ivory Coast (Apostolescu, 1961);

### *Sapucariella honigsteini* Puckett and Andreu 2016

#### Pl. 3. Figure 5a-b

1984 *Brachycythere angulata* Grékoff, 1951 – Honigstein, p. 16, pl. 5, figs. 1–7, pl. 15, Figure 2 (note muscle scar).

1985 *Brachycythere angulata* Grékoff, 1951 – Honigstein et al., pl. 11, Figure 51.

1985 *Brachycythere angulata* Grékoff, 1951 – Lipson-Benitah et al., Figure 5p.

1986 *Brachycythere angulata* Grékoff, 1951 – Honigstein, pl.1, figs. 1–4, 6.

2016 *Sapucariella honigsteini* Puckett and Andreu, nov. sp. pl. 10, Figs. 1–9, 12

**Material:** 40 specimens of Essen section (samples: C71, C74, C75, C81-C85, C87, C100, C102, C127- C143, S60).

**Measurements:** sample C71, S60, C, L: 0.83, H: 0.53, W:0.45

**Description of the specimens:** Carapace large, robust, with a smoothly and broadly rounded anterior margin and greatest anterior extremity just below mid-height, a very broadly convex ventral margin that is upturned in the posterior part leading to an acuminate posterior margin with greatest extremity at approximately height, and a broadly convex dorsoposterior margin with a very open to barely perceptible dorsoposterior angle with greatest height just behind prominent eyespot at approximately length; ventrolateral area swollen, with greatest width just above venter, well-rounded in larger morphs and more angular in smaller morphs. Left valve overlaps right, with greatest overlap along dorsal and ventral margins. Eyespot distinctive, with prominent postocular depression. Surface punctate, with widely-

## CHAPTER III SYSTEMATIC

varying degrees of punctuation ranging from nearly smooth to distinctively punctate. Hinge typical of genus, in right valve with anterior tooth, subjacent socket, finely crenulate median bar, and crenulate posterior tooth; hinge of left valve complements that of right. Anterior marginal pore canals occur in pairs.

**Remarks:** This species is named in honor of Dr. Avi Honigstein, Geological Survey of Palestine, for his contributions to Cretaceous ostracode studies of Palestine. Table 9 presents measurements of *Sapucariella honigsteini* nov. sp.

**Occurrences :** Coniacian-Santonian of Essen Formation.

Genus *Trachyleberidea* Bowen, 1953

*Trachyleberidea* gr. *geinitzi* (Reuss, 1874)

### Pl. 3. Figure 6a-c

1874 *Cytheregeinitzi* n. sp.- Reuss, p. 146, pl. II, Figure 4 a, b.

1980 *Trachyleberidea geinitzi* (Reuss)- Babinot, pl. 27, Figure 3–14.

1985 *Trachyleberidea* gr. *geinitzi* (Reuss)-Vivière, p. 203, 204, pl. 14, Figure 10, 11; pl. 15, figs. 1–4.

2006 *Trachyleberidea geinitzi* (Reuss)- Andreu and Bilotte, p. 67, pl. 4, figs. 9–10.

2008 *Trachyleberidea geinitzi* (Reuss)- El Nady et al., p. 555, pl. VI, Figure 13.

2017 *Trachyleberidea* gr. *geinitzi* (Reuss)- Jomaa-Salmouna et al., pl. 3, fig 6a–c.

**Material:** 12 specimens (samples: E1, E3, E5)

**Measurements:** sample **E1, C**, adult; **L: 0.91; H: 0.33; W: 0.24.**

**Occurrence:** Coniacian of Boukezez Formation

**Distribution :** Coniacian–Campanian of Tunisia (Jomaa-Salmouna, 2017); Turonian of South-Eastern France (Andreu and Bilotte, 2006); late Turonian of Egypt (El-Nady et al., 2008); Coniacian of Algeria (Vivière, 1985); Coniacian of Tunisia; Late Cretaceous (Babinot, 1980);

Genus *Trachyleberidea* Bowen, 1953

*Trachyleberididae* sp.,

### Pl. 3. Figure 7a-b

**Material:** 46 specimens of Essen section (samples: C23, C32, C56-C59, C72, C84, C85, C89, C100, C101, C123, C131, C140, C172, S1, S20, S48, S47)

**Measurements:** C23, S1 **L: 0.66; H: 0.42; W: 0.26.**

**Occurrences :** Coniacian –Santonian of Essen Formation.

**Distribution :** Upper Cretaceous of Algeria (Vivière, 1985), and Morocco (Donze et al., 1982),

## CHAPTER III SYSTEMATIC

Genus *Spinoleberis* Deroo, 1966

*Spinoleberis yotvataensis* Rosenfeld, 1974

### Pl .3. Figure 8a-d

1968 *Cythereis* EmJS 1333 Grékoff, pl. 1, Figure 10 a–b.

1981 *Spinoleberis yotvataensis* Rosenfeld- Bismuth et al., p. 235, pl. 11, figs. 4–6.

1985 *Spinoleberis?* gr. *yotvataensis* Rosenfeld- Vivière, p. 191, pl. 12, figs. 4–9.

1989 *Spinoleberis?* *yotvataensis?* Rosenfeld- Majoran, p. 27, pl. 16, figs. 10–12.

1995 *Spinoleberis yotvataensis* Rosenfeld - Bismuth et al., p. 137, pl. 2, Figure 12.

2008 *Spinoleberis yotvataensis* Rosenfeld - El Nady et al., p. 555, pl. VI, figs. 10–12.

2016 *Spinoleberis yotvataensis* Rosenfeld - Benmansour et al., p. 201, pl 26, figs. 12–20.

2017 *Spinoleberis yotvataensis* Rosenfeld-Jomaa-Salmouna et al., p38.pl. 3, Figure 5a–c

**Material:** 147 specimens (samples: E1, E3, E5, E36 - E45, E63, E69, E71)

**Measurements:** sample **E5, E36, C**, 8a-b: Female, 88c-d: Male; **L:** 0.66; **H:** 0.36; **W:** 0.36.

**Remarks:** Our specimens are predominantly smooth, with tubercles clearly visible on the surface of the valves. Significant phenotypic variations in this species have been mentioned by Vivière (1985), Andreu-Boussut (1991) and Benmansour (2016).

**Occurrence:** Coniacian and Santonian of Boukezez Formation and Essen Formation.

**Distribution:** Middle Turonian of Tunisia (Bismuth et al., 1981) and Algeria (Grekoff, 1968, Majoran, 1989); Coniacian–Campanian of Dj. Dyr, Tebessa, from Algeria (Vivière, 1985); Turonian–Coniacian of Morocco (Bismuth et al., 1995); Middle Turonian–Lower Coniacian of Tunisia (Jomaa-Salmouna et al., 2017); Coniacian of Egypt (El Nady et al., 2008); Santonian of Morocco (Algouti et al., 2015); Campanian from Mena and El Kantara from Algeria (Benmansour et al., 2016);

Genus *Cythereis* Jones, 1849

*Cythereis* gr. *rawashensis* Van den Bold, 1964

### Pl .4. Figure 1

1964 *Cythereis rawashensis* n. sp.-Van den Bold, p. 124, pl. 15, figs. 1 a, b, 2 a, b.

1985 *Cythereis* gr. *rawashensis* Van den Bold-Vivière, p.180–184, pl. 10, figs. 1–16.

1991 *Cythereis rawashensis* Van den Bold-Shahin, p. 141, pl. 3, figs. 13, 14.

2017 *Cythereis* gr. *rawashensis* Van den Bold -Jomaa-Salmouna et al., pl. 3, Figure 3a–c.

**Material:** 15 specimens (samples: E3, E36– E45)

**Measurements:** sample **E36, C**, adult male; **L:** 0.63; **H:** 0.33; **W:** 0.10.

**Remarks:** the present material has a marked wing, clavicular spines and prominent marginal denticles with accentuated reticulation on the dorsal part.

## CHAPTER III SYSTEMATIC

**Occurrence:** Coniacian and Santonian of Boukezez Formation.

**Distribution :** Mid-Turonian–Campanian of Egypt (Van den Bold, 1964); Turonian and Coniacian of Algeria (Vivière, 1985) and Tunisia (Jomaa-Salmouna et al., 2017); Cenomanian–Late Turonian from Sinai, Egypt (Shahin, 1991);

### *Cythereis* sp. 1

#### Pl .4. Figure 2

**Material:** 5 specimens samples: E3, E36– E45(Boukezez) and 65 specimens samples C2, C5, C13, C53-C57, 77-C80, C84-C88, S42, S47, S53 (Essen).

**Measurements:** sample **E3, C42, C, L:** 0.6 3; **H:** 0.33; **W:** 0.10.

**Description of the specimens:** Carapace subrectangular. The posterior outline is sub-triangular and with denticulations along the periphery. The anterior outline is symmetrically rounded. The dorsal and ventral margins are straight. Subcentral tubercle positioned in front of the mid-length. Two robust tubercles located in the posterodorsal and posteroventral regions. Small tubercles distributed in the valves surface. Prominent rounded ocular tubercle.

**Occurrence:** Coniacian and Santonian of Boukezez and Essen Formations.

### *Cythereis* sp. 2

#### Pl .4. Figure 3

**Material:** 6 specimens (samples: E1, E36, E45, E71) of Boukeez and **12** specimens of Essen (samples: C80, C127, C140, C180, S14, S15, S42, S47).

**Measurements:** Sampele **E36, C, L:** 0.64; **H:** 0. 36; **W:** 0.15.

**Description of the specimens:** Subrectangular in lateral view, lanceolate in dorsal view. Maximum height located at the anterior cardinal angle, maximum width at mid-length. The ventral and dorsal margins are straight. The anterior margin is rounded and present denticules; the posterior one is sub-triangular. The central tubercle is prominent and located in the central part of the valves surface; eye tubercle small. Carapace reticulated, with two large ribs, in the ventrolateral and dorsal regions; presents three spines on the posteroventral margin.

**Remarks:** Our species is similar to *Cythereis cretaria* described in Campanian of Egypt (Bold, 1964), which presents an acute median part of the posterior end and small spines on the posteroventral margin.

**Occurrence:** Coniacian and Santonian of Boukezez and Essen Formations

### *Cythereis* sp.,3

#### Pl. 4. Figure 4

**Material:** **26** specimens of Essen section (samples: C26, C33, C42-C45, C57-C60).

**Measurements:** **C26**

## CHAPTER III SYSTEMATIC

**Remarks :** These specimens are like Algeriana in possessing lateral ridges consisting of disconnected tubercles and a predominantly smooth intercostal shell surface. There is also a well developed posteroventral boss below the ventral ridge. The size and overall shape, however, differ markedly from Algeriana. The earapae is subtrapezoidal to subtriangular in lateral aspect. Contrary to Algeriana, the hinge-ear is more pronounced as is also the eye-tubercle and particularly the subcentral tubercle. The anterior margin is rimmed and faintly studded, though not as broad and evenly rounded as in Algeriana. The triangular posterior margin is also rimmed and bears a few rounded denticles along its convex ventral section (see ventral view) ; its dorsal section is straight and reaches below mid-height. The ventral surface is coarse and irregular. Sexual dimorphism appears to be present, with the presumed males being longer.

**Occurrences :** Coniacian of Essen Formation.

*Cythereis fahrioni bigrandis* Majoran, 1989

### Pl. 4. Figure 5a-b

1963 *Cythereis fahrioni* Bischoff 31-33, Pl. 12, figs 90-93, figure 94

1981 *Cythereis cf. fahrioni* Bischoff; Bismuth et al., 23 1, p1.9, figs 6- 8

1988 *Cythereis cf. fahrioni* Bischoff; Athersuch: p1. 3, figs 5,6

**Material:** 22 specimens of Essen section (samples: C57-C60, C130, C159, C160, S3).

**Measurements:** C60, C, L: 0.50; H: 0.32; W: 0.25.

**Description:** The carapace is medium to large in size, with a fully reticulate surface and a subrectangular to trapezoidal outline in lateral view. Its greatest height occurs at the moderately to strongly developed hinge ear. The left valve slightly overlaps the right along the dorsal part of the posterior margin. The eye tubercle is hemispherical and distinctly prominent. The anterior margin is broadly rounded with a slight oblique orientation and is ornamented with coarse denticles alternating with fine papillae along its frontal edge (visible in ventral view). In lateral view, a narrow rim extends from the eye tubercle and runs parallel to the anterior margin, reaching the junction with the ventral margin. This rim bears short pore conuli or sieve plates, which can occasionally be celate in the ventral region. The ventral margin appears sinuous due to a pronounced inflexure where it meets the anterior margin. The dorsal margin is straight. The posterior margin is triangular in the right valve and more rounded in the left, with its convex ventral portion decorated similarly to the anterior margin. The lateral surface displays a uniform reticulation. Distinct plications are present on the valve surface, forming a subcentral tubercle and three lateral ridges. The dorsal ridge extends beyond the dorsal margin, creating a shallow furrow along the valve border. The ventral

### CHAPTER III SYSTEMATIC

surface is triangular and characterized by rounded fossae. The maximum width is located across the posteromedian region. Both the internal and external morphological features are consistent with the genus *Cythereis*, as defined by Van Morkhoven (1963, pp. 179–182) and Damotte (1977).

**Remarks :** Bischoff (1963) originally described this species from the Albian of Lebanon. Later, Bismuth et al. (1981) and Athersuch (1988) reported *C. cf. fahrioni* from the Albian–Cenomanian of Tunisia and the Albian of Oman, respectively. These specimens are regarded here as true representatives of the species. The material from the Bordj Ghdir section is also considered conspecific, with the postero-terminal knob of this ridge appearing noticeably more pronounced.

**Occurrence :** Coniacian and Santonian of Essen Formation

**Distribution :** In Algeria, MAJORAN, 1989 described *C. fahrioni bigrandis* in the Upper Albian of Bordj Ghdir and Ras-El-Oued.

#### *Cythereis kosticensis* Pokorny, 1963

##### Pl. 4. Figure 6a-b

**Material:** 22 specimens of Essen section (samples: C10, C25, C44, C84-C82, C174-C177, S32- S34, S42).

**Measurements:** C10, L: 0.46; H: 0.22; W: 0.15.

**Occurrences :** Coniacian-Santonian Essen Formation

**Distribution :** Turonian

#### *Cythereis namousensis* Bassoullet & Damotte, 1969

##### Pl. 4. Figure 7a-b

1969 *Cythereis namousensis* Bassoullet & Damotte, pp. 134, 135, pl. 1, figs 3 a-d.

1974 *Cythereis namousensis* Bassoullet & Damotte.– Rosenfeld & Raab, p. 17, pl. 3, figs 17, 18.

1977 *Cythereis namousensis* Bassoullet & Damotte.– Boukhary *et al.*, p. 158, pl. 1, Figure 5a-d.

1980 *Cythereis namousensis* Bassoullet & Damotte.– Ben Youssef, p. 78, pl. 6, figs 5-8.

1981 *Cythereis namousensis* Bassoullet & Damotte.– Bismuth *et al.*, p. 232, pl. 9, figs 9-10.

1983 *Cythereis (Rehacythereis) namousensis* Bassoullet & Damotte.– Gargouri-Razgallah, p. 154, pl. 29, Figure 1.

1985 *Rehacythereis cf. namousensis* (Bassoullet & Damotte).– Babinot & Basha, pp. 260, 261.

1985 *Cythereis cf. namousensis* Bassoullet & Damotte.– Vivière, pp. 174, 175, pl. 8, figs 6, 7.

1989 *Cythereis namousensis* Bassoullet & Damotte.– Majoran, p. 21, pl. 10, figs 13-16.

### CHAPTER III SYSTEMATIC

- 1991 *Cythereis namousensis* Bassoullet & Damotte.– Shahin, p. 145, pl. 3, Figure 12.
1994. *Cythereis namousensis* Bassoullet & Damotte.– Shanin *et al.*, p. 56, pl. 3, figs 21, 22.  
cf. 1995. *Cythereis namousensis* Bassoullet & Damotte.– Bismuth *et al.*, p. 135.
1995. *Cythereis namousensis* Bassoullet & Damotte.– Abdallah *et al.*, p. 531, Figure 20.10.
2001. *Cythereis namousensis* Bassoullet & Damotte.– Ismail, figs 13.9, 10.
2001. *Cythereis namousensis* Bassoullet & Damotte.– Morsi & Bauer, p. 392, pl. 4, figs 10, 11.
2002. *Cythereis namousensis* Bassoullet & Damotte.– Bassiouni, p. 70, pl. 15, figs 13-16.
2009. *Cythereis namousensis* Bassoullet & Damotte.– Boukhary *et al.*, pp. 24, 25, pl. 2, figs 1-5.
2010. *Cythereis namousensis* Bassoullet & Damotte.– Morsi & Wendler, p. 199, Figure 6.15-20.
- 2016 *Cythereis namousensis* Bassoullet & Damotte.– Mebarki *et al.*, Pl. III, Figure 33-36

**Material:** 73 specimens (samples: E39- E45, E53, E64)

**Measurements:** sample **E64**, **C, L:** 0.44; **H:** 0.12; **W:** 0.25.

**Remark:** *Cythereis namousensis* and *C. algeriana*, which are larger, are morphologically similar.

**Occurrence:** Santonian of the Essen Formation.

**Distribution:** Late Cenomanian of the Guir Basin, Western Saharan Atlas (Bassoullet & Damotte, 1969) and NE Algeria (Vivière, 1985). Middle and Late Cenomanian of Tunisia (Bismuth *et al.*, 1981, 1995; Gargouri-Razgallah, 1983). Cenomanian from Egypt (Boukhary *et al.*, 1977; Shahin, 1991; Shahin *et al.*, 1994; Ismail, 2001; Morsi & Bauer, 2001; Bassiouni, 2002; Boukhary *et al.*, 2009), from the Levant (Rosenfeld & Raab, 1974; Rehacythereis cf. *namousensis* in Babinot & Basha, 1985;

**Type species:** *Cytherinae ornatissima* Reuss, 1846

***Cythereis algeriana* Bassoullet & Damotte, 1969**

#### **Pl. 4. Figure 8a-b**

- 1969 *Cythereis algeriana* Bassoullet & Damotte, pp. 132, 133, pl. 1, figs 1 a-d.
- 1972 *Cythereis algeriana* Bassoullet & Damotte.– Damotte & Saint-Marc, p. 278, pl. 1, Figure 4.
1973. *Cythereis algeriana* Bassoullet & Damotte.– Grosdidier, pl. 12, Figure 95a-e.
- 1974 *Cythereis algeriana* Bassoullet & Damotte.– Rosenfeld & Raab, p. 17, pl. 3, figs 19, 20.
- 1981 *Cythereis algeriana* Bassoullet & Damotte.– Bismuth *et al.*, pp. 230, 231, pl. 10, Figure 15.

### CHAPTER III SYSTEMATIC

1981 *Cythereis algeriana* Bassoullet & Damotte.– Al-Abdul- Razzaq & Grosdidier, p. 188, pl. 1, Figure 4.

1983 *Cythereis (Rehacythrereis) algeriana* Bassoullet & Damotte.– Gargouri-Razgallah, p. 154, pl. 30, figs 6, 7.

1985 *Cythereis algeriana* Bassoullet & Damotte.– Vivière, p. 175, pl. 8, figs 8, 9.

1989 *Rehacythrereis algeriana* (Bassoullet & Damotte).– Babinot & Bourdillon-de-Grissac, pp. 289, 290).

1988 *Cythereis algeriana* Bassoullet & Damotte.– Athersuch, pl. 3, figs 11, 12.

1991 *Cythereis algeriana* Bassoullet & Damotte.– Andreu, pp. 618-620, pl. 56, figs 1-4.

1994 *Cythereis algeriana* Bassoullet & Damotte.– Shahin *et al.*, p. 54, pl. 3, figs 14, 15.

2001 *Cythereis algeriana* Bassoullet & Damotte.– Morsi & Bauer, pp. 391, 392, pl. 4, figs 4, 5.

2013 *Cythereis algeriana* Bassoullet & Damotte.– Andreu *et al.*, pl. 7, figs 30, 31 ; pl. 8, figs 1-5.

2013a *Cytherella aegyptiensis* Colin and El Dakkak.– Shahin *et al.*, p. 107, Pl. 1 Figs. 1, 2,

2016 *Cythereis algeriana* Bassoullet & Damotte.– Mebarki *et al.* ., pl. III, Figure 29-32

**Matériel** : 83 specimens (samples: C8, C12, C15, C17, C29, C33, C38, C49, C52, C56, C61-C63, C65-C67, C73-C75, C147, C154, C159, C164, S13, S47-S62)

**Measurements** : **C73, C, L**: 0.36; **H**: 0.22; **W**: 0.20.

**Remarks**: Size smaller than that of the type species.

**Occurrence**: Conaician and Santonian of the Essen Formation.

**Distribution**: Late Cenomanian of the Guir Basin, the Western Saharan Atlas (Bassoullet & Damotte, 1969), and NE Algeria (Vivière, 1985).

Cenomanian-Lower Turonian of Morocco (Andreu, 1991; Andreu *et al.*, 2013). Middle and Late Cenomanian of Tunisia (Bismuth *et al.*, 1981; Gargouri-Razgallah, 1983). Cenomanian of Egypt (Shahin *et al.*, 1994; Morsi & Bauer, 2001) and Kuwait (Al-Abdul-Razzaq & Grosdidier, 1981). Middle and Upper Cenomanian of the Levant (Damotte & Saint-Marc, 1972; Rosenfeld & Raab, 1974). Upper Albian-Lower Cenomanian of Iran (Grosdisier, 1973). Upper Albian-Upper Cenomanian of Oman (Athersuch, 1988; *Rehacythereis algeriana* in Babinot & Bourdillon-de-Grissac, 1989).

Genus *Protocosta* Bertels, 1969

*Protocosta babinoti* Piovesan, Cabral and Colin, 2014

**Pl. 4. Figure 9 a-b**

## CHAPTER III SYSTEMATIC

2000 *Cythereis?* sp. P8 Viviers, Koutsoukos, Silva-Telles and Bengtson, p. 433, Figure 19, 3–4.

2014a *Protocosta babinoti* Piovesan, Cabral and Colin, p. 329, pl. 6, figs. K–P.

2014b *Protocosta babinoti* Piovesan, Cabral and Colin- Piovesan et al., p. 335, pl. 5, figs. K–P.

2020 *Protocosta babinoti* Piovesan, Cabral and Colin- Piovesan et al., p. 87, Figure 4D–E.

**Material:** 71 specimens 4 specimens Essen (samples: E36– E45, E53, E56, E58, E61, S42)

**Measurements:** sample **E61**, **C**, **L**: 0.79; **H**: 0.43; **W**: 0.27.

**Description of the specimens:** Very large reticulated carapace, subrectangular in lateral view. Dorsal margin almost straight. Ventral margin slightly concave anteriorly. Rounded anteriormargin. Posterior margin is somewhat triangular. Both margins are compressed. Maximum height is at anterior cardinal angle. Maximum width is in front of mid-length while is maximum length at mid-height. Left valve overlaps right one along all margins. The dorsal rib is convex while the ventral rib is almost straight. The middle rib is sinuous and moderate in its anterior part. A small distinct ocular tubercle is present while the subcentral tubercle is underdeveloped.

**Remarks :** *Protocosta babinoti* Piovesan, Cabral and Colin, 2014, very similar to *Cythereis?* sp. P8. Viviers, 2000 in Santonian–lower Campanian from Potiguar Basin Jandaira Fm in shape and ornamentation. Left valve overlaps right one along all margins. A small distinct ocular tubercle is present while the subcentral tubercle is underdeveloped.

**Occurrence:** Coniacian of Boukezez Formation and Santonian of Essen Formation.

**Distribution:** Coniacian and Santonian in Tunisia (Jomaa-Salmouna et al., 2017); Santonian–Campanian of the Potiguar Basin (Piovesan et al, 2014b) ; Santonian–Campanian of the Potiguar Basin, Brazil (Piovesan et al., 2014a and b; Viviers et al., 2000);

### *Paraplatycosta* sp.

#### **Pl. 4. Figure 10a-b**

2014b *Paraplatycosta* POT 1- Piovesan, Cabral and Colin, p. 331, pl. 7, figs. D–E.

**Material:** 2 specimens (sample: E45)

**Measurements:** sample **E45**, **C**, juveniles; **L**: 0.50; **H**: 0.20; **W**: 0.12.

**Description of the specimens:** Reticulated carapace. Subrectangular in lateral view and subtrapezoidal in dorsal view. Anterior margin rounded, posterior margin triangular. Maximum height at anterior cardinal angle, maximum width at posterior third, maximum length below mid-height. Presence of subcentral, ocular tubercles and two fine ribs: median and ventral. Two tubercles occur near the posteroventral and posterodorsal regions.

## CHAPTER III SYSTEMATIC

**Remarks:** This species differs from *Paraplatycosta* aff. *talayninensis* Santonian–Campanian of the Potiguar Basin, Brazil described by (Piovesan et al., 2014b) due the presence of tubercles in the posterodorsal and posteroventral margins, less developed ribs and the position of maximum length, which is below the midheight.

**Occurrences:** Santonian of Boukezez Formation.

**Distribution :** Santonian–Campanian of the Potiguar Basin, Brazil in Brazil (Piovesan et al., 2014b).

Genus *Paraplatycosta* Dingle, 1971

*Paraplatycosta* aff. *talayninensis* Andreu, 1995

### Pl. 4. Figure 11

2014 b *Paraplatycosta* aff. *talayninensis* Andreu- Piovesan et al., p.331, pl. 7, figs. A–C

**Material:** 8 specimens of Boukezez Formation and 105 specimens of Essen Formation (samples: E36, E41, E43, E53, E54, C1,C2, C6, C7, C11-C57, C65-C75, C84-C90, C115, C164, C169-C180, S1-S7, S15, S27, S60 )

**Measurements:** sample **S1, C, L:** 0.55; **H:** 0.26; **W:** 0.24.

**Remarks:** Our specimens have affinities with *P. talayninensis* described by Andreu (1995) in Morocco, but are more elongate and with irregular size of the reticula. Despite the similarities in outline between the species, our material is smaller than those mentioned by Benmansour et al., 2016, which could be related with the ontogeny.

**Occurrence:** Coniacian and Santonian of Boukezez and Essen Formation. **Distribution :** Santonian–Campanian of the Potiguar Basin, Brazil (Piovesan et al., 2014b);

Genus *Haughtonileberis* Dingle, 1969

*Haughtonileberis dinglei* Piovesan, Cabral & Colin, 2014

### Pl. 4. Figure 12

1992 *Dumontina* sp. Okosun, p. 330, pl. 1, figs. 21, 25.

2014a *Haughtonileberis dinglei* Piovesan et al., p. pl.5, Figure M–S.

**Material:** 8 specimens (samples: E36, E41, E43, E53, E54)

**Measurements:** Sample **E36, C, L:** 0.55; **H:** 0.26; **W:** 0.24.

**Remarks:** This species is similar of the Morocco species *Haughtonileberis propeplanus* described by Andreu (1995) from the late Santonian of Morocco, but differs by the much more developed anteromarginal rib, the stronger spines in the anterior margin and the dorsal and the median rib, which are not linked.

**Occurrence:** Santonian of Boukezez Formation

### CHAPTER III SYSTEMATIC

**Distribution :** Turonian–Santonian of Nigeria (Okosun, 1992); Turonian, Potiguar Basin, Brazil (Piovesan et al., 2014a);

Subfamily Buntoniinae Apostolescu, 1961

Genus *Protobuntonia* Grekoff, 1954

*Protobuntonia numidica* Grekoff, 1954

#### Pl. 4. Figure 13a-b

1954 *Protobuntonia numidica* n. gen. n. sp. Grekoff, p. 400, text-Figure 1

1959 *Buntonia (Protobuntonia) numidica* Grekoff– Reyment et Elofson, p. 163, pl. 1, Figure 3

1964 *Protobuntonia numidica* Grekoff– Van Den Bold, p. 126, pl. 13, figs. 16–17

1966 *Protobuntonia numidica* Grekoff – Masoli, p. 126, pl. 2, Figure 9

1973 *Protobuntonia numidica* Grekoff – Bellion et al., p. 19, pl. 4, figs. 30– 34

1973 *Protobuntonia numidica* Grekoff – Said, p. 226, pl. 25, Figure 9

1982 *Protobuntonia numidica* Grekoff – Reyment, p. 412, Figure 2a

1985 *Protobuntonia numidica* Grekoff – Vivière, p. 236, pl. 22, figs. 5–8

1987 *Protobuntonia numidica* Grekoff - Damotte and Fleury, p. 107, pl.3, Figure 15

1996 *Protobuntonia numidica* Grekoff - Andreu and Tronchetti, p.61, Pl. 6, Figure 16

2016 *Protobuntonia numidica* Grekoff- Benmansour et al., 2016, p. 193, pl. 22, 27-28; S–figs. 9, 1-4.

**Material:** 14 specimens of Bouezez section and 3 specimens of Essen section (samples: E44, E45, E71, C29, C127, S48-S44)

**Measurements:** sample **E44, S44, C**, adult; **L:** 0.79; **H:** 0.43; **W:** 0.27.

**Occurrence:** Santonian of Bouezez and Coniacian- Santonian of Essen Formation.

**Distribution :** Turonian–Coniacian of Morocco (Andreu and Tronchetti, 1996); late Turonian–late Santonian of Morocco (Reyment et Elofson, 1959); late Turonian–Campanian to Dj. Dyr, Algeria (Vivière 1985); Turonian–Lower Campanian of Morocco (Masoli, 1966; Reyment, 1982); late Turonian–Maastrichtian of Algeria (Bellion et al., 1973); Turonian–Thanetian of Algeria (Grekoff, 1954); Santonian–Campanian of Egypt (Van Den Bold, 1964); Coniacian to Maastrichtian of South-West Constantine, Algeria (Damotte and Fleury, 1987); Campanian of Tighanimine and Mena, Algeria (Benmansour 2016); Thanetian of Tunisia (Said, 1973); Subfamily Pterygocytherinae Puri, 1957

Genus *Pterygocythere* Hill, 1954

*Pterygocythere aff. allinensis* Grekoff and Deroo, 1956

#### Pl. 5. Figure 1a-b

### CHAPTER III SYSTEMATIC

aff. 1956 *Alatacythere allinensis* n. sp. – Grekoff and Deroo, p.229, pl. XLVII, Figure 34–35.

**Material:** 6 specimens (samples: E36, E41, E28, C180, C123-C127, C85-C88, C59-C70)

**Measurements:** sample **E36, C, L: 0.69; H: 0.53; W: 0.36.**

**Occurrence:** Santonian of Boukezez Formation.

**Distribution :** Coniacian of Morocco (Algouti et al., 2022),

*Pterygocythere* sp.,

**Pl. 5. Figure 2**

**Material:** 6 specimens (samples: C12, C13, C127)

**Measurements:** sample **E36, C, L: 0.69; H: 0.53; W: 0.36.**

**Occurrence:** Lower Coniacian of Essen Formation.

Genre *Taracythere* AYRESS, 1995

*Taracythere antakaranaensis* nov. sp. Jean-François Babinot, Jean-Paul Colin, Auran  
Randrianasolo 2009

**Pl. 5. Figure 3a-c**

1979. *Cythereis* DS3 GREKOFF – COLLIGNON *et alii*, p. 236, Pl. 4, Figure 14a-b.

2009 *Taracythere antakaranaensis* nov. sp. Babinot, pl. 2, figs. 12-19, p. 10

**Material:** specimens of Essen section (samples: C3, C5, C25, C80, C84, C85, C169-C176, S1, S6, S28).

**Measurements:** **S1, C, L: 0.56; H: 0.32; W: 0.25.**

**Description of the specimens:** Species assigned to the genus *Taracythere* characterized by a subrectangular carapace, a non-raised triangular posterior end, and complex ornamentation.

**Remarks:** The genus *Taracythere* was described by Ayress (1995) for species of *Trachyleberididae* without an ocular tubercle or cardinal lobe from the Eocene of New Zealand. Subsequently, Jellinek & Swanson (2003) revised this genus based on current material. In this study, they demonstrate that this genus is not restricted to New Zealand and that other species that can be assigned to it are known from the Paleogene of the Indian Ocean, notably *Actinocythereis orientalis orientalis* Guernet, 1985, and *Actinocythereis orientalis rete* Guernet, 1993 (see also Guernet & Galbrun, 1992). *Taracythere antakaranaensis* nov. sp., by its general morphology (posterior end not raised, presence of a muscular nodule, and well-individualized and nodular ventral and dorsal ridges), is much closer to the Paleogene forms of the Indian Ocean. The ornamentation affects the entire surface of the valves.

**Occurrences :** Coniacian and Santonian of Essen Formation.

## CHAPTER III SYSTEMATIC

**Distribution :** Lower Cenomanian Abattoir section, Andranomaimbo Formation, terminal Albian (Vraconian) to Lower Cenomanian of Madagascar.

**Family:** Bairdiidae

**Genus:** *Peloriops*

***Peloriops pustulata* (Rosenfeld & Raab, 1974)**

**Pl. 5. Figure 4a-c**

1974 *Planileberis pustulata* n.sp. Rosenfeld in Rosenfeld & RAAB, p. 19, pl. 3, fi gs. 2–5; pl. 6, fi gs. 1–4

1977 *Planileberis pustulata* Rosenfeld – Boukhary et al., p. 159, pl. 1, fi gs. 1a–d

1979 *Peloriops ulosa* n.sp. Al-abdul-Razzaq, p. 51, pl. 1, fi gs. 4–5, 11, 15; pl. 2, fi g.3

1981a *Cythereis ziregensis* Bassoullet & Damotte–Bismuth et al., p. 234, pl. 8, fi gs. 9–12

1988 *Peloriops ulosa* Al-abdul-Razzaq–Athersuch, p. 1203, pl. 4, fi g. 10–11 pars 1989 *Peloriops ziregensis?* (Bassoullet & Damotte) – MAJORAN, p. 24, pl. 15, fi gs. 4–13; non pl. 15, fi gs. 1–3

1991 *Peloriops* sp. Szczechura et al., p. 25, pl. 8, fi g. 8

1994 *Peloriops ulosa* Al-abdul-Razzaq – Athersuch 1994, p. 263, pl. 12.2, fi gs. 2, 4

1994 *Planileberis pustulata* Rosenfeld – Shahin et al., p. 57, pl. 3, fi gs. 29–31

2001 *Peloriops pustulata* (Rosenfeld) – Morsi & Bauer, p. 394, pl. 5, fi gs. 6–7, 9

2002 *Peloriops pustulata* (Rosenfeld) – BASSIOUNI, p. 88, pl. 21, fi gs. 9–13

2009 *Peloriops pustulata* Rosenfeld and Raab,-Boukhary et al., pl. 2, figs. 8–10

2013a *Peloriops postulata* Rosenfeld- Shahin et al., p.113 , pl. 4 figs. 21, 22

**Material:** 13 specimens of Essen section (samples: C158- C169, S6, S58-S62).

**Measurements:** C158, C, L: 0.66–0.70 ; H: 0.37–0.47; W: 0.24–0.31.

**Description of the specimens:** The carapace of *P. pustulata* is elongate, ranging from subrectangular to subovale in lateral view. The dorsal margin appears straight to slightly convex, while the ventral margin is gently concave. The anterior end is broadly rounded, contrasting with the posterior end, which is more tapered and subacute. This species is of medium size for the genus, with valve lengths, although dimensions may vary slightly. The most distinctive feature of *P. pustulata* is its characteristic surface ornamentation, consisting of numerous small, rounded to irregular pustules or tubercles. These pustules may be evenly distributed or more concentrated in the central and posterior parts of the carapace, serving as a

### CHAPTER III SYSTEMATIC

key diagnostic trait that differentiates this species from other members of the genus *Peloriops*, which usually display smoother or striated surfaces.

**Remarks :** The representative of this species closely resembles specimens previously assigned to *Cythereis* (now correctly referred to as *Peloriops*) *pustulata*, originally described by Rosenfeld (1974) from the Cenomanian of Palestine, as well as *Peloriops sphaerommata* described by Al-Abdul-Razzaq (1974) from the Cenomanian of Kuwait. Similar observations regarding the relationships among these species were reported by Bismuth et al. (1981), Athersuch (1988), and Majoran (1989), with some authors even suggesting that *P. sphaerommata* may be closely related to other recognized species. In 1983, Al-Abdul-Razzaq proposed placing *P. sp haerommata* in synonymy with *P. ziregensis*. However, Majoran (1989) questioned whether these species are truly conspecific and tentatively assigned his Cenomanian specimens from Algeria to *P. ziregensis* with uncertainty. The primary differences among these taxa involve variations in size and ornamentation details, which may reflect intraspecific variability. Due to the lack of a clear photograph of the *P. ziregensis* holotype and the presence of only a single specimen of *Peloriops* sp., in the our ostracode collection, its taxonomic status remains unresolved.

**Occurrences :** Upper Coniacian-Santonian of Essen Formation.

**Distribution:** This species was first described from the Cenomanian of Palestine (Rosenfeld & Raab, 1974). It is also known from the Cenomanian of Algeria (Majoran, 1989), Tunisia (BISMUTH et al., 1981a), Kuwait (AL-Abdul-Razzaq, 1979), and Egypt (Boukhary et al., 1977; SHahin et al., 1991; Szczechura et al., 1991; Morsi & Bauer, 2001; Bassiouni, 2002), Upper Cenomanian in south of Ain Sukhna, western side of the Gulf of Suez, Egypt (Bouhary et al., 2009)

Genus *Reticulocosta* Grundel, 1974

***Reticulocosta kanaanensis* (Rosenfeld 1974, in Rosenfeld & Raab 1974)**

#### **Pl. 5. Figure 5a-c**

1974 *Cythereis rawashensis kanaanensis* Rosenfeld, n. s sp., in Rosenfeld & Raab, p. 17, pl. 3, figs 23–25; pl. 6, figs 5–6.

2002 *Reticulicosta kanaanensis* (Rosenfeld), Bassiouni, p. 77, pl. 18, figs 9, 10.

2010 *Reticulicosta kanaanensis* (Rosenfeld), Morsi, p. 200, Figure 7, figs 3–8

**Material :** 132 specimens of Essen section (samples : C24-C27, C28, C140-C168, C178, S5, S48).

## CHAPTER III SYSTEMATIC

**Measurements :** Sample S5, C, L : 0.5 - 0.7 m, H : 0.35-0.4, W : 0.25-0.30

**Occurrences :** Coniacian- Santonian of Essen Formation.

**Distribution :** This species was previously recorded from levels assigned to the Lower Turonian in Palestine (Rosenfeld & Raab 1974), Egypt (Bassiouni 2002) and Jordan (Schulze et al. 2004). Upper Cenomanian from Central Jordan (Morsi et Wendler, 2010).

Family Cytheruridae Müller, 1894  
Genus *Metacytheropteron* Oertli, 1957

***Metacytheropteron* sp.**

**Pl. 5. Figure 6a-c**

**Material:** 17 specimens (samples: E45, E64, E71, C13, C15, C19, C20, C27, C38, C45, C55-C75, C88-C99, C108, C127, C143, C130, C151, C156, C159, C169, C172- C175, C180, S1, S5).

**Measurements:** sample E71, S1, C, juvenile; L: 0.46; H: 0.12; W: 0.21.

**Description of the specimens:** Small reticulated carapace, subovale in lateral view, oval in dorsal view. The anterior margin is rounded; the posterior is narrow. Anterior margin obliquely round, posterior margin forming a small caudal process. The greatest width is just behind the mid-length. Ventral outline slightly convex.

**Remarks:** This species is close to *Centrocythere cheguigaensis* described by Damotte (1984) in Barremian of Algeria. However, *C. cheguigaensis* has well-developed ribs and the eye-tubercle is well marked.

**Occurrence:** Santonian of Boukezez Formation and Essen Formation

Genre *Amphicytherura*

***Amphicytherura* aff. *yakhiniensis* Rosenfeld 1974**

**Pl. 5. Figure 7a-b**

**Material:** 174 specimens of Essen section (samples: C1, C108, C127, C130, C156, C168-C180, S1, S2).

**Measurements:** Sample C1, S1, C, L: 0.44- 0.55 ; H: 28 - 0.36; W: 1.5 - 1.6.

**Description of the specimens:** The carapace of *Amphicytherura* aff. *yakhiniensis* is small to medium-sized. In lateral view, the carapace is subrectangular to subovale, with a nearly straight to slightly convex dorsal margin and a broadly concave ventral margin. The anterior margin is well rounded, while the posterior margin is more tapered and slightly pointed. The surface of the carapace is ornamented with a distinct reticulate pattern forming irregular polygonal meshes, with the central area slightly depressed and surrounded by moderately developed marginal ridges. Weak radial ribs may occur near the anterior region. The hinge is

### CHAPTER III SYSTEMATIC

of the lophodont type, typical of the genus *Amphicytherura*, and displaying a vertical alignment when visible in well-preserved specimens.

**Remarks :** *Amphicytherura* aff. *yakhiniensis* Rosenfeld, 1974 (in Rosenfeld and Raab, 1974) from Coniacian, is morphologically close to *Amphicytherura* (*Sondagella*) *gigantodistincta* Andreu, 1991 from the Aptian-Cenomanian of Morocco and probably to *Fissocarinocythere?* *Hexagona* Singh, 1997 from the Cenomanian of the Jaisalmer basin. *A.* aff. *A. yakhiniensis* Rosenfeld, 1974 has also been recorded from Cenomanian-Turonian of Bagh Formation.

**Occurrences:** Coniacian- Lower Santonian of Essen Formation.

**Distribution:** The original species *A. yakhiniensis* was described by Rosenfeld (1974) from Campanian–Maastrichtian deposits of Palestine.

Genus: *Clithrocytheridea*

#### *Clithrocytheridea kaufmani* Hazel, 1968

#### Pl. 6. Figure 1a-c

**Material:** 15 specimens of Essen section (samples: C29, C72, C78-C81, C146, S47, S60).

**Measurements:** sample S60, C, L: 0.70- 0.85; H: 0.38- 0.48; W: 1.7- 1.8.

**Description of the specimens:** Subovale in lateral view. The dorsal margin is relatively straight to gently arched; the ventral margin is slightly concave to straight. The anterior margin is broadly rounded, while the posterior margin is more narrowly rounded to subtruncate. Medium-sized for the genus. Valves are ornamented with distinct longitudinal costae (ribs), running from the anterior to the posterior ends. These costae are raised and evenly spaced, separated by shallow furrows. In well-preserved specimens, the costae may show fine granulation or be smooth.

**Remarks:** *Clithrocytheridea kaufmani* was first described by Hazel (1968) from Upper Cretaceous (Cenomanian to Maastrichtian) marine sediments of the Gulf and Atlantic Coastal Plains (USA). The species is notable for its prominent longitudinal costae and subrectangular shape, distinguishing it from closely related *Clithrocytheridea* species that may have less pronounced ribbing or different valve proportions.

**Occurrences:** Coniacian and Santonian of Essen Formation.

**Distribution :** Upper Cretaceous (Cenomanian to Maastrichtian) of USA (Hazel, 1968)

## CHAPTER III SYSTEMATIC

Genus *Asciocythere* Swain, 1952  
*Asciocythere* aff. *aegyptiana* (Morsi 2000)  
**Pl. 6. Figure 2a-c**

**Material:** 56 specimens of Essen section (samples: C29, C42, C60-C62, C70-C71, C151, C156- C159, C168).

**Measurements:** sample C29, C, L:0.65- 0.85; H:0.35- 0.50; W:1.6- 1.8.

**Description of the specimens:** oval in lateral view, rounded without angles; maximum height at the front of the carapace, maximum length below mid-height.

**Remarks :** The specimens assigned to *Asciocythere* aff. *aegyptiana* closely resemble the original description of *A. aegyptiana* Bate, 1972, particularly in their general outline and surface ornamentation. However, some morphological differences were observed that prevent a precise assignment to the nominal species, the surface shows fine reticulation with weak to moderate ridges, slightly less pronounced than in *A. aegyptiana*. Central area more depressed, with marginal ridges less developed.

**Occurrences :** Coniacian of Essen of Essen section

**Distribution :** Campanian of Mena (Algeria) Benmansour, 2017

Family Xestoleberididae Sars, 1928  
Genus *Xestoleberis* Sars 1928  
*Xestoleberis* sp.  
**Pl. 6. Figure 3a-b**

**Material:** 73 specimens (samples: E39- E45, E53, E64, C20, C60-C65, C72-C80).

**Measurements:** sample E64, C20, C, L: 0.44; H: 0.12; W: 0.25.

**Description of the specimens:** Small, smooth carapace. Rounded in lateral view and ovate in dorsal view. Maximum height located in the middle. Maximum length below mid-height; maximum thickness located towards the rear. Anterior region lower than the posterior one. The ventral outline straight, dorsal outline strongly convex.

**Remarks:** *Xestoleberis* sp. is different from to *Xestoleberis tunisiensis* described by Benmansour (2016) in Algeria; *X. tunisiensis* shows a more rounded ventral margin.

**Occurrence:** Santonian of Boukezez Formation and Lower Coniacian of Essen Formation.

Famille Bythocyprididae maddocks, 1969  
Genre *Bythocypris* BRADY, 1880  
*Bythocypris* sp.,

**Pl. 6. Figure 4**

1994 *Bythocypris* sp., Shahin p.40, Pl. 1 Figure 22

## CHAPTER III SYSTEMATIC

2007 *Bythocypris* sp., Andreu, p355, pl. 2, Figure 19

**Material :** 34 specimens of Essen section (samples : C19, C102, C125, S1, S43, S35, S57, S62).

**Measurements :** C19, S5, C, L: 0.48; H: 0.32; W: 0.25.

**Description of the specimens :** Carapace subrectangular in lateral view, with its maximum height and length in the middle of the carapace. The anterior margin is broadly rounded, and the posterior margin is obliquely rounded. The ventral margin is straight. The dorsal margin is convex, and the posterodorsal margin slopes gently. The left valve is slightly larger than the right. The surface of the carapace is smooth. In dorsal view, the carapace has an elliptical, elongate shape with its maximum width in the center.

**Remarks :** Very rare, poorly preserved specimens with closed carapaces. The generic attribution it self remains uncertain. *Bythocypris* ? sp. SAUVAGNAT 1999 from the Lower Aptian of the Jura has a more elongated carapace.

**Occurrences :** Coniacian and Santonian of Essen Formation.

**Distribution :** Tuvalian – Carnian, *Tropites subbullatus* *Anatropites spinosus* zones, Monte Gambanera, Central Eastern Sicily, Italy (Sylvie, 2020), Lower Aptian of the Jura (Sauvagnat, 1999), Upper Bedoulian of Pichouraz (Babinot J.-F, 2007).

### *Bythocypris mohani* Singh 1997

#### Pl. 6. Figure 5

2007 *Bythocypris mohani* Singh- Andreu, p. 355, pl. 2, Figure 17-18.

**Material :** 10 specimens of Essen section (samples: C56, C59-C60, C71, S49)

**Measurements :** sample C56, C, L : 0.50–0.65; H : 0.30–0.40; W : 0.11- 0.19.

**Description of the specimens :** small ostracod characterized by an subrectangular carapace with moderately convex dorsal and ventral margins. The anterior margin is broadly rounded and slightly expanded, while the posterior margin is narrower, slightly tapering, and more pointed. The valves are smooth, thin-shelled, and moderately inflated, with the greatest height located slightly anterior to mid-length. The hinge is simple, lacking prominent teeth or sockets, and no surface ornamentation is present. This species is distinguished from closely related taxa by its more elongate outline and relatively narrow posterior extremity. The carapace

**Occurrence :** Coniacian-Santonian of Essen Formation.

**Distribution :** Upper Cretaceous, specifically the Cenomanian to Turonian. It was first described from the Kachchh Basin, western India (Singh, 1997) and later identified in several

## CHAPTER III SYSTEMATIC

regions of the Tethyan realm, including Tunisia (Ben Youssef, 1980; Bismuth et al., 1981), Algeria (Vivière, 1985), and northern Morocco (Donze et al., 1982). Coniacian from the Jaisalmer Basin, Rajasthan, India Andreu et al., (2007)

**Family Brachycytheridae Puri, 1954**  
**Genus *Brachycythere* Al Exander, 1933**

***Brachycythere* sp.,**

**Pl. 6. Figure 6**

2007 *Brachycythere* sp., Andreu, p357, pl. 3, figs. 21-22

**Material:** 23 specimens of Essen section (samples: C20, C28, C32, C38-C47, C52, C58)

**Measurements:** sample C52, C, L: 0.55- 0.75; H: 0.35- 0.50; W: 0.15- 0.25.

**Description of the specimens :** subrectangular to subquadrate carapace with moderately convex dorsal and ventral margins. The anterior margin is broadly rounded with a slight ventral projection, while the posterior margin is narrower, more tapered, and sometimes exhibits a weak posteroventral spine or angular extension. The valves are moderately thick and robust, with the greatest height located slightly anterior to mid-length. The surface ornamentation consists of a distinct reticulate pattern of polygonal meshes, occasionally forming weak nodes or ridges along the marginal areas. The hinge is lophodont, typical of the family Trachyleberididae, with well-developed cardinal and terminal elements. These features suggest adaptation to relatively high-energy shallow marine environments.

**Remarks :** The specimens are assigned to the genus *Brachycythere* based on their characteristic outline, reticulate ornamentation, and hinge structure. However, due to the absence of some diagnostic characters such as the exact configuration of marginal ridges and nodes, a precise species-level identification is not possible.

**Occurrences :** Coniacian of Essen Formation.

**Distribution :** Cenomanian to the Maastrichtian, with its abundance peaking during the Turonian–Coniacian interval. Tunisia (Glantzboeckel & Magné, 1959; Ben Youssef, 1980; Bismuth et al., 1981), Algeria (Vivière, 1985), and Morocco (Donze et al., 1982)

**Family: Cytheruridae**

**Genus: *Perissocytheridea***

***Perissocytheridea ascalopha* (Van den Bold), 1964)**

**Pl. 6. Figure 7a-c**

## CHAPTER III SYSTEMATIC

**Material:** 96 specimens of Essen section (samples: C2, C20- C21, C28-C39, C53-C60, C141-C180, S1, S60).

**Measurements:** sample C2, S60, C, L: 0.4- 0.5; H:0.3- 0.35; W:0.12-0.22.

**Description:** Subtriangular to subrectangular in lateral view, with moderate lateral compression. Small to medium-sized. The dorsal margin is usually straight to slightly convex, and the ventral margin is gently concave. The anterior end is broadly rounded, while the posterior is more tapered and subacute to pointed. The valve surface is characterized by a fine to moderately well-developed reticulate pattern. Central and subcentral areas may show faint ridges or costellae. No strong nodes or spines are usually present, though some specimens may exhibit subtle swelling near the postero dorsal region.

**Remarks:** *Perissocytheridea ascalapha* was first described by van den Bold (1964) from the Paleogene of the Caribbean region and has since been reported from Late Cretaceous to early Paleogene deposits in various shallow marine environments. *P. ascalapha* is readily distinguished from *P. punctillata* by its reticulate ornamentation and more tapered posterior. *P. limbata* tends to be more rectangular with less posterior tapering and has faint longitudinal ridges or costae, unlike the more subtle reticulation in *P. ascalapha*. Specimens referred to as *P. sp. aff. ascalapha* may show similar outline and ornamentation but differ subtly in proportions or reticulation density these may represent geographic or stratigraphic variants or undescribed species.

**Occurrences :** Coniacian-Santonian of Essen

**Distribution :** recorded in Cenomanian-Maastrichtian (Late Cretaceous) of North Africa, notably in Tunisia (Glintzboeckel & Magné, 1959; Ben Youssef, 1980; Bismuth et al., 1981), Algeria (Vivière, 1985), and Morocco (Donze et al., 1982).

### Subfamily Buntoniinae APOSTOLESCU, 1961

#### Genus Soudanella APOSTOLESCU, 1961

##### *Soudanella laciniosa triangulata* Apostolescu; 1961

##### Pl. 6. Figure 8

1961 *Soudanella laciniosa triangulata* Apostolescu, p.810, pl.7, figs.130-135.

1963 *Soudanella* cf. *S. laciniosa triangulata* Apostolescu- Barsotti, p.1525, pl.3, Figure 20.

1970 *Soudanella laciniosa triangulata* Apostolescu- Bassiouni, pl.3, Figure 11.

## CHAPTER III SYSTEMATIC

1979 *Soudanella laciniosa triangulata* Apostolescu- Neufville, p.153, Pl.6, figs 1a-b.

1982 *Soudanella laciniosa triangulata* Apostolescu- Donze et al., p.295, pl.12, figs. 2-3.

1990 *Soudanella laciniosa triangulata* Apostolescu-Bassiouni & Luger, p.847, pl.24, Figure 18.

1991 *Soudanella laciniosa triangulata* Apostolescu- Ismail, p.167, pl.31, figs 14-16.

1992 *Soudanella laciniosa triangulata* Apostolescu- Ismail, p.51, pl.2, Figure 10.

1995 *Soudanella laciniosa triangulata* Apostolescu- Aref, p.128, pl.1, Figure12.

2000 *Soudanella laciniosa triangulata* Apostolescu- Bassiouni & Morsi, p.67, pl.12, figure 6.

2000 *Soudanella laciniosa triangulata* Apostolescu- Shahin, p.22, figure 7 (20-23).

2004 *Soudanella laciniosa triangulata* Apostolescu- Ismail & Ied, p.115, pl. 5 figs. 14-15.

2005 *Soudanella laciniosa triangulata* Apostolescu- Ismail & Ied, pl.5–Figure11. 135.

**Material:** 11 specimens of Essen section (samples: C44, C159).

**Measurements:** sample **C44, C, L:** 0.35 - 0.45; **H:** 0.28 - 0.35; **W:**0.10- 0.19.

**Description of the specimens:** *Soudanella triangulata* The ornament of the anterior zone is effaced or it may appear “smeared”. The anterior furrow is always deeply incised. The posterior of the carapace is extended. The lateral ribbing is broader and flatter than in typical *laciniosa* but the number of costae is the same. Some individuals have lost the full lateral ornament and there are smooth centro-lateral fields. In Nigeria, the main occurrence of the *triangulata*-type is the Ilaro sequence.

**Occurrence:** Coniacian of Essen

**Distribution:** This species was described from the Paleocene of Senegal (Apostolescu, 1961), Libya (Barsotti (1963), Nigeria (Reyment, 1963) and Brazil (Neufville, 1979), Maastrichtian – Paleocene of Algeria (Damotte and Fleury, 1987) Paleocene – Lower Eocene of Tunisia (Donze et al. 1982), Lower Eocene of Jordan (Bassiouni, 1970). In Egypt, it was recorded from the Paleocene - Lower Eocene of southern Egypt (Bassiouni & Luger, 1990), Northern Galala (Ismail, 1991), Red Sea Coast (Aref, 1995), Middle- Upper Eocene of South Sinai (Shahin, 2000), Lower Eocene of Farafra Oasis (Bassiouni & Morsi, 2000), and Paleocene-Lower Eocene of northeastern Sinai (Ismail & Ied, 2004) ; Lower Eocene of Eastern desert Egypt (Ismail & Ied, 2005).

### *Arculicythere semilunata* Singh 1997

#### Pl. 6. Figure 9

**Material:** 8 specimens of Essen section (samples: C49, C159-C160, C175).

**Measurements:** **C49 C, L:** 0.30 - 0.45; **H:** 0.20 - 0.25; **W:**0.10- 0.15.

## CHAPTER III SYSTEMATIC

**Description of the specimens:** subtriangular to subovate carapace with a strongly arched dorsal margin and a broadly concave to nearly straight ventral margin. The anterior margin is broadly rounded and expanded, whereas the posterior margin is narrower, slightly pointed, and more tapering. The valves are moderately inflated, with the greatest height located slightly anterior to mid-length. The surface ornamentation consists of a distinct reticulate pattern forming irregular polygonal meshes, more pronounced around the marginal areas. A well-developed marginal ridge follows the outline of the carapace, being especially prominent ventrally and posterodorsally. The hinge is lophodont, typical of the family Trachyleberididae, with clearly developed cardinal and terminal elements. No strong nodes or tubercles are present, although weak swellings may occur in the mid-posterior region.

**Remarks :** This species is assigned to the genus *Arculicythere* based on its strongly arched dorsal margin, prominent marginal ridge, and reticulate ornamentation. It differs from closely related species, such as *A. angularis* and *A. triangulata*, by having a more evenly curved dorsal margin, a less angular posterior end, and a semilunate overall shape, which inspired its species name.

**Occurrences :** Coniacian of Essen

**Distribution:** first described by Singh (1997) from Cenomanian–Turonian sediments of the Kachchh Basin, western India, The genus *Arculicythere* is widely distributed across the Tethyan realm, with related species reported from Tunisia (Ben Youssef, 1980; Bismuth et al., 1981), Algeria (Vivière, 1985), and Morocco (Donze et al., 1982)

### *Monoceratina trituberculata* Rosenfeld (1974)

#### Pl. 6. Figure 10

**Material:** 3 specimens of Essen section (samples: S60, S44)

**Measurements:** S60, C, L: 0.45 - 0.60; H: 0.25 - 0.35; W: 0.14- 0.19.

**Description of the specimens:** Species showing small to medium sizes. The profile of the two carapaces is generally asymmetrical, elliptical in shape, domed, most often on one side, and presenting two or three distinct bulges on the dorsal surface. The ventral part is very compressed. The ornamentation is poorly preserved.

**Occurrences :** Upper Santonian of Essen section

**Distribution:** *Monoceratina ? trituberculata* is a cosmopolitan but rare species, identified in Cenomanian deposits from several regions. It has been reported in Morocco and Algeria (Vivière, 1985; Slami, 2019), as well as Tunisia (Glantzboeckel & Magné, 1959; Ben Youssef, 1980; Bismuth et al., 1981; Gargouri, 1983). Records also include Kuwait, where it

## CHAPTER III SYSTEMATIC

was described as *Exophthalmocythere? bituberculata* by Al Abdul Razzaq (1977), and Gabon, where the same taxon was cited by Grosdidier (1979).

### Genre *Aphrikanocythere* Damotte et Oertli; 1982

#### *Aphrikanocythere phumatoides* Damotte et Oertli; 1982

#### Pl. 6. Figure 11

1982 *Aphrikanocythere phumatoides* DAMOTTE et OERTLI, Pl. 2, Figure 22-23

1978 *Atlanticytherel* sp. SAID, p. 242, pl. 27, Figure 4-6

1982 *Aphrikanocythere phumatoides* n. sp. – DAMOTTE et OERTLI in DONZE et al., p. 288, pl. 6, Figure 8-9

**Material:** 9 specimens of Essen section (samples: C11-C14, C120, S53)

**Measurements:** S53, C, L: 0.5-0.7; H: 0.4- 0.5; W: 0.2- 0.3.

**Description of the specimens:** The carapace is subrectangular to subovate in lateral view, with a moderately convex dorsal margin and a relatively straight ventral margin. The anterior end is broadly rounded, while the posterior end is narrower, often appearing subacute or angular. This species is medium-sized. The surface ornamentation is coarsely reticulate to punctate-reticulate, frequently featuring longitudinal costae along with distinct nodes or ridges. The central field is typically marked by a complex network of ridges forming polygonal cells, and in some specimens, a median ridge or a pronounced anterodorsal node may be present. Slight variations in ornamentation can occur, influenced by ontogenetic

**Remarks:** The specimens are assigned to the genus *Phumatoides* based on the carapace shape, trachyleberidid hinge, and characteristic reticulate/costate ornamentation. They show close affinity to forms described by Damotte & Oertli (1982), especially in terms of surface sculpture and valve proportions, though specific identification at the species level is not confirmed due to minor morphological variations or lack of complete diagnostic features. *Phumatoides* is a characteristic component of Late Cretaceous to Paleogene marine ostracod assemblages, frequently found in shallow to moderately deep marine environments.

**Occurrence :** Coniacian-Santonian of Essen section.

**Distribution:** Tunisia: *Aphrikanocythere phumatoides* was described in the middle and upper Maastrichtian of the Kef section. Algeria: this species is rare in the Maastrichtian (zones MCs 10? and MCs 11) of Dj. Dyr.

## CHAPTER III SYSTEMATIC

### Legend ostracods :

**Plate 1:** **1a-c:** *Cytherella ovata* Roemer, 1841; **a:** left view, **b:** right view, **c:** dorsal view; E3; **2a-2d:** *Cytherella* aff. *gabonensis* Neufville, 1973; **a:** left view, **b:** internal view, left valve, **c:** dorsal view, **d:** right view; E3; **3a-b:** *Cytherella mediatlasica* Andreu, 1996; **a:** left view, **b:** dorsal view; E3; **4a-c:** *Cytherella* sp., **a:** right view, **b:** dorsal view, **c:** left view; E53; **5a-b:** *Cytherella* aff. *contracta* Van Veen, 1932.

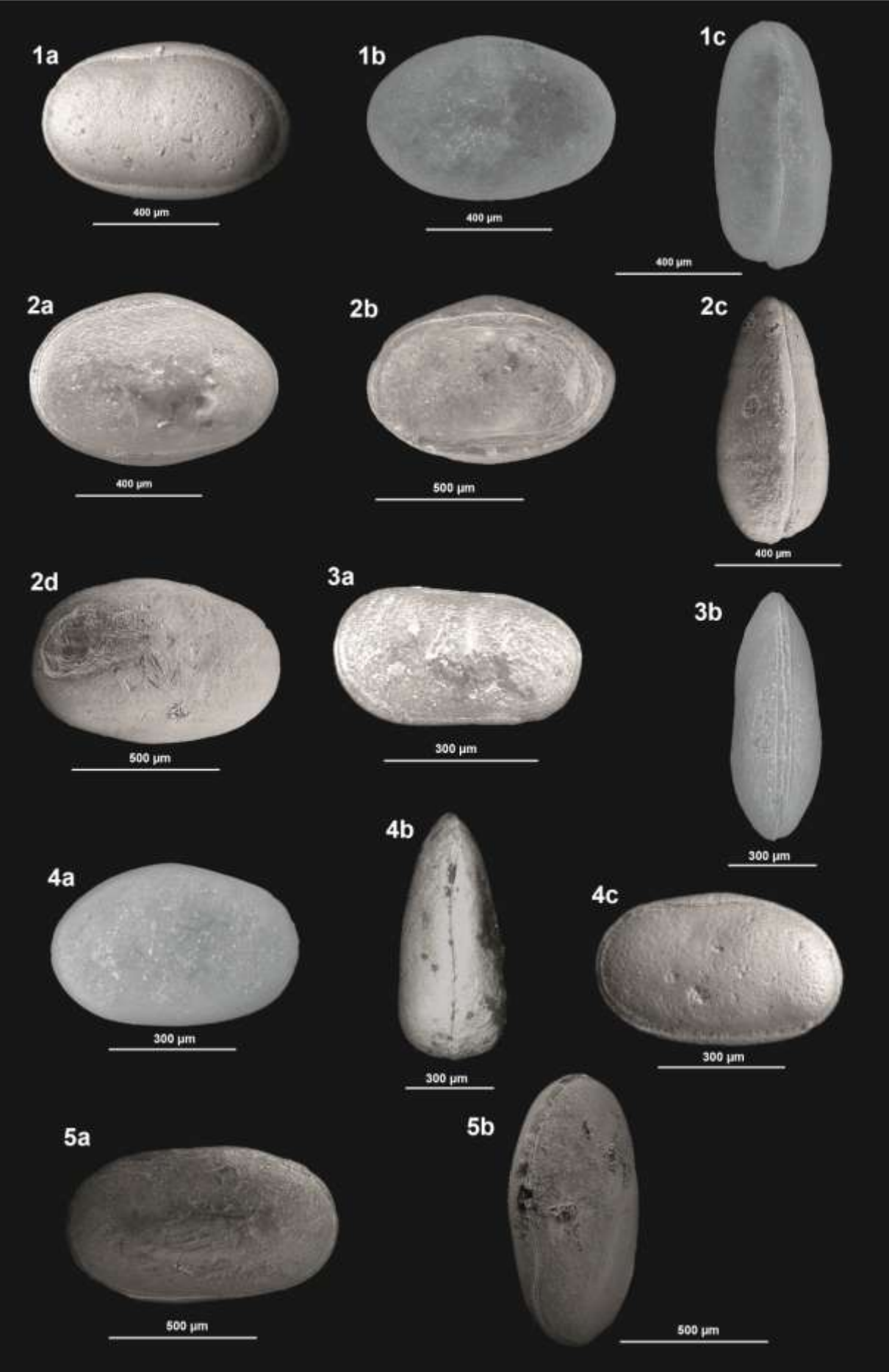
**Plate 2:** **1a-b:** *Cytherella gombiensis* Apostolescu, 1963; **2a-c:** *Cytherella* aff. *elongata* Donze, 1964; **3a-b:** *Cytherella* aff. *austinensis* Alexander, 1929; **4a-b:** *Cytherella aegyptiensis* Colin; **5a-c:** *Paracypris mdaouerensis* Bassoullet and Damotte, 1969; **a:** left view; **b:** right view; **c:** dorsal view; E36; **6a-b:** *Paracypris dubertreti* Damotte and Saint-Marc, 1972; **a:** right view; **b:** ventral view; E37; **7a-b:** *Paracypris* aff. *posteriuseracuminatus* Andreu, 1996; **a:** left view, **b:** dorsal view; E36; **8a-b:** *Paracypris* aff. *caudata* (Bold, 1964); **9 a-e:** *Paracypris chekhami*, Trabelsi, Sames, Nasri, Piovesan, Elferhi, Skanji, Houla, Soussi and Wagreich, 2020.

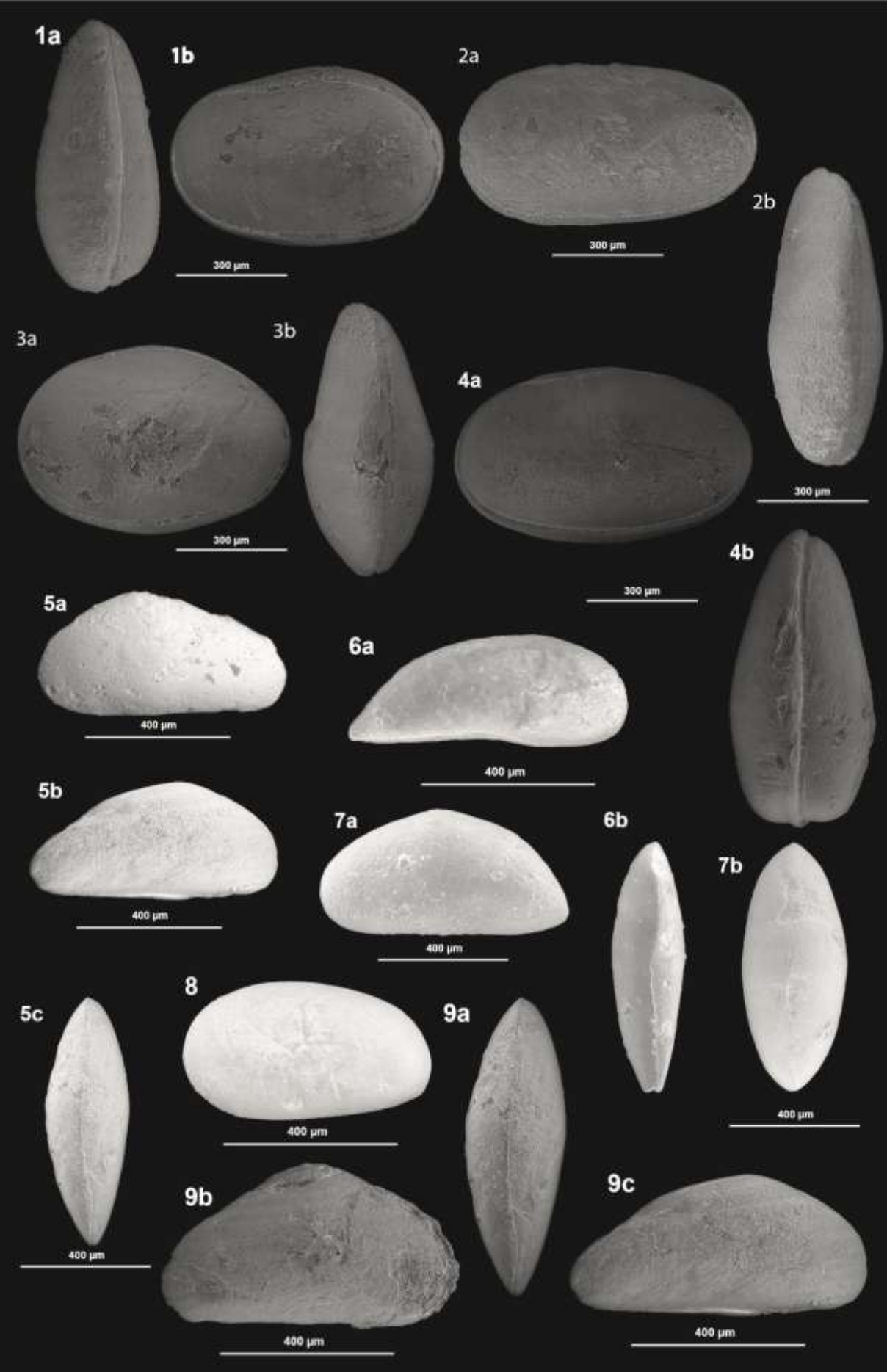
**Plate 3:** **1a-b:** *Ovocytheridea triangularis* Piovesan, Cabral and Colin 2014; **a:** right view; **b:** dorsal view; E3; **2a-b :** *Limburgina* sp.; **a:** left view, **b:** dorsal view; E36; **3a-b:** *Aysegulina* sp., **4a-c:** *Sapucariella parvoangulata* Andreu and Puckett, 2016; **a:** left view, **b:** right view, **c:** dorsal view; E36; **5:** *Sapucariella honigsteini* Puckett and Andreu, 2016; **6 a-c:** *Trachyleberidea* gr. *geinitzi* (Reuss, 1874); adult; **a:** left view, **b:** right view, **c:** dorsal view; E1; **7a-b:** *Trachyleberididae* sp.; **8a-d:** *Spinoleberis yotvataensis* Rosenfeld, 1974; 8a-b Female, 88c-d : Male **a, d:** left view, **b, c:** dorsal view; E5, E36.

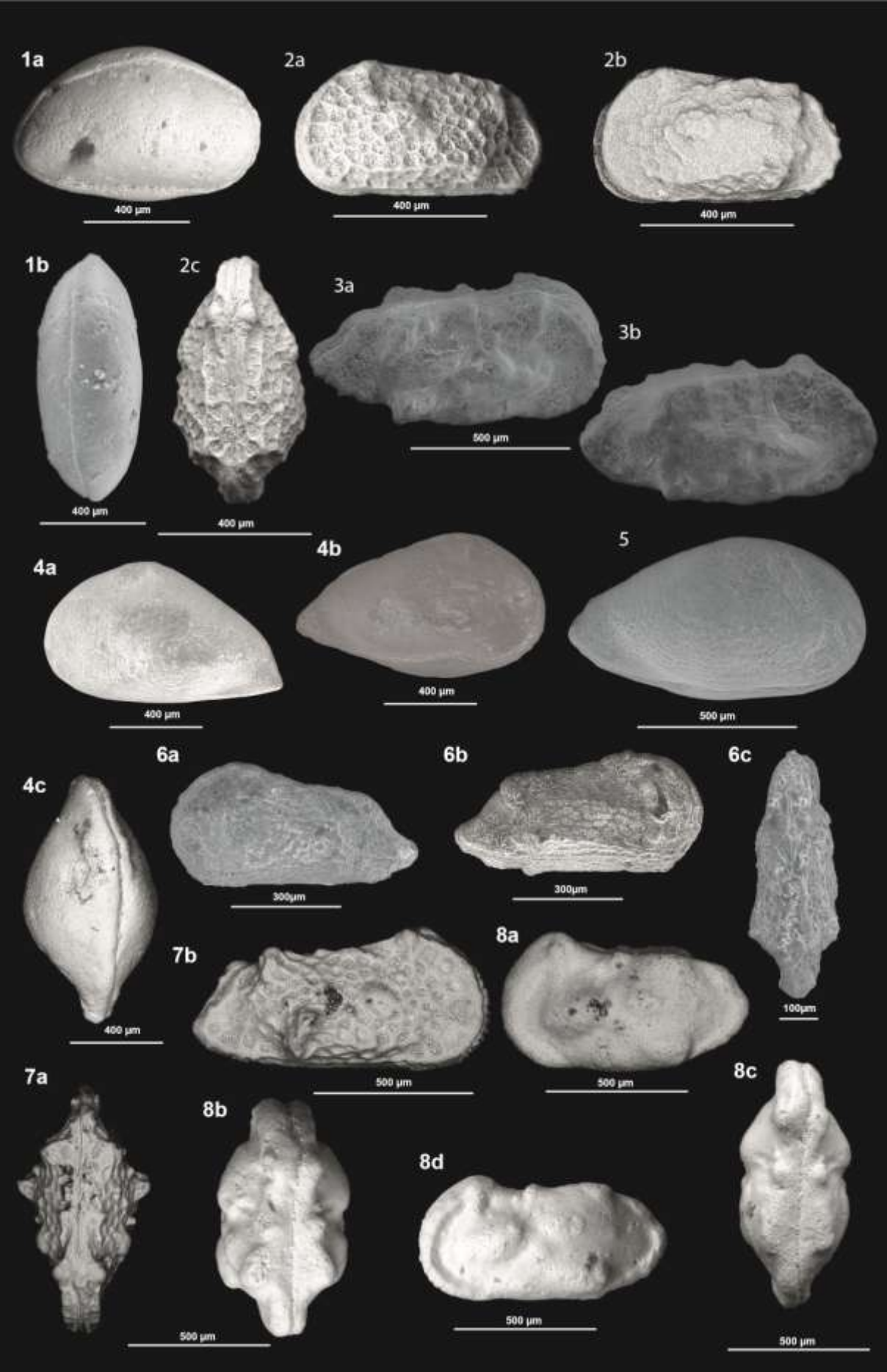
**Plate 4 :** **1:** *Cythereis* gr. *rawashensis* Van den Bold, 1964; adult; right view; E36; **2:** *Cythereis* sp 1., left view; E3 ; **3:** *Cythereis* sp. 2; right view; E36; **4:** *Cythereis* sp. 3; male; **5a-b:** *Cythereis fahrioni bigrandis* Majoran, 1989; **6a-b:** *Cythereis kosticensis* Pokorny, 1963 ; **7a-b :** *Cythereis namousensis* Bassoullet & Damotte, 1969; **8a-c:** *Cythereis algeriana* Bassoullet et Damotte 1969 ; **9a-b:** *Protocosta babinoti* Piovesan, Cabral and Colin, 2014; **a:** dorsal view; **b:** left view; E61; **10a-b:** *Paraplatycosta* sp., **a:** dorsal view, **b:** left view; E45; **11:** *Paraplatycosta* aff. *talayninensis* Andreu, 1995; left view; E53; **12:** *Haughtonileberis dinglei*, right view; E36; **13 a-b:** *Protobuntonia numidica* Grekoff, 1954; **a:** right view, **b:** dorsal view; E44;

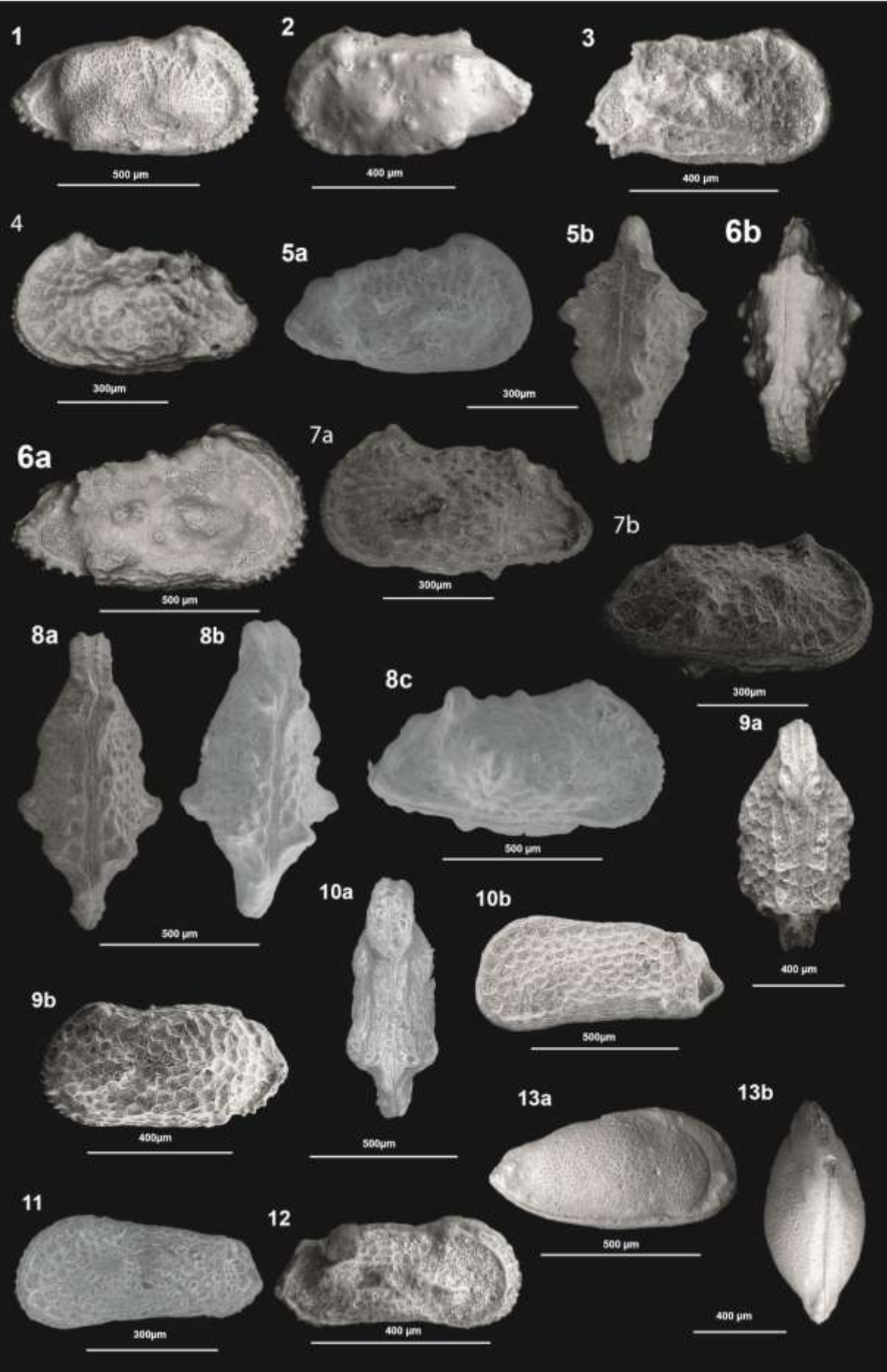
**Plate 5 :** **1a-b:** *Pterygocythere* aff. *allinensis* Grekoff and Deroo, 1956; **a:** right view; E36; **b:** dorsal view; E36; **2:** *Pterygocythere* sp., **3a-c:** *Taracythere antakaranaensis* Jean-François Babinot, Jean-Paul Colin, Auran Randrianasolo, 2009; **4a-c:** *Peloriops pustulata* (Rosenfeld and Raab, 1974); **5a-b:** *Reticulocosta kenaanensis* Rosenfeld & Raab (1974); **7a-c:** *Metacytheropteron* sp., **a:** ventral view, **b:** dorsal view, **c:** left view; E71; **8a-c :** *Amphicytherura* aff. *yakhiniensis* Rosenfeld 1974.

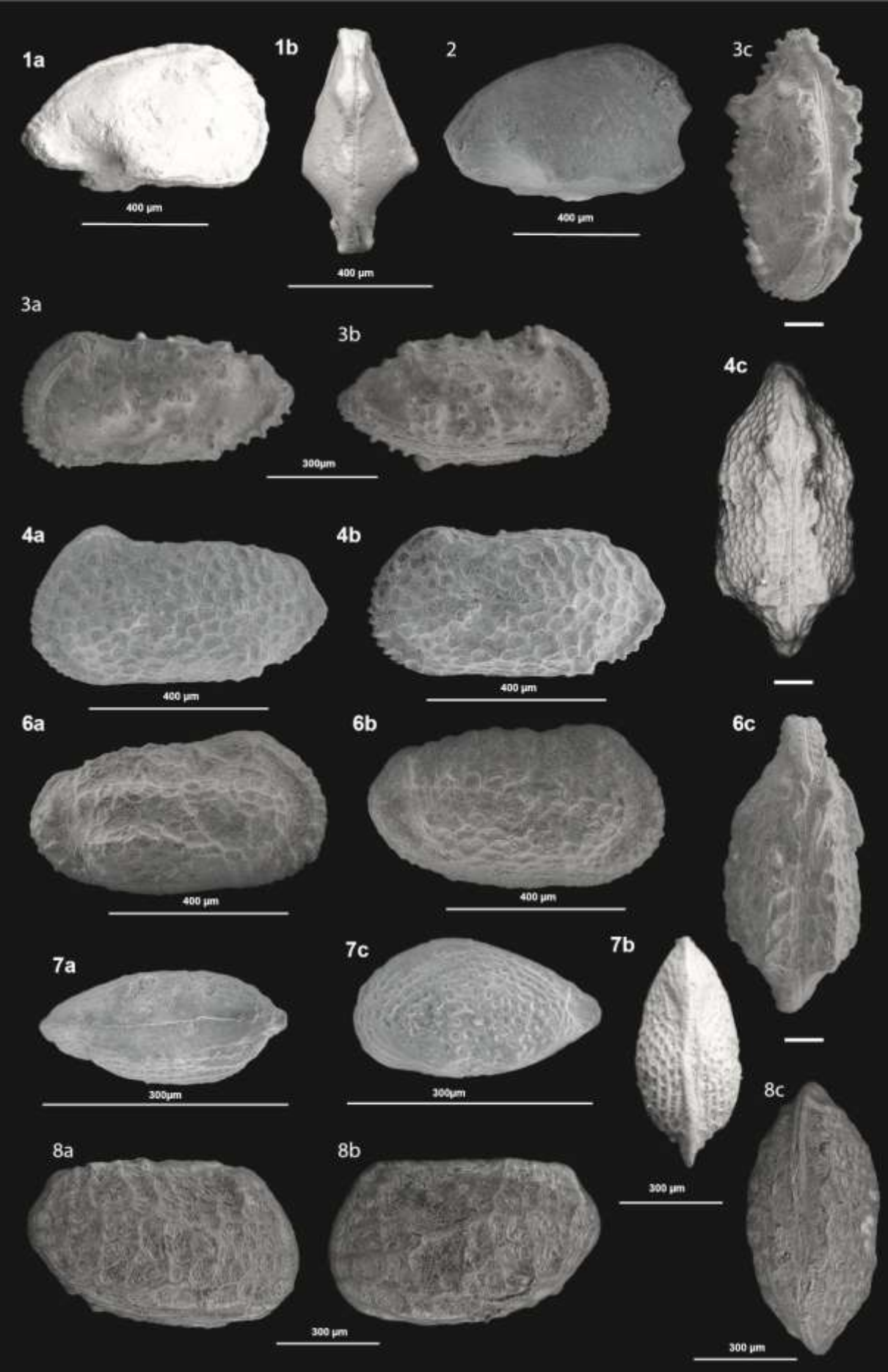
**Plate 6 :** **1:** *Clithrocytheridea kaufmani* Hazel, 1968; **2a-c:** *Asciocythere* aff. *aegyptiana* (Morsi 2000); **3a-c :** *Xestoleberis* sp., **a:** ventral view; **b:** dorsal view; **c:** right view; E64. **4:** *Bythocypris* sp. ; **5:** *Bythocypris mohani* Singh 1997; **6:** *Brachyocythere* sp. ; **7a-c:** *Perissocytheridea ascalopha* (Van den Bold), 1964 ; **8:** *Soudanella laciniosa triangulata* Apostolescu (1961); **9:** *Arculicythere semilunata* Singh 1997; **10:** *Monoceratina trituberculata* Rosenfeld (1974) ; **11:** *Aphrikanocythere phumatoides* Damotte et Oertli, 1982.

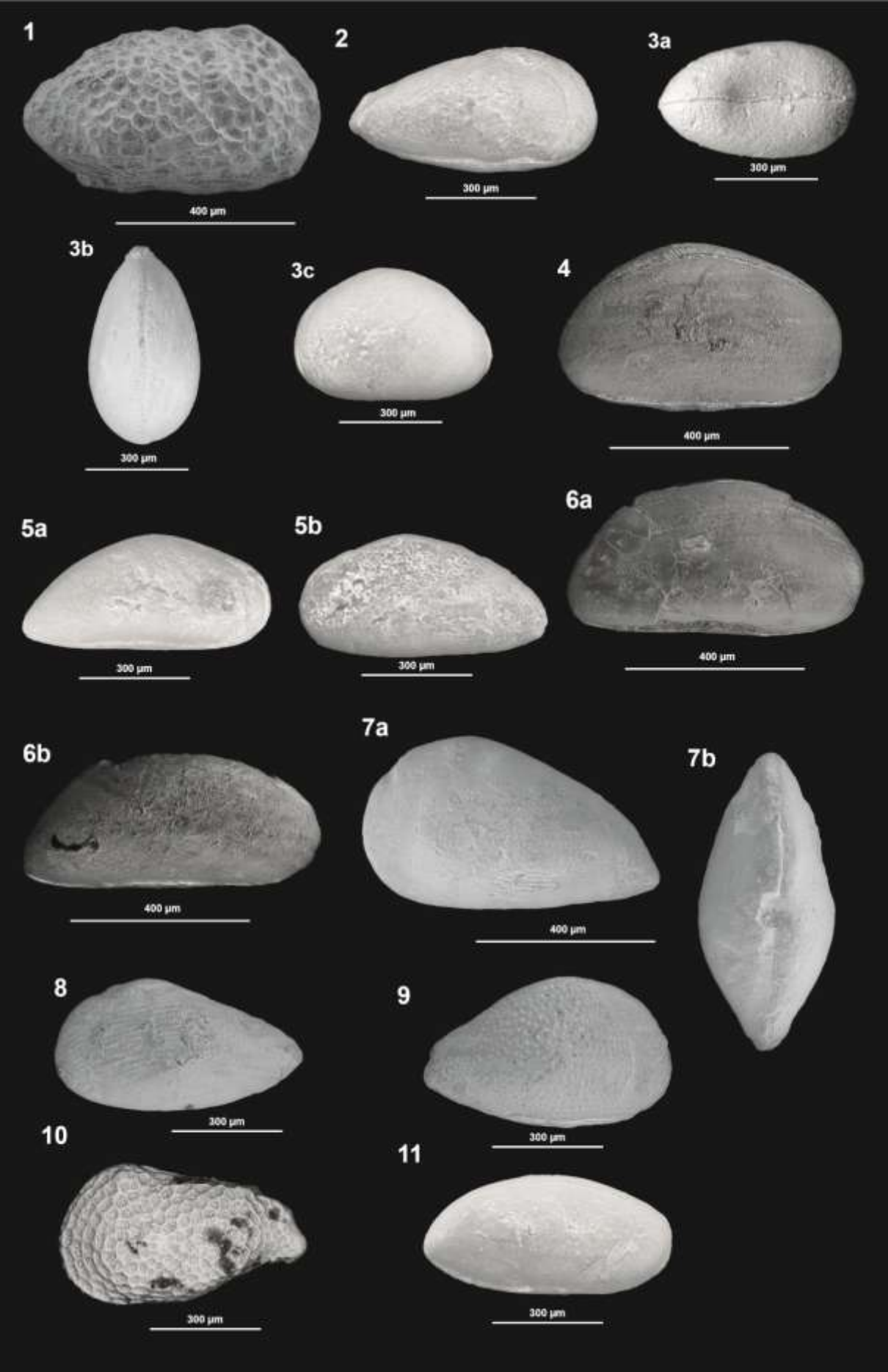












## CHAPTER III SYSTEMATIC

### Planktonic Foraminifera

**Family:** Globotruncanidae

**Genus:** *Marginotruncana* Reiss, 1957

*Marginotruncana renzi* (Gandolfi, 1942)

#### Pl. 1. Figure 1a-c

**Material:** C1-C120 (2460 specimens)

**Description :** The test is trochospiral, appearing biconvex to planoconvex in lateral view, with a distinct and continuous peripheral keel (carina). The spiral side is slightly convex, whereas the umbilical side tends to be more strongly convex, particularly in adult specimens. The final whorl generally consists of 5 to 7 chambers that gradually increase in size, with chambers exhibiting a subtriangular to ovate outline. The wall is calcareous, finely perforate, and marked by radial pustules, especially concentrated on the spiral side and along the keel. These pustules may merge to form short, irregular ridges. Sutures on the spiral side are curved and depressed, often bordered by faint costellae, while on the umbilical side they are radial and slightly depressed. The keel is sharp, well developed, and continuous around the test periphery. The aperture is interiomarginal, extending from the extraumbilical to umbilical area as a narrow slit, typically accompanied by a small tegillum, a characteristic feature of *Marginotruncana*. In some specimens, the aperture may be partially obscured by secondary lamination or overgrowth. Though larger adult forms may occur depending on ontogenetic stage and preservation quality.

**Remarks:** *Marginotruncana renzi* is distinguished from other species in the genus by its moderately convex spiral side, well-developed keel, and evenly pustulate wall texture. Compared to *M. marginata*, *M. renzi* shows fewer chambers per whorl and a less compressed profile, while differing from *M. sigali* by its more regular chamber arrangement and less angular periphery. This species is commonly found in Turonian to early Santonian marine deposits and serves as a biostratigraphic marker in the Upper Cretaceous.

**Occurrence :** Lower-Middle Coniacian

**Distribution :** Turonian to early Santonian

## CHAPTER III SYSTEMATIC

**Genus:** *Marginotruncana* Reiss, 1957

*Marginotruncana caronae* Peryt, 1980

### Pl. 1. Figure 2a-c

**Material:** C1-C120 (1986 specimens)

**Distribution:** The test is trochospiral, ranging from biconvex to slightly planoconvex, with a sharply keeled and angular periphery. The spiral side is moderately convex, while the umbilical side appears flatter or, in some specimens, slightly concave. The final whorl typically consists of 5 to 6 chambers that are subtriangular to subrectangular in shape, gradually increasing in size toward the periphery. These chambers are well defined and display slight inflation near the outer margin. The wall is calcareous, finely perforate, and pustulose, with pustules sometimes merging to form short ridges or nodes, especially near the periphery and around the umbilicus. Suture on the spiral side are curved and may be slightly raised or depressed, often bordered by faint costellae or pustules. On the umbilical side, sutures are radial and deeply incised, commonly associated with prominent pustules or nodal thickenings. The peripheral margin is strongly angular to carinate, bearing a sharp, continuous keel. The aperture is interiomarginal, extending from the umbilical to the extraumbilical region as a narrow slit, frequently partially covered by a tegillum or secondary lamination. In well-preserved specimens, the aperture is visible along the base of the final chamber. The test diameter between 0.35 mm and 0.55 mm, depending on the ontogenetic stage.

**Remarks:** *Marginotruncana caronae* can be distinguished from closely related species such as *M. renzi* and *M. marginata* by its more compressed test profile, characteristic pustulose ornamentation, and consistent chamber arrangement. First described by Peryt (1980), this species has been reported from Upper Cretaceous (Coniacian–Santonian) marine deposits, particularly within the Tethyan realm and neighboring basins. Its sharply keeled periphery and pustulose wall texture suggest an adaptation to open marine environments, likely inhabiting warm outer shelf to upper slope settings under well-oxygenated water conditions. Owing to its distinctive morphology and stratigraphic range, *M. caronae* is an important biostratigraphic indicator in Upper Cretaceous planktonic foraminiferal zonation frameworks.

**Occurrence :** Lower-Middel Coniacian

## CHAPTER III SYSTEMATIC

**Genus:** *Marginotruncana* Reiss, 1957

*Marginotruncana* cf. *sigali* 1952

### Pl. 1. Figure 3a-b

**Material:** C1-C120 (2215 specimens)

**Distribution:** The test is trochospiral and moderately biconvex, with a distinct angular periphery defined by a sharp, continuous keel. The spiral side is gently convex, whereas the umbilical side appears flatter to slightly concave in mature specimens. The final whorl typically consists of 5 to 7 chambers that gradually increase in size, becoming more inflated toward the final chamber. Chambers are subtriangular to subangular in outline. Sutures on the spiral side are curved and clearly incised, sometimes bordered by faint pustules or costellae, while those on the umbilical side are radial, deeply depressed, and generally more pronounced. The calcareous wall is finely perforate and decorated with fine pustules, particularly concentrated around the umbilical area and along the periphery. In some specimens, the keel is bordered by a band of coarser pustulation. The aperture is interiomarginal, extending from the extraumbilical to the umbilical region as a narrow slit, partially covered by a tegillum, a typical feature of the genus.

**Remarks:** The specimens are assigned to *Marginotruncana* cf. *sigali* due to their overall similarity in test shape, chamber arrangement, keel development, and wall ornamentation. However, slight differences in chamber inflation and keel sharpness prevent a definitive identification at the species level. *M. sigali* is a well-documented Coniacian to early Santonian taxon widely used in planktonic foraminiferal biostratigraphy. It is recognized by its relatively compressed test, angular periphery, and moderate pustulation. The occurrence of this form indicates deposition in a warm, open-marine environment, likely corresponding to outer shelf to upper slope settings, under normal salinity and well-oxygenated conditions.

**Occurrence :** Lower-Middel Coniacian

## CHAPTER III SYSTEMATIC

**Genus:** *Marginotruncana* Reiss, 1957

*Marginotruncana sinuosa* Porthault, in Donze et al., 1970

### Pl. 1. Figure 4a-c

1979b *Marginotruncana sinuosa* Porthault – Robaszynski and Caron, p. 147, pl. 74, figs 1-2; pl. 75, figs 1-2.

1985 *Marginotruncana sinuosa* Porthault – Caron, p. 61, figs 27.9-11.

### Material : C35-C180 (2897 specimens)

**Description :** The test is trochospiral, moderately to slightly biconvex, and generally flat, with a wide umbilicus. The spiral side is gently convex, displaying crescentic chambers with raised, beaded sutures, while the umbilical side appears more flattened to slightly concave. The periphery is marked by a continuous, well-developed double keel, which is narrow in the posterior part of each chamber and widens toward the anterior part. The final whorl consists of five to six elongate chambers, which are subtriangular to subangular in outline and exhibit a slightly sinuous curvature, a key diagnostic trait of this species. On the spiral side, the sutures are curved to sigmoidal, slightly raised or bordered by low pustules or delicate costellae. On the umbilical side, the sutures are strongly beaded and V-shaped, clearly delineating the chambers. The chamber surface is undulating, with pustules concentrated around the umbilicus, along the sutures, and near the keel. The wall is calcareous and finely perforate, providing a finely textured appearance. The aperture is interiomarginal, extending from the umbilical toward the extraumbilical region as a narrow slit, usually accompanied by a small tegillum (apertural cover), which is characteristic of the genus. This combination of a distinct double keel, chamber morphology, and aperture features distinguishes the species from other *Marginotruncana* members.

**Remarks:** The name *sinuosa* refers to the sinuous sutures visible on the spiral side, which serve as a distinctive feature separating this species from other members of the genus. *Marginotruncana sinuosa* is primarily found in Turonian to Coniacian strata of the Upper Cretaceous, where it serves as an important biostratigraphic marker. It differs from *M. renzi* by its more strongly curved sutures and from *M. sigali* by its less compressed test and more irregular chamber outlines. The occurrence of this species reflects deposition in warm, open-marine conditions, most likely in outer shelf to upper slope settings with normal salinity, typical of mid-Cretaceous planktonic foraminiferal communities.

## CHAPTER III SYSTEMATIC

**Occurrences :** Coniacian of Essen Formation

**Distribution :** Robaszynski and Caron (1979a) Coniacian and younger; Caron (1985) Coniacian to Santonian (D. primitiva to lower D. asymetrica Zone); Georgescu (1996) Coniacian to upper Santonian; Gale et al. (2008) Santonian to lowermost Campanian

**Genus:** *Marginotruncana* Reiss, 1957

***Marginotruncana pseudolinneiana* Porthault, 1970**

### Pl. 2. Figure 1a-c

1967 *Marginotruncana pseudolinneiana* Pessagno, p. 310, pl. 65, figs 24-27.

1979b *Marginotruncana pseudolinneiana* Pessagno – Robaszynski and Caron, p. 123, pl. 67, figs 1-2; pl. 68, figs 1-2.

1985 *Marginotruncana pseudolinneiana* Pessagno – Caron, p. 61, figs 26.7-8.

**Material:** C1-C120, S1-S62 (3234 specimens)

**Description of the Specimens:** The test is lobate and trochospiral, exhibiting an extremely flat, often spirally concave form, with a flat umbilical side. Its periphery is sharply truncated by a broad double keel, the margins of which are either smooth or only faintly beaded. The test consists of 2.5 to 3 whorls of progressively enlarging chambers, with the final whorl containing 7 to 8 chambers. On the spiral side, the chambers are crescent-shaped and separated by raised, curved sutures that may be smooth or slightly beaded. On the umbilical side, the chambers are subrectangular, divided by slightly curved, elevated sutures that are mostly smooth or only faintly beaded. The umbilicus is wide and bordered by a gently raised umbilical shoulder. The primary aperture is interiomarginal, positioned extraumbilical-umbilical, and appears as a low, arched opening. The outer wall, except for the double keel, is composed of radial hyaline material and is perforate, while the double keel itself is radial hyaline but imperforate. The septal walls are microgranular hyaline with sparse perforations.

**Remarks:** According to Pessagno (1967), *Marginotruncana pseudolinneiana* is externally very similar to *G. linneiana*. However, it can be distinguished by several key features: The primary aperture is distinctly extraumbilical-umbilical in position. The spiral side of the test is notably flatter and often concave. Chambers are predominantly crescent-shaped on the spiral side, whereas those of *G. linneiana* are more typically petaliform. It lacks the coarse beading on the sutures and keels that characterize *G. linneiana*. Occurrences :

**Occurrences :** Lower- Middel Coniacian, Santonian of Essen Formation

## CHAPTER III SYSTEMATIC

**Distribution :** Robaszynski and Caron (1979a) middle Turonian to Coniacian; Caron (1985) middle Turonian to Santonian (upper *H. helvetica* to *D. asymetrica* Zone); Georgescu (1996) (?upper) Santonian to lower Campanian, Gale et al. (2008) in the Waxahachie spillway section only in the Santonian.

Genus *Globotruncana* CUSHMAN, 1927

*Globotruncana linneiana* d'Orbigny 1956

### Pl. 2. Figure 2a-c

1956 *Globotruncana linneiana* (d'Orbigny) pl 9, figure 2a-c

1839 *Rosalina linneiana* D'ORBIGNY, p. 101, pi. 5, figs. 10-1 2.

1956 *Globotruncana linneiana* (d'Orbigny). - BRONNIMANN and BROWN., pp. 540-542, pl. 20, figs. 13-17; pl. 21, figs. 16-18.

1972 *Globotruncana linneiana* (d'Orbigny) Plate 9, figure 2a-c, p. 101, pi. 5, figs. 10-1 2

### Material: S1-S62 (740 specimens)

**Remarks :** Specimens from Libya have been compared to the neotype of *G. linneiana* proposed by Brennimann and Brown (1956, pp. 540-542, pl. 20, figs. 13-15) and were found to be identical. *G. linneiana* is closely related to *G. tricarinata* (Quereau) and *G. coronata* Bolli, and in the past these forms have often been regarded as subspecies of either *G. lapparenti* Brotzen (e.g. Bolli, 1945; Hagn and Zeil, 1954) or *G. linneiana* (e.g. Barr, 1962; van Hinte, 1963; Martin, 1964). (The author considers *G. lapparenti* to be a junior synonym of *G. linneiana*.) In Libya, although there are sometimes transitional specimens between the typical forms, these three species have distinct stratigraphic ranges, and their recognition has proven to be of considerable value in stratigraphic studies.

**Occurrence :** Santonian of Essen Formation

**Distribution:** *G. linneiana* has been recovered from several surface exposures in northern Cyrenaica and from many wells in the northern Sirte Basin. This species ranges from Santonian to middle Campanian and is most common in the lower Campanian. In the Santonian (lower *G. elevata* Zone), there are often numerous transitional forms between *G. linneiana* and *G. coronata* Bolli.

## CHAPTER III SYSTEMATIC

**Genus:** *Globotruncana* Cushman, 1927

***Globotruncana bulloides* Vogler, 1941**

### Pl. 2. Figure 3a-c

**Material:** S10-S50 (600 specimens)

**Description of the Specimens:** The test is low trochospiral, ranging from planoconvex to biconvex, with a broadly rounded peripheral margin that may occasionally display a weak or discontinuous keel. The spiral side is gently convex, while the umbilical side is flatter to slightly concave. The final whorl typically comprises 5 to 6 chambers that increase moderately in size. These chambers are globular to ovate, giving the test its distinctive inflated or “bulloidal” appearance. Sutures on the spiral side are curved to slightly oblique and range from flush to slightly depressed. On the umbilical side, the sutures are radial, distinct, and usually depressed, converging around a small, open umbilicus. The calcareous wall is finely perforate and bears low pustulose ornamentation, most commonly concentrated along the sutures and near the umbilical region. This ornamentation is generally less pronounced compared to other *Globotruncana* species. The keel, when present, is weak and discontinuous, and may be poorly developed or absent altogether, especially in juvenile or poorly preserved specimens. The aperture is interiomarginal, extending from the umbilical to extraumbilical area as a narrow slit bordered by a thin lip. In some individuals, it may be partially obscured by secondary lamination or a tegillum.

**Remarks:** *Globotruncana bulloides* is characterized by its globular chambers and a less sharply defined peripheral margin, setting it apart from more strongly keeled or angular species such as *G. arca* and *G. linneiana*. Its wall texture, combined with its low-profile test, makes it a distinctive taxon for identifying early to middle Turonian stratigraphic intervals. This species is typically associated with open marine environments, reflecting warm, outer shelf to upper slope conditions with normal salinity and well-oxygenated waters. Due to its broad geographic distribution and easily recognizable morphology, *G. bulloides* is widely utilized in biostratigraphic and paleoecological studies of the mid-Cretaceous.

**Occurrence :** Upper Santonian of Essen Formation

***Globotruncana arca* (Cushman, 1926)**

### Pl. 3. Figure 1a-c

## CHAPTER III SYSTEMATIC

1926 *Globotruncana arca* (Cushman), pl. 6, figure 7a-c

1926 *Pulvinulina arca* Cushman, p. 23, pl. 3, Figure 1 a-c.

1967 *Globotruncana arca* (Cushman). - Pessagno, pp. 321- 323, pl. 79, figs. 5-8; pi. 90, figs. 6-8; pl. 96, figs. 7-8, 17.

1968 *Globotruncana arca* (Cushman). Barr, p. 315, pl. 39, Figure 3a-c .

1972 *Pulvinulina arca* Cushman p. 23, pl. 3, Figure 1 a-c.

1984 *Globotruncana arca* (Cushman).- Robaszynski and others, p. 182, 184, pl. 1, figs. 2-3; pl. 4, figs. 1-3.

1988 *Globotruncana arca* (CUSHMAN).- O ZKAN and KO YLU OG LU, p. 381, pl. 1, figs. 4, 6.

2006 *Globotruncana arca* (CUSHMAN).- Sari, Pl. 1, Figure 15

2014 *Globotruncana arca* (Cushman), pl 6, figure 7a-c

### **Material: S50- S62 (291 specimens)**

**Description of the specimens:** Test moderately high trochospiral; profile nearly symmetrical, moderately convex on both spiral and umbilical sides, but spiral side especially more convex; two distinct keels separated by a large peripheral band, equally developed and parallel throughout the last whorl; keel band tilted towards the umbilical side. Sutures on the spiral side raised and beaded; adumbilical ridges well developed; umbilicus wide and deep.

**Remarks :** *Globotruncana arca* differs from *G. mariei* in its two generally widely spaced and well-marked keels. It differs from *G. rosetta* in generally having a more convex spiral side and in the presence of two widely spaced distinct keels on all chambers. The species differs from *G. falsostuarti* in the presence of two widely separated keels throughout the last whorl. It differs from *G. orientalis* in the presence of two widely spaced keels on all chambers. It is also distinguished from *Contusotruncana fornicata* by having less elongated and less undulating chambers on the spiral side.

**Occurrence:** Upper Santonian of Essen Formation

**Distribution :** The author (Barr, 1968a, p. 315) recently recorded *Globotruncana arca* from the lower Maastrichtian portion of the Atrun Limestone in the Wadi al Atrun-Wadi Merghes area in northern Cyrenaica. This species is fairly common in the uppermost Campanian and

## CHAPTER III SYSTEMATIC

Maastrichtian strata of the Sirte Basin and northern Cyrenaica, Maastrichtien of Algeria (Benmansour, 2017)

### *Globo truncana elevata* (Brotzen) 1934

#### Pl. 3. Figure 2a-c

1934 *Rotaliae levata* BROTZEN, p. 66, pl. 3, Figure C.

1953 *Globo truncana andori* DE KLASZ, pp. 233-235, pl. 6, Figure 1 a-c.

1955 *Globo truncana elevata elevata* (Brotzen) - DALBIEZ, p. 169, text-Figure 9a-c.

1956 *Globo truncana elevata*(Brotzen) - KNIPSCHEER, pp. 51-52, pl. 4, figs. 1-3, 5; text-Figure 1.

1962 *Globo truncana rosetta* (Carsey). - BARR, pp. 575-576, pl. 70, Figure 4a-c.

#### **Material: S50- S62 (246 specimens)**

**Description of the specimens:** The test of *Globo truncana elevata* is trochospiral, ranging from biconvex to strongly biconvex, with a highly elevated and prominently inflated spiral side, while the umbilical side is flatter to slightly concave. The peripheral keel is sharp, well developed, and continuous, forming a distinct angular margin. The final whorl consists of 5 to 7 chambers that are inflated, robust, and subtriangular to subglobular in outline, increasing progressively in size toward the periphery. These thick chambers contribute to the elevated profile of the test. On the spiral side, the sutures are deep and curved, sometimes bordered by faint costellae or small pustules, whereas on the umbilical side, the sutures are radial, deeply incised, and clearly defined. The calcareous wall is finely perforate and displays moderate pustulose ornamentation, with occasional short costellae on the spiral side. This ornamentation is generally less prominent than in some related *Globo truncana* species. The keel is sharply defined and continuous, often accentuated by pustules or fine nodules along its edge. The aperture is interiomarginal, extending from the umbilical to extraumbilical area, and is often partially covered by a tegillum.

**Remarks :** The test of *G. elevata* is arranged in a low trochospiral and is characterized by a nearly plano-convex shape. The spiral side is nearly flat except for a small conical central portion. The umbilical side is strongly convex. The umbilicus is relatively small, and on the umbilical side sutures are radial and depressed. The surface of the test is smooth except for the three or four earliest chambers of the final whorl on the umbilical side, which are coarsely hispid.

**Occurrence :** Upper Santonian of Essen Formation

## CHAPTER III SYSTEMATIC

**Distribution :** *G. elevata* ranges from the uppermost *G. concavata concavata* Zone (upper Coniacian) to late Campanian in Libya. Knipscheer (1956) reported a similar range in Bavaria, and, although Dalbiez (1955, pp. 167, 169) recorded a Campanian range for this species in Tunisia, he showed on his range chart an overlap in the uppermost occurrence of *G. ventricosa carinata* (= *G. concavata*) and the lowermost occurrence of *G. elevata*. It therefore appears that the stratigraphic range of *G. elevata* in Tunisia is the same as that observed in Libya.

### *Contusotruncana plummerae* (Bolli, 1957)

#### Pl. 3. Figure 1a-c

**Material: S10-S62 (657 specimens)**

**Description :** The test of *Contusotruncana plummerae* is trochospiral and distinctly biconvex, with a periphery that is broadly rounded to slightly angular. The spiral side is convex, whereas the umbilical side appears flattened to weakly concave. In the final whorl, there are typically 5 to 7 chambers that are subtriangular to subrectangular in outline. These chambers are moderately inflated and increase gradually in size toward the terminal chamber. On the spiral side, the sutures are curved and deeply incised, sometimes bordered by fine costellae or small pustules. On the umbilical side, the sutures are radial and sharply defined, clearly separating the chambers. The wall is calcareous and finely perforate, displaying fine pustules or low costellae concentrated along the sutures and peripheral margin, creating a subtly roughened surface texture. The periphery is marked by a sharp, continuous keel, which may be bordered by fine pustules, enhancing its definition. The aperture is interiomarginal, extending from the umbilical to extraumbilical area, and may be partially covered by a thin lamella or tegillum.

**Remarks:** *Contusotruncana plummerae* is distinguished by its biconvex test, well-developed sharp keel, and moderate pustulose ornamentation. It is a characteristic species of the Upper Cretaceous, most commonly recorded in Turonian to Coniacian deposits. Owing to its distinct morphology and stratigraphic range, it is widely utilized as an index fossil in Late Cretaceous biostratigraphy.

**Occurrence :** Upper Santonian of Essen Formation

**Distribution:** *C. plummerae* ranges from the Santonian to Maastrichtian stages, with its peak abundance and greatest biostratigraphic importance during the Campanian.

## CHAPTER III SYSTEMATIC

### *Dicarinella canaliculata* (Reuss 1854)

#### Pl. 3. Figure 4a-c

**Material:** C1- C180 (1532 specimens)

**Description:** The test is trochospiral in form, with a flattened spiral and umbilical side, and its periphery is distinctly truncated by a broad, double keel. It consists of two to two and a half whorls, with six to seven chambers typically present in the final whorl. The chambers of the last whorl are crescent-shaped to petaloid when viewed spirally, but appear distinctly wedge-shaped on the umbilical side. On the spiral side, the sutures are curved, slightly elevated, and generally lack beading, while on the umbilical side, they are straight, radial, and depressed. The umbilical surface often bears coarse, beadlike rugosities on the chamber walls. Stout portici with infralaminar accessory apertures extend into a small umbilicus. The primary aperture is interiomarginal and extraumbilical, forming a slightly arched opening. The outer wall is radial, hyaline, and perforate, except along the double keel, which is radial, hyaline, and imperforate. The septal walls are microgranular hyaline with sparse perforations, while the portici are also microgranular hyaline, likely with few perforations.

**Remarks:** *M. canaliculata* (Reuss) has been one of the most frequently misidentified species of planktonic Foraminifera in the Upper Cretaceous (see synonymies of *Globotruncana linneiana* (dOrbigny) and *Globotruncana lapparenti* s.s. Brotzen) and has long served as a waste basket term for a number of double keeled species of *Globotruncana* and *Marginotruncana*.

**Occurrence :** Coniacian of Essen Formation

**Distribution :** Cretaceous, Upper Cretaceous (Turonian-Santonian).

**Genus** *Dicarinella* Porthault in Donze et al., 1970

### *Dicarinella primitiva*

#### Pl. 4. Figure 1a-c

1955 *Globotruncana* (*Globotruncana*) *ventricosa primitiva* DALBIEZ. - DALBIEZ : p.171 fig 6

1979 *Dicarinella primitiva* DALBIEZ. - ROBASZYNSKI & CARON : p.96 pl 60 figs 1a-c

1979b *Dicarinella primitiva* (Dalbiez, 1955) – Robaszynski and Caron, p. 93, pl. 60, figs 1-2.

1985 *Dicarinella primitiva* DALBIEZ– CARON, 46,47 figs 18.4-5; 11, 13, 15.

## CHAPTER III SYSTEMATIC

### **Material: C1- C120 (1969 specimens)**

**Description:** The test is of moderate size, with a slightly to distinctly lobate periphery marked by either a single double keel or two closely spaced keels. The spiral side is flat to slightly concave, featuring curved, limbate sutures. The final whorl typically contains six chambers that increase in size progressively. On the umbilical side, a broad umbilicus is present, with six moderately inflated chambers generally visible. Test medium-sized, trochospiral with flat spiral and low conical umbilical side, outline elongate to subcircular, lobate, with narrow double keel. Spiral chambers petaloid, in the earlier part globular, sutures indistinct to slightly depressed. Umbilical chambers inflated, sutures radial and depressed.

**Occurrences:** Lower – Middle Coniacian of Essen Formation.

**Distribution:** Robaszynski and Caron (1979a); Uppermost Turonian to Coniacian; Caron (1985) Coniacian to lower Santonian (D. primitiva to D. concavata Zone).

### *Dicarinella asymetrica* (Sigal, 1952)

#### **Pl. 4. Figure 2a-c**

1952 *Globotruncana asymetrica* Sigal, p. 35, Figure 35.

1955 *Globotruncana (Globotruncana) ventricosa* White subsp. *carinata* Dalbiez, p.171, figs 8a-c.

1962 *Glt.concavata (Brotzen) carinata* Dalbiez – Edgell, p. 43, pl. 1, figs 1-3.

1963 *Globotruncana concavata carinata* Dalbiez – Küpper, p. 618, pl. 4, figs 4a-c.

1970 *Globotruncana asymetrica* Sigal, Porthault Figure 8/1-3

1979b *Dicarinella asymetrica* (Sigal, 1952) – Robaszynski and Caron, p. 61, pl. 51, figs 1-2; pl. 52, figs 1-2.

1985 *Dicarinella asymetrica* (Sigal) – Caron, p. 43, figs 17.3-4.

2007 *Dicarinella asymetrica* (Sigal, 1952) – Lamolda, Peryt and Ion, p.28, figs 5M1-2, 6F1-2.

### **Material: S10- S50 (573 specimens)**

**Description :** Test large, planoconvex, loosely enrolled, subcircular, with flat spiral and elevated umbilical side. Umbilicus wide and deep, surrounded by high conical chambers with ad-umbilical ridge. Spiral sutures strongly curved raised and beaded, umbilical sutures radial depressed. Periphery with a double keel.

## CHAPTER III SYSTEMATIC

**Remarks:** The species can be differentiated from *Dicarinella concavata* in having an angular chambers profile and in the presence of flat to slightly concave, or sometimes by strongly convex spiral side

**Occurrence :** Santonian of Essen Formation

**Distribution :** This species is common in the upper part of the pelagic limestones of the Kometan Formation in both sections. It is restricted to the *D. asymetrica* Zone. The last appearance (LA) is at the top of the *D. asymetrica* Zone (83.64 Ma) and the FA is at the base of the *D. asymetrica* Zone (86.66 Ma) according to Gradstein et al. (2012). Robaszynski and Caron (1979a) Coniacian and younger; Caron (1985) Upper Santonian (*D. asymetrica* Zone); Georgescu (1996) (?late) Santonian; Petrizzo (2003) first occurrence in the lower third of Texanites ammonite zone, near the base of Santonian, last occurrence in the lowermost Campanian chron 33R; Gale et al. (2008) all Santonian to lower Campanian. Lamolda et al. (2007) upper Coniacian to Santonian.

**Family** Rugoglobigerinidae subbotina, 1959  
**Genus** *Archaeoglobigerina* PESSAGNO 1967

### **Archaeoglobigerina sp**

#### **Pl. 4. Figure 3a-c**

**Material :** C1-S62 (4067 specimens)

**Description :** Test trochospiral; chambers subspherical; chambers successively increasing in size, except for the final chamber which is somewhat smaller than the penultimate; spiral sutures curved, depressed; radial umbilical sutures, depressed; periphery with weakly developed double carinae.

**Occurrence :** Coniacian and Santonian of Essen Formation

**Distribution :** Campanian-Lower Maastrichtian. From Algeria Benmansour, 2017

**Family:** Hedbergellidae

**Genus:** *Muricohedbergella*

**Species:** *Muricohedbergella flandrini* (Bolli, 1957)

#### **Pl. 4. Figure 5a-c**

1970 *Hedbergella flandrini* Porthault, p. 64, pl. 10, figs 1-3.

## CHAPTER III SYSTEMATIC

1979a *Hedbergella flandrini* Porthault – Robaszynski and Caron, p. 129, pl. 24, figs 1-2pl. 25, figs 1-3.

1985 *Hedbergella flandrini* Porthault – Caron, p. 57, figs 25.12-14.

2011 *Muricohedbergella flandrini* (Porthault) – Huber and Leckie, p. 84.

### **Material: C1- C120 (2559 specimens)**

**Description :** The test of *Muricohedbergella flandrini* is small, trochospiral, and ranges from globular to slightly elongate, with a low to moderately elevated trochospire. In lateral view, it is typically planoconvex to biconvex. The final whorl is composed of approximately 5 to 7 chambers that are subglobular to slightly inflated. These chambers are well separated and clearly defined by distinct sutures. Sutures are curved and well-marked, sometimes slightly depressed but not deeply incised. The wall is calcareous and smooth to finely perforate, lacking prominent ornamentation or pustules, giving it a clean appearance. A keel is generally absent or very faintly developed in this species. The aperture is interiomarginal, positioned at the base of the final chamber, and appears as an arch-shaped slit bordered by a thin lip. Specimens are small,

**Remarks:** *Muricohedbergella flandrini* serves as an important biostratigraphic marker for the Early to Middle Cretaceous, particularly within the Aptian to Albian stages. It is widely utilized in the correlation of pelagic marine sediments and plays a key role in refining Cretaceous stratigraphy. This species is indicative of open marine, pelagic environments characterized by warm, well-oxygenated waters with normal salinity. Its smooth test and diminutive size distinguish it from other hedbergellids that possess more pronounced ornamentation or strongly inflated chambers.

**Occurrence :** Lower- Middel Coniacian of Essen Formation

**Distribution:** This taxon is primarily recorded from the Aptian to lower Albian stages of the Early Cretaceous, dating to approximately 125–100 million years ago. It has been documented worldwide in pelagic marine deposits, including regions across Europe, North Africa, the Middle East, and the Americas. Due to its distinctive morphology and consistent stratigraphic occurrence, *M. flandrini* is widely used for correlating marine strata across diverse paleogeographic settings. Caron (1985) upper Turonian to lower Santonian (upper

## CHAPTER III SYSTEMATIC

Marginotruncana sigali to lower D. asymetrica Zone); Georgescu (1996) (?upper) Santonian; Gale et al (2008) in the lower part of the Santonian, nearly absent in the upper Santonian and lowermost Campanian.

Family Heterohelicidae

Subfamily Gublerininae

Genus *Sigalia*

***Sigalia carpatica* Salaj, Samuel, (1963)**

### Pl. 4. Figure 5a

1963 *Sigalia carpatica* Salaj and Samuel, p. 105, pl. 7, figs 2-3.

1966 *Sigalia carpatica* Salaj and Samuel – Salaj and Samuel, p. 227, Table 37, Figure 2.

1991 *Sigalia decoratissima carpatica* Salaj and Samuel – Nederbragt, p. 368, pl. 11, figs 2-3.

2007 *Sigalia carpatica* Salaj and Samuel, 1963 – Lamolda, Peryt and Ion, p. 28, figs 4M. P1-2, S1-2

#### **Material: S1-S9 (49 specimens)**

**Description of the specimens:** Test biserial, subtriangular, laterally compressed, periphery rounded. Chambers broad, curved, sutures thick limbate, partly *Schackoina* cf. *cenomana* (Schacko) *Schackoina multispinata* (Cushman and Wickenden) *Sigalia carpatica* Salaj and Samuel Hans EGGER, Omar MOHAMED & Fred RÖGL beaded, wall smooth.

**Remarks :** A similar test to *Sigalia decoratissima*, but this one becomes multi layered in adulthood. It is mucous and beaded. Its wall is smooth.

**Occurrences :** Lower Santonian of Essen Formation

**Distribution:** Nederbragt (1991) Santonian (lower to middle part of D. asymetrica Zone); Georgescu (1996) first occurrence around the Coniacian-Santonian boundary. Lamolda et al. (2007) upper Coniacian to lower Santonian.

**Family** Hedbergellinidae Loeblich & Tappan, 1961

**Genus** *Whiteinella* Pessagno, 1967

***Whiteinella baltica* Douglas & Rankin, 1969**

### Pl. 5. Figure 1a-c

1969 *Whiteinella baltica* Douglas and Rankin, p. 198, text-figs 9 A-C.

## CHAPTER III SYSTEMATIC

1979a *Whiteinella baltica* Douglas and Rankin – Robaszynski and Caron, p. 169, pl. 35, figs 1-4; pl. 36, figs 1-2.

1985 *Whiteinella baltica* Douglas and Rankin – Caron, p. 79, figs 37.1-3.

**Material :** C1-S62 (4347 specimens)

**Description:** The trochospire of this species is low, resulting in a nearly symmetrical profile, very globose and rugose chambers, and radial and depressed sutures. The outline is squarely lobed, and the umbilicus is generally narrow.

**Occurrence:** Coniacian and Santonian of the Essen Formation

**Distribution:** This species is reported from the Upper Cenomanian up to the Coniacian-Santonian boundary. In our material, it is very common in the Coniacian-Santonian.

Robaszynski and Caron (1979a) Upper Cenomanian to Coniacian and younger; Caron (1985) upper Cenomanian to Lowermost Santonian (*Rotalipora cushmani* to *D. concavata* Zone); Georgescu (1996) Upper Cenomanian to middle Santonian

### *Whiteinella archaeocretacea* Pessagno, 1967

#### Pl. 5. Figure 2a-c

**Material :** C1-S62 (4825 specimens)

**Description:** The test of *Whiteinella* is finely perforated calcareous, lobed in outline. It has globose chambers with a pustular surface and a rounded profile, with radial and depressed sutures arcuate in the last chambers. The umbilicus is generally wide with a main opening outside the umbilical-umbilical cavity. *Whiteinella archaeocretacea* species has a lobed outline, initially globose chambers, then elongated in the coiling direction, and radial and depressed suture lines. The main opening is almost umbilical, and the umbilicus is shallow and more or less wide.

**Occurrence:** Coniacian and Santonian of Essen Formation

**Distribution:** It is noted from the Late Cenomanian, in France, Italy, England, Tunisia, and Morocco and the Cenomanian-Turonian transition in Algeria (Khoudhair, 2015; Slami et al., 2019) Campanian-Lower Maastrichtian in Algeria (Benmansour, 2017)

**Age:** Latest Cenomanian through early Turonian.

## CHAPTER III SYSTEMATIC

### *Whiteinella* sp.,

#### Pl. 5. Figure 3a-c

**Material :** C1-S62 (4565 specimens)

**Description:** *Whiteinella* sp. is distinguished by globular cells, some rounded and others lobed, and straight and oblique suture lines. The whorl is well individualized.

**Occurrence :** Coniacian and Santonian of the Essen Formation

**Distribution :** Turonian, Coniacian

### **Family:** Huberellidae

### *Huberella praehuberi*, Georgescu, 2007

#### Pl. 5. Figure 4a-c

**Material:** C8- C80 (14 specimens)

**Description :** The test is elongate and tubular, displaying a coiling pattern that ranges from trochospiral to planispiral. It may be straight or slightly curved, typically exhibiting a fusiform (spindle-shaped) outline. It consists of multiple rectangular to trapezoidal chambers arranged in a linear or gently curved sequence, with chambers gradually increasing in size toward the aperture. The sutures are straight, transverse, and clearly marked, distinctly separating each chamber. The wall is agglutinated, composed of fine sediment particles bound together, giving the surface a rough, granular appearance. The aperture is simple and terminal, appearing as a slit or opening at the distal end of the test. Specimens generally range from 0.3 mm to 0.7 mm in length, depending on their growth stage.

**Remarks:** *Huberella praehuberi* is a benthic, agglutinated foraminifer first described by Georgescu (2007). It is characterized by its elongate, tubular form and distinctive chamber arrangement. This species plays a significant role in reconstructing paleoenvironmental conditions of marine shelf to slope settings during the Upper Cretaceous. The genus *Huberella* is distinguished from other agglutinated foraminiferal genera by its unique combination of test shape, chamber structure, and sutural patterns. Accurate identification relies on well-preserved specimens, particularly those retaining clear surface features and aperture morphology.

**Occurrence :** Lower Coniacian of Essen Formation

**Distribution :** Upper Cretaceous (Turonian), Georgescu, (2007).

## CHAPTER III SYSTEMATIC

**Genus** *Pseudotextularia* Hofker, 1951

*Pseudotextularia* sp.,

**Pl. 5. Figure 5a-c**

**Material:** C1-C180 (4144 specimens)

**Description :** The test is typically elongate and cylindrical, sometimes slightly curved, with a coiling pattern that ranges from trochospiral to planispiral. However, due to preservation issues, the exact coiling is often difficult to determine. The test is usually laterally compressed. The chambers are rectangular to trapezoidal and arranged in a straight or slightly curved linear series, gradually increasing in size toward the aperture. The exact number and shape of chambers can vary among specimens. Sutures are straight, transverse, and clearly defined, providing distinct separation between adjacent chambers. The wall is agglutinated, consisting of fine sediment particles bound together, producing a rough, granular surface appearance. The aperture is generally simple, located terminally as a slit or opening at the end of the test, and may sometimes be bordered by a delicate lip or slight thickening. Specimens commonly measure between 0.3 mm and 0.6 mm in length, though size may vary depending on preservation and growth stage.

**Remarks:** The specimens are attributed to the genus *Pseudotextularia* based on their elongated form and agglutinated wall composition. However, precise species-level identification is not possible due to incomplete morphological features or poor preservation. This genus is widely distributed in Upper Cretaceous marine sediments, particularly within deeper shelf to slope settings. The agglutinated wall structure suggests adaptation to environments characterized by variable sediment input and fluctuating energy conditions. Further study of better-preserved material, especially focusing on aperture structure and chamber organization, would enable more accurate taxonomic classification.

**Occurrence :** Coniacian of Essen Formation

**Family** Textulariidae

**Genus** *Pseudotextularia* Hofker, 1951

*Pseudotextularia nuttalli* (Voorwijk, 1937)

**Pl. 5. Figure 6a-c**

1937 *Guembelina nuttalli* Voorwijk, p. 192, pl. 2, figs 1-9.

1989 *Pseudotextularia nuttalli* (Voorwijk) – Nederbragt, p. 204, pl. 8, figs 2-3; text-Figure 9.

## CHAPTER III SYSTEMATIC

1991 *Pseudotextularia nuttalli* (Voorwijk) – Nederbragt, p. 364, pl. 10, figs 4, 6.

2007 *Pseudotextularia nuttalli* (Voorwijk, 1937) – Lamolda, Peryt and Ion, p. 28, figs 4N1-2, O1-2.

### **Material: C1- C120 (2661 specimens)**

**Description :** The test of *Pseudotextularia nuttalli* is elongate and cylindrical, displaying a trochospiral to slightly planispiral coiling pattern. The chambers are arranged in a linear to slightly curved series, with the test often laterally compressed and occasionally showing a gentle curvature. In the final whorl, there are typically 10 to 15 chambers. These chambers are rectangular to trapezoidal in outline, strongly compressed laterally, and gradually increase in size toward the aperture. The sutures are straight and transverse, clearly demarcating the boundaries between chambers, and may show a subtle indentation along the ventral side. The wall is agglutinated, consisting of fine sediment particles irregularly arranged and cemented by organic or calcareous material. This composition gives the surface a rough, granular texture. The aperture is simple, occurring as a terminal slit or opening at the end of the test, and is sometimes bordered by a faint lip. Test dimensions typically range from 0.3 mm to 0.6 mm in length, with a diameter of approximately 0.1 mm to 0.2 mm.

**Remarks:** *Pseudotextularia nuttalli* is a characteristic agglutinated benthic foraminifer, widely recognized in Upper Cretaceous marine sediments for its distinct elongate, cylindrical morphology. It is particularly common in deep marine shelf and slope settings, often associated with low-oxygen or quiet depositional environments. This species is valuable in paleoenvironmental studies, especially for identifying facies variations linked to oxygenation levels. Compared to related genera, *Pseudotextularia* is set apart by its agglutinated wall structure and its distinctively elongate, linear chamber arrangement.

**Occurrence :** Lower- Middel Coniacian of Essen Formation

**Distribution:** Nederbragt (1991) Coniacian to Maastrichtian; Gale et al. (2008) in the Santonian and very rare in the lower Campanian. *Praegublerina pseudotessera* (Cushman) *Pseudotextularia nuttalli* (Voorwijk)

## CHAPTER III SYSTEMATIC

### *Planohétérohélix globulosa*, (Ehrenberg, 1839)

#### Pl. 5. Figure 7

**Material:** S1– S46 (256 specimens)

**Description:** The test is globular to subglobular, showing a predominantly trochospiral or slightly planispiral coiling. Its overall form is rounded, lacking elongation. Chambers are numerous, strongly inflated, and closely packed, arranged in a multiserial pattern during early growth stages, often becoming biserial in later stages. Chamber size increases gradually toward the aperture. Sutures are curved and deeply incised, providing clear separation between the chambers. The wall is calcareous and finely perforate, with a smooth surface that may display subtle, fine ornamentation. The aperture is typically interiomarginal, appearing as a slit or rounded opening located at the base of the final chamber.

**Remarks :** *Planohétérohélix globulosa* is a widely distributed benthic foraminifer, recognized for its globular form and strongly inflated chambers, which help distinguish it from other species within the same genus. It commonly inhabits marine shelf environments and plays a key role in paleoenvironmental and paleogeographic reconstructions. Its abundance and wide occurrence make it a reliable taxon for correlating marine deposits.

**Occurrence :** Santonian of Essen Formation

**Distribution:** This species has been reported in marine sediments across a broad range of regions: Europe: Present in Cretaceous to Recent deposits from areas such as France, Germany, and the United Kingdom. North Africa: Found in Mediterranean marine basins, including Algeria and Morocco. Middle East: Occurs in Cenozoic marine sequences. Americas: Documented along both Atlantic and Pacific coasts, from Cretaceous to modern marine sediments. *P. globulosa* spans a long stratigraphic range, extending from the Late Cretaceous through the Cenozoic, with occurrences even in some Recent marine sediments.

#### Genus *Planohedbergella*

### *Planohedbergella cf. escheri*, (Kaufmann, 1865)

#### Pl. 5. Figure 8a-c

1865 *Nonionina escheri* KAUFMANN, p. 198, text-figs. 110a–e

### CHAPTER III SYSTEMATIC

1952 *Globigerinella escheri escheri* (Kaufmann). – BRÖNNIMANN, p. 46–49, text-figs. 22, 23

1977 *Globigerinelloides escheri* (Kaufmann). – MASTERS, p. 409–412, pl. 11, figs. 4–5

**Material: C1- C120 (1905 specimens)**

**Description of the specimens:** Surface with evenly scattered fine to medium, sharply pointed pustules and often a smooth interpustule area. Test planispirally coiled, biumbilicate, moderately evolute with a shallow umbilicus, moderately to strongly lobate and subcircular in equatorial outline, test axially compressed with an elliptical peripheral margin, symmetrical in edge view, nearly always uniapertural; chambers axially compressed, slightly inflated, enlarging relatively rapidly in size throughout ontogeny, total chambers in adult specimens usually coiled in 1.5 whorls, sutures radial, depressed; interiomarginal aperture centered on equatorial margin with a circular arch extending up the final chamber face and sometimes extending part way toward the umbilicus, bordered by a narrow lip; relict apertures sometimes visible surrounding the umbilicus.

**Remarks:** reveals sufficient similarity among *Planohedbergella escheri* (Kaufmann, 1865)

**Occurrences :** Lower- Middel Coniacian of Essen Formation

**Distribution :** recorded in early Coniacian *Dicarinella concavata* Zone (Georgescu and Huber 2008), ranges through the late Campanian *Radotruncana calcarata* Zone (Huber et al. 2022). Occurs in low to middle latitude sequences; specimens have not been identified at high southern or northern latitudes.

**Genus:** *Planohétérohélix*

***Planoheterohelix reussi* (Cushman, 1938)**

**Pl. 5. Figure 9a-b**

1938 *Guembelina reussi* CUSHMAN.

1970 *Heterohelix globulosa* EHRENBERG.

**Material: C1- S62 (4705 specimens)**

**Description of the specimens:** The test of this species is small, with an elongate to oval shape and a planispiral coiling that varies from evolute to slightly involute. The spiral side is usually flat to slightly convex, while the umbilical side tends to be flattened or slightly concave. The chambers are numerous, initially arranged in a biserial pattern, sometimes

### CHAPTER III SYSTEMATIC

transitioning to a triserial arrangement in later growth stages. They are generally rectangular to trapezoidal in form and gradually increase in size, although the final chambers enlarge more rapidly. Chambers display fine ribbed ornamentation and are finely perforated. Sutures are straight to gently curved, distinctly separating the chambers, and are typically flush with the test surface or slightly depressed. The wall is calcareous and microperforate, with a generally smooth surface lacking prominent pustules. The aperture is terminal, appearing as a simple slit or rounded opening at the end of the last chamber, often bordered by a delicate lip. This species differs from *H. globulosa* by its more elongated overall shape, making it a distinguishing morphological feature.

**Remarks :** *Planohétérohélix reussi* is a common benthic foraminifer in Upper Cretaceous marine deposits, typically inhabiting shelf to upper slope environments. It serves as a valuable biostratigraphic tool for correlating Cretaceous strata, owing to its distinctive coiling pattern and progressive chamber arrangement from biserial to triserial forms. This species is frequently associated with moderate to low-energy depositional settings characterized by well-oxygenated bottom waters. It differs from closely related genera by its unique planispiral coiling and the developmental transition in chamber arrangement observed during growth.

**Occurrences :** Coniacian and Santonian of Essen Formation

**Distribution:** *Planohétérohélix reussi* has a broad geographic distribution and has been documented in numerous Late Cretaceous marine basins worldwide. In Europe, it has been found in France, Germany, Spain and the United Kingdom. Notable occurrences in North Africa include Morocco and Algeria. In the Middle East, records include Saudi Arabia and neighbouring regions, while in North America, the species is well represented in the Gulf of Mexico and in several outcrops across the southwestern United States. This species is primarily associated with Late Cretaceous deposits, with its stratigraphic range most firmly established between the Campanian and Maastrichtian stages. Although occasional findings outside this range have been reported, most studies confirm its highest abundance and reliability within this time interval. Due to its widespread occurrence and well-defined temporal range, *P. reussi* serves as a valuable index fossil for correlating marine strata of the Late Cretaceous period. Additionally, *P. reussi* has been identified in Upper Cretaceous deposits ranging from the Upper Cenomanian to the Maastrichtian, with reported occurrences in West Africa, the Atlantic realm, the Americas, and Europe (Caron, 1985; Leckie, 1987; De Klasz et al., 1995; Keller et al., 2001; Keller & Pardo, 2004).

## CHAPTER III SYSTEMATIC

### Legend Planktonic Foraminifera

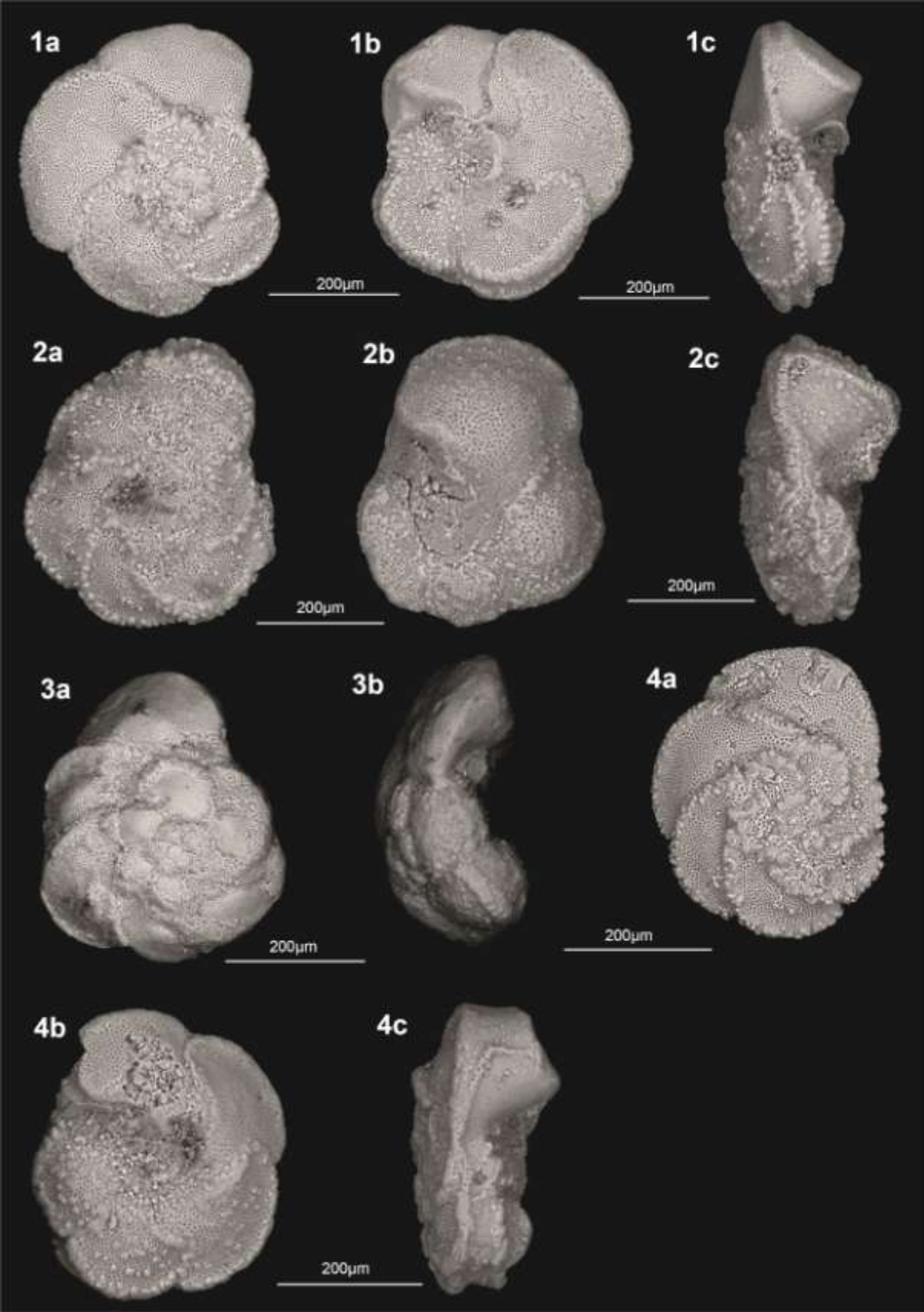
**Plate 1:** **1a-c:** *Marginotruncana renzi* (Gandolfi, 1942) sample C3; **2a-c:** *Marginotruncana caronae* Peryt, 1980 sample C100; **3a-b:** *Marginotruncana* cf. *sigali* (Reichel, 1950) sample C160; **4a-c:** *Marginotruncana sinuosa* Porthault, in Donze et al., 1970; sample C121.

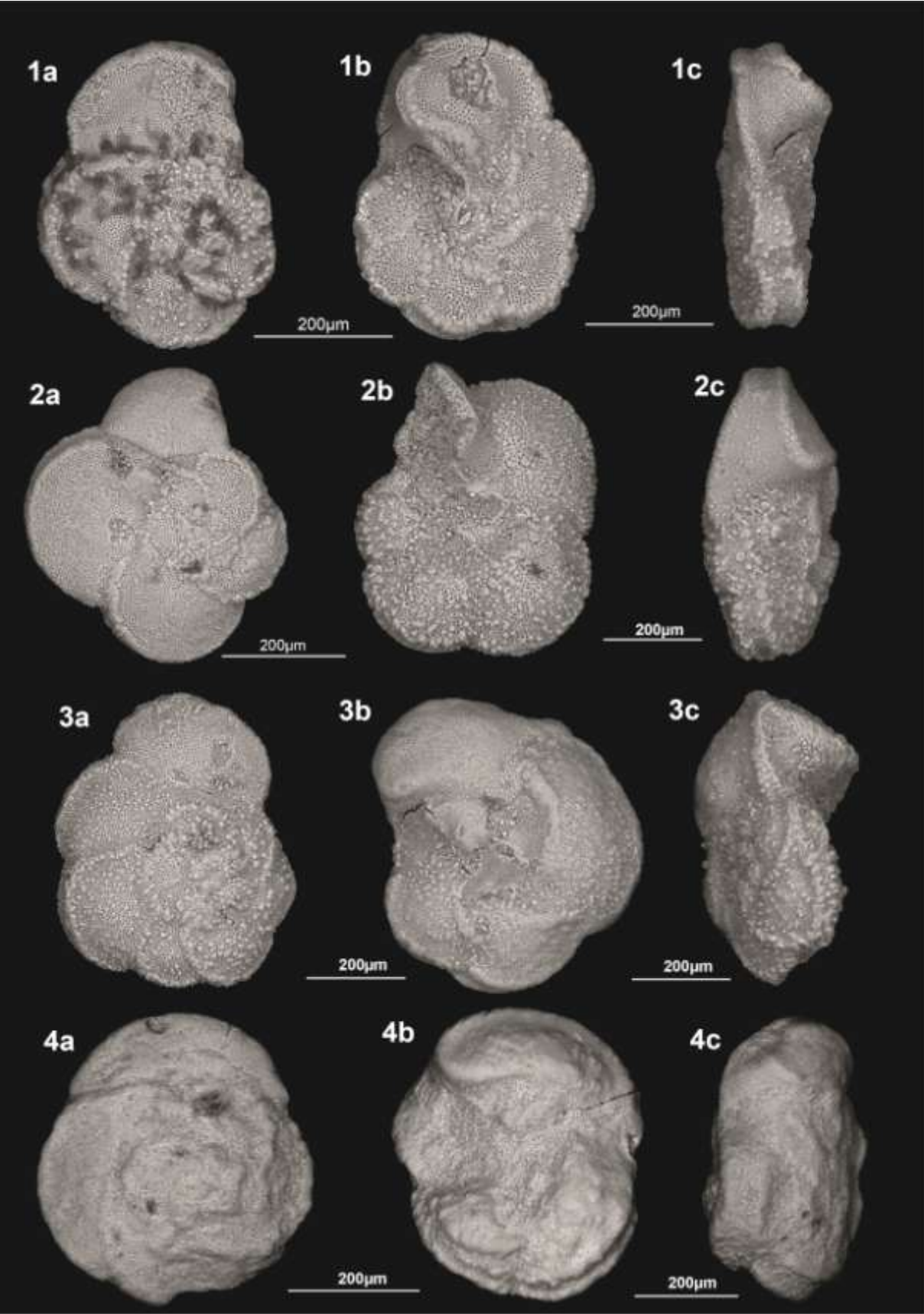
**Plate 2:** **1a-c:** *Marginotruncana pseudolinneiana* Pessagno, 1967 sample C35; **2a-c:** *Globotruncana linneiana* (d'Orbigny, 1839) sample C100; **3a-c:** *Globotruncana bulloides* Vogler, 1941 sample S25; **4a-c:** *Globotruncana* sp., Sample C30.

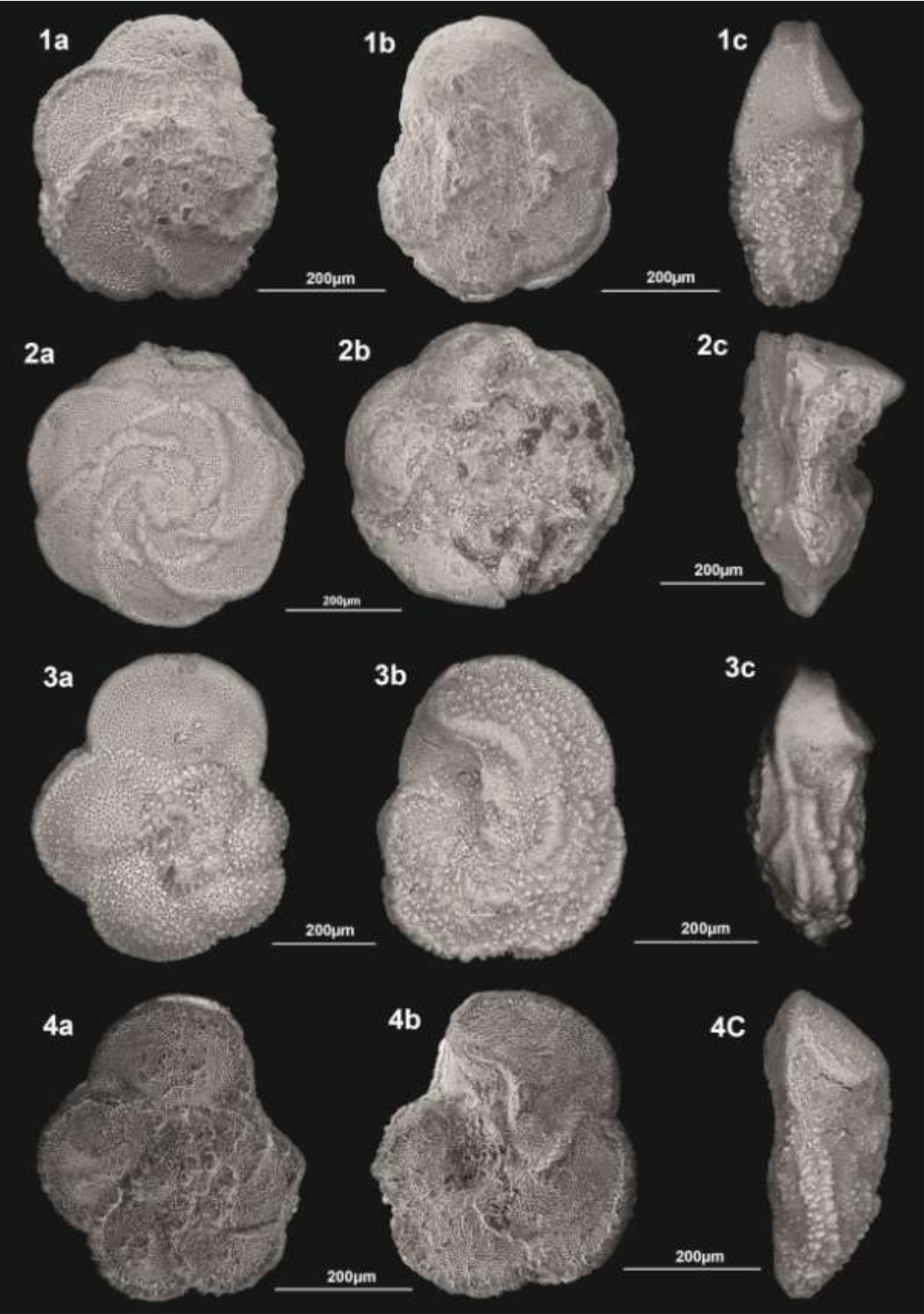
**Plate 3:** **1a-c:** *Globotruncana arca* (Cushman, 1926) sample S20 ; **2a-c:** *Globotruncanita elevata* (Brotzen, 1934) sample S47; **3a-c:** *Contusotruncana plummerae* (Gandolfi, 1955) sample S10 ; **4a-c:** *Dicarinella canaliculata* (Reuss 1854) sample C170.

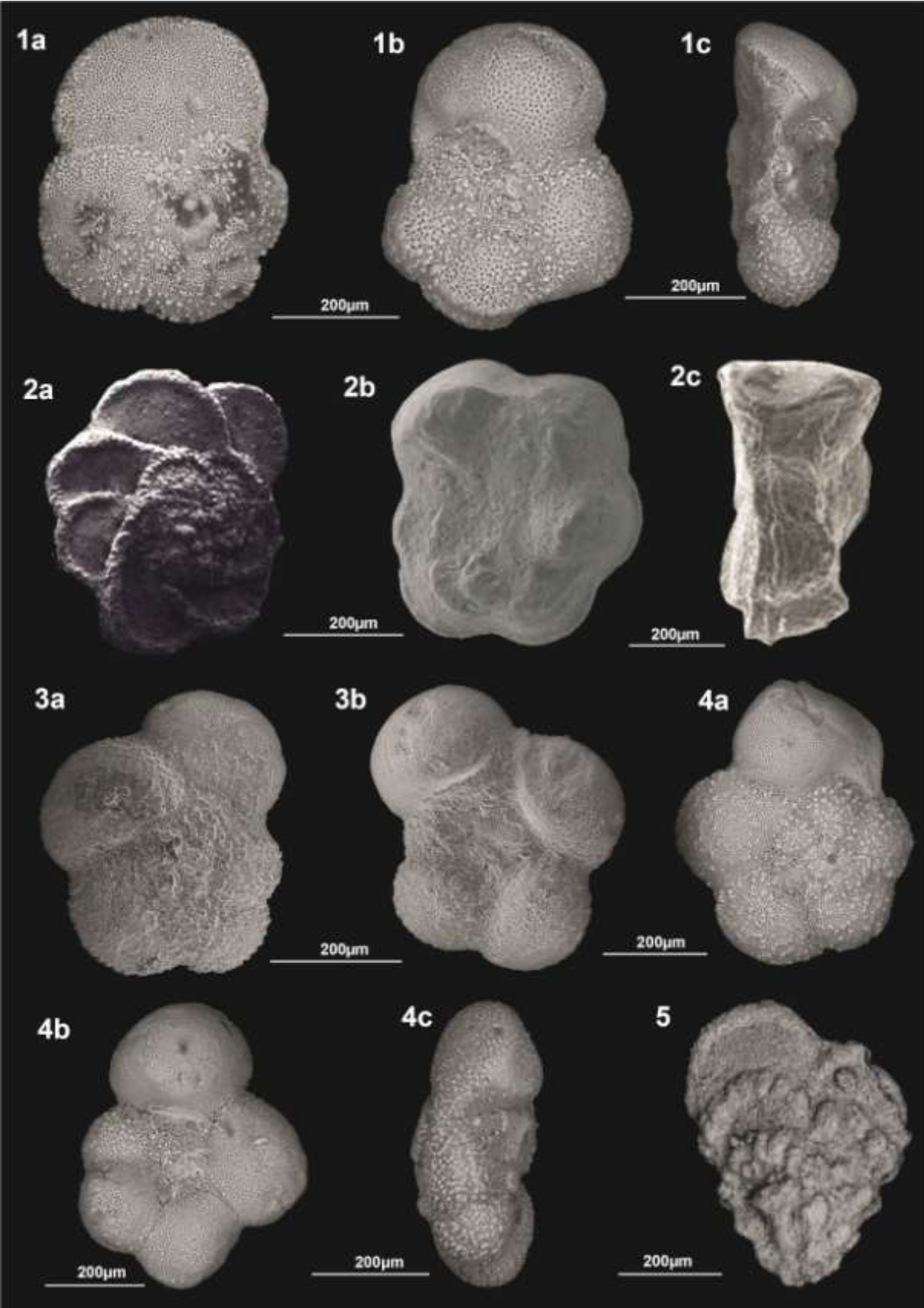
**Plate 4:** **1a-c:** *Dicarinella primitiva* (Dalbiez, 1955) sample C100 ; **2a-c:** *Dicarinella asymetrica* (Sigal, 1952) sample S10 ; **3a-b:** *Archaeoglobigerina* sp., sample C35; **4a-c:** *Muricohedbergella flandrini* (Porthault, in Donze et al., 1970) sample C89; **5:** *Sigalia carpatica* Salaj & Samuel, 1963 sample S3.

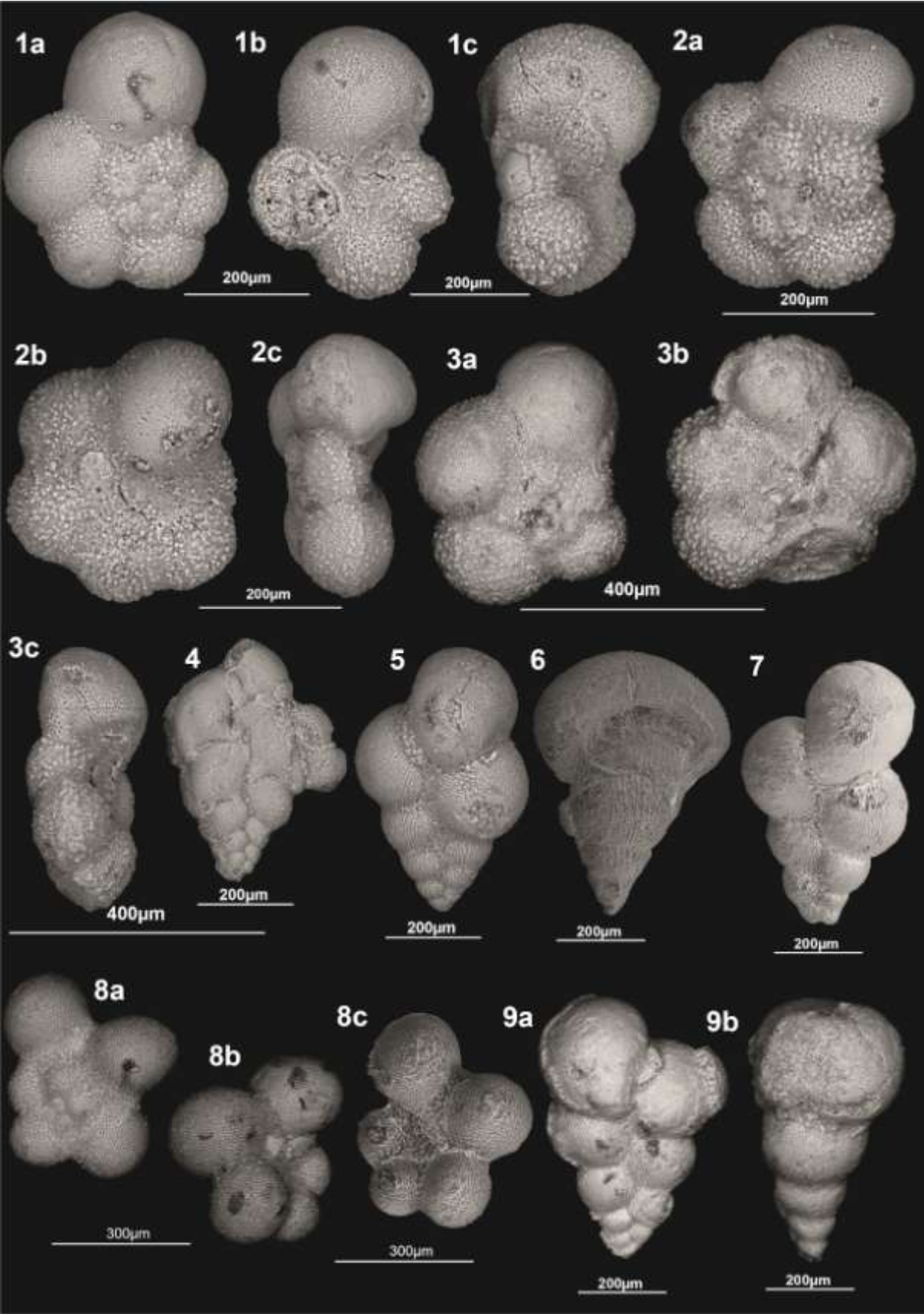
**Plate 5:** **1a-c:** *Whiteinella baltica* Douglas and Rankin , 1969, sample C1; **2a-c:** *Whiteinella archaeocretacea* Pessagno, 1967 sample C3; **3a-c:** *Whiteinella* sp., sample C4 ; **4:** *Huberella praehuberi* Georgescu 2007 sample C80; **5:** *Pseudotextularia* sp., sample C15; **6:** *Pseudotextularia nuttalli* (Voorwijk, 1937) sample C 64; **7:** *Planohétérohélix globulosa* (Ehrenberg, 1840) sample C18; **8a-c:** *Planohedbergella* cf. *escheri*, (Kaufmann, 1865) sample C64; **9a-b:** *Planohétérohélix reussi* (Cushman, 1938), sample C3.











## CHAPTER III SYSTEMATIC

### Benthic Foraminifera

Family Gavelinellidae

Subfamily Gavelinellinae

Genus *Gavelinella*

*Gavelinella* sp.,  
Pl. 6. Figure 1a-b, 4

**Material:** C1- S21 (2674 specimens)

**Description:** Free, calcareous, planispiral, almost bilaterally symmetrical, semi-involute test. The dorsal side is more convex than the ventral side. The periphery is narrowly rounded. The last whorl is composed of 9-12 chambers. The sutures are slightly curved on both sides of the test. The umbilical depression on the spiral side is often filled with secondary calcite.

**Occurrence :** Coniacian- Lowe Santonian of Essen Formation

**Distribution:** Santonian to Maastrichtian, Benmansour, 2017.

Family Gavelinellidae

Subfamily Gavelinellinae

Genus *Notoplanulina*

*Notoplanulina* sp.,

**Material:** C98-C100, S11-S52, S55, S60, S62 (711 specimens)

**Description of the specimens:** Test about 1 mm in diameter, flattened, low trochospiral coil of about three whorls, six to thirteen rapidly flaring chambers in the final whorl, planoconvex, spiral side flat and evolute, sutures strongly curved, raised, and limbate, umbilical side involute, chambers inflated, sutures curved and depressed, umbilicus open and deep or may be partly covered by umbilical chamber extensions or folia, periphery angular and carinate; wall calcareous, optically granular, finely perforate except for the imperforate thickened sutures; aperture an areal transverse slit bending sharply to an interiomarginal continuation along the base of the chamber face. U. Cretaceous (Coniacian to Maastrichtian); New Zealand; Argentina; USA: California. (Loeblich & Tappan, 1987, Foraminiferal Genera and Their Classification)

**Occurrences :** Middel Coniacian, Upper Santonian of Essen Formation

**Distribution :** Upper Cretaceous (Coniacian to Maastrichtian), Malumián & Masiuk, 1977

## CHAPTER III SYSTEMATIC

Family Nonionidae

Subfamily Nonioninae

Genus Nonionella

*Nonionella* sp.,  
Pl. 6. Figure 2

**Material:** S1- S52 (595 specimens)

**Description of the specimens:** The test is slightly compressed and arranged in a low trochospiral coil with a rounded periphery. The spiral side is partially evolute, surrounding an umbonal boss, while the umbilical side is involute. Chambers are numerous, broad, and low, with whorls that gradually increase in size, sometimes producing a slightly flaring test. Each chamber has a flap-like extension that overhangs the umbilicus, with successive chambers overlapping one another. Sutures are curved and depressed, and the periphery remains rounded. The wall is calcareous, optically granular, and finely perforated, with a smooth surface lacking pustules. The aperture is a small, nearly equatorial interiomarginal arch that extends slightly onto the umbilical side. This form ranges from the Upper Cretaceous (Coniacian) to the Holocene and is cosmopolitan in distribution.

**Occurrences :** Middel Coniacian- Santonian of Essen Formation

**Distribution :** Upper Cretaceous (Maastrichtian) Benmansour, 2017

**Suborder** Spiroplectamminina Cushman, 1927

**Superfamily** Spiroplectamminacea Cushman, 1927

**Family** Textulariopsidae Loeblich & Tappan, 1982

*Eobigenerina* sp.,

Pl. 6. Figure 3

**Material:** S1- S52 (403 specimens)

**Description of the specimens:** The test begins with an early biserial stage that makes up at least one-third of the total adult length, followed by a loosely biserial stage. This is succeeded by a short, open uniserial section and concludes with a terminal uniserial stage composed of low, rounded chambers in cross-section. The wall is solid, noncanaliculate, and smoothly finished, consisting of fine agglutinated particles bound by organic material. It is often well silicified and resistant to dissolution in HCl. The aperture is terminal, small, and rounded, positioned on a collar or short neck.

**Remarks :** It differs from *Bigenerinaby* possessing a solid, non canaliculate wall that is resistant to acid dissolution. Unlike *Aaptotoichus*, it has a well-developed biserial portion, a

## CHAPTER III SYSTEMATIC

short apertural neck, and a finely agglutinated test wall. It is distinguished from *Bimonilina* by having chambers that are strictly uniserial rather than lax-uniserial, along with a rounded terminal aperture. Additionally, it differs from *Rashnovammina* and *Bicazammina* by the presence of a truly uniserial terminal section with horizontal sutures between the final chambers.

**Occurrences :** Santonian of Essen Formation

**Distribution :** Very abundant in the Cenomanian–Turonian boundary interval, abundant to rare in the Turonian, and very rare in the Cenomanian. Upper Pennsylvanian to Eocene; Australia; USA: Kansas, Texas; Indian Ocean; North Atlantic; Barents Sea; Alpine-Carpathian region: Romania, Poland, Czech Republic, Austria, Germany, Italy

**Family** Cibicididae

**Subfamily** Cibicidinae

**Genus** Cibicidoides

**Cibicidoides sp.,**

**Pl. 6. Figure 5**

**Material:** C99- S45 (1017 specimens)

**Description:** Trochospiral test, conical to subconical. The chambers are triangular to trapezoidal. The opening is basal. The internal walls are slightly curved.

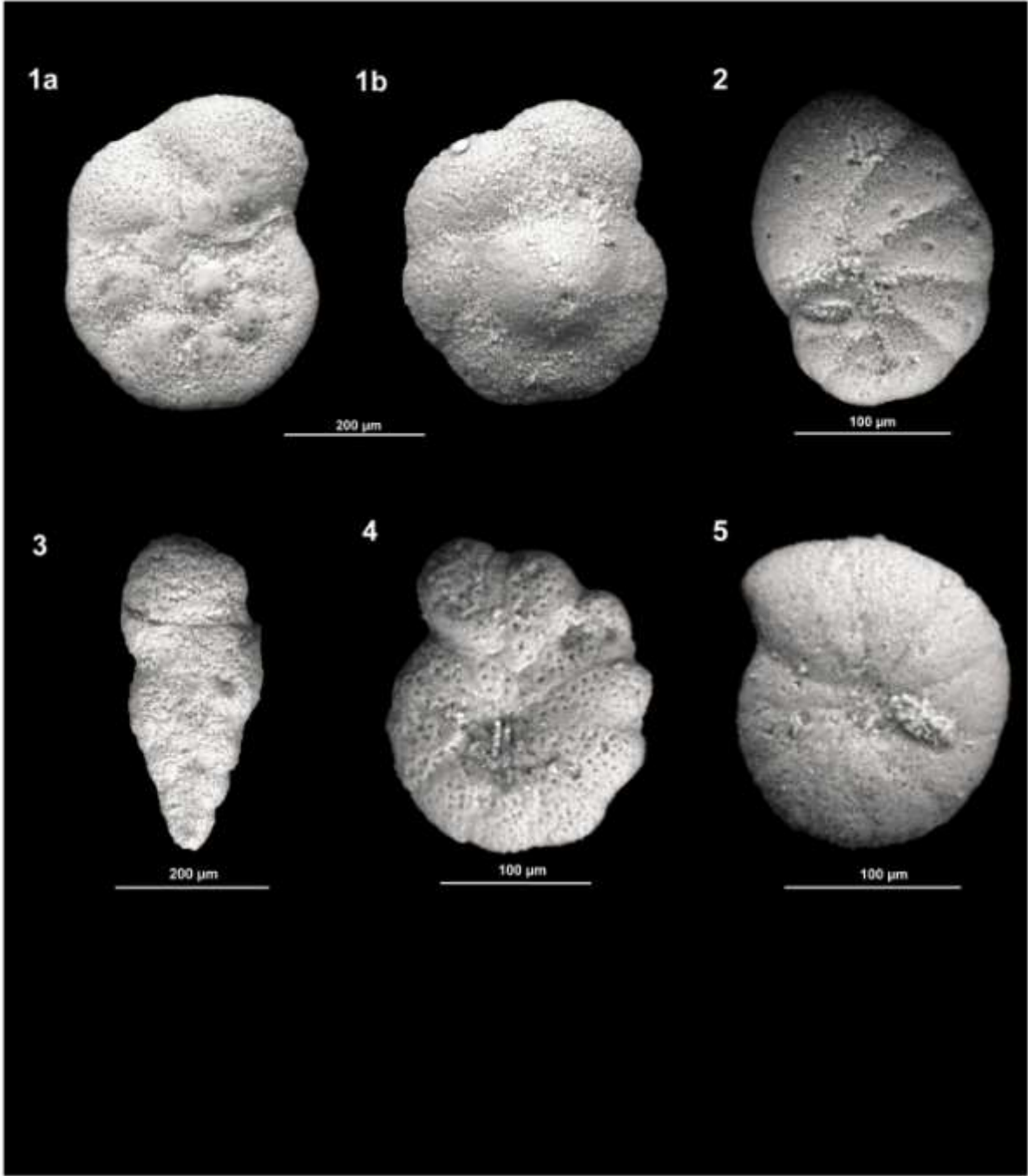
**Occurrence :** Lower, Upper Coniacian- Upper Santonian of Essen Formation

**Distribution:** Late Cretaceous (Ben mansour, 2017)

CHAPTER III SYSTEMATIC

Legend Benthic Foraminifera :

Plate 6: 1a-b: *Gavelinella* sp; 2: *Nonionella* sp.; 3 : *Eobigenerina* sp. 4, 5 : *Cibicidoides* sp.



***CHAPTER IV***  
***BIOSTRATIGRAPHY***

## CHAPTER IV BIOSTRATIGRAPHY

### 1. Introduction

The first Symposium on Cretaceous Stage Boundaries (Birkelund et al., 1984) reached a broad agreement that the first appearances (FO) of the ammonite subgenus *Texanites* (*Texanites*) and the inoceramid bivalve *Cladoceramus* (= *Platyceramus*) *undulatoplicatus* (Roemer) represent the most reliable biostratigraphic markers for defining stage boundaries. Although *Texanites* (*Texanites*) has been used across a wide geographic area, its rarity in the classical northwestern European sections reduces its usefulness there as a stratigraphic indicator (Hancock, 1991). By contrast, *Platyceramus undulatoplicatus* is geographically widespread and morphologically distinctive, making it easy to recognize. In North African successions, *Platyceramus siccensis* (Pervinquière) commonly occurs together with *Texanites* and has been suggested as an additional marker for identifying the base of the Santonian Stage (Lamolda et al., 2014). The genus *Platyceramus* is known to have first appeared during the Coniacian–Santonian interval (Seitz, 1961, 1967).

In the report of the working group on the Santonian to the second symposium on the limits of the Cretaceous stages (Lamolda and Hancock, 1996), the *Texanites* FO was rejected because it lies below the lower limit of *Platyceramus undulatoplicatus* and had been cited in assemblages with inoceramids normally considered coniacian (Lamolda and Hancock 1996). The first occurrence (FO) of *Platyceramus undulatoplicatus* was confirmed as the main marker of the base of the Santonian stage. The FO of the planktonic foraminifer *Sigalia carpatica* was accepted as a secondary marker of the basal Santonian. It is widespread in the Mediterranean region of the Tethys, is associated with *Inoceramus siccensis* and *Texanites* in Tunisia, and in northern Spain (Navarre) its FO is very close to the lowest occurrence of *Platyceramus undulatoplicatus*.

Dalbiez (1956) was the first to present a preliminary description of Santonian foraminifera in the Kef region, Salaj (1980) used the distribution of foraminifera from the El Kef section and other sections in northern Tunisia, to subdivide the *Dicarinella asymetrica* zone, which he considered characteristic of the Santonian, into three successive sub-zones (*Sigalia carpatica* sub-zone, *Ventilabrella decoratissima* sub-zone and *Globotruncana manaurensis* sub-zone).

In eastern Algeria, the Coniacian and Santonian interval remains poorly documented, with only a few palaeontological studies devoted to this stratigraphic interval (Durozoy, 1956;

## CHAPTER IV BIOSTRATIGRAPHY

Nemouchi et al., 2024). Previous research has mainly been based on ammonite assemblages (Dubourdiou, 1956), notably *Muniericeras* sp., *Peroniceras* sp., *Barroisiceras* sp., *Forresteria* sp. and *Harleites* ? nov. sp. However, these taxa, recorded below the occurrence of *Texanites texanus* at the end of the Santonian, provide limited stratigraphic resolution, leaving the boundary between the Coniacian and Santonian indistinct. The assemblages of inocera in the Constantinois and Monts du Mellegue regions, Voûte (1967) documented various forms assigned to the following species in the Lower Coniacian of the Chebka des Sellaoua ; these include *Inoceramus sublabiatus*, *Inoceramus* sp. cf. *sublabiatus*, *Inoceramus inconstans*, *Inoceramus inconstans* var. *planus*, *Inoceramus mantelli*, *Inoceramus striato-concentricus*, *Inoceramus* aff. *striato-concentricus* and *Inoceramus undulatus*. In the Khémisssa region (Monts de Medjerda), David (1960) cited the species *Inoceramus* gr. *labiatus*.

In Tébessa, Vivière (1985) reported the species *Inoceramus (Platyceramus) siccensis* Dans le Djebel Dyr. Van Der Fliert (1955) mentioned the species *Inoceramus brongnarti* and *Inoceramus cycloides* var. *siccensis* in the Lower Senonian of Jebel Frikitia.

Despite the abundance and wide distribution of the outcrops, the absence of reliable radiometric dating and macrofaunal data in these deposits presents a significant challenge for accurately delineating stage boundaries (Nemouchi et al., 2024). In light of this limitation, biostratigraphic analyses based on microfossils offer considerable potential. Accordingly, the present study employs planktonic foraminifera to refine age estimations and facilitate a more precise reconstruction of the palaeoenvironment within the study area.

## CHAPTER IV BIOSTRATIGRAPHY

Age (Ma)	Author		Gradstein et al., (2012) Tethyan Ammonoids	Robaszynski et al., (2000), Tunisia Ammonite zone	Present Work
	Age				
83.5	Santonian	E	<i>Platyceras</i> <i>Polyopsis</i>	interval of Texanites	
		Lt			
		M			
		E			
85.8 86.3	Coniacian	Lt	<i>Paratexanites</i> <i>serratomagnum</i>	interval of <i>Paratexanites</i> & <i>Protexanites</i>	
M					
E					
88.6 89.8	Turonian	Lt			

**Table IV.1 :** Stratigraphic framework and the Ammonit biozones identified in the study section at Djebel Essen.

Age (Ma)	Author		Lamolda et al., (2011) Olazagtia Inoceramid zone	Present Work
	Age			
83.5	Santonian	E	<i>Platyceramus</i> <i>undulaplicatus</i>	
		Lt		
		M		
		E		
85.8 86.3	Coniacian	Lt	<i>Magadiceramus</i> <i>subquadratus</i>	
M				
E				
88.6 89.8	Turonian	Lt		

**Table IV. 2:** Stratigraphic framework and the Inoceramids biozones identified in the study section at Djebel Boukezez.

# CHAPTER IV BIOSTRATIGRAPHY

Age (Ma)	Age	Author	Stratigraphic zone	Zone	Zone	Zone	Zone	Zone	Zone	Zone	Zone	Zone	Zone	Zone	Zone	Zone
100	Senonian	El Ghazal and El Ghazal, 2016	Senonian	Senonian	Senonian	Senonian	Senonian	Senonian	Senonian	Senonian	Senonian	Senonian	Senonian	Senonian	Senonian	Senonian
90	Senonian	El Ghazal and El Ghazal, 2016	Senonian	Senonian	Senonian	Senonian	Senonian	Senonian	Senonian	Senonian	Senonian	Senonian	Senonian	Senonian	Senonian	Senonian
80	Senonian	El Ghazal and El Ghazal, 2016	Senonian	Senonian	Senonian	Senonian	Senonian	Senonian	Senonian	Senonian	Senonian	Senonian	Senonian	Senonian	Senonian	Senonian
70	Senonian	El Ghazal and El Ghazal, 2016	Senonian	Senonian	Senonian	Senonian	Senonian	Senonian	Senonian	Senonian	Senonian	Senonian	Senonian	Senonian	Senonian	Senonian
60	Senonian	El Ghazal and El Ghazal, 2016	Senonian	Senonian	Senonian	Senonian	Senonian	Senonian	Senonian	Senonian	Senonian	Senonian	Senonian	Senonian	Senonian	Senonian
50	Senonian	El Ghazal and El Ghazal, 2016	Senonian	Senonian	Senonian	Senonian	Senonian	Senonian	Senonian	Senonian	Senonian	Senonian	Senonian	Senonian	Senonian	Senonian
40	Senonian	El Ghazal and El Ghazal, 2016	Senonian	Senonian	Senonian	Senonian	Senonian	Senonian	Senonian	Senonian	Senonian	Senonian	Senonian	Senonian	Senonian	Senonian
30	Senonian	El Ghazal and El Ghazal, 2016	Senonian	Senonian	Senonian	Senonian	Senonian	Senonian	Senonian	Senonian	Senonian	Senonian	Senonian	Senonian	Senonian	Senonian
20	Senonian	El Ghazal and El Ghazal, 2016	Senonian	Senonian	Senonian	Senonian	Senonian	Senonian	Senonian	Senonian	Senonian	Senonian	Senonian	Senonian	Senonian	Senonian
10	Senonian	El Ghazal and El Ghazal, 2016	Senonian	Senonian	Senonian	Senonian	Senonian	Senonian	Senonian	Senonian	Senonian	Senonian	Senonian	Senonian	Senonian	Senonian

**Table IV. 3:** Stratigraphic correlation of the identified biozones to previous zones in adjacent areas.

## 2. Results

### 2.1. Ammonites Zones

#### **Hemitissotia morreni Total Range-Zone (T. R. Z.) Upper Coniacian**

This biozone corresponds to the total time of existence of the marker taxon. It's occurs through about 268 m in the Essen section (samples C170 to C180).

It also closely resembles certain *Hemitissotia batnensis* Peron. The exact interpretation of Coquand's *Ammonites Morreni* is difficult and what disagreements exist in its description, figuration and classification. Coquand, in fact, who had taken over Haan's *Ceratites* genus to classify the ammonites of Algeria whose partitions have rounded saddles, classified the species we are dealing with not in this *Ceratites* genus but in the *Ammonites*. Moreover, in describing the *Ceratites Fourneli*, whose external form is similar to that of *Ammonites Morreni*, he specifies that these fossils are distinguished in that the former possesses the remarkable characters of the *Ceratites*, unlike the latter.

Pervinquière (1907) and Chancellor et al (1994) considered *H. batnensis* Peron (1897) and *H. czini* Peron (1897) to be synonyms of *H. morreni*.

**Stratigraphic distribution:** Lower Senonian of Refana, near Tébessa; Algeria (Peron 1896), Upper Turonian of Tunisia (Coquand, 1862), North Africa (Tunisia and Algeria; Chancellor et al., 1994), and the Middle East (Palestine ; Parnes, 1964).

### 2.2. Inocerames Zones

#### **Inoceramus sicicensis Total Range-Zone (T. R. Z.) Santonian :**

## CHAPTER IV BIOSTRATIGRAPHY

This biozone corresponds to the total time of existence of the marker taxon. It occurs through about 90 m in the Boukezez section (samples E45) associated with irregular echinoids (*Mecaster fourneli* Agassiz, 1847).

Several authors considered that the FO of *Inoceramus siccensis* is located at the Coniacian/Santonian (C/S) boundary (e.g. Farouk et al., 2017), Lower Santonian (e.g. *Inoceramus siccensis* Pervinquière (1912), (SIGAL, 1952), Van der Fliert, (1955), Dubourdiou, (1956), David (1960), Coquand, (1862), Voûte, (1967), Vila, (1980), Birkelund et al., (1984), Vivière, (1985), Robaszynski et al., 1998, Rami et al., 1997, El Amri (2004), Walaszczyk, (2006), El Manai (2009), Midell Santonian (e.g. Voûte (1951).

This species is related to the *Inoceramus (Platyceramus) cycloides* (Wegner) group. It is known only from North Africa, where it occurs in great quantities together with rare *Texanites* at Djebel Fguira Salah, Tunisia (Birkelund et al., 1984).

**Stratigraphic distribution:** This species was reported in the Upper Turonian of Dyr el Kef (Tunisia) by Pervinquière (1912). In Algeria, it is known from the Coniacian-Santonian boundary at El Kantara (Aurès). It has also been cited in the same period in Constantinois and the Monts du Mellegue (Dubourdiou, 1956; Van der Fliert, 1955 and Voûte, 1967) and in the Nementchas (Vivière, 1985).

### 2.3. Foraminifera Zones

#### **Dicarinella primitiva Total Range-Zone (T. R. Z.) Early- Middle Coniacian**

This biozone corresponds to the total time of existence of the marker taxon. It occurs through about 200 m in the Essen section (samples C1 to C120). The dominant planktic species are: *Heterohelix globulosa*, *H. reussi*, *Pseudotextularia nuttalli*, *Pseudotextularia* sp, *Whiteinella baltica*, *W. archaeocretacea*, *W. sp.*, *Archaeoglobigerina* sp., *Hastigerinoides subdigitata*, *Marginotruncana marginata*, *M. rensi*, *M. caronae*, *M. coronata*, *M. pseudolinneiana*, *M. cf. sigali*, *Globotruncana linneiana*, *Muricohedbergella flandrini*, *Planohedbergella cf. escheri*. (Figure 01)

**Stratigraphic distribution :** Several authors considered that the FO of *Dicarinella primitiva* is located at the Early Coniacian (e.g. Premoli Silva & Boersma, 1977; Caron, 1978, 1985; Robaszynski & Caron, 1979; Wonders, 1980; Birkelund et al., 1984; Marks, 1984a, b; Abdel-Kireemet et al., 1995; El Albani et al., 1999; Premoli Silva and Verga, 2004; Abawi & Mahmood, 2005; El Amri and Zaghib-Turki, 2005; El Amri, 2008), Rami, A., et al., 2016; Ogg

## CHAPTER IV BIOSTRATIGRAPHY

et al., 2016; Bentaher et al., 2023; Sulaiman et al., 2023). Usually, this biozone is determined at the base of the *Dicarinella concavata* interval zone (Caron, 1985 ; Gradstein et al., 2008 Ogg et al., 2016). Wonders (1980) adopted the *Dicarinella primitiva* biozone to designate the whole of the Coniacian. According to Salaj(1980), this biozone represents the upper part of the Lower Coniacian and most of the Upper Coniacian. However, other previous studies have assigned the *Dicarinella primitiva* biozone to the Late Turonian to Early Coniacian (Nederbragt, 1991; Salaj, 1997; Robaszynski et al., 1990; Robaszynski and Caron, 1995; Gebhardt, 2004, 2008; Premoli Silva and Verga, 2004; Elamri et al., 2014). While others suggest that the species *D. primitiva* appears in the terminal part of the Middle Turonian (Robaszynski et al., 1990) or at the end of the Turonian (Robaszynski and Caron, 1995 ; Salaj, 1997; Premoli-Silva and Sliter, 1999; Gebhardt, 2004; Elamri et al., 2014; Vahidinia et al., 2014; Jaff et al., 2015). In addition, Bellier (1983) designated it as a subzone to mark the upper part of the *Marginotruncana Schneegansi* zone of the Upper Turonian. In this study, we attribute the whole *Dicarinella primitiva* biozone to Lower- Middle Coniacian

### **Marginotruncana sinuosa Partial range zone Upper Coniacian**

This biozone is defined as the time interval, including the marker fossil, between the extinction of *Dicarinella primitiva* and the first appearance of *Sigalia carpatica*. It is located between the samples C35- C180 (145m thick) in the Essen section. In this biozone, various species occur: *Heterohelix globulosa*, *H. reussi*, *Pseudotextularia nuttalli*, *Pseudotextularia* sp, *Whiteinella baltica*, *W. archaeocretacea*, *W.* sp, *Archaeoglobigerina* sp, *Hastigerinoides subdigitata*, *Dicarinella canliculata*, *Marginotruncana coronata*, *M. sigali*, *M. pseudolinneian*, *Muricohedbergella flandrini*.

**Stratigraphic distribution** : According to Bellier (1983), Birkelund et al. (1984), Kauffman et al. (1996) and Vahidinia et al. (2016), the appearance of *Marginotruncana sinuosa*, together with the deployment of the *Dicarinella primitiva - concavata* group, can provisionally be used as a marker to distinguish the Coniacian from the Turonian. Elsewhere, *Marginotruncana sinuosa* has been recorded in the *Dicarinella Primitiva Interval Zone* and *Dicarinella Concavata Interval Zone*, which date from the Early to Late Coniacian, respectively (Jaff et al., 2015; Elamri et al., 2016; Sulaiman et al., 2023) and may even exceed the Santonian in the *Dicarinella asymetrica Total Range Zone* (Elamri and Zaghib-Turki, 2004 ; Sulaiman et al. 2023). According to Elamri et al., (2016), the *M. sinuosa*, species exceed the Santonian/Campanian boundary where the *marginotruncanids* suffered gradual extinction. It has been recorded in the *Globotruncanita elevata/Globotruncana* area

## CHAPTER IV BIOSTRATIGRAPHY

Partial Range Zone (PRZ), which dates from the Early-Middle Campanian. However, Rami et al. (2016) report that *M. sinuosa* is extinct before the end of the Zone with *Globotruncana arca* Cushman which dates from the Lower Campanian.

In the present work, this species marks the Upper Coniacian in the absence of *Dicarinella concavata* Brotzen.

### **Sigalia carpatica Partial range Zone early Santonian**

This biozone is determined by the interval between the first and last occurrence of the index taxon. It is represented by samples S1-S9 (25m thick) in the Essen section. Its appearance is not synchronous with that of *Dicarinella asymetrica*, but is more common with *Globotruncana linneiana*. The dominant planktic species are: *Heterohelix globulosa*, *H. reussi*, *Whiteinella baltica*, *W. archaeocretacea*, *Hastigerinoides subdigitata*, *Archaeoglobigerina* sp, *Globotruncana linneiana*, *Marginotruncana coronata*, *M. pseudolinneiana*.

**Stratigraphic distribution** : The occurrence of *Sigalia carpatica* has been much debated by many authors. In fact, this species is not always a common one in series rich in planktonic foraminifera (Elamri and Zaghib-Turki, 2004; Jaff et al., 2015; Elamri et al., 2016; Sulaiman et al., 2023). However, taking into account the distribution of planktonic foraminifera by Salaj (1980), the Santonian in Tunisia is subdivided into three successive sub-zones at: *Sigalia carpatica*, *Ventilabrella decoratissima* and *Globotruncana manaurensis*. This subdivision was also adopted by Bellier (1983), and Robaszynski and Caron (1995) where *Sigalia carpatica* marks the lower Santonian. A number of authors (e.g. Salaj and Samuel, 1966; Rami et al., 2016) indicate the contemporary occurrence of *Sigalia carpatica* to that of *Dicarinella asymetrica* and consider it to be a sub-zone of the *Dicarinella asymetrica* (T. R. Z.) before the occurrence of *Sigalia decoratissima*, marking the lower Santonian. This view is confirmed by Bellier (1983), who admits that the simultaneous occurrence of *Sigalia carpatica* and *Dicarinella asymetrica* marks the lower limit of the Santonian. In fact, Salaj (1980) had already mentioned that the occurrence of these two species is simultaneous and can only be synchronous. Similarly, Nederbragt (1990), Robaszynski et al (2000), Elamri and Zaghib-Turki (2002) and Jaff and Al-Kahtany (2020) found that the occurrence of *Sigalia carpatica* was much later than that of *Dicarinella asymetrica*. It should also be noted that according to Wagreich (1992) and Jaff and Al-Kahtany (2020), *Sigalia carpatica* appeared in the latest Coniacian.

## CHAPTER IV BIOSTRATIGRAPHY

The present study examines the FO of *Sigalia carpatica* from the Early Santonian.

### **Dicarinella asymetrica Interval Zone Middle-Upper Santonian**

This biozone encompasses the first occurrence of the index taxon from the LO of *Sigalia carpatica* at the FO *Globotruncanita elevata*. This biozone represented by around 116m of strata in the Essen section (362–478 m), from sample numbers S10- S46. It is characterized by the co-existence of several dominant planktic foraminifera species are : *Heterohelix globulosa*, *Planoheterohelix globulosa*, *Whiteinella baltica*, *W. archaeocretacea*, *Archaeoglobigerina* sp, *G. arca*, *G. linneiana*, *Contusotruncana plummerae*.

**Stratigraphic distribution:** Some studies (Lamolda et al., 2007, 2014 ;Coccioni and Premoli-Silva, 2015; Gale et al., 2007); Soycan and Hakyenez, 2018) proposed a duration from the latest Coniacian to the Santonian for *Dicarinella asymetrica* biozone. However, Marks (1984), Farouk et al. (2017), Lamolda et al. (2014), Elamri and Zaghib-Turki (2004, 2005) and Elamri (2008) proposed the first occurrence (FO) of *Dicarinella asymetrica* could be used as a marker for defining the Coniacian/Santonian boundary. It's highest occurrence (HO) defines the Santonian-Campanian boundary (Caron, 1985; Sliter, 1989; Gale et al., 1995; Ozkan-Altiner and Ozcan, 1999; Sari (2006, 2009); Babazadeh et al., 2007; Jaff, 2015 ; Rami, 1998; Wagneich et al., 2010).

Indeed, many authors (Postuma, 1971; Sigal, 1977 ; Robaszynski et al., 1979 ;Jaffet al., 2015) assigned the *Dicarinella asymetrica* Total Range Zone an approximate indicator for the early to late Santonian. Others (Marks 1984; Premoli-Silva and Sliter, 1994, 1999; Arz, 1996; Mancini et al., 1996; Robaszynski et al., 2000 ; Wan et al., 2005; Djaffal et al., 2015; Elamri and Zaghib-Turki, 2004; Sari 2006, 2009; Farouk and Faris, 2012; Ogg and Hinnov, 2012; Elamri et al., 2014, 2016; Kochhann et al., 2014; Vahidinia et al., 2014 ; Jaff et al. 2015; Farouk et al. 2017 ; Bentahar et al., 2023) indicate that this biozone is an indicator of the early Santonian. On the other hand, some studies (e.g. Robaszynski et al., 1984; Aref and Ramadan, 1990; Nederbragt, 1991; Robaszynski and Caron, 1995; Ayyad et al., 1996; Petrizzo, 2000, 2002; Bauer et al., 2001 ; Mancini and Puckett, 2005; Georgescu, 2006; Sari, 2006; Dimitrova and Valchev, 2007; Ameen and Gharib, 2014; Hussain and Al-Sheikhly, 2015) specify in detail that the *Dicarinella asymetrica* Total Range Zone corresponds to the middle-late Santonian.

It is important to mention that the current zone can be matched to the *Rosita fornicata* Zone recorded by (Abawi and Hammoudi, 1997) and (Abawi and Mahmood, 2005) in northern Iraq, the *Dicarinella asymetrica*-*Ventilabrella eggeri* Zone recorded by (Rajabi, 2020) in Iran,

## CHAPTER IV BIOSTRATIGRAPHY

as well as the *Globotruncana linneiana* Zone identified by (Petrizzo et al., 2020) in the southern mid-to high latitudes region and (Peryt et al., 2022) in Poland and eastern Ukraine.

It can also be correlated with the *Sigalia decoratissima* subzone of Kalsz (I. Z.) of Rami et al., (2016) in Tunisia. On the other hand, Salaj (1980), Gradstein et al. (2008) and Rami et al. (2016) considered the *Sigalia decoratissima* subzone as a separate zone indicating the Middle Santonian.

In the present study, this biozone was determined in lower- upper Santonian

### **Globotruncanita elevata Partial range zone, latest Santonian**

This biozone is limited to the LO of *D. asymetrica* and the FO of *Globotruncanita elevata*.

It represents 49m in the Essen section (samples S47 to S62). The dominant planktic species are : *Heterohelix globulosa*, *Globotruncana arca*, *Globotruncanita elevata*, *Marginotruncana coronata* Bolli and *Globotruncana linneiana* d'Orbigny. The *Globotruncanita elevata* biozone is characterized by the dominance and abundance of globotruncanids and heterohelicids but most notably by the persistent occurrence of the eponymous zone fossil.

**Stratigraphic distribution:** Following some authors (e.g. Salaj, 1980, 1997) the first appearance of *G. elevata* is equated with different levels within the Santonian in the North African and Mediterranean regions. Although, El Gammal and Orabi (2019), reported previously that *Globotruncanita elevata* is marked the Santonian/Campanian Boundary Event. It is ranges, also, from the Santonian and the beginning of the Campanian (Sulaiman et al., 2023), or from the Santonian to middle Campanian Barr (1972). Indeed, the current partial range zone can be correlated to the *Globotruncanita elevata* zone recorded in the Early Campanian by Caron (1985) and by many other studies at different locations, such as: (Premoli Silva and Bolli, 1973; Wonders, 1980; Robaszynski et al., 1984, 2000; Dowsett, 1984, 1989; Honigstein et al., 1987; Sliter, 1989; Almogi-Labinet et al., 1991; Abdel-Kireemet et al., 1995; Ayyad et al., 1996; Mancini et al., 1996; El Albani et al. 1999; Robaszynski, 1998; Ozkan-Altiner & Ozcan, 1999; Zapata et al., 2003; Chacon et al., 2004; Abawi and Mahmood, 2005; Babazadeh et al., 2007; Dimitrova and Valchev, 2007; Li et al., 2011; Ljubović-Obradović et al., 2011; Farouk and Faris, 2012; Ogg & Hinnov, 2012; Abdo, 2013; Ameen and Gharib, 2014; Elamri and Zaghib-Turki, 2014; Elamri et al., 2014; Fereydoonpour et al., 2014; Kochhann et al., 2014; Jaff, 2015 ; Farouk et al., 2016; Ogg et al., 2016 ; Al-Dulaimi and Saeed, 2017; Orabi, 2019; Li et al., 2020 ; Chabbi et al., 2021).

It is worthy to mention that the present biozone correlates to the *Globotruncana mariei* biozone recorded by (Modaresnia et al., 2012) in northern Iran at the early Campanian, and the *Globotruncana arca* biozone identified by (Peryt et al., 2022) in Poland and eastern

## CHAPTER IV BIOSTRATIGRAPHY

Ukraine at the early Campanian. It can also be correlated with the *Marginotruncana manauensis* Subzone mentioned by Rami et al., 2016 in Tunisia centro-septentrional which dates from the upper Santonian.

In the present study, this biozone was determined in the latest Santonian.

Ma	Stage	Standard zones	Essen Section
84	Santonian	<i>Dicarinella asymetrica</i>	<i>Globotruncanita elevata</i>
85			<i>Dicarinella asymetrica</i>
			<i>Sigalia carpatica</i>
86	Coniacian	<i>Dicarinella concavata</i>	<i>Marginotruncana sinuosa</i>
87			
88			<i>Dicarinella primitiva</i>
89			

**Table IV.4 :** Stratigraphic framework and the planktic foraminiferal biozones identified in the study section at Djebel Essen.

### Conclusion

In the eastern part of the Saharan Atlas, particularly in the regions of Tébessa and Batna, the Coniacian and Santonian stages have been biostratigraphically dated using ammonites, inoceramids, and planktonic foraminifera. The lower and middle Coniacian are identified by the presence of *Dicarinella primitiva*, while the upper Coniacian is marked by *Marginotruncana sinuosa* and *Hemitissotia morreni*. The Santonian stage is dated primarily through planktonic foraminifera, with the lower Santonian indicated by *Sigalia carpatica*, and the middle to upper Santonian defined by *Dicarinella asymetrica*, *Globotruncanita elevata*, and the inoceramid *Inoceramus siccensis*.

***CHAPTER V***  
***RESULTS,***  
***INTERPRETATION***  
***AND DISCUSSION***

## CHAPTER V RESULTS, INTERPRETATION AND DISCUSSION

### 1. Introduction

The reconstruction of palaeoenvironmental conditions represents a crucial aim within the fields of sedimentology and palaeontology, offering valuable insights into historical climatic, oceanographic, and ecological scenarios. In this chapter, we examine and interpret the environmental contexts of the sedimentary sequence under investigation by analyzing the spatial and temporal distribution of both macrofaunal and microfaunal assemblages. Particular attention is directed towards two significant groups of microfauna (ostracods and foraminifera) due to their heightened sensitivity to environmental factors such as salinity, oxygen concentrations, water depth, and substrate characteristics.

Macrofaunal remains, which encompass visible fossilized organisms like bivalves and echinoderms, provide critical information regarding the ecological structure and energy dynamics of the palaeoenvironment. When assessed alongside microfaunal indicators, especially ostracods and foraminifera, a more nuanced and multi-dimensional reconstruction of the environment can be achieved.

This chapter delivers a comprehensive interpretation of the palaeoenvironmental evolution within the study area. It synthesizes faunal distribution data with sedimentological insights and established regional palaeogeographic models. The ecological preferences and environmental tolerances of the identified taxa are utilized to deduce essential palaeoenvironmental parameters, including water salinity, depth variations, and potential anoxic occurrences.

### 2. Results

#### 2.1. Macrofaunal assemblages

##### 2.1.1. Essen section

The section studied in Djebel Essen, the examined 242 samples of the 533m long sections, only 23 samples contain macrofossils. A total of 204 specimens were identified at the species level. These individuals belong to 33 species: 24 bivalves, 4 gastropods, one cephalopod, and 4 irregular echinoids.

Bivalves are mainly heterodonts, oysters, and plicatulid. The echinoids are all spatangoid and of the same genus (*Mecaster*). The scarcity of the fauna and the low diversity can refer to either diagenetic dissolution of the aragonitic shells or environmental stress (Abdelhady and

## CHAPTER V RESULTS, INTERPRETATION AND DISCUSSION

Fürsich, 2014). Most of the identified species exhibit long vertical distributions. The UPGMA clustering based on Jacquard similarity was used to subdivide the studied samples into meaningful assemblages. It reveals four assemblages, as shown in Figure (1, 2). Based on NPMANOVA, these assemblages exhibit significant differences (as shown in Table 1, Table 2). These distinct patterns are well-characterized on the NMDS plot, where no overlap in the scatter plot was observed (see Figure 3, Figure 4). The community structure of these assemblages was used to interpret their paleoenvironments.

### **Agelasina plenodonta Assemblage**

This faunal assemblage predominates in the lower Coniacian of the Essen Formation (C1 to C50) and comprises eleven species: three echinoids and eight bivalves. Among them, *Agelasina plenodonta* is the most abundant, making up 43% of the assemblage (Figure 3), followed by *Pycnodonte (Phygraea) vesicularis vesicularis* at 16%, and *Mecaster batnensis*, which contributes less than 13%. Overall, the assemblage displays low diversity, with a Shannon diversity index of 1.21 and a Simpson index of 0.61 (Table 1).

The majority of the taxa (84%) are infaunal, while epifaunal forms are scarce, representing just 16% (Table 1). Suspension feeders dominate the trophic structure (92%), whereas deposit feeders are relatively rare (16%, Table 2). Mobile taxa are more prevalent than stationary ones (Table 2). The predominance of infaunal and mobile organisms suggests that the substrate was soft to soupy in consistency (Abdelhady and Fürsich, 2014; Abdelhady and Mohamed, 2017).

### **Cucullaea Assemblage**

This assemblage characterizes the middle Coniacian of the Essen Formation (C70 to C150) and is represented by only four bivalve species: *Cucullaea thevestensis*, *Cucullaea diceras*, *Oscillopsa dichotoma*, and *Cucullaea trigona*. Each of the first three species contributes more than 25% to the assemblage, while *C. trigona* makes up approximately 23% (Figure 3). The infaunal suspension feeder *Cucullaea* dominates the assemblages, accounting for 75% of the total composition.

Species diversity is notably low, and the assemblage is best described as paucispecific. The Shannon diversity index is 0.83, and the Simpson index is 0.50 (Table 1). Infaunal taxa are predominant (75%; Table 2), while epifaunal forms are relatively scarce. The trophic structure is entirely composed of suspension feeders (100%), with no deposit feeders present (Table 2). Mobile species are more common than stationary ones.

## CHAPTER V RESULTS, INTERPRETATION AND DESCUSION

### Oscillopha-Plicatula Assemblage

This assemblages predominates in the upper Coniacian of the Essen Formation (C160 to C180) and includes a total of twelve species. Among these, *Plicatula ferryi* accounts for 32%, while *Oscillopha dichotoma* comprises 31% of the assemblage (Table 1). Overall, the diversity within this assemblages is low. The Shannon diversity index is 0.91, and the Simpson diversity index is 0.48 (both values are reported in Table 1). Epifaunal taxa prevail constituting 68 % (Table 1). Infaunal organisms are less abundant. Additionally, suspension-feeders dominate, accounting for 92 %, while deposit-feeders are rare (8 %; see Table 3). Mobile taxa are less common, while stationary organisms make up two-thirds of the assemblages.

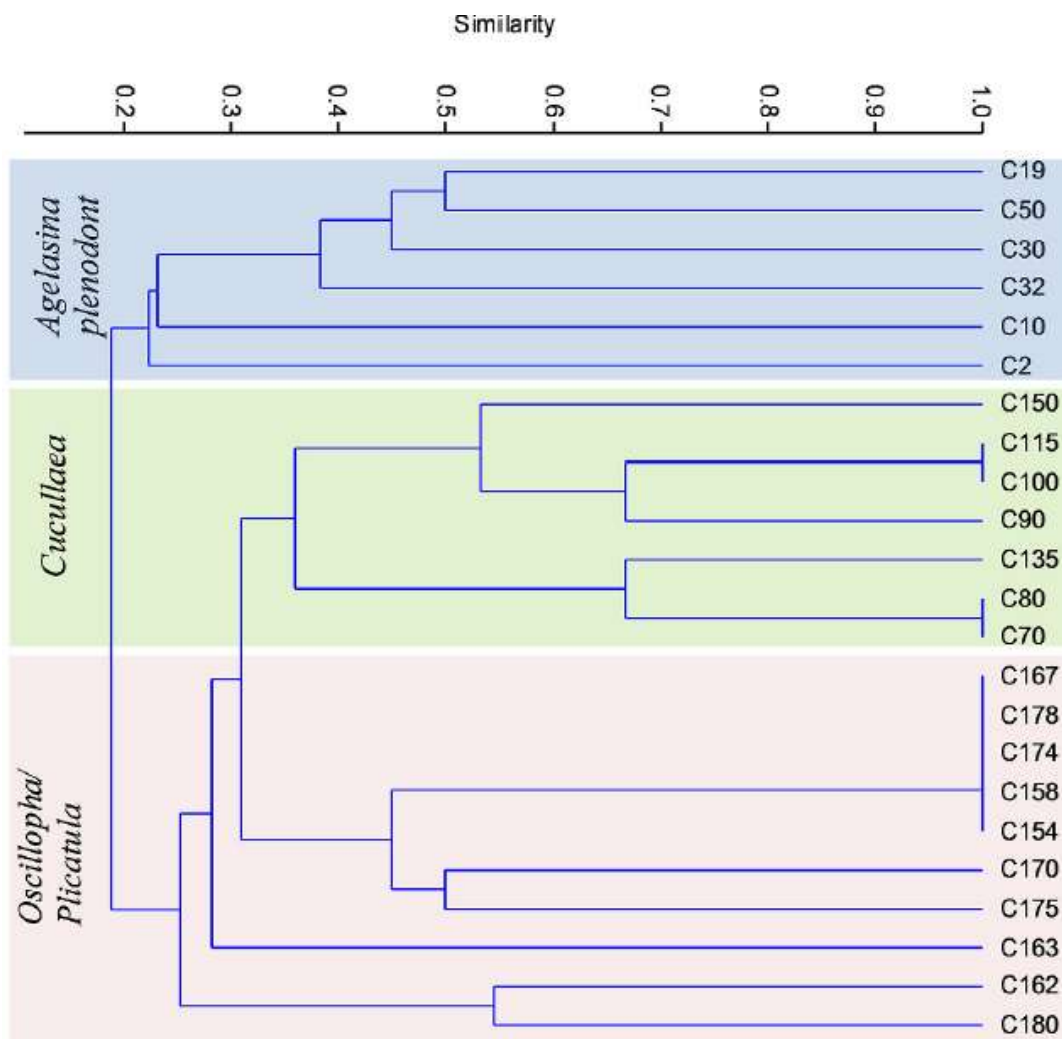


**Figure V. 1:** UPGMA cluster analysis using Bray-Curtis method. This analysis produced three clusters of sample groups based on relative abundances of the macrofossils of coniacian in Essen section.

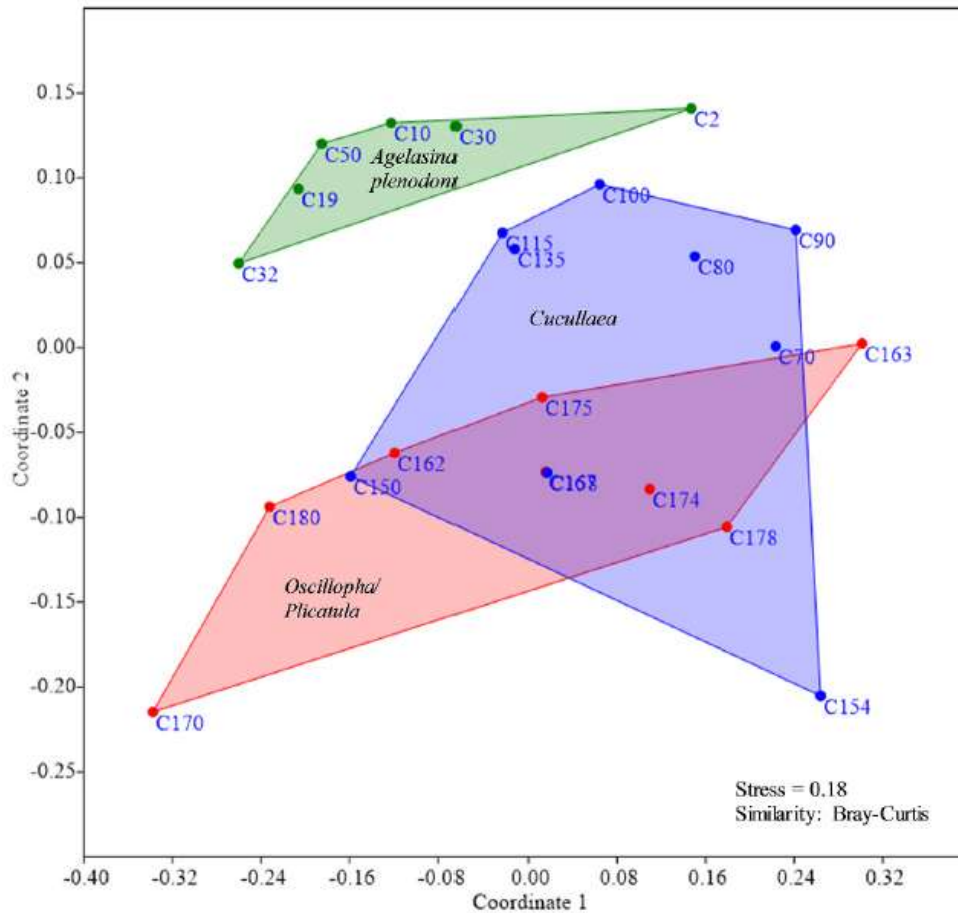


**Figure V. 3:** 2D-NMDS (Bray-Curtis similarity) plot shows the identified assemblages of coniacian in Essen section.

	Oscillopha/Plicatula	Cucullaea	Agelasina plenodonta
<i>Oscillopha-Plicatula</i>	0		
<i>Cucullaea</i>	0.0025	0	
<i>Agelasina plenodonta</i>	0.0006	0.0168	0

**TableV. 1 :** Summary of the NPMANOVA test among the identified assemblages of coniacian in Essen section.

**Nuculana cf. mariae Assemblage**

This assemblage predominates in the Santonian of the Essen Formation (S1 to S62). They are characterised a less biodiverse a macrofaunal assemblage composed mainly of bivalves associated with numerous echinoids and rare gastropods, generally of the same species. In order of abundance, we note the presence of: *Nuculana cf. mariae* (D’Orbigny, 1844) accounts for 23%, *Arctica cordata* (Sharpe1850), *Rostrocardia papieri* (Coquand, 1862), *Astare gigantea* deshaves, 1842, *Plicatula fourenli* (Coquand, 1862), *Plagiostoma*

## CHAPTER V RESULTS, INTERPRETATION AND DESCUSSION

*subsimplex* (Thomas & Peron 1891), *Granocardium desvauxi* coquand 1862, *Plicatula ferryi* (coquand 1862) and *Hemiaster* cf. *bibansensis* Péron & Gauthier, 1881 and the gastropod: *Aporrhaisourneli* (Coquand, 1862). Overall, the diversity within this assemblages is low. Epifaunal taxa prevail constituting 68 % (Table 1). Infaunal organisms are less abundant. Additionally, suspension-feeders dominate, while deposit-feeders are rare. Mobile taxa are less common.

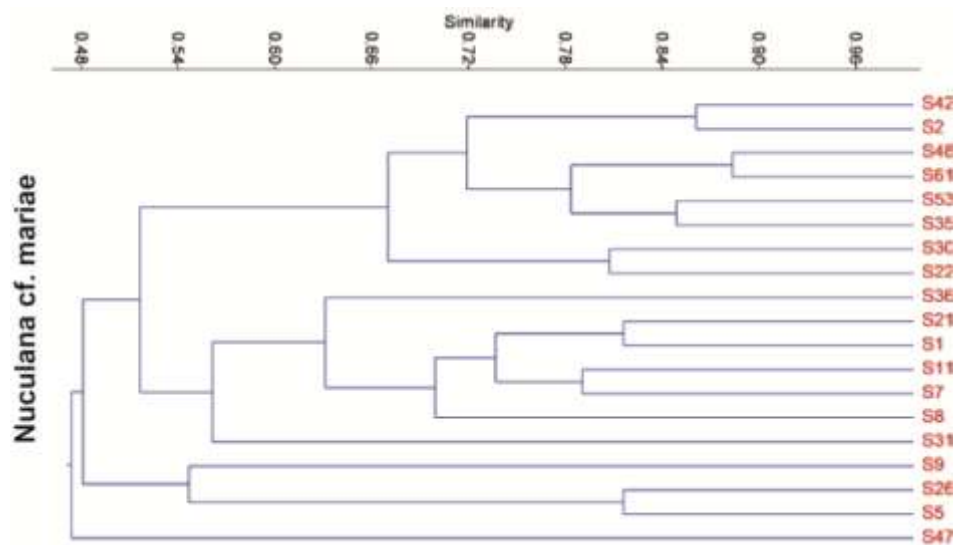


**Figure V. 2:** UPGMA cluster analysis using Bray-Curtis method. This analysis produced **three un** cluster of sample groups based on relative abundances of the macrofossils of santonian in Essen section.

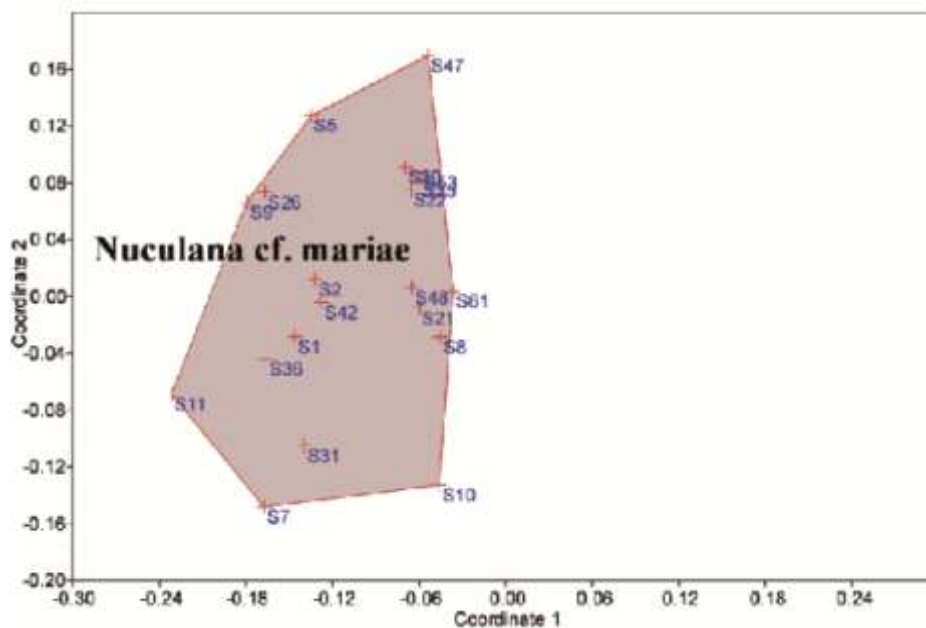


**Figure V. 4:** 2D-NMDS (Bray-Curtis similarity) plot shows the identified assemblages of santonian in Essen section.

CHAPTER V RESULTS, INTERPRETATION AND DESCUSSION

<b>NPMANOVA</b>	<b>Nuculana cf. mariae</b>
<b>Nuculana cf. mariae</b>	<b>0</b>

**Table : 2 :** Summary of the NPMANOVA test among the identified assemblages of Santonian.

Association		<i>Agelasina plenodonta</i>	<i>Cucullaea</i>	<i>Oscillopha-Plicatula</i>	
Diversity indices	Samples	6	7	10	
	Species	11	4	12	
	Individuals	56	39	100	
	Dominance	0.39	0.50	0.52	
	Simpson	0.61	0.50	0.48	
	Shannon	1.21	0.83	0.91	
	Evenness	0.83	0.85	0.81	
Biotic traits	Epifauna	16	25	68	
	Infauna	84	75	32	
	Suspension-feeders	84	100	92	
	Deposit-feeders	16	0	8	
	Mobile	84	75	32	
	Stationary	16	25	68	
	Aragonite	84	75	23	
	Calcite	16	25	76	
	Interpretation	Water-energy	Low	Low	Moderate
		Substrate	Soft	Soft	Firm
Nutrient		Mesotrophic	Oligotrophic	Oligotrophic	
Sedimentation rate		Moderate	Low	Low	
Environment		Restricted lagoon			

**Table V. 3 :** Summary of the characteristics of the identified associations of Essen section.

**2.1.2. Boukezez section**

The section studied in Djebel Boukezez, the examined 29 samples of the 160m long sections, only 7 samples contain macrofossils. A total of 65 individuals were identified at the species level. These individuals belong to 8 species: 13 bivalves, 8 gastropods, 33 irregular echinoids, 10 regular echinoids and one inoceramed.

Bivalves are mainly *Plicatula ventilabrum*, *Paraesafaba* sp., and *Rachiosoma rectilineatum*. The echinoids are all spatangoid and of the same genus (*Hemiaster*) and regular echinoids *Phymosoma thevestense* and *Phymosoma sulcatum*. The scarcity of the fauna and the low diversity can refer to either diagenetic dissolution of the aragonitic shells or environmental stress (Abdelhady and Fürsich, 2014). Most of the identified species exhibit long vertical distributions. The UPGMA clustering based on Jacquard similarity was used to

## CHAPTER V RESULTS, INTERPRETATION AND DESCUSSION

subdivide the studied samples into meaningful assemblages. It reveals one assemblage, as shown in Figure 5. Based on NPMANOVA, these assemblages exhibit significant differences (Table 4). These distinct patterns are well-characterized on the NMDS plot, where no overlap in the scatter plot was observed (Figure 6). The community structure of these assemblages was used to interpret their paleoenvironments.

### Hemiaster fourneli – Paraesa faba Assemblage

This faunal assemblage predominates in the lower section of the Boukezez Formation (E1 to E5) and comprises eleven species: three echinoids and eight bivalves. Among them, irregular echinoids (*Hemiaster fourneli* Agassiz and Dessor, 1847), regular echinoids (*Phymosoma thevestense* Péron and Gauthier, 1880), is the most abundant, making up 48 % of the assemblage (Figure 5, Figure 6), followed by bivalves (*Paraesa faba* at 22.58%, *Plicatula ventilabrum* Coquand, 1880 which contributes less than 16.12% and *Rachiosoma rectilineatum* Péron and Gauthier, 1881) is the least abundant 3.22%, and gastropods (*Cimolithium* sp., and *Nerinea* sp.), Overall, the assemblage displays low diversity. Infaunal organisms are less abundant. Additionally, suspension-feeders dominate, while deposit-feeders are rare. Mobile taxa are less common.

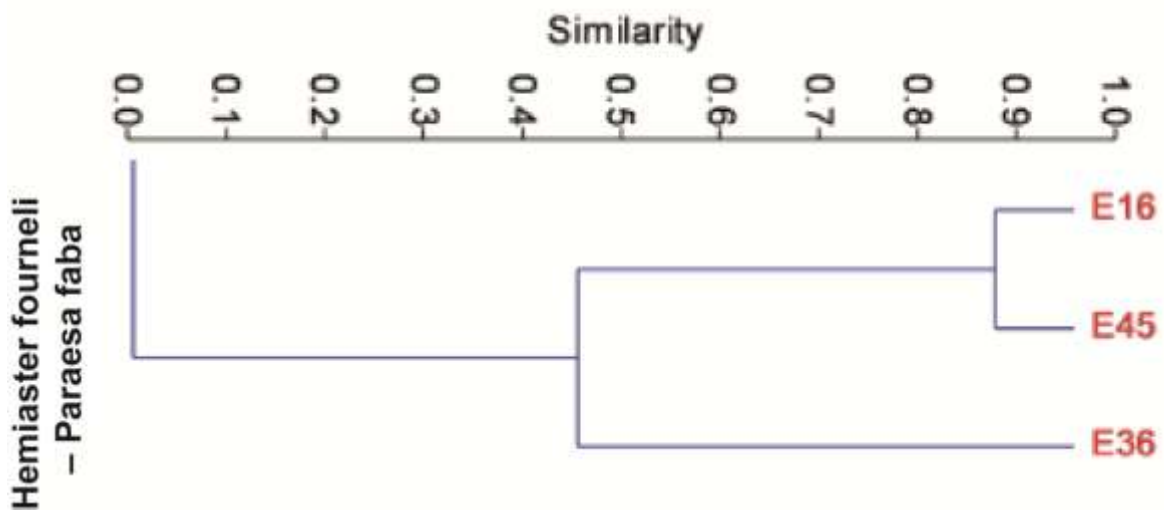


**Figure V. 5:** UPGMA cluster analysis using Bray-Curtis method. This analysis produced **three un** clusters of sample groups based on relative abundances of the macrofossils of Boukezez section.

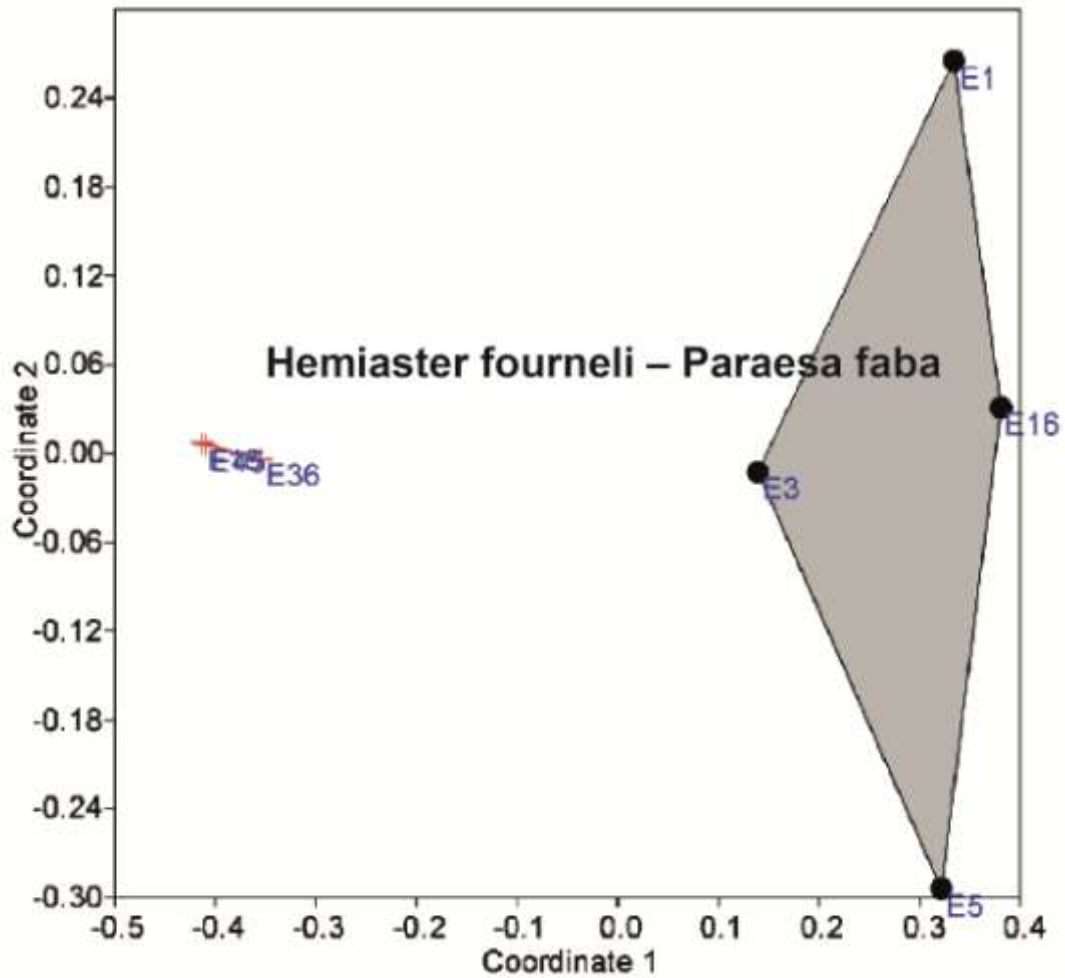


**Figure V. 6:** 2D-NMDS (Bray-Curtis similarity) plot shows the identified assemblage in Boukezez section.

	San	Con
San	0	0.0298
Con	0.0298	0

**Table : 4 :** Summary of the NPMANOVA test among the identified assemblage in Boukezez section.

Based on the fossil record and ecological preferences of the species *Plicatula ventilabrum*, *Paraesafaba* sp., *Rachiosoma rectilineatum*, and the echinoids *Phymosoma thevestense* and *Phymosoma sulcatum*, it can be inferred that these organisms inhabited a shallow, warm, and well-oxygenated marine environment rich in nutrients. *Plicatula ventilabrum*, typically attached to hard substrates, indicates a moderately energetic, shallow marine setting with stable sedimentation and firmgrounds such as reefs or hardgrounds

## CHAPTER V RESULTS, INTERPRETATION AND DISCUSSION

(Skelton, 2013). The small-sized mollusks *Paraesa faba* and *Rachiosoma rectilineatum* suggest soft-bottom conditions with calm waters, favorable for microbenthic communities that thrive on fine sediments rich in organic matter (Kiel, 2010). Furthermore, the presence of echinoids like *Phymosoma thevestense* and *Phymosoma sulcatum* supports the interpretation of a neritic environment with sandy to muddy substrates and good bottom-water ventilation, consistent with their known ecological distribution in Cretaceous deposits (Smith & Jeffery, 2000). Collectively, these taxa point to a stable, biodiverse, shallow marine ecosystem characteristic of the neritic zone during the Late Cretaceous.

### 2.2. Ostracods and foraminifera assemblage

#### 2.2.1. Essen section

A total of 242 samples, 8021 specimens and 49 ostracods species were identified. The grouping of samples based on their ages, revealed a little overlap in the PCA plots (Figure 7). The first three components comment on 56 % for ostracods (Figure 7A-B) and 68 % in case of foraminifera (Figure 7 C-D). These patterns are well characterized by the NPMANOVA test, where a significant difference was found ( $p < 0.001$ ). The composition of the trophic nucleus (>80 %) for the Coniacian and Santonian assemblages reveals slight differences in the dominant ostracod species within these periods (Table 5).

#### **Cytherella aff. austinensis- Cytherella aff. contracta Assemblage**

In the *Cytherella aff. austinensis- Cytherella aff. contracta* Assemblage of Essen section 330m, *Cytherella aff. austinensis* is the most abundant species, comprising 33.3 % of the Assemblage. This is followed by *Cytherella aff. Contracta* (8.7%), *Spinoleberis yotvatensis* (7.9%), and *Cytherella gambiensis* (7.2%). These species together dominate the trophic nucleus, which accounts for 80.1 % of the Coniacian assemblage. Additional contributions come from species like *Paracypris mdaouerensis* (4.3%) and *Paracypris aff. posteriusacuminatus* (4.1%), along with minor contributions from others such as *Amphicytherura aff. yakhiniensis* and *Cytherella aegyptiensis*. The trophic nucleus for the Coniacian accounts for 81.1 % of the total assemblage.

#### **Cytherella aff. austinensis - Cytherella aff. elongata Assemblage**

The *Cytherella aff. austinensis - Cytherella aff. elongata* Assemblage of Essen section 200m features *Cytherella aff. austinensis* as the dominant species, accounting for 24.5% of the trophic nucleus. Other significant contributors include *Cytherella aff. elongata* (16.9%) and *Paracypris mdaouerensis* (15.5%), highlighting a shift in dominance compared to the Coniacian. The contribution of *Cytherella ovata* decreases markedly to 6.2% in the Santonian,

## CHAPTER V RESULTS, INTERPRETATION AND DISCUSSION

while species such as *Spinoleberis yotvatensis* (4.1%) and *Cythereis algeriana* (3.4%) play smaller roles. The trophic nucleus for the Santonian accounts for 80.4% of the total assemblage. These shifts in the trophic nucleus suggest ecological and environmental changes between the two stages.

The comparison of ostracod assemblages between the Coniacian and Santonian stages highlights significant differences in numerical and functional diversity (Table 6). The Coniacian stage exhibits higher diversity and abundance, with 47 total species and 7766 individuals, compared to 41 species and 1041 individuals in the Santonian. The average number of species and individuals per sample also declines notably from 11.75 and 43.14 in the Coniacian to 5.81 and 16.79 in the Santonian, respectively. These results indicate a marked reduction in population size and diversity during the Santonian.

Diversity indices further emphasize these shifts. The Coniacian stage shows greater overall diversity, with higher Simpson (0.80) and Shannon (2.02) indices compared to the Santonian (0.70 and 1.45, respectively; Table 5; Figure 7). However, evenness increases from 0.67 in the Coniacian to 0.85 in the Santonian, suggesting a more balanced distribution of individuals among species during the latter stage. Functional group analysis reveals shifts in dominance and ecological composition. Ostracods are more abundant in the Coniacian (43.6%) than in the Santonian (34.1%), while foraminifera, particularly benthic forms, dominate in the Santonian (66.5%, with 37.2% benthic; Figure 7) compared to the Coniacian (57.0%, with 18.2% benthic). Among ostracods, smooth forms decrease from 31.8% in the Coniacian to 23.4% in the Santonian, while ornamented forms remain relatively stable. Foraminiferal subgroups show similar trends, with a decline in globular forms (20.6% to 13.1%) and an increase in keeled forms (8.0% to 10.0%) and benthic foraminifera (Figure 7). The Santonian shows a decline in foraminiferal diversity compared to the Coniacian, with fewer species (15 vs. 19; Table 6) and a lower number of individuals (190.82 vs. 329.32). However, diversity indices such as Simpson (0.93 vs. 0.91) and Shannon (2.77 vs. 2.56) suggest a more stable community in the Santonian. Dominance increases slightly (0.09 vs. 0.07), indicating a few species became more dominant, while evenness remains similar (0.89 vs. 0.87).

In summary, the Coniacian is significantly different from the Santonian, where the Coniacian is more diverse, containing more smooth ostracods, more globular and keeled and planktic foraminifera. The Santonian is marked by diversity decrease and high dominance Index (Figs. 7). What is also interesting is the negative relationship between the ostracods and foraminifera.

## CHAPTER V RESULTS, INTERPRETATION AND DESCUSSION

These patterns suggest significant ecological and environmental changes between the Coniacian and Santonian, resulting in reduced diversity and altered community structure. The increased proportion of benthic foraminifera in the Santonian may reflect shifts in habitat conditions or ecological pressures during this time (Table 5).

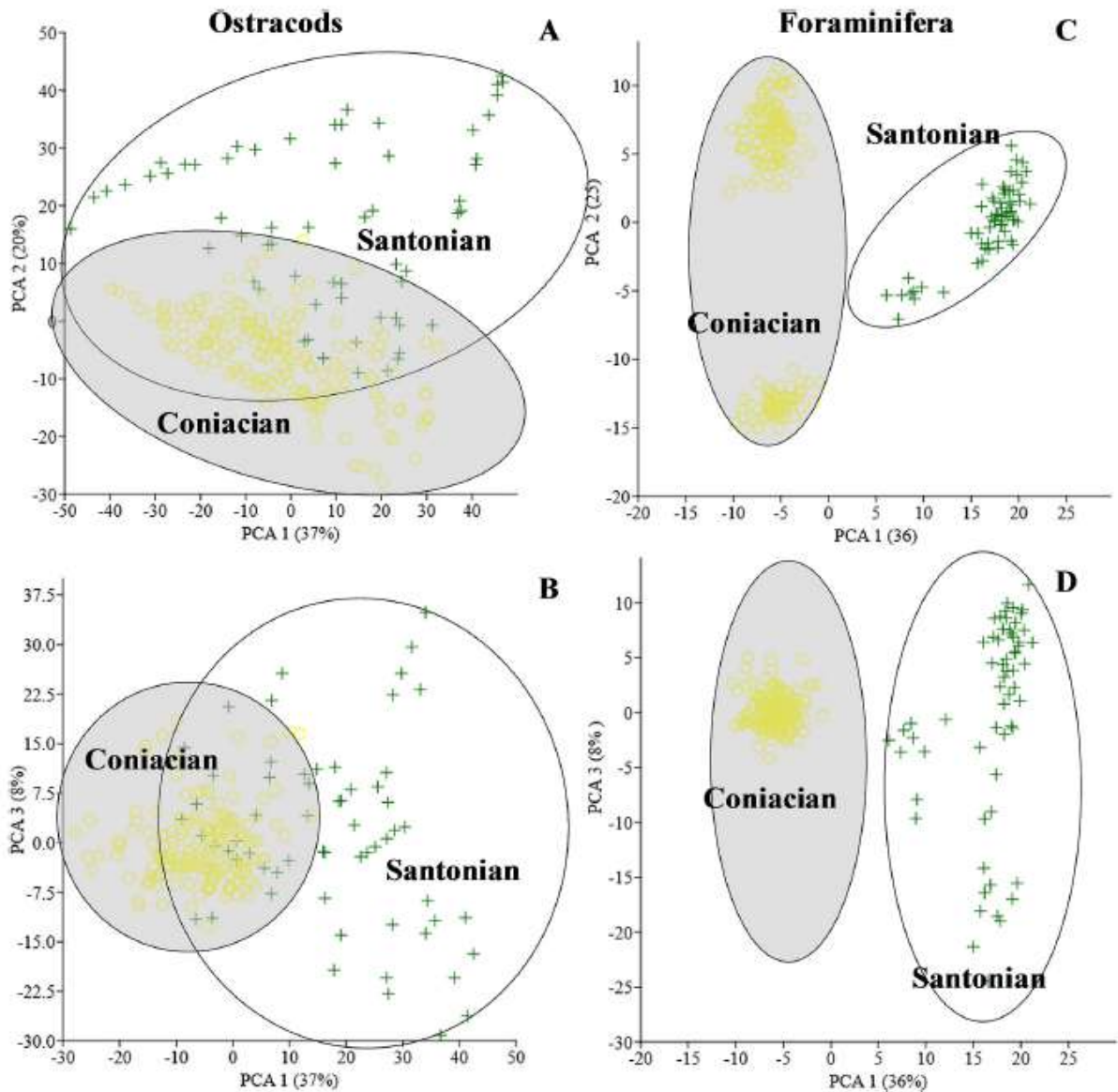


**Figure V. 7 :** PCA plots of the faunal assemblages categorized based on their ages; A-B) Ostracods; C- D) Foraminifera. Note the little overlap among the Coniacian and the Santonian assemblages, suggesting marked fauna changes. Green crosses: Santonian samples, yellow circles: Coniacian samples.

## CHAPTER V RESULTS, INTERPRETATION AND DESCUSSION

	Coniacian Species %	Santonian Species %
Ostracods	<i>Cytherella</i> aff. <i>austinensis</i> 33.3 <i>Cytherella</i> aff. <i>contracta</i> 8.7 <i>Spinoleberis yotvatensis</i> 7.9 <i>Cytherella gambiensis</i> 7.2 <i>Cytherella ovata</i> 6.7 <i>Cytherella</i> aff. <i>elongata</i> 5.1 <i>Paracypris mdaouerensis</i> 4.3 <i>Paracypris</i> aff. <i>posteriorusacuminatus</i> 4.1 <i>Cytherella gambiensis</i> 2.7 <i>Amphicytherura</i> aff. <i>yakhiniensis</i> 2.2 <i>Cytherella aegyptiensis</i> 1.7 <b>Trophic nucleus 81.1</b>	<i>Cytherella</i> aff. <i>austinensis</i> 24.5 <i>Cytherella</i> aff. <i>elongata</i> 16.9 <i>Paracypris mdaouerensis</i> 15.5 <i>Cytherella ovata</i> 6.2 <i>Spinoleberis yotvatensis</i> 4.1 <i>Cythereis algeriana</i> 3.4 <i>Cytherella</i> aff. <i>Contracta</i> 3.0 <i>Paraplatycosta</i> aff. <i>talayniensis</i> 1.9 <i>Cythereis namousensis</i> 2.2
Foraminifera	Foraminifera <i>Marginotruncana coronata</i> 7.2 <i>Pseudotextularia</i> sp. 7.0 <i>Heterohelix reussi</i> 6.7 <i>Whiteinella archaeocretacea</i> 6.2 <i>Marginotruncana sigali</i> 6.0 <i>Whiteinella baltica</i> 5.9 <i>Whiteinella</i> sp. 5.8 <i>Archaeoglobigerina</i> sp. 5.0 <i>Marginotruncana sinuosa</i> 4.9 <i>Pseudotextularia nuttalli</i> 4.5 <i>Muricohedbergella flandrini</i> 4.3 <i>Marginotruncana pseudolinneiana</i> 4.3 <i>Gavelinella</i> sp. 4.3 <i>Marginotruncana renzi</i> 4.1 <i>Marginotruncana</i> cf. <i>sigali</i> 3.7 <i>Marginotruncana caronae</i> 3.3 <b>Trophic nucleus 80.1</b>	<b>80.4</b> <i>Whiteinella</i> sp. 9.5 <i>Whiteinella archaeocretacea</i> 9.5 <i>Archaeoglobigerina</i> sp. 9.4 <i>Whiteinella baltica</i> 7.3 <i>Globotruncana linneiana</i> 6.3 <i>Heterohelix reussi</i> 6.0 <i>Marginotruncana pseudolinneiana</i> 5.9 <i>Notoplanulina</i> sp. 5.8 <i>Contusotruncana plummerae</i> 5.6 <i>Globotruncana bulloides</i> 5.1 <i>Eobigenerina</i> sp. 5.1 <i>Dicarinella asymetrica</i> 4.9
	<b>Trophic nucleus 80.1</b>	<b>Trophic nucleus 83</b>

**Table V. 5 :** Trophic nucleus (>80 %) composition of the identified assemblages of Essen section.

		Coniacian	Santonian
General	Total samples	180	62
	% Ostracods	43.6	34.1
	% Foraminifera	57.0	66.5
	% Smooth ostracods	31.8	23.4
	% Ornamented ostracods	11.8	10.4
	% Benthic foraminifera	18.2	37.2
	% Planktonic foraminifera	38.8	29.3
	% Globular foraminifera	20.6	13.1
	% Keeled foraminifera	8.0	10.0
	% Heterohilixides	10.4	6.5
Ostracods	Average species	11.75	5.81
	Average individuals	43.14	16.79
	Average Dominance	0.20	0.30
	Average Simpson	0.80	0.70
	Average Shannon	2.02	1.45
	Average Evenness	0.67	0.85
Foraminifera	Average species	19	15
	Average individuals	329.32	190.82
	Average Dominance	0.07	0.09
	Average Simpson	0.91	0.93
	Average Shannon	2.56	2.77
	Average Evenness	0.87	0.89

**Table V. 6 :** Summary of the differences between the two identified ostracod assemblages of Essen section.

### 2.2.2. Boukezez section

A high presence of ostracods generally coincides with an abundance of benthic foraminifera, suggesting that these two groups share similar environmental preferences, in particular well-oxygenated and stable seabed conditions. However, a major environmental change is observed when the disappearance of ostracods is accompanied by a significant

## CHAPTER V RESULTS, INTERPRETATION AND DISCUSSION

increase in calcispheres and globular planktonic foraminifera. This change probably indicates a transition to a deeper, less oxygenated or more open environment, unfavourable to the benthic fauna but favourable to the development of planktonic organisms. The boundary between the Coniacian and Santonian periods is particularly marked by the total absence of ostracods. At this stage, the fossil assemblages are dominated by planktonic foraminifera and opportunistic benthic forms, which are known for their ability to survive in stressful or unstable environmental conditions.

A total of 23 samples, 1387 specimens and 23 ostracod species were identified. The distribution of the identified species indicates vertical fluctuations in Boukezez section, where marly horizons are rich in the ostracods. In addition, the Coniacian/Santonian transition is unfossiliferous. Hierarchical clustering was applied to the ostracod occurrence matrix using different similarity coefficients to identify potential clusters (assemblages). The quality of the fit for stratigraphically-constrained clustering was low ( $< 0.5$ ). The Jaccard similarity retained the best fit ( $CCC = 0.86$ ) and also saved the stratigraphic pattern if the dendrogram splatted into three clusters at similarity more than 0.36. Moreover, these three clusters are well characterized in the NMDS plot (Figure 8), where no overlap among samples of different clusters were found. Santonian samples have low NMDS axis 1 values, while lower samples of both late Coniacian and early Santonian have higher scores on the NMDS axis 1 (Figure 8). Although both late Coniacian and early Santonian have similar NMDS axis one scores, they are well differentiated on NMDS axis 2 score, where the late Coniacian samples have higher scores and the early Santonian ones have lower scores (Figure 8). However, PERMANOVA test indicated that the community composition of late Coniacian samples (E1-E5) and the earliest Santonian (E21- E29) are not significantly different. Therefore, both were grouped together and all samples of the section were grouped into two main assemblages

### **Cytherella ovata – Spinolebris yotvatensis Assemblage**

The *Cytherella ovata*– *Spinolebris yotvatensis* Assemblage, which constitute the Upper coniacian of Boukezez Formation (55m) and is dominated by smooth carapaces of the family *Cytheracea* (46%; Table 7) and has lower species diversity ( $Shannon = 1.27$ ;  $Simpson = 0.6$ ) and higher dominance (0.4).

### **Paracypris aff. posteriusacuminatus- Ovocytheridea triangularis Assemblage**

The *Paracypris* aff. *posteriusacuminatus*- *Ovocytheridea triangularis* Assemblage is dominating the lower santonian of Boukezez Formation (55-160m) and has higher diversity ( $Shannon = 1.62$ ;  $Simpson = 0.7$ ) and lower dominance (0.29).

CHAPTER V RESULTS, INTERPRETATION AND DESCUSSION

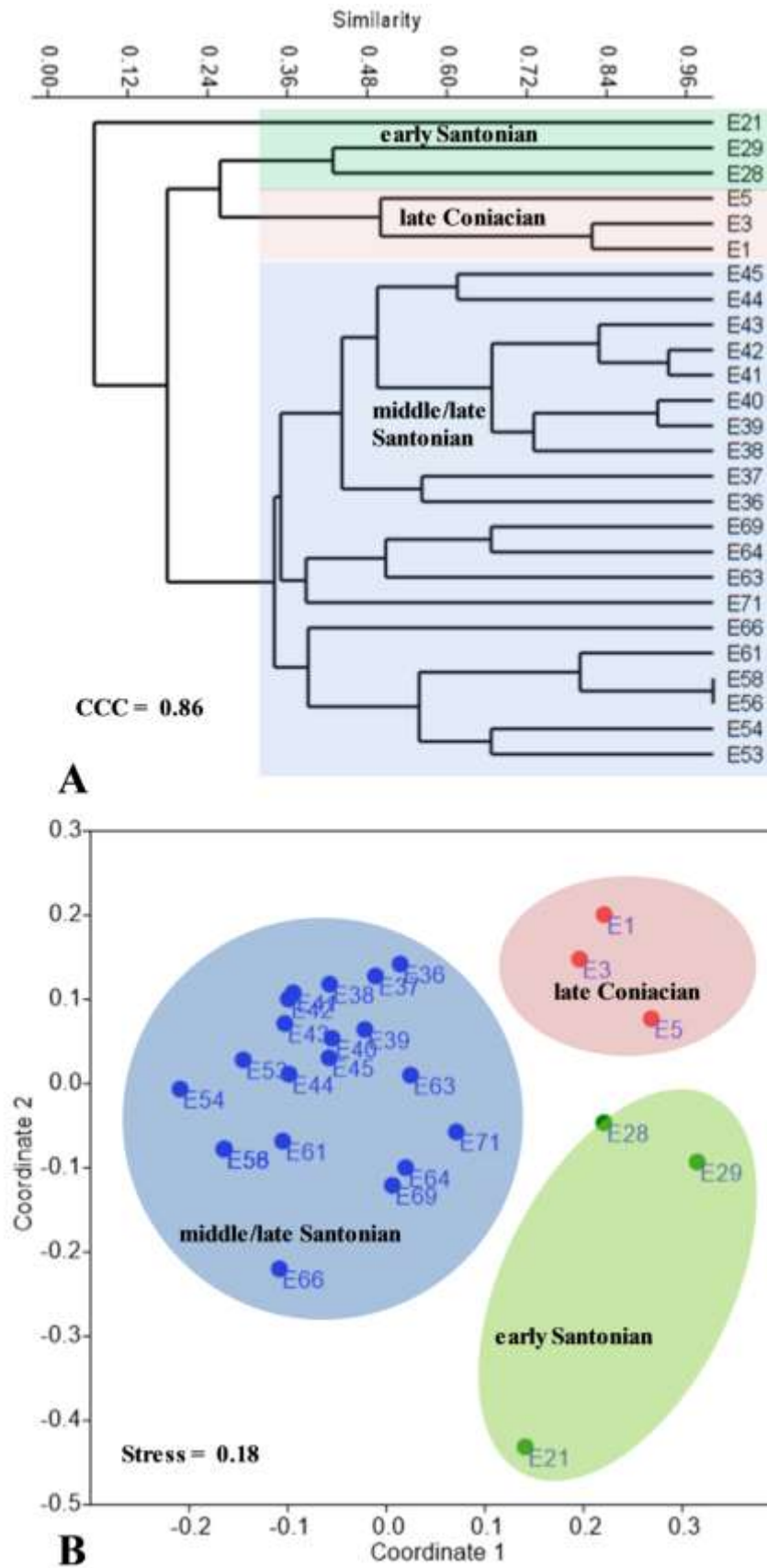


Figure V. 8 :2D-NMDS plot visualize the relationship among the proposed clusters (assemblages).

## CHAPTER V RESULTS, INTERPRETATION AND DESCUSSION

	<i>Cytherella</i> Assemblage	<i>Paracypris</i> Assemblage
Age	Late Coniacian/early Santonian	Santonian
Avg water depth <sup>+</sup>	75	88
Total individuals	320	1067
Total species	10	25
Number of samples	3	23
Avg species	6	8.95
Avg Individuals	60	51.35
Avg Dominance	0.40	0.29
Avg Simpson	0.60	0.71
Avg Shannon	1.27	1.62
Avg depth (m)	75	87
Total smooth %	68	32
Avg smooth	98	27
Avg % Cytheroidea	30	47
Avg % Cypridoidea + Bairdioidea	29	23
Avg % Cytherelloidea	41	30

**Table V. 7 :** Summary of the differences between the two identified ostracod assemblages of Boukezez section.

### 3. Paleoenvironmental discussion and interpretation

The distribution pattern and the faunal diversity of the macrofaunes (Bivalves, echinoids and molusks) and microfaunals (ostracods, planktonic and benthic foraminifera) can be linked directly to different abiotic variables (e.g., depth, salinity, temperature, and the nature of the substrate characteristics). In addition, they can be used as indicators of eustatic variations (Babinot, 1995; Slipper, 2005; Al-Shareefi et al., 2010; Sayed et al., 2022). Variations in macrofaunal assemblages provide valuable insights into past marine and terrestrial environments, including factors such as salinity, substrate type, water depth, oxygenation levels, and energy conditions (Kidwell & Bosence, 1991 ; Fürsich & Oschmann, 1993 ; Brett & Baird, 1986 ; Hallam, 1992 ; Walker & James, 1992). High macrofaunal diversity is generally indicative of stable, well-oxygenated environments with favorable ecological niches, whereas low diversity may suggest stressful conditions, such as hypersalinity, anoxia, or rapid environmental changes (Fürsich & Oschmann, 1993; Brett & Baird 1986 ; Harper & Peck, 2016; Kidwell & Bosence, 1991; Hallam, & Wignall, 1997). The composition and distribution of macrofauna thus serve as key indicators for reconstructing palaeoecological settings and understanding the evolutionary responses of communities to palaeoclimatic and

## CHAPTER V RESULTS, INTERPRETATION AND DISCUSSION

palaeogeographic changes (e.g., Kidwell & Brenchley, 1994; Brett & Baird, 1997). This makes macrofaunal analysis essential in palaeoenvironmental studies, particularly when integrated with sedimentological and geochemical data. The diversity of ostracods is linked to the chemical stability of their environment, with their abundance generally reflecting trophic richness (Babinot and Crumière-Airaud, 1990; cited in Tchenar et al., 2020). Moreover, ostracods serve as excellent indicators of eustatic (sea-level) fluctuations (Babinot, 1995; Park et al., 2000; Slipper, 2005; Al-Shareefi et al., 2010; Sayed et al., 2022).

Thus, the vertical lithological trends, microfacies profiles, macrofaunal assemblages, and quantitative analyses of ostracod distribution, along with data from planktonic and benthic foraminifera within the sedimentary succession, have enabled the palaeoenvironmental reconstruction of the Coniacian–Santonian interval at the Essen and Boukezez sections.

### 3.1. Paleoxygenation

During the Late Cretaceous, an Oceanic Anoxic Event (OAE 3) occurred across the Coniacian–Santonian interval (Marz et al., 2009), coinciding with persistently high global sea levels (Haq et al., 1988) and a long-term global cooling trend (Friedrich et al., 2012). In the Eastern Pontides region of northeastern Turkey, suboxic conditions have been reported for Turonian–Coniacian strata, which were subsequently followed by a gradual deepening of the depositional environment (Özyurt et al., 2023). Despite the occurrence of OAE 3, black shale deposition appears to have been limited geographically, with occurrences primarily documented in the Atlantic and Caribbean regions (Arthur and Schlanger, 1979; Jenkyns et al., 1994; Arthur et al., 1990; Wagner et al., 2004; Jones et al., 2007; Wapreigh, 2012), as well as the Tarfaya Basin in Morocco (Prauss, 2015). In contrast, such deposits are notably absent in the Pacific and Tethyan realms (Wapreigh, 2012). As a result, OAE 3 is interpreted as a regionally confined anoxic event within the Atlantic, unlike the more globally pervasive OAE 2 (Wapreigh, 2005, 2009). Some researchers (e.g., Wapreigh, 2009) have also suggested that OAE 3 was more characteristic of shallow marine environments, marked by the presence of redoxic sediments known as Cretaceous Oceanic Red Beds (CORBs). Supporting this, Kalanat et al. (2022) demonstrated that the Coniacian–Santonian boundary interval in the Eastern Tethys was deposited under oxic conditions, a finding also corroborated by Nemouchi et al. (2024). Shallow-water environments are generally less prone to anoxia than deeper settings, as oxygen levels tend to decrease with depth (Richards, 1957). Furthermore, oligotrophic conditions, characterized by low nutrient input and reduced sedimentation rates,

## CHAPTER V RESULTS, INTERPRETATION AND DISCUSSION

are less conducive to the development of anoxic conditions, which are typically associated with eutrophic settings (Almroth-Rosell et al., 2021). However, although dysoxic conditions might be considered, the dominance of infaunal organisms indicates that oxic conditions prevailed, with sufficient oxygen penetrating the substrate to support benthic life (Abdelhady and Fürsich, 2014). A key factor contributing to the decline in ostracod assemblages during the Santonian is likely the decrease in oxygen availability, resulting from restricted water circulation (Babinot and Tronchetti, 1983).

At the Essen section, litho- and biofacies evidence from the current study indicate persistent oxic conditions with no significant fluctuations in oxygen levels. The middle to Upper Coniacian interval, commonly associated with the widespread anoxic event OAE-3 marked by black shale deposition in various global locations was not identified in the Essen section. This absence suggests sedimentation occurred in an isolated, shallow shelf lagoon. The lack of black shale and glauconite both common indicators of OAE-3 and frequently found at the Coniacian–Santonian boundary in the equatorial Atlantic and adjacent epicontinental seas (Mansour and Wagreich, 2022; Lamolda et al., 2014) further supports the interpretation that the Essen section represents a shallow, restricted lagoonal environment (Chikhi-Aouimeur et al., 2011). Furthermore, a comparison of ostracod assemblages across the Coniacian–Santonian boundary reveals a substantial drop in both numerical and functional diversity. The Coniacian is characterized by higher species richness and abundance, while the Santonian exhibits a marked reduction in both metrics. During the Santonian, planktonic foraminiferal diversity declined, marked by the extinction of certain species and the appearance of new taxa that coexisted with benthic foraminifera. Although ostracods remained present, their overall abundance decreased significantly. The persistence and continued proliferation of genera such as *Whiteinella* and *Heterohelix* beyond the Coniacian and Santonian transition reflect their adaptability to environmental stress, including low-oxygen conditions (Caron and Homewood, 1983). The taxonomic replacement of *Marginotruncana* by *Globotruncana* and *Globotruncanita*, along with the evolutionary shift from *Dicarinella primitiva* to *D. asymetrica* prior to the end of the Santonian, may have been influenced by episodes of mild dysoxia (Schlanger and Jenkyns, 1976; Caron and Homewood, 1983). This decline in planktonic foraminifera and ostracods during the Santonian (Table 6) may be linked to environmental stress, possibly associated with Oceanic Anoxic Event 3 (OAE3). However, the lithofacies in the study area do not exhibit clear indicators of anoxic conditions. On the contrary, the increasing abundance of benthic foraminifera (Figs 9, 10),

## CHAPTER V RESULTS, INTERPRETATION AND DISCUSSION

typically more sensitive to anoxia suggests otherwise. This pattern may reflect the influence of mild dysoxia, perhaps associated with a nearby expanding anoxic zone such as that of the Tarfaya Basin, or the development of species adapted to anaerobic metabolism (Langlet, 2014). Therefore, if dysoxic conditions were present, they were likely spatially or temporally limited (see Mansour and Wagreich, 2022).

During the Coniacian and Santonian interval can be reconstructed the paleooxygenation based on the ecological structure of macro- and microfaunal assemblages. In the lower Coniacian, the *Agelasina plenodonta* Assemblage is dominated by infaunal, mobile suspension-feeding bivalves (84% infaunal and 92% suspension feeders), notably *Agelasina plenodonta*, which accounts for 43% of the total fauna. The predominance of infaunal, burrowing organisms, combined with the presence of echinoids, suggests that bottom and pore waters were well oxygenated to slightly dysoxic, allowing sustained bioturbation and filter feeding within a soft, muddy substrate (Abdelhady and Fürsich, 2014; Abdelhady and Mohamed, 2017). The subsequent *Cucullaea* Assemblage in the middle Coniacian exhibits a similar ecological pattern, with 75% infaunal suspension feeders, indicating stable oxic to mildly dysoxic conditions at the sediment water interface. However, both assemblages display very low diversity (*Shannon index* 1.21– 0.83), pointing to environmental stress such as high sedimentation, salinity fluctuations, or nutrient variability rather than persistent anoxia (Hallam, 1984; Wignall and Hallam, 1991).

A major ecological shift occurs in the upper Coniacian, marked by the *Oscillophora–Plicatula* Assemblage, which is dominated by epifaunal and sessile taxa (68%), while infaunal forms become less abundant. This transition reflects a change toward shallower, possibly more agitated conditions with higher oxygenation at the sediment surface, restricting deep burrowing (Kidwell and Bosence, 1991). In the Santonian, the *Nuculana cf. mariaae* Assemblage is characterized by low diversity, with epifaunal and stationary taxa still dominant. Microfaunal data reinforce this trend: ostracod diversity and abundance sharply decline from the Coniacian (47 species, 7766 individuals) to the Santonian (41 species, 1041 individuals), while benthic foraminifera increase significantly, representing 37.2% of the total microfaunal assemblage. This negative relationship between ostracods and foraminifera suggests an ecological reorganization, likely linked to environmental stress and possible shifts in bottom-water chemistry (Caron and Homewood, 1983; Abdelhady and Mohamed, 2017). Throughout the Essen section, the continued presence of diverse bivalves, echinoids, and

## CHAPTER V RESULTS, INTERPRETATION AND DISCUSSION

benthic foraminifera argues against persistent basin-wide anoxia, such as that associated with the global Oceanic Anoxic Event 3 (OAE3), which is marked by widespread black shale deposition elsewhere (Wendler, 2013; Lamolda et al., 2014). Instead, the faunal composition points to predominantly oxic to moderately dysoxic conditions within a shallow, restricted shelf or lagoonal setting, where episodic environmental stresses (e.g., salinity variations, turbidity, or increased sedimentation) periodically reduced diversity and favored opportunistic taxa (Hallam, 1987; Wignall, 1994). The upward trend from infaunal to epifaunal dominance, coupled with the increase in stationary forms and benthic foraminifera, likely reflects a progressive shallowing and stabilization of substrate conditions toward the Santonian. This interpretation is consistent with sedimentological evidence for restricted shallow-marine deposition and with the absence of black shales or geochemical indicators of persistent euxinia within the Essen Formation (Dubourdieu, 1956; Nemouchi et al., 2024, 2025).

In summary, the paleooxygenation record of the Essen section reveals that, while the macrofaunal and microfaunal communities experienced significant ecological fluctuations across the Coniacian and Santonian transition, there is no evidence for prolonged anoxic events. Instead, the observed patterns are best explained by local paleoenvironmental dynamics in a restricted epicontinental basin under generally well-oxygenated shallow-marine conditions, punctuated by episodic stress episodes.

In Boukezez section based on the fossil record and the geographic distribution of the mentioned macrofauna, it can be inferred that these species inhabited a shallow, warm, nutrient-rich marine environment characterized by stable sedimentary conditions and good oxygenation. The bivalve *Plicatula ventilabrum* is considered an indicator of shallow marine settings with hard or mixed substrates, as it typically attaches to firm surfaces such as rocks or coral reefs. Its presence suggests a moderately energetic environment with stable sedimentation and sufficient oxygen supply (Skelton, 2013). Small-sized taxa such as *Paraesa faba* and *Rachiosoma rectilineatum* are classified as micromollusks, which often inhabit fine-grained sediments in calm, shallow marine environments, indicating stable water conditions and high organic content (Kiel, 2010). The echinoids *Phymosoma thevestense* and *Phymosoma sulcatum* are echinoderms typically found in shallow, semi-open marine settings. They are indicative of well-oxygenated sandy or muddy seafloors and are often associated with biologically rich neritic environments (Smith and Jeffery, 2000). The distribution patterns and overall faunal diversity of ostracods are generally influenced by various abiotic factors

## CHAPTER V RESULTS, INTERPRETATION AND DISCUSSION

such as water depth, salinity, temperature, and substrate characteristics. Overall, the two identified ostracod assemblages exhibit distinct faunal compositions. The *Cytherella ovata*-*Spinoleberis yotvataensis* is primarily composed of smooth-shelled forms, whereas the succeeding *Paracypris* aff. *posteriusakuminatus*-*Ovocytheridea triangularis* is dominated by ornamented carapaces. The *Cytherella ovata*-*Spinoleberis yotvataensis* is characterized by an abundance of disarticulated valves, which suggest deposition in a shallow, high-energy marine environment, likely within the neritic zone (Andreu, 1991; Andreu et al., 1998; Al-Shareefi et al., 2010; Amami-Hamdi et al., 2016), under normal salinity conditions (Depeche, 1984), warm temperatures (Morkhoven, 1963; Peypouquet et al., 1981; Depeche, 1984; Whatley, 1995; Bonnet et al., 1999), and well-oxygenated waters (Andreu, 1991). The relatively low species diversity may reflect oligotrophic conditions (Guernet and Molina, 1995). Notably, ostracods are absent in intervals where planktonic foraminifera dominate. The exclusive presence of *Planoheterohelix globulosa*, without accompanying ostracods, indicates dysoxic conditions (Yao et al., 2018). Thus, the depositional setting associated with level E12 (Table 4) appears unfavorable for ostracod habitation. In contrast, this interval shows a proliferation of planktonic foraminifera and calcispheres in laminated limestone, suggesting increased productivity under dysoxic to potentially euxinic conditions, as described by Bryant et al., (2021) for *Planoheterohelix globulosa* dominance during OAE2.

Conversely, throughout the Santonian succession, the more diverse *Paracypris* aff. *posteriusakuminatus*-*Ovocytheridea triangularis* Assemblage is marked by an increased abundance of benthic foraminifera. The presence of *Gavelinella* alongside ostracods indicates a shallow, nutrient-rich (eutrophic) environment. This assemblage is dominated by ornamented, thick, and often articulated carapaces (e.g., *Cythereis* and *Protocosta*), which point to deposition on an open platform under rising sea level (Andreu, 1991). The elevated diversity of this assemblage reflects stable ecological conditions, including temperate waters, normal salinity, and well-oxygenated environments. These interpretations are supported by the co-occurrence of benthic foraminifera such as *Eobigenerina*, *Gavelinella*, and *Cibicidoides* (Yao et al., 2018; Cetaan et al., 2008). Additionally, genera like *Paracypris* and *Cythereis* are typically found within the photic zone, particularly in carbonate-rich substrates (Babinot, 1995; Andreu, 2002; Shirazi et al., 2014; Trabelsi et al., 2015; Salel et al., 2016; Jomaa-Salmouna et al., 2017), which are often enriched in magnesium (Tchenar et al., 2020). The passage of Coniacian and Santonian where ostracoda are absent and *Planoheterohelix globulosa* is present reflect environmentally unfavorable conditions, characterized by

## CHAPTER V RESULTS, INTERPRETATION AND DISCUSSION

lowoxygen (dysoxia) and possibly highly anoxic (euxinic) conditions, resulting from high production activity associated with global oxygenation events (OAE2) and a deeper marine environment. The dominance of oxygen-tolerant foraminifera and absence of the ostracod suggest dysoxic to moderately anoxic settings. However, the lack of organic-rich black shales points to only partial development of Oceanic Anoxic Event 3 (OAE3), likely due to regional differences. Laminated limestones with calcispheres and *Planoheterohelix globulosa* suggest intermittent bottom-water ventilation. Overall, the evidence indicates warm sea temperatures and mild stratification, leading to oxygen stress but not full anoxia. The reduced diversity of benthic fauna likely reflects environmentally stressful conditions, such as low oxygen levels, extreme nutrient regimes (either eutrophic or oligotrophic), or fluctuations in salinity (Abdelhady and Fürsich, 2014; Jain et al., 2023). In the Boukezez section, ostracods are absent from the marl intervals beneath laminated wackestone limestones (beds E7–E12). In contrast, two foraminiferal taxa *Gavelinella* and *Heterohelix* are notably abundant. Both genera have been documented in high-stress settings during the Late Cretaceous. *Gavelinella*, in particular, is among the five taxa commonly associated with oxygen-depleted, organic-rich environments of the Cretaceous (Friedrich et al., 2006). Its proliferation, especially during OAE2, is often referred to as the "*Gavelinella acme*," linked to reduced oxygen levels in both bottom and upper waters (Boudinot et al., 2020). *Gavelinella* has been widely recognized in OAE2 deposits as a dominant benthic epifaunal form (Amaglio et al., 2023). According to Amaglio et al., (2023), *Gavelinella* appears in environments with varying oxygen concentrations, suggesting that not only its presence but also its abundance may indicate oxygen stress, as seems to be the case in the study section. Similarly, *Heterohelix* a small planktonic foraminifer has been shown to tolerate low oxygen and often dominates stressed intervals, particularly following extreme events during the Cretaceous Paleogene (Pardo and Keller, 2008). It is likely that stratification of the water column during transgressive phases led to dysoxic conditions, with significant oxygen depletion at the sediment water interface. This would explain the absence of ostracods and the decline in sensitive benthic foraminiferal species (Figure 10). The abundance of planktonic foraminifera in this interval supports the interpretation of a deepening environment. While the absence of ostracods may reflect harsh conditions linked to OAE3, the lithological record lacks clear indicators of anoxia. For instance, the laminated wackestones of bed E12, though rich in *Heterohelix globulosa*, may indicate dysoxia rather than full anoxia. The absence of organic-rich black shales or dark carbonates hallmarks of OAE3 within the Coniacian and Santonian interval in this section suggests that the event was not strongly developed here, consistent with previous findings

## CHAPTER V RESULTS, INTERPRETATION AND DISCUSSION

(Wagreich, 2009; Wagreich and Mansour, 2022). According to these studies, organic-rich sedimentation during OAE3 was mostly confined to low-latitude Atlantic regions and nearby shallow seas. Previous authors (e.g., Arthur and Schlanger, 1979; Jenkyns, 1980; Arthur et al., 1990; Wagner et al., 2004; Jones et al., 2007; Wagreich, 2009) have similarly noted that black shale deposits in this interval were spatially restricted. In the Boukezez section, laminated limestones containing calcispheres and *Heterohelix globulosa* serve as biostratigraphic markers of the Coniacian–Santonian transition. Overall, this interval is thought to have had sufficient oxygen levels in both shallow and deeper marine settings across the Tethys, Indian Ocean, and large portions of the Pacific (Wagreich, 2009). Further up section, in beds E16–E20, the fossil-rich limestones characterized by abundant bioclasts such as bivalves, gastropods, and echinoid plates point to well-oxygenated and ecologically stable conditions. However, the continued absence of ostracods suggests a delayed recovery, highlighting their heightened sensitivity to even moderate environmental stress compared to other benthic organisms. Infaunal ostracods, which tend to have smooth carapaces, are more tolerant of low oxygen levels, while epifaunal forms typically feature ornamentation such as keels or spines and are associated with coarser sediments, higher-energy environments, and better oxygenation (Bodergat, 1983; Anadon et al., 2002). Numerous studies (e.g., Geiger, 1990; Dole-Olivier et al., 2000) indicate that smooth-shelled species tend to dominate under low-oxygen conditions, in contrast to their ornamented counterparts a trend also observed in benthic foraminifera (Kaiho, 1994). The predominance of smooth ostracods during the latest Coniacian and earliest Santonian further supports the presence of dysoxic conditions during this time.

### 3.2. Paleotemperature

At the Essen section, the taxonomic richness of both foraminifera and ostracods shows a noticeable decline toward the late Santonian. These findings are consistent with those of Petrizzo et al., (2022), who reported a decrease in the absolute and relative abundance of calcareous plankton assemblages and epifaunal, oxic foraminifera in the southern high latitudes during the late Santonian. This faunal shift was attributed to a cooling event, evidenced by bulk carbonate and foraminiferal  $\delta^{18}\text{O}$  records, which primarily impacted the upper water column (see also Friedrich et al., 2012a, 2012b; O'Brien et al., 2017; Huber et al., 2018a, 2018b; Petrizzo et al., 2022). Additional confirmation of this mid-to late Santonian cooling was provided by Jenkyns et al. (1994) and later supported by Haq (2014a, 2014b).

## CHAPTER V RESULTS, INTERPRETATION AND DESCUSSION

The appearance of *Archaeoglobigerina* is considered a significant evolutionary development, indicative of adaptation to cooler marine environments (Caron, 1983). According to Lipps (1979), if oceanic water masses descended in tandem with a pronounced temperature drop, only cold-tolerant species would have persisted. The relative abundance of benthic taxa may suggest that cooling had a greater impact on surface waters than on deeper waters or the seafloor. Notably, the decline in foraminiferal diversity began earlier, in the late Coniacian, implying that other environmental factors may have also contributed to this shift. During the Coniacian and Santonian interval can be inferred from the ecological structure of both macrofaunal and microfaunal assemblages. The lower Coniacian *Agelasina plenodonta* Assemblage, characterized by a predominance of infaunal, mobile, suspension-feeding taxa such as *Agelasina plenodonta* and *Pycnodonte (Phygraea) vesicularis vesicularis*, suggests deposition under warm, shallow, well-oxygenated marine conditions with soft substrates (Abdelhady & Fürsich, 2014; Abdelhady & Mohamed, 2017). Such assemblages are typical of subtropical to tropical environments, indicating elevated paleotemperatures, consistent with global mid-Cretaceous greenhouse conditions (Wilson & Norris, 2001; Friedrich et al., 2012). During the middle Coniacian, the dominance of the *Cucullaea* Assemblage, with low diversity and a high abundance of infaunal suspension feeders, indicates a relatively stable but warm environment with limited ecological niches, consistent with a shallow shelf lagoonal setting. The upper Coniacian *Oscillopho-* *Plicatula* Assemblage shows an increase in epifaunal taxa and stationary forms, suggesting a gradual shift toward slightly cooler and more stable conditions, possibly linked to minor regional sea-level fluctuations. Microfaunal data support these interpretations: Coniacian ostracod assemblages exhibit high diversity and dominance of smooth-shelled taxa such as *Cytherella* aff. *austinensis*, which are typically associated with warm, open-marine conditions (Whatley et al., 2003; Donze et al., 1982). The transition into the Santonian is marked by a pronounced decline in ostracod diversity and abundance, alongside an increase in benthic foraminifera (from 18.2% in the Coniacian to 37.2% in the Santonian), indicating environmental cooling and a shift toward more stressed benthic conditions (Haynes et al., 2015; Huber et al., 2018). These faunal shifts, combined with the paucispecific *Nuculana* cf. *mariae* Assemblage and the prevalence of epifaunal stationary taxa, suggest a drop in paleotemperature during the Santonian, possibly associated with the global climatic transition following the mid-Cretaceous thermal maximum (Voigt et al., 2004; Robinson et al., 2017). Thus, the Essen section records a warm, tropical Coniacian sea that gradually cooled into the Santonian, accompanied by changes in marine biodiversity and community structure.

## CHAPTER V RESULTS, INTERPRETATION AND DISCUSSION

At Boukezez section, the Coniacian is significantly different from the Santonian, where the Coniacian is more diverse, containing more smooth ostracods, ~~more globular and keeled~~ and planktic foraminifera. The Santonian is marked by diversity decrease and high dominance Index. These patterns suggest significant ecological and environmental changes between the Coniacian and Santonian, resulting in reduced diversity and altered community structure. The increased proportion of benthic foraminifera in the Santonian may reflect shifts in habitat conditions or ecological pressures during this time. The *Cytherella ovata* – *Spinoleberis yotvatensis* Assemblage, from the upper Coniacian, is dominated by smooth-shelled taxa of the family Cytheruridae (notably *Cytherella ovata*, representing 46% of *Cytheracea*). This assemblage suggests deposition in cooler, deeper marine environments, likely on the outer shelf to upper slope, under low-energy and potentially oxygen-poor conditions. The low species diversity ( $Shannon = 1.27$ ;  $Simpson = 0.60$ ) and relatively high dominance (0.40) reflect ecological stress or thermal stability in a cool, oligotrophic setting. Although *Spinoleberis yotvatensis*, typically found in warm marginal marine environments, is present, its occurrence likely indicates ecological tolerance or transport rather than local warm conditions. This assemblage likely represents the interior continental platform under environmental stress, despite being formed under a relatively warm yet thermally stable climate. By contrast, the *Paracypris* aff. *posteriusacuminatus* – *Ovocytheridea triangularis* Assemblage, characteristic of the lower Santonian of the Boukezez Formation, reflects a warmer, open-marine setting associated with a relative sea-level rise. The presence of ornamented forms and the high diversity indices ( $Shannon = 1.62$ ;  $Simpson = 0.70$ ), along with low dominance (0.29), suggest eutrophic, well-ventilated, and ecologically stable conditions in shallow, subtropical neritic environments. This assemblage contains associated benthic foraminifera such as *Gavelinella* and *Cibicidoides*, which further support the interpretation of oxygenated, nutrient-rich bottom waters, favorable for benthic communities. The ostracods in the passage of Coniacian and Santonian, are abundant in marly beds alternating with benthic foraminifera, the higher species diversity denotes the establishment of ecological conditions featuring temperate waters, the benthic and planktonic fossil assemblages indicate environmentally stressed conditions during the Coniacian and Santonian, including low oxygen, salinity fluctuations, and variable nutrient levels.

### 3.3. Sea level

## CHAPTER V RESULTS, INTERPRETATION AND DISCUSSION

During the Coniacian and Santonian periods, global sea level was characterised by widespread transgression, reaching one of the highest peaks in the Late Cretaceous. According to Haq (2014), this rise in sea level resulted mainly from the absence of polar ice caps and the thermal expansion of the oceans linked to a globally warm climate. In addition, the increased activity of the mid-ocean ridges has contributed to a reduction in the volume of the ocean basins, inducing flooding of the continental margins. Miller et al., (2020) confirm this trend by identifying a series of short- and medium-duration eustatic cycles superimposed on a general rise in sea level, affecting sedimentary deposits in numerous basins, particularly in Europe, North Africa and North America. These conditions favoured the development of broad carbonate platforms and shallow marine basins, with sedimentation rich in organic matter, reflecting stratification of the waters and sometimes partial anoxia in certain basins. Environmental factors such as water depth and the intensity of upwelling may have caused the selective elimination of specialised species.

At Essen section, the Coniacian stage, although shorter in duration than the preceding Cenomanian and Turonian stages, has received relatively limited attention in the literature due to its restricted outcrops and reduced spatial extent, which are largely the result of a prolonged global sea-level fall during this time (Haq, 2014). This regression led to a significant reduction in shallow-marine habitats, contributing to the low diversity of Coniacian macrofauna, a pattern observed not only in Algeria but also across North Africa and the Middle East (Abdelhady et al., 2023). In the Eastern Saharan Atlas, this pattern was further influenced by local tectonic activity associated with Triassic diapirism, which created isolated shallow-water environments with limited faunal exchange (Dubourdieu, 1956; Perthuisot, 1978; Perthuisot & Rouvier, 1992). During the Turonian, the opening of the Trans-Saharan seaway facilitated faunal connections between the Tethys to the east and the South Atlantic to the west, encouraging widespread biotic exchange along marginal marine environments (Adamu et al., 2023). This connectivity explains the similarities between Algerian faunas and those of adjacent regions in North and West Africa. However, during the Coniacian, a gradual first-order sea-level fall reduced these connections and promoted the development of more localized faunal assemblages (Callapez et al., 2015). By the Middle Coniacian, a brief transgressive event was associated with the Oceanic Anoxic Event 3 (OAE3) and black shale deposition in the Atlantic Ocean (Meyers et al., 2006). Nevertheless, in the Essen section, no evidence of black shale or major facies changes was observed, and only minor faunal variations were recorded, suggesting that the area remained isolated and well-oxygenated, outside the direct influence of OAE3 (Mansour & Wagreich, 2022).

## CHAPTER V RESULTS, INTERPRETATION AND DISCUSSION

The macrofossil assemblage is dominated by oysters such as *Pycnodonte*, which are highly eurytopic and able to tolerate variable environmental conditions, unlike rudists that dominated earlier Aptian–Turonian carbonate platforms but disappeared locally due to increased terrigenous influx and siliciclastic sedimentation (Stanley, 1970; Bottjer, 1985; Chikhi-Aouimeur, 2003). The cooccurrence of *Pycnodonte* with spatangoid echinoids points to moderately deep lagoonal environments, likely exceeding 15 m in depth, rather than very shallow tidal flat conditions (Ferreira Soares, 1968; Kauffman, 1967; Nemouchi et al., 2024). The scarcity of macrofauna during this interval reflects a combination of environmental stressors, including reduced habitat area and fluctuating energy conditions, which selectively eliminated highly specialized taxa unable to withstand even minor environmental perturbations (Lipps & Mitchell, 1976). This interpretation is supported by the microfossil record, which reveals highly diverse planktonic foraminiferal assemblages dominated by keeled genera such as *Dicarinella* and *Marginotruncana*, indicating warm, open-marine waters of variable depths during the Coniacian (Caron, 1983). The abundant and diverse ostracod assemblages, particularly smooth-shelled taxa like *Cytherella*, suggest well-oxygenated bottom waters and stable substrates (Piovesan et al., 2014). The presence of *Paracypris mdaouerensis* further indicates deposition within a restricted infralittoral zone (Slami et al., 2022). In addition, benthic foraminifera such as *Gavelinella* and *Cibicidoides*, typical of mid-neritic settings, reinforce the interpretation of a shallow shelf with good water circulation (Rodrigues et al., 2018; Amaglio et al., 2023; Taylor et al., 2017).

A clear paleoenvironmental transition is observed from the Coniacian to the Santonian. During the late Coniacian, the dominance of taxa such as *Cytherella* and *Spinoleberis*, with their eurybathic nature, indicates environments with relatively stable energy regimes but subject to periodic fluctuations. At the Coniacian–Santonian boundary, the disappearance of ostracods and proliferation of calcispheres and planktonic foraminifera reflect a deepening event and a shift to more open, pelagic conditions unfavorable for benthic fauna (Huber et al., 2018). In the early Santonian, a resurgence of more diverse ostracod communities, including *Paracypris* and *Ovocytheridea*, alongside increased benthic foraminiferal diversity, signals a return to shallower, better-circulated waters, likely linked to a relative sea-level fall and progradation of the carbonate platform. This transition highlights a dynamic interplay between global sea-level changes, regional tectonics, and terrigenous input, which together shaped the energy regimes and ecological structure of the Boukezez section. Such patterns are consistent with other Upper Cretaceous Tethyan shelf deposits, which

## CHAPTER V RESULTS, INTERPRETATION AND DISCUSSION

document similar faunal turnovers and environmental shifts during the Coniacian– Santonian transition (Voigt et al., 2004; Friedrich et al., 2012; Abdelhady & Mohamed, 2017).

At Boukezez section, in northeastern Algeria provides an exceptional record of relative sea-level fluctuations during the Coniacian and Santonian interval along the southern Tethyan margin. The lower part of the section (E1–E5) is characterized by the *Hemiaster fourneli*– *Paraesa faba* Assemblage, which includes abundant irregular echinoids (*Hemiaster fourneli*) and regular echinoids (*Phymosoma thevestense*, *Phymosoma sulcatum*), together with small infaunal and epifaunal bivalves such as *Plicatula ventilabrum*, *Paraesa faba*, and *Rachiosoma rectilineatum*. The dominance of *Plicatula ventilabrum*, a taxon typically cemented to firm substrates, indicates deposition in a moderately energetic shallow-marine setting, probably situated above storm wave base where intermittent currents and wave action reworked the seafloor (Skelton, 2013). In contrast, the presence of *Paraesa faba* and *Rachiosoma rectilineatum*, which favor soft, fine-grained substrates, suggests periodic low-energy conditions conducive to the accumulation of organic-rich sediments (Kiel, 2010). This mixed faunal composition points to a low to moderate-energy neritic environment, with alternating phases of stable, low-energy sedimentation and episodic high-energy events such as storms or tidal currents. Microfaunal evidence corroborates this interpretation: in the upper Coniacian, the *Cytherella ovata*– *Spinoleberis yotvatensis* ostracod assemblage exhibits low species diversity ( $Shannon = 1.27$ ;  $Simpson = 0.60$ ) and high dominance (0.40), features typical of a restricted lagoonal or inner-shelf setting with limited environmental variability (Whatley et al., 2003).

Toward the Coniacian and Santonian transition, a significant paleoenvironmental change is recorded by the disappearance of ostracods and a concomitant increase in calcispheres and planktonic foraminifera, particularly *Heterohelix globulosa*. This shift indicates a deepening event and reduced benthic oxygen levels, unfavorable for benthic communities but favorable for pelagic taxa, marking a transition to more open-marine, low-energy conditions (Haynes et al., 2015; Huber et al., 2018). In the early Santonian, the *Paracypris* aff. *posteriusacuminatus*– *Ovocytheridea triangularis* ostracod assemblage shows higher diversity ( $Shannon = 1.62$ ;  $Simpson = 0.70$ ) and lower dominance (0.29), reflecting improved water circulation and increased nutrient availability, consistent with slightly more open and oxygenated shallow-marine conditions. The uppermost part of the section Santonian shows a return to abundant ostracods, diverse echinoids, and grainstone-dominated facies, indicating regressive and progradational conditions, with highly oxygenated, shallow

## CHAPTER V RESULTS, INTERPRETATION AND DISCUSSION

infralittoral to intertidal environments and vigorous hydrodynamic energy (Piovesan et al., 2014; Rodrigues et al., 2018).

Overall, the Boukezez section record a complete transgressive–regressive (T–R) cycle. During the late Coniacian, deposition took place under moderately energetic, shallow neritic conditions with well-ventilated bottom waters. A subsequent deepening phase around the Coniacian–Santonian boundary is reflected by the disappearance of benthic ostracods and the predominance of planktonic foraminifera, marking a Maximum Flooding Surface (MFS) and a shift toward a pelagic-dominated system. This was followed in the early Santonian by a regressive phase, as indicated by the re-establishment of diverse benthic assemblages and shallow-water grainstone facies, suggesting progradation of coastal and lagoonal environments during a relative sea-level fall. These results are consistent with global eustatic sea-level trends for the Coniacian and Santonian interval (Haq, 2014; Voigt et al., 2004) and align with patterns documented in other Upper Cretaceous Tethyan shelf successions (Abdelhady & Mohamed, 2017; Friedrich et al., 2012), although the absence of black shale horizons suggests that the Boukezez area remained isolated from Oceanic Anoxic Event 3 (OAE3), likely due to its position within a semi-restricted shallow shelf lagoon.

### 3.4. Paleoenergy

Hydrodynamic energy is integral to the development of sedimentary environments, serving as a key element in paleoenvironmental reconstructions.

Environments with high energy are typically defined by coarser, well-sorted sediments and notable sedimentary structures like cross-bedding and ripple marks. In contrast, low-energy environments tend to gather fine-grained, organic-rich deposits with restricted physical disturbance. These energy conditions not only determine sediment textures but also impact the distribution and preservation of biological remains, rendering energy a crucial factor in fossil taphonomy and ecological interpretation. Indicators in sedimentology, such as grain size distribution, bedding structures, and sediment fabric, are routinely utilized to infer historical energy conditions. Therefore, understanding energy dynamics is vital for interpreting depositional environments, basin evolution, and the climatic or tectonic forces that have influenced environmental changes in the geological past.

At Essen section, in the *Agelasina plenodonta* Assemblage of Lower coniacian of the Essen Formation, the dominance of suspension feeders implies that nutrient particles remained suspended in the water column, possibly due to agitation, or that the fauna were adapted to oligotrophic conditions. The assemblage is found within marly clay sediments, indicating a low-energy aquatic environment (Burchette and Wright, 1992; Wilmsen et al.,

## CHAPTER V RESULTS, INTERPRETATION AND DISCUSSION

2010). High mobility and bulldozing behavior may have hindered the establishment of sessile or attached species, accounting for the low abundance of epifaunal taxa. Moreover, bioturbation and bulldozing activities likely redistributed sediment and returned organic material to the water column, enabling suspension feeders to access nutrients even in low-energy settings. In the *Cucullaea* Assemblage of middle Coniacian of the Essen Formation, The extremely lower diversity suggests environmental stress or harsh conditions. Low nutrient availability and food shortage could also contribute to this unique ecological assemblages. Overall, this assemblages likely existed in a soupy substrate within low-energy semi-closed lagoon with fluctuating water salinity and temperature (the stressful conditions herein), where only a few taxa could adapt to such a challenging habitat. In the *Oscillopho-Plicatula* Assemblage of Upper coniacian of the Essen Formation, The dominance of epifaunal guild and stationary taxa suggests that the substrate was firm (Abdelhady and Mohamed, 2017). The dominance of suspension-feeders suggests that nutrient particles remained in the water column (likely due to water agitation). The assemblages occur within marly clay sediments, which typically indicate low water-energy conditions (Burchette and Wright, 1992; Wilmsen et al., 2010). Low water-energy environments may allow sediments to become cemented, providing a habitat for attached/sessile taxa. A low sedimentation rate likely contributed to sticky sediments (Abdelhady and Fürsich, 2014). Lower diversity suggests environmental stress or harsh conditions. Despite this, oxic conditions prevailed due to the dominance of infaunal taxa (Abdelhady and Fürsich, 2014). The overall low diversity may be related to low nutrient availability (oligotrophy) in the stressful conditions herein. This assemblages likely lived in a sticky substrate within a low water-energy, closed lagoon. In the *Nuculana cf. mariae* Assemblage of Santonian of the Essen Formation, The dominance of suspension-feeders suggests that nutrient particles remained in the water column (likely due to water agitation). The assemblages occur within marly clay sediments, which typically indicate low water-energy conditions (Burchette and Wright, 1992; Wilmsen et al., 2010). Low water-energy environments may allow sediments to become cemented, providing a habitat for attached/sessile taxa. This assemblages likely lived in a sticky substrate within a low water-energy, closed lagoon. The assemblages of the Essen Formation reflect predominantly low-energy depositional conditions within marly clay substrates and semi-closed lagoons. The dominance of suspension feeders across all assemblages indicates that nutrients were retained in the water column, either by limited agitation or bioturbation, while low sedimentation rates produced sticky substrates that hindered sessile taxa. Extremely low diversity in the *Cucullaea* and *Oscillopho-Plicatula* assemblages points to oligotrophic,

## CHAPTER V RESULTS, INTERPRETATION AND DISCUSSION

stressful conditions, whereas the *Agelasina plenodonta* and *Nuculana cf. mariae* assemblages highlight the role of bulldozing and sediment cementation in sustaining suspension-feeding communities. Collectively, these faunas demonstrate that hydrodynamic energy exerted a primary control on substrate consistency, nutrient availability, and ecological structure in the Essen Formation. The *Cytherella aff. austinensis*-*Cytherella aff. contracta* Assemblage is dominated by *Cytherella aff. austinensis* and related taxa, forming over 80% of the trophic nucleus, with higher diversity (*Shannon* = 2.02; *Simpson* = 0.80) and greater species abundance than the Santonian. In contrast, the *Cytherella aff. austinensis*-*Cytherella aff. elongata* Assemblage shows a shift in dominance toward *Cytherella aff. elongata* and *Paracypris mdaouerensis*, with reduced diversity (*Shannon*= 1.45; *Simpson*= 0.70) and fewer species and individuals per sample. Functional trends reveal a decline in smooth ostracods and globular foraminifera, alongside an increase in keeled and benthic foraminifera, reflecting ecological restructuring. Overall, the Coniacian represents a more diverse and abundant phase, whereas the Santonian reflects reduced diversity but greater ecological stability.

At Boukezez section, representing Upper Coniacian to Santonian deposits, reveals a clear paleoenvironmental and paleoenergy evolution based on integrated lithological, macrofaunal, and microfaunal evidence. The lower part of the section (E1–E5), corresponding to Unit 1, is dominated by the *Hemiaster fourneli*–*Paraesa faba* Assemblage, which is composed mainly of irregular echinoids (*Hemiaster fourneli*), regular echinoids (*Phymosoma thevestense*, *Phymosoma sulcatum*), and small infaunal and epifaunal bivalves such as *Plicatula ventilabrum*, *Paraesa faba*, and *Rachiosoma rectilineatum*. The dominance of *Plicatula ventilabrum*, a cemented suspension feeder attached to firm substrates, indicates moderately energetic shallow-marine conditions above the storm wave base, where intermittent currents and wave activity periodically reworked the seafloor (Skelton, 2013). In contrast, the co-occurrence of soft-sediment dwellers such as *Paraesa faba* and *Rachiosoma rectilineatum* points to low-energy phases characterized by calm water conditions and the deposition of fine, organic-rich sediments (Kiel, 2010). The alternation of marl and limestone beds with mudstone and wackestone textures in this unit further supports deposition in a low- to moderate-energy neritic setting, with episodic high-energy storm or tidal events (Smith & Jeffery, 2000). Ostracod assemblages in the same interval, notably the *Cytherella ovata*–*Spinoleberis yotvatensis* Assemblage, are dominated by smooth-shelled Cytheracea species, typical of restricted, quiet, and stable environments with limited hydrodynamic energy. The low species diversity (*Shannon*= 1.27; *Simpson*= 0.60) and high dominance (0.40) recorded here reinforce the interpretation of a protected lagoonal or inner-shelf environment with

## CHAPTER V RESULTS, INTERPRETATION AND DISCUSSION

limited water circulation (Whatley et al., 2003). A significant environmental perturbation is observed at the Coniacian–Santonian boundary, marked by the disappearance of ostracods and the sudden proliferation of calcispheres and planktonic foraminifera (e.g., *Heterohelix globulosa*). This shift indicates a rapid deepening event and a transition to more open-marine, less oxygenated conditions unfavorable to benthic macro- and microfauna (Haynes et al., 2015; Huber et al., 2018). Lithologically, this interval (Unit 2, E7–E20) is dominated by bioclastic wackestones and packstones with large invertebrate fragments, representing medium to high-energy subtidal to mid-platform settings, gradually passing upward into laminated limestones rich in planktonic organisms, suggesting a temporary shift toward pelagic sedimentation during peak transgression. In the overlying Unit 3 (E21–E72), corresponding to the Santonian, a resurgence of ostracods is observed in the *Paracypris* aff. *posteriusacuminatus*–*Ovocysteridea triangularis* Assemblage. This group exhibits higher diversity (*Shannon* = 1.62; *Simpson* = 0.70) and lower dominance (0.29), reflecting more open-marine, well-circulated conditions with greater nutrient availability. The associated limestone microfacies evolve upward from packstone to grainstone textures, with abundant pelletoids, bryozoans, and echinoid fragments, indicating deposition in very shallow, high-energy environments, probably within the upper intertidal to shallow subtidal zones. The presence of hardgrounds and dolomitized limestones in the uppermost part of the section suggests repeated episodes of emersion and reworking under strong hydrodynamic influence.

Overall, the Boukezez section records a transition from a protected, low- to moderate-energy neritic environment during the late Coniacian, characterized by well-ventilated bottom waters and periodic storm influence, to a deeper, low-energy and more pelagic setting at the Coniacian–Santonian boundary, followed by a return to very shallow, high-energy environments during the Santonian as a result of renewed shallowing and progradation of the carbonate platform. This evolutionary pattern mirrors regional trends observed in other Tethyan shelf settings, where the Coniacian and Santonian transition is marked by faunal turnovers, increased planktonic dominance, and significant paleoceanographic changes linked to global sea-level and climatic fluctuations (Voigt et al., 2004; Friedrich et al., 2012; Abdelhady & Mohamed, 2017).

### 3.5. Paleosalinity

Salinity is widely recognized as a critical paleoenvironmental proxy due to its strong sensitivity to climatic, hydrological, and oceanographic processes. In geological archives, shifts in salinity are often inferred through multiple lines of evidence, including fossil assemblages. Microorganisms such as foraminifera and ostracods, are especially sensitive to

## CHAPTER V RESULTS, INTERPRETATION AND DISCUSSION

salinity changes, making their fossilized remains powerful tools for reconstructing ancient aquatic environments. Collectively, salinity reconstructions contribute significantly to our understanding of paleoclimate variability, basin evolution, and the response of aquatic systems to long-term environmental change.

At the Essen section, salinity shows a progressive increase from the Lower Coniacian through to the Santonian. At the base Agelasina plenodonta Assemblage (C1–C50), the faunal dominated by *Agelasina plenodonta* (43 %) and *Pycnodonte (Phygraea) vesicularis* (16 %), with *Mecaster batnensis* among echinoids, a diverse planktonic foraminiferal load, and an abundant ostracod assemblage indicates marine connectivity but benthic stress consistent with upper mesohaline to polyhaline conditions driven by episodic freshwater input (low diversity; dominance of suspension feeders) (Abdelhady & Fürsich, 2014; Colin & Peypouquet, 1979). In the Middle Coniacian (C70–C150), a strongly paucispecific, *Cucullaea* dominated infaunal assemblage (75 % *Cucullaea*) combined with continued marine planktonic indicators suggests persistent polyhaline conditions under stronger estuarine/nearshore influence; arcid bivalves documented euryhalinity explains their dominance despite open-marine planktonic signals (Fürsich & Werner, 1988; Abdelhady & Mohamed, 2017). A significant ecological change is recorded in the faunal association dominating the upper part of the Essen Formation (C160–C180) is characterized by a low-diversity macrofauna, mainly composed of the epifaunal suspension-feeding bivalves *Plicatula ferryi* (32%) and *Oscillopsis dichotoma* (31%). The predominance of euryhaline oysters suggests deposition under relatively stable conditions compared to earlier Coniacian Assemblages, but still within a low-diversity framework reflecting environmental stress. Importantly, the concomitant record of abundant ammonites (*Hemitissotia morreni*) and a diversified planktonic foraminiferal community (including *Heterohelix globulosa*, *Pseudotextularia nuttalli*, *Whiteinella baltica*, *Dicarinella canaliculata*, *Marginotruncana coronata*, among others) provides clear evidence of open-marine influence and fully marine water masses. This interpretation is reinforced by the ostracod assemblage, which includes a wide spectrum of *Cytherella* species (*C. ovata*, *C. aff. contracta*, *C. gambiensis*, *C. aegyptiensis*, *C. austinensis*), as well as *Paracypris*, *Ovocytheridea*, and *Xestoleberis*, all of which are generally associated with normal-marine salinity conditions. Taken together, these lines of evidence indicate deposition under upper polyhaline to euhaline conditions, reflecting a near-normal marine setting with reduced freshwater influence and enhanced connection to open-marine environments. The continued low diversity of the benthic macrofauna likely results from substrate or hydrodynamic stress rather than salinity reduction, since the microfaunal indicators strongly point toward stable,

## CHAPTER V RESULTS, INTERPRETATION AND DISCUSSION

fully marine conditions. By the Santonian, the *Nuculana cf. mariae* Assemblage (S1-S62) reflects a further shift towards normal marine conditions, with the prevalence of echinoids and suspension-feeding epifauna in fine-grained deposits suggesting near-normal salinity. Overall, these successions document a clear salinity trend from stressed meso/polyhaline conditions in the early Coniacian toward increasingly stable euhaline conditions by the Santonian, a pattern that aligns with a regional transgressive trajectory and the progressive reduction of freshwater influence.

At Boukezez section, the *Hemiaster fourneli*– *Paraesa faba* Assemblage, which dominates the lower part of the Boukezez Formation (E1-E5), is characterized by a predominance of echinoids, notably the spatangoid *Hemiaster fourneli* and the regular echinoid *Phymosoma thevestense*, which together constitute nearly half of the assemblage. These taxa are generally considered stenohaline and representative of normal marine conditions. Accompanying bivalves, such as *Paraesa faba* and the euryhaline oyster *Plicatula ventilabrum*, also support deposition in polyhaline to upper euhaline environments, where salinity values likely approach near-normal marine levels. The community is dominated by suspension-feeders, while infaunal and mobile elements are less common, suggesting deposition in well-oxygenated waters with firm substrates. Although overall diversity remains low, this pattern is more plausibly attributed to episodic environmental stress and selective diagenetic loss of aragonitic shells rather than to a sustained reduction in salinity. Taken together, the faunal composition and ecological structure indicate that this assemblage records deposition under polyhaline to upper euhaline conditions, tending toward near-normal stable marine salinity. The absence of typical marine taxa such as ammonites may reflect fluctuating salinity levels. Furthermore, limited nutrient availability and food scarcity likely contributed to the formation of this distinctive ecological community. The occurrence of echinoids suggests normal water salinity. The overall low diversity may be related to low nutrient availability (oligotrophy) in the stressful conditions herein. Where the distribution of ostracod assemblages in the Boukezez section reveals clear vertical fluctuations in paleosalinity across the Coniacian and Santonian interval, particularly rich in ostracods, whereas the Coniacian/Santonian transition is unfossiliferous, likely reflecting unfavorable environmental conditions. Cluster analyses (*Jaccard similarity*,  $CCC = 0.86$ ) and NMDS ordination identified two major ostracod assemblages. The *Cytherella ovata*– *Spinoleberis yotvatensis* Assemblage, which characterizes the Upper Coniacian (55 m), is dominated by smooth-shelled *cytheraceans* (46%) and exhibits low diversity (*Shannon* = 1.27; *Simpson* = 0.6) and

## CHAPTER V RESULTS, INTERPRETATION AND DISCUSSION

high dominance (0.4). The prevalence of smooth, thin-shelled forms (*Cytherella*, *Spinoleberis*) taxa generally associated with deeper, reduced salinity tolerance suggests deposition under relatively mesohaline to polyhaline conditions, possibly on the outer shelf where freshwater influence remained episodically significant (Colin & Peypouquet, 1979; Whatley & Boomer, 2000; Benson, 1972). In contrast, the *Paracypris* aff. *posteriusacuminatus*–*Ovocytheridea triangularis* Assemblage, dominating the Lower Santonian (55–160 m), displays higher diversity (*Shannon*= 1.62; *Simpson*= 0.7) and lower dominance (0.29). The abundance of robust, ornamented taxa such as *Paracypris* and *Ovocytheridea*, which are tolerant of more stable marine salinities, indicates a transition toward euhaline conditions (Boomer et al., 2003; Horne et al., 2002). This faunal shift, together with higher NMDS axis 1 scores in Coniacian samples compared to the Santonian, reflects a progressive reduction of freshwater input and stabilization of marine conditions during the early Santonian. The lack of significant faunal difference between the latest Coniacian (E1–E5) and the earliest Santonian (E21–E29) as shown by PERMANOVA suggests a gradual rather than abrupt salinity transition across the boundary. Overall, the ostracod assemblages document an ecological trajectory from stressed, mesohaline/polyhaline communities in the Upper Coniacian toward more diverse, euhaline assemblages in the Santonian, consistent with a long-term transgressive trend.

### 3.6. Substrate

The substrate, defined as the underlying surface or material upon which sediments accumulate and organisms live, plays a critical role in paleoenvironmental reconstructions. Its composition not only influences sedimentation dynamics but also controls the geochemical conditions and biological assemblages preserved in the geological record. Substrate properties affect key environmental parameters such as redox conditions, porosity, and stability, which in turn influence fossil preservation and sediment diagenesis. In marine and lacustrine systems, for instance, carbonate substrates often facilitate the preservation of calcareous microfossils (e.g., foraminifera, ostracods), while siliciclastic or muddy substrates are associated with more dynamic environments, such as estuaries, deltas, or continental margins (Nichols, 2009). Recent studies, such as that by Vleeschouwer et al. (2020), have highlighted how changes in substrate composition across stratigraphic sections can indicate shifts in depositional environments and climatic regimes. Thus, understanding substrate characteristics is essential for accurate paleoenvironmental and paleogeographic reconstructions, especially when integrated with sedimentological, geochemical, and paleontological data.

## CHAPTER V RESULTS, INTERPRETATION AND DISCUSSION

At Essen section, the macrofaunal, ostracods and foraminiferal assemblages of the Essen Formation collectively indicate a substrate evolution from soft, soupy, fine-grained muds during the Coniacian to more compacted and heterogeneous marly substrates in the Santonian. In the Coniacian, macrofaunal associations: the *Agelasina plenodonta* Assemblage of the lower Coniacian, characterized by low diversity and dominance of infaunal suspension-feeders, indicates a soupy substrate with limited firm ground colonization (Abdelhady & Fürsich, 2014; Abdelhady & Mohamed, 2017). A soft to soupy substrate is the stressful conditions herein and may explain the general low diversity. This association existed in a soupy substrate within a low water-energy restricted lagoon (Chikhi-Aouimeur et al., 2011). Corroborated by the dominance of smooth-shelled cytherellids (*Cytherella* aff. *austinensis*, *C.* aff. *contracta*) a diverse and abundant ostracods assemblages, coupled with a higher contribution of globular and planktic foraminifera, reflects deposition on soft, low-energy outer-shelf floors, where cohesive muddy substrates and reduced near-bed energy favored smooth forms and intermittent oxygen stress near the sediment–water interface (Murray, 2006; Boomer et al., 2003; Peypouquet, 1977). Similarly, the *Cucullaea* and *Oscillophaplicatula* Assemblage of the middle to upper Coniacian are paucispecific and dominated by infaunal taxa, Epifaunal taxa are less abundant, Suspension feeders are exclusively dominant (100 %), while deposit-feeders are absent, with *Oscillophaplicatula* abundance suggesting adaptive strategies to soft-bottom habitats, consistent with Seilacher's (1984) observations on *oyster* adaptations to muddy substrates, the dominance of infaunal guild taxa suggests that substrate was likely soft (Abdelhady and Mohamed, 2017). Macrofaunal the *Nuculana* cf. *mariae* Assemblage dominance of epifaunal and stationary guilds implies firmer substrates and harsher environmental conditions, with very low diversity suggesting ecological stress, although oxic conditions were maintained (Abdelhady & Fürsich, 2014; Abdelhady & Mohamed, 2017). By contrast, the Santonian records a decline in ostracod abundance and diversity, increased evenness, and a rise in benthic foraminifera, pointing to more consolidated, marly substrates and greater benthic control (Murray, 2006; Sen Gupta, 1999). The combination of ostracods–foraminiferal signals and macrofaunal guild structures thus documents a clear environmental transition; from soft, unstable muddy substrates in the Coniacian, favorable to infaunal bivalves and ostracod-rich communities, to firmer, more compacted marly grounds in the Santonian, increasingly dominated by benthic foraminifera and epifaunal macrofauna under more stressful but relatively stable benthic conditions (Chikhi-Aouimeur et al., 2011; Rosenfeld & Raab, 1983).

## CHAPTER V RESULTS, INTERPRETATION AND DISCUSSION

At the Boukezez section, the substrate conditions of the Boukezez Formation, as reconstructed from both macrofaunal and microfaunal assemblages, indicate a transition from soft, nutrient-rich muds in the Coniacian to more stable, compacted substrates in the Santonian. The *Hemiaster fourneli*–*Paraesa faba* Assemblage of the lower Coniacian is dominated by irregular echinoids *Hemiaster fourneli* and bivalves such as *Paraesa faba*, *Plicatula ventilabrum*, and *Rachiosoma rectilineatum*, with suspension-feeders prevailing and infaunal elements relatively scarce. The presence of *Plicatula ventilabrum*, which typically attaches to firm substrates, suggests patchy hardgrounds or firmgrounds within a predominantly soft-bottom environment (Skelton, 2013). By contrast, small infaunal taxa *Paraesa faba*, *Rachiosoma rectilineatum* and gastropods *Cimolithium* and *Nerinea* point to fine-grained, organic-rich sediments favorable to microbenthic communities (Kiel, 2010). This mixed signal indicates deposition in a shallow neritic setting with localized firm substrates but overall soft, soupy sediment, consistent with interpretations from comparable Cretaceous bivalve assemblages (Abdelhady & Fürsich, 2014; Abdelhady & Mohamed, 2017). The concurrent ostracod assemblages reinforce this view: the *Cytherella ovata*–*Spinoleberis yotvatensis* Assemblage of the upper Coniacian is dominated by smooth-shelled cytheraceans (46%), indicative of soft-mud substrates with intermittent oxygen stress at the seafloor (Peypouquet, 1977; Boomer et al., 2003). This assemblage exhibits low species diversity ( $Shannon= 1.27$ ;  $Simpson= 0.6$ ) and high dominance (0.4), features typical of stressed benthic communities on unstable muddy bottoms. At the Coniacian–Santonian boundary, the disappearance of ostracods, coupled with a sharp increase in calcispheres and globular planktonic foraminifera, signals a major environmental change towards deeper, less oxygenated, and more open marine conditions unfavorable to benthic organisms but favorable to planktonic proliferation (Murray, 2006; Sen Gupta, 1999). The Santonian *Paracypris* aff. *posteriusacuminatus*–*Ovocytheridea triangularis* Assemblage, by contrast, displays higher diversity ( $Shannon= 1.62$ ;  $Simpson= 0.7$ ) and lower dominance (0.29), pointing to a more heterogeneous benthic environment with relatively firmed marly substrates. Macrofaunal evidence from the *Nuculana* cf. *mariae* Assemblage corroborates this interpretation, as the dominance of epifaunal and stationary guilds implies firmer grounds, while extremely low diversity reflects stressful or unstable conditions (Abdelhady & Fürsich, 2014; Chikhi-Aouimeur et al., 2011). Collectively, the combined faunal signals document a substrate evolution from soft, soupy, and unstable muddy bottoms in the Coniacian, dominated by infaunal bivalves and smooth ostracods, to firmer, more compacted marly substrates in the Santonian, characterized by stronger benthic foraminiferal presence and epifaunal

## CHAPTER V RESULTS, INTERPRETATION AND DISCUSSION

macrofaunal dominance under increasingly stressed environmental conditions. In summary, this assemblage most likely developed within a soft, soupy substrate, semi-enclosed lagoon characterized by fluctuating salinity and temperature stressful conditions under which only a few specialized taxa could survive. Such lagoonal settings are typically marked by fine-grained sediments, soft substrates, and low faunal diversity. For more detail on the lithofacies and biofacies of lagoonal environments.

### 4. Coniacian- Santonian transition

In Essen section, the Coniacian is significantly different from the Santonian, where the Coniacian is more diverse, containing more smooth ostracods, more globular and keeled and planktic foraminifera. The Santonian is marked by diversity decrease and high dominance Index. What is also interesting is the negative relationship between the ostracods and foraminifera. These patterns suggest significant ecological and environmental changes between the Coniacian and Santonian, resulting in reduced diversity and altered community structure. The increased proportion of benthic foraminifera in the Santonian may reflect shifts in habitat conditions or ecological pressures during this time. Benthic foraminifera, which may be affected more by anoxia is increasing. This can be explained by a small degree of dysoxia due to the development of a large anoxic zone (Schlanger and Jenkyns, 1976) not far from the study area, the low diversity of the benthic fauna may be the result of a stressed environmental conditions such as reduced oxygen availability, extreme (low/high) eutrophic levels, reduced salinity (Abdelhady and Fürsich, 2014; Jain et al., 2023). The distinction between the Coniacian and Santonian is less clear-cut due to the absence of clear biogenic markers and the prevalence of sedimentary lacunae. The middle–upper Coniacian boundary, typically linked to the Oceanic Anoxic Event 3 (OAE-3) and marked by widespread black shale deposition, is absent in the Essen section. This absence indicates sedimentation within an isolated shelf lagoon (Nemouchi et al., 2024). Shallow marine settings are generally less prone to anoxic conditions than deeper environments, as oxygen availability decreases with depth (Richards, 1957). Moreover, oligotrophic conditions, characterized by limited nutrient and sediment supply, contrast with the eutrophic settings usually associated with anoxia (Almroth-Rosell et al., 2021). These factors support the interpretation that OAE-3 was confined to the equatorial Atlantic and adjacent epicontinental seas (Mansour and Wagreich, 2022). The lack of black shales (Mansour and Wagreich, 2022) and glauconites (Lamolda et al., 2014) features commonly recorded at the Coniacian–Santonian boundary in equatorial

## CHAPTER V RESULTS, INTERPRETATION AND DISCUSSION

Atlantic regions further suggests that the Essen section was deposited in shallow, restricted shelf lagoons (Chikhi-Aouimeur et al., 2011, Nemouchi et al., 2024). In contrast, the Santonian experienced a reduction in the diversity of planktonic foraminifera, marked by the extinction of certain species and the rise of others that cohabited with benthic foraminifera. While ostracods remained present, their populations saw a notable decline. The ongoing proliferation of *Whiteinella* and *Heterohelix* beyond the Coniacian-Santonian boundary suggests their ability to withstand environmental pressures, including anoxic conditions (Caron and Homewood, 1983). Furthermore, an analysis of ostracod communities from the Coniacian and Santonian stages indicates considerable disparities in both numerical and functional diversity. The lithofacies do not exhibit clear evidence of such anoxia. Additionally, benthic foraminifera, which may be more adversely affected by anoxia, are on the rise. This phenomenon can be attributed to a slight degree of dysoxia resulting from the formation of a substantial anoxic zone (Schlanger and Jenkyns, 1976).

In the Boukezez section Herein, the ostracods are absent in marls underlain by laminated wackestone limestones of beds E7-E12. In contrast, two foraminifers are abundant include *Gavelinella* and *Planoheterohelix*. Both were recorded in high stress environments during the Late Cretaceous of many localities. *Gavelinella* was found to be one of five taxa dominating the oxygen-depleted and organic-rich environments of the Cretaceous (Friedrich et al., 2006). During the OAE2, the *Gavelinella* acme was associated with deoxygenation in bottom waters (and even upper water column; Boudinot et al., 2020). In general, the OAE 2 interval was dominated by the benthic calcareous epifaunal *Gavelinella* sp. (Amaglio et al., 2023). However and according to Amaglio et al. (2023), *Gavelinella* was found in settings with variable oxygen levels. The repeated occurrences in anoxic/dysoxic setting suggest that their abundance (not only occurrence) can be related to oxygen deficiency as the case in the study section.

Similarly, Pardo and Keller (2008) found that the small *Heterohelix* is low-oxygen tolerant and is dominating high stress horizons after extreme events of the Cretaceous-Paleogene interval. Probably, stratification of the water column associated with deepening was result in dysoxia, where oxygen level decreased significantly at sediment-water interface, and thus, ostracods and benthic foraminifer species could not survive (Figure 13). The dominance of the planktonic foraminifera at this interval supports a deeper water condition.

The absence of ostracods could be related to stressful environmental conditions within OAE3. But the oxygen deficiency has no clear lithologic footprint. Laminated wackestones of

## CHAPTER V RESULTS, INTERPRETATION AND DISCUSSION

bed E12 is not an obvious criterion. Although this bed contains abundant *Planoheterohelix globulosa*, they may represent only dysoxia and not anoxia. The absence of the marked organic carbon-rich black shales and dark carbonates of the OAE3 of Coniacian-Santonian interval indicates that the event was not pronounced in the study site. This is in same line with previous investigations (e.g., Wagreich, 2009; Mansour and Wagreich, 2022). According to the Wagreich and Mansour (2022), organic-rich sedimentation was mainly restricted to low-latitude Atlantic and adjacent shallow seas. Certain authors (e.g., Arthur and Schlanger, 1979; Jenkyns, 1980; Arthur et al., 1990; Wagner et al., 2004; Jones et al., 2007; Wagreich, 2009) have previously noted a restricted occurrence of black shales in the Coniacian and Santonian interval. In Boukezez section, laminated limestones hosting calcispheres and *Planoheterohelix globulosa* are regarded as a biochronological marker for the Coniacian-Santonian transition. In general, the Coniacian-Santonian was a time of enough oxygen in shallow and deep seas in the Tethys, Indian, and large areas of the Pacific (Wagreich, 2009).

The fossiliferous nature of the limestones of the beds E16 to E20 and the dominance of bioclastics (bivalves, gastropod, and echinoid plates) indicate well-oxygen conditions and more stable environment. Absence of ostracods at this horizon indicates a delay in their recovery and hint to more sensitivity to moderate and low environmental stress, relatively to other benthic groups.

Ostracods that are living infaunally usually have smooth carapaces and they are adapted for low-oxygen availability, while those living epifaunally have usually ornamented surfaces with keels or spines and also they usually found in coarser sediments of higher water-energy and enough oxygen (Bodergat, 1983; Anadón et al., 2002). Generally and based on numerous investigations (e.g., Geiger, 1990, Dole-Olivier et al., 2000), the species with smooth carapaces can dominate low-oxygen environments and contrast the ornamented ones. The latter is also comparable to the phenomenon seen in benthic foraminifera (Kaiho, 1994). The dominance of smooth forms in latest Coniacian and earliest Santonian supports dysoxic conditions.

## CHAPTER V RESULTS, INTERPRETATION AND DISCUSSION

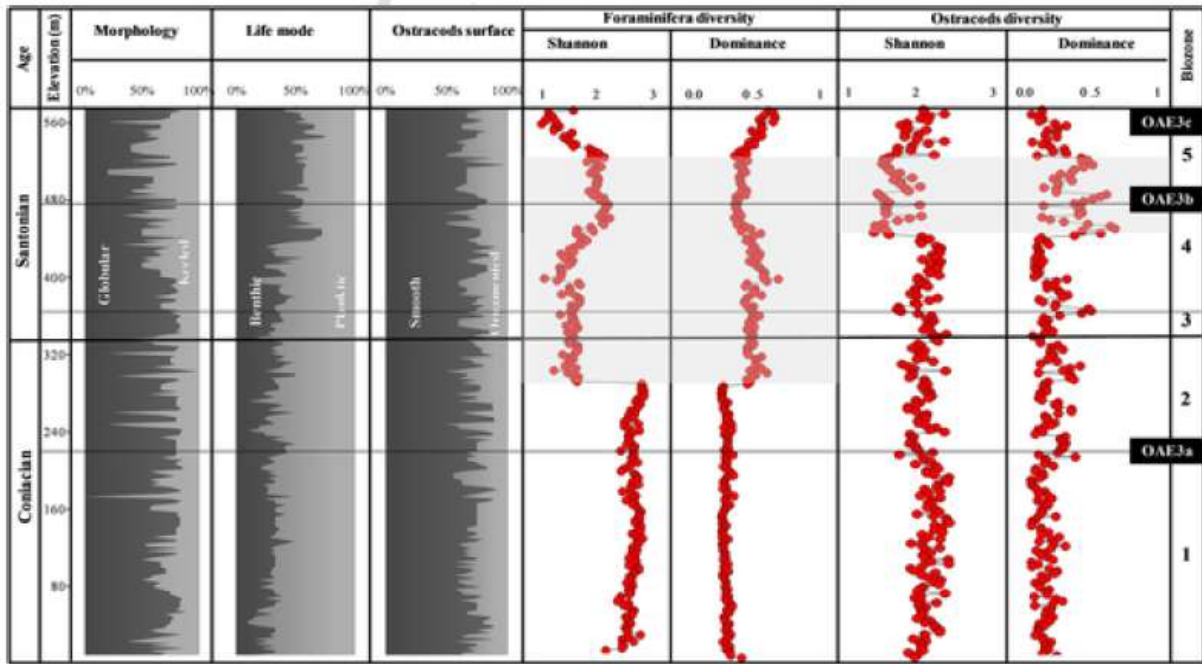


**Figure V. 9.** Box plots show marked differentiation between the ostracods/foraminifera of Coniacian and the Santonian assemblages.

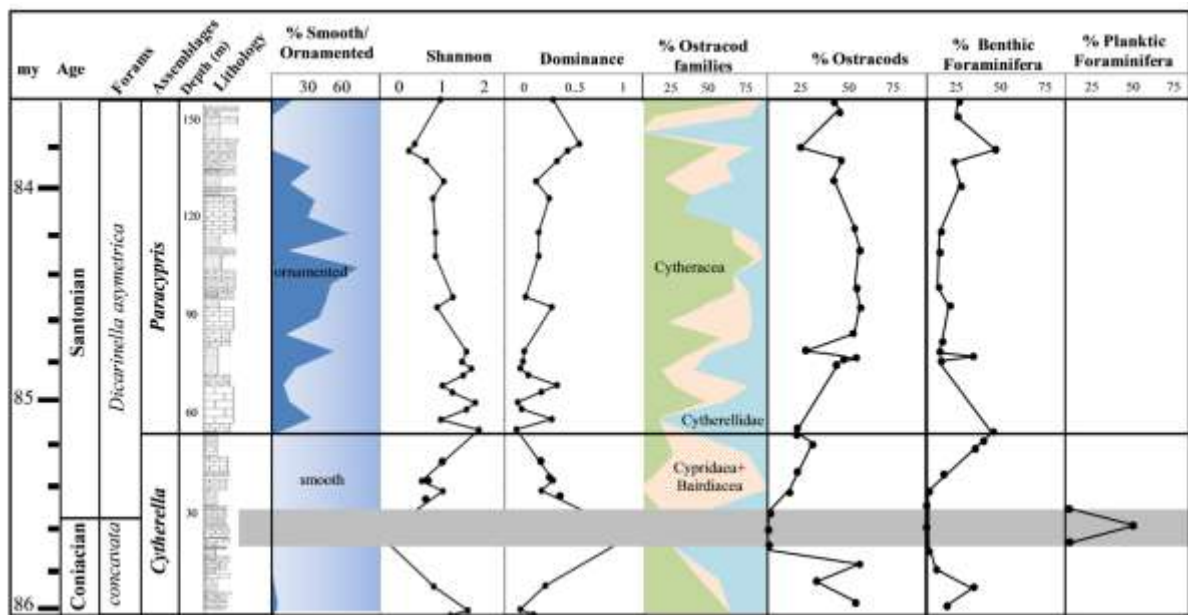


**Figure V. 10:** Stratigraphic framework of the Boukezez section. Shaded area denotes the Coniacian- Santonian transition.

### 5. Paleobiogeography

The identified species predominantly exhibit Tethyan affinities and have been reported from Upper Cretaceous deposits across North Africa and the Middle East (West Asia), as documented by Seeling and Bengtson (1999), Jaitly and Mishra (2009), Moussavou (2015), Benzaggagh (2016), and Ghenim et al. (2019). Several species, such as *Pycnodonta*

## CHAPTER V RESULTS, INTERPRETATION AND DISCUSSION

*(Phygraea) vesicularisvesicularis*, *Amphidonteconica*, *Protocardiahillana*, and *Oscillopha dichotoma*, display a cosmopolitan distribution and have been recorded globally. In contrast, *Idonearca trigona* and *Meretrix desvauxi* appear to be restricted to North Africa. The presence of numerous regionally restricted species supports the idea of a biogeographic link between the study area and the Tethyan Ocean, suggesting that any environmental restriction affecting the basin was likely spatially or temporally limited. Notably, although *Idonearca trigona* and *Meretrix desvauxi* possess planktotrophic larvae typically associated with broader dispersal these species show a limited geographic range (Abdelhady and Fürsich, 2015), implying that abiotic factors may have been more influential than biotic traits in controlling their distribution.

The biogeographic distribution of the identified species whether restricted or widespread cannot be attributed solely to their larval development strategies. Other factors, such as environmental tolerance and adaptability to stress, likely play a significant role. For example, the broad distribution of Cretaceous oysters, both within the study area and globally (Ahmad et al., 2015), is probably linked to their ability to withstand a wide range of environmental conditions. This same resilience may also account for the success of modern oysters, which often thrive in habitats affected by intense anthropogenic pressures, including eutrophic lakes, deltas, lagoons, coastal wetlands, and shallow marine environments. Therefore, the biogeographic patterns observed in the fossil assemblage are likely shaped by a combination of both biotic and abiotic influences.

This continental margin of the Tethyan appears to be a pathway for ostracods faunal exchanges, characterized by significant dispersion linked to an increase in water depth during the Santonian (Benmansour et al., 2016). The extensive geographic range of ostracods along both the northern and southern Tethyan margins indicates opportunities for migration and exchanges between these different regions (Babinot and Colin, 1988 and 1992; Carbonnel, 1990; Colin and Hochuli, 1992; Luger, 2003; Khalil, 2020; Bekhouch et al., 2023; Bendala et al., 2023). As all ostracods are active mobile, they have the chance to be dispersed for longer distances (Abdelhady and Fürsich, 2015). Although many species are widespread in North Africa, similarity among countries based on their ostracods fauna is less than that of the Turonian. The general low faunal similarity in the Coniacian-Santonian can be related to the less pronounced marine transgression relatively to that of the Cenomanian-Turonian (Abdelhady et al., 2023). Similarly, Piovesan et al. (2014a) attributed the narrower geographic ranges of the Santonian–Campanian ostracods, comparatively to the

## CHAPTER V RESULTS, INTERPRETATION AND DISCUSSION

Cenomanian–Turonian, to the paleobathymetry. The existed similarity between North Africa and West Africa may indicate continued extensive faunal exchange between the two regions via the Trans-Sahara-Seaway (see Reyment, 1980; Elewa and Abdelhady, 2020). Elewa and Abdelhady (2020) suggested that in addition to the Trans-Sahara-Seaway, the dispersion along the continental margin of the southern Tethyan through Gibraltar corridor to the continental margin of West Africa towards the southern Atlantic is also possible. The wide geographic distribution of some ostracods species in North Africa and the Middle East suggests also that these areas share similar paleoenvironmental conditions (e.g., water salinity, energy, dissolved oxygen, and food supply), facilitating exchanges along the South Tethyan margin (Jomaa-Salmouna et al., 2017). The dispersion towards the south (as indicated by an earlier/older occurrence by key taxa in the North; Sarr, 1995; Elewa and Abdelhady, 2020) indicates also that temperature gradient was not very steep during the Coniacian-Santonian interval (Zakharov et al., 2012) or that cooling by the Santonian (Petrizzo et al., 2022) made migration toward the south a favorable trend for many ostracod species. The very low similarity of the identified taxa with those from United States indicates that the migration via the North Atlantic was highly restricted. The latter can be also attributed to increasing depth of the Atlantic (Murphy and Thomas, 2013) or due to the Santonian cooling (Petrizzo et al., 2022), where southern migration will be more favorable.

## CHAPTER V RESULTS, INTERPRETATION AND DESCUSSION

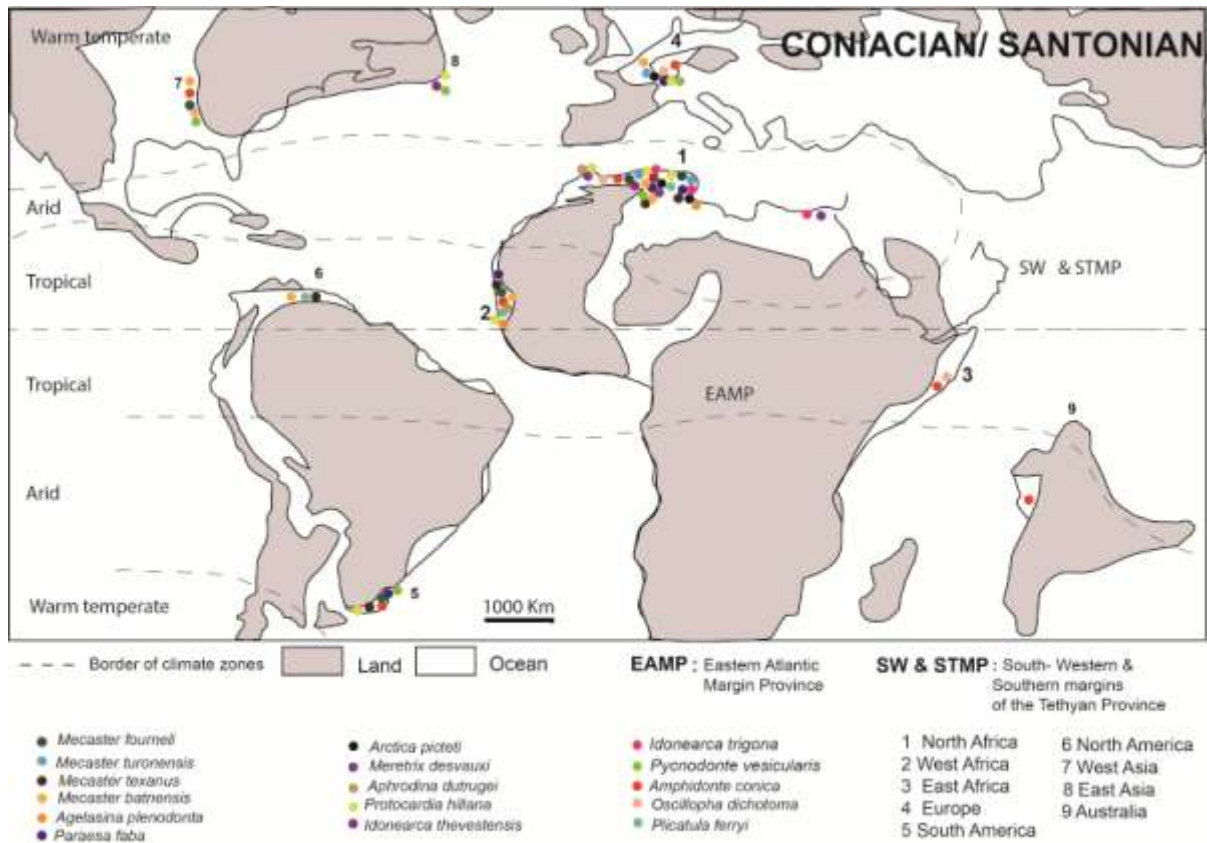


**Figure 11a** : Geographic distribution of the identified macrofaunal species in the study section.

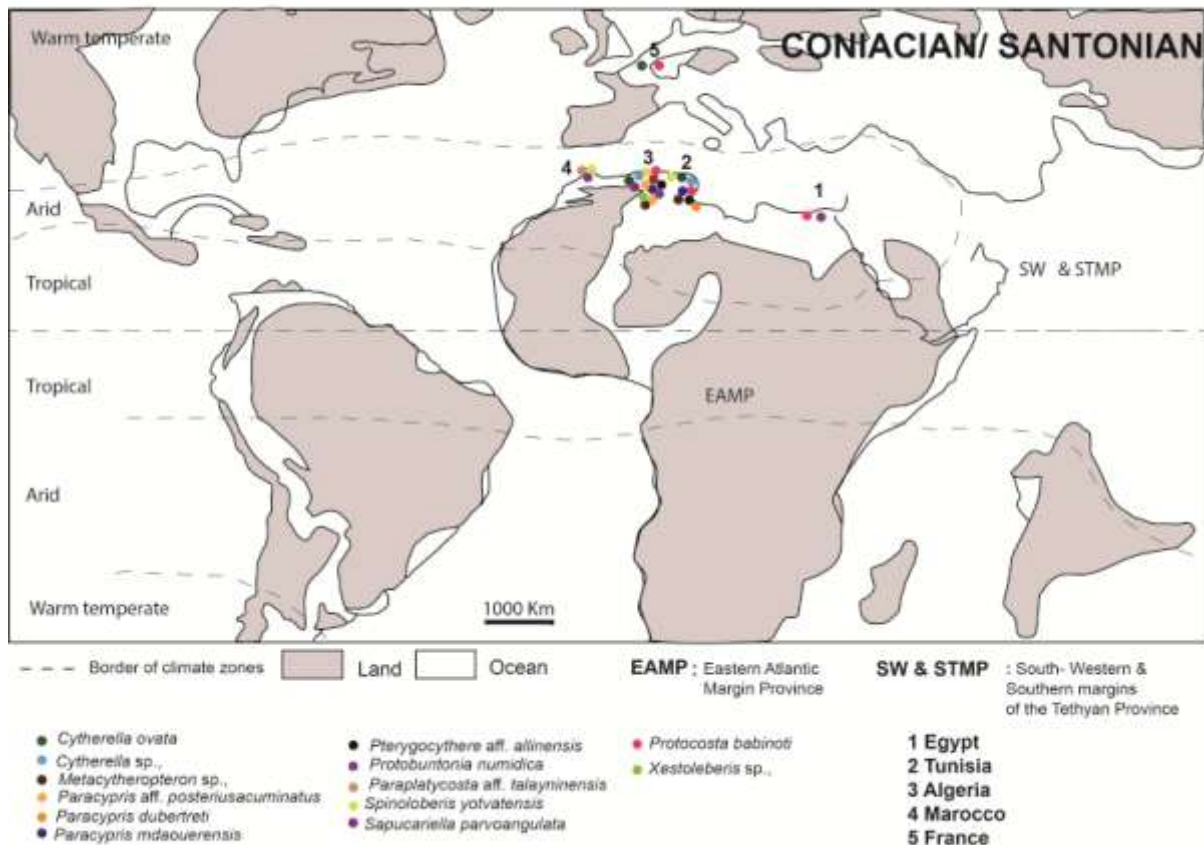


**Figure 11b :** Geographic distribution of the ostracods taxa identified in the study section. 1: Egypt, 2:Tunisia, 3: Algeria, 4: Morocco, 5: France.

## 6. Regional correlation

During the middle Turonian to Santonian, an extensive shallow water carbonate platforms developed on the southern margin of the Tethys (Tunisia and East Algeria). During the Turonian to Santonian period, extensive shallow-water carbonate platforms emerged along the southern edge of the Tethys, specifically in Tunisia and East Algeria. These platforms were shaped by extensional fault systems (Camoin, 1991). In the South-East Constantinois Basin of Algeria, Cheriet and Benzagouta (2016) assessed Coniacian- Santonian outcrops, identifying them as potential reservoirs characterized by low porosity and permeability. Such features may arise from deposition within restricted shelf lagoons and diminished hydrodynamics.

The Coniacian and Santonian series found in the Aures Mountains of northeastern Algeria is marked by sedimentation processes dominated by marls (Bentahar et al., 2023).

## CHAPTER V RESULTS, INTERPRETATION AND DISCUSSION

Bentahar et al., 2023 examined three sections from the Aures Mountains and noted the existence of two distinct Coniacian- Santonian formations. The lower formation is approximately 300 meters thick and comprises carbonate marls interspersed with limestone banks that host gastropods, sea urchins, lamellibranchs, and the ammonite *Tissotia tissoti*, which is indicative of the Coniacian age. Conversely, the upper marly formation, abundant in *Palenticeras polypsis*, corresponds to the Santonian age. Rudists, which are of significant biostratigraphic importance and have been utilized to date various Late Cretaceous sections, are prevalent in the upper Turonian of the Aures Mountains. Noteworthy rudist species include *Distefanella lombricalis*, *Bournonia*, *Vaccinites*, *Hippurites*, *Plagioptychus*, and *Durania*. For additional information, consult the works of Busson et al. (1999) and Chikhi-Aouimeur (1992, 2003). Nevertheless, the demarcation between the Turonian and Coniacian remains inadequately defined (Bentahar et al., 2023; Benzerouel et al., 2024). In the Aures region, the rudist limestones are overlain by marly beds that contain the ammonite *Tissotia*, which corroborates the Coniacian age of the strata (Chikhi-Aouimeur, 2003). The studied Essen Formation can be correlated to the lower formation, El assas Formation at El assas section, of Bentahar et al., 2023.

Essen and Boukezez sections highlights both stratigraphic continuity and paleoecological variability across the Coniacian and Santonian interval. The Essen Formation (Nemouchi et al., 2024, 2025) exhibits a thick, homogeneous marl succession (533 m) with abundant benthic macro-invertebrates, particularly bivalves and echinoids, and only a limited presence of gastropods. Its Coniacian deposits (300 m) are overlain by Santonian strata (200 m), separated by a 3 m bioconstructed limestone bench, with the lower boundary resting on a Turonian rudist limestone bar (Dubourdiou, 1956). In contrast, the Boukezez section is thinner (160 m) and consists of alternating marls and limestones (Yahiaoui, 1990; Laffitte, 1939), where the exposed record spans only the Upper Coniacian to Santonian. Despite these lithological differences, micropaleontological data allow for a meaningful correlation. In the Essen section, the Coniacian is characterized by the *Cytherella* aff. *austinensis*– *Cytherella* aff. *contracta* Assemblage, with a trophic nucleus strongly dominated by *Cytherella* aff. *austinensis* alongside *Spinoleberis yotvatensis* and *Cytherella gambiensis*, whereas the Santonian shows a shift to the *Cytherella* aff. *austinensis*– *Cytherella* aff. *elongata* Assemblage, marked by increased representation of *Cytherella* aff. *elongata* and *Paracypris mdaouerensis*. Similarly, the Boukezez section records a transition from the *Cytherella ovata*– *Spinoleberis yotvatensis* Assemblage in the upper Coniacian, dominated by smooth-shelled

## CHAPTER V RESULTS, INTERPRETATION AND DISCUSSION

*Cytheracea* with low diversity and high dominance, to the *Paracypris* aff. *posteriusacuminatus*– *Ovocytheridea triangularis* Assemblage in the lower Santonian, characterized by greater diversity and reduced dominance. These parallel faunal turnovers in both sections reflect ecological restructuring across the Coniacian–Santonian boundary, most likely linked to regional paleoenvironmental changes affecting both diversity patterns and community composition.

### 7. Conclusion

The macrofaunal and microfaunal assemblages of the Essen and Boukezez sections reveal significant local palaeoenvironmental variability during the Coniacian–Santonian. The Essen section reflects soft-substrate, low-energy settings marked by infaunal dominance, moderate environmental stress, and fluctuating conditions. In contrast, Boukezez indicates firmer substrates, greater habitat stability, and well-oxygenated neritic environments. Both sections record faunal and ecological shifts linked to sea-level fluctuations, temperature changes, and oxygen availability, highlighting the complex interplay of regional palaeogeography, substrate consistency, and climatic influences. These findings underscore the importance of local depositional settings in shaping marine community structure within the broader Tethyan.

***GENERAL  
CONCLUSION***

## GENERAL CONCLUSION

The analysis of Coniacian and Santonian formations in the Tébessa and Bellezma-Batna mountains, located in northern Algeria (Eastern Saharan Atlas), conducted through a multidisciplinary approach integrating lithological, paleontological, biostratigraphic, and paleoenvironmental studies, has led to the following main conclusions:

From a structural perspective, the two studied areas belong to the Eastern Saharan Atlas domain in northeastern Algeria. The Essen section, located in Tébessa, is part of the Mellegue Mountains, while the Boukezez section, situated in Batna, belongs to the Bellezma-Batna Mountains. These regions occupy a transitional position between the Saharan basement to the south and the Tellian domain to the north. They are characterized by particularly thick Mesozoic to Cenozoic sedimentary successions, shaped by Alpine tectonic processes.

From lithological and paleontological perspectives, the two studied sedimentary successions, located at Jebel Essen (Tébessa) and Jebel Boukezez (Batna), both record the Coniacian and Santonian interval, yet display significant differences in thickness, lithological composition, and fossil assemblages. The Essen Formation reaches a substantial thickness of approximately 533 meters, dominated by marly deposits interbedded with fossiliferous limestone layers. In contrast, the Boukezez Formation is considerably thinner (around 160 meters) and is composed predominantly of carbonate facies. At Jebel Essen, four distinct biogenic units were identified based on the distribution of macro- and microfossils, comprising diverse assemblages of bivalves, echinoids, cephalopods, foraminifera, and ostracods. A marked faunal turnover is evident at the Coniacian–Santonian boundary, characterized by the first occurrence (FO) of *Dicarinella asymetrica* and a transition from highly diverse to low-diversity faunal communities. In contrast, the Boukezez section shows lower overall fossil diversity, particularly among ostracods and foraminifera, and is dominated by echinoid-rich two assemblages, indicative of shallower, higher-energy depositional conditions.

The Coniacian and Santonian transition is clearly expressed at Jebel Essen by a 3 meter-thick bioclastic limestone bed, while at Boukezez, this transition is less well-defined due to sedimentary discontinuities and the absence of precise biostratigraphic markers.

Taken together, these findings refine the regional biostratigraphic framework and highlight local paleoenvironmental contrasts: Jebel Essen reflects a deeper, more stable, and fossil-rich marine setting, whereas Jebel Boukezez represents a shallower, more dynamic

environment with intermittent sedimentation, both shaped by Late Cretaceous sea-level fluctuations.

From biostratigraphical perspectives of the Essen and Boukezez formations refines the Coniacian and Santonian stratigraphic framework in northeastern Algeria. In the Essen section, five planktonic foraminiferal zones were identified, from the *Dicarinella primitiva* Zone (Lower–Middle Coniacian) to the *Globotruncanita elevata* Zone (Latest Santonian), with the FO of *Dicarinella asymetrica* marking the Coniacian/Santonian boundary. In the Boukezez Formation, the *Inoceramus siccensis* Zone, associated with *Mecaster fourneli*, defines the lower Santonian. The integration of foraminiferal, ammonite, and inoceramid data reveals a clear faunal turnover at the boundary, reflecting significant paleoenvironmental changes linked to regional sea-level fluctuations. These results provide robust correlations with other Tethyan regions and improve understanding of the Coniacian and Santonian transition.

The analysis of macrofaunal assemblages from the Essen and Boukezez sections reveals a generally low diversity and scarcity of fossils, mainly composed of bivalves, echinoids, and rare gastropods. In the Essen section, four distinct assemblages were identified, showing a transition from infaunal, mobile taxa in the lower Coniacian to more epifaunal, suspension-feeding communities by the Santonian. This reflects gradual environmental changes from soft, soupy substrates to firmer, moderately energetic settings. In the Boukezez section, one assemblage dominated by echinoids (*Hemiaster*, *Phymosoma*) and bivalves (*Plicatula*, *Paraesa faba*) suggest a shallow, warm, and well-oxygenated marine environment with mixed substrates.

Overall, both sections indicate deposition in a neritic setting with limited ecological diversity, likely influenced by fine sedimentation, occasional oxygen stress, and stable shallow-marine conditions during the Late Cretaceous. These results provide valuable insights for regional and Tethyan-scale stratigraphic correlations of the Coniacian and Santonian interval.

The analysis of ostracod and foraminiferal assemblages from the Essen and Boukezez sections highlights distinct ecological and environmental shifts across the Coniacian and Santonian transition. At Essen, the Coniacian interval is marked by high taxonomic diversity and abundance, with assemblages dominated by smooth-shelled ostracods and a prevalence of planktic foraminifera, including globular and keeled forms. In contrast, the Santonian record a notable decline in diversity, an increase in benthic foraminifera, and a higher dominance

index, all of which point to environmental stress and changing habitat conditions. In the Boukezez section, ostracods are well represented during the Coniacian but vanish near the stage boundary, coinciding with a sharp rise in planktic foraminifera and opportunistic benthic species. This pattern reflects a shift from well-oxygenated, shallow neritic environments to deeper, less stable, or oxygen-depleted settings. In summary, the Coniacian and Santonian show marked paleoecological differences. The former exhibits greater diversity and ecological complexity, while the latter is characterized by simplified communities, dominated by benthic forms. A particularly noteworthy observation is the inverse relationship between ostracod and foraminiferal abundance, suggesting distinct ecological responses to changing environmental pressures. The rise in benthic foraminifera during the Santonian likely reflects adaptation to altered substrates, oxygenation levels, or increased environmental stress during this interval. Overall, both sections record a significant faunal turnover at the Coniacian–Santonian boundary, reflecting a deterioration of benthic habitats and a reorganization of marine communities during this time.

These changes suggest a major faunal turnover linked to substrate modification, reduced oxygenation, and overall environmental instability. Collectively, the data indicate that the Coniacian was a period of ecological complexity and favorable marine habitats, whereas the Santonian represents a time of environmental stress and community restructuring, marking a critical phase in the paleoenvironmental evolution of the region.

The paleoenvironmental record of the Essen and Boukezez sections reflects predominantly oxic, shallow-marine conditions throughout the Coniacian and Santonian interval, with only localized and short-lived episodes of dysoxia. At the Essen section, the absence of black shales and glauconite, along with the persistence of diverse macrofaunal and benthic foraminiferal assemblages, indicates that Oceanic Anoxic Event 3 (OAE3) did not strongly impact this region. Instead, the faunal patterns suggest deposition within a restricted, shallow shelf lagoon, where occasional environmental stresses such as salinity fluctuations, increased sedimentation, or turbidity temporarily reduced diversity. The Boukezez section records a comparable trend, with early Coniacian assemblages dominated by infaunal suspension feeders such as *Agelasina plenodonta*, indicative of well-oxygenated, soft-bottom conditions. A transition to epifaunal dominance in the upper Coniacian reflects a shift toward shallower and more agitated environments, followed by a Santonian decline in both macro- and microfaunal diversity, linked to episodic oxygen stress and possible mild dysoxia. While ostracod assemblages decrease sharply at the boundary, the concurrent rise of planktonic

foraminifera (*Heterohelix*, *Globotruncana*) and benthic forms like *Gavelinella* suggests intermittent stratification and oxygen depletion, rather than persistent anoxia.

Overall, both sections document regional paleoenvironmental changes driven by eustatic sea-level fluctuations, with a gradual deepening at the Coniacian and Santonian transition followed by progradation and shallowing in the early Santonian. These findings align with broader Tethyan trends while highlighting that, in northeastern Algeria, OAE3 was only weakly expressed, with dysoxic conditions limited in extent and duration.

In summary, the transition from the Coniacian to the Santonian reflects a gradual environmental shift from shallow, stable, and well-oxygenated marine settings with high biodiversity, to more variable environments characterized by a decline in diversity and signs of episodic oxygen stress. This indicates that local ecosystems responded to global sea-level and climatic changes, while the region was less affected by major anoxic events compared to other parts of the Tethys realm.

The paleotemperature evolution recorded at the Essen and Boukezez sections reflects a transition from warm, well-oxygenated shallow marine conditions during the Coniacian to cooler and more environmentally stressed settings in the Santonian. In the Essen section, high diversity of foraminifera and ostracods in the lower Coniacian suggests tropical, stable conditions, while the late Santonian is marked by a pronounced decline in diversity and abundance, indicating a cooling event and changes in marine community structure, consistent with global climatic trends (Petrizzo et al., 2022; Friedrich et al., 2012). At the Boukezez section, the Coniacian assemblages are characterized by high diversity and dominance of smooth-shelled ostracods and keeled planktonic foraminifera, reflecting warm, open-marine environments. In contrast, the Santonian shows reduced diversity, higher dominance, and a greater proportion of benthic foraminifera, indicating cooler, stressed, and shallower conditions. These shifts suggest a regional response to global sea-level changes and mid-Cretaceous cooling, with the Coniacian and Santonian transition representing a turning point marked by ecological reorganization and declining biodiversity.

Overall, the comparison shows a paleotemperature gradient from the cooler, deeper, and stressed environments of the Coniacian (*Cytherella ovata*– *Spinoleberis yotvatensis* Assemblage) to the warmer, shallower, and ecologically richer environments of the Santonian (the *Paracypris* aff. *posteriusacuminatus*– *Ovocytheridea triangularis* Assemblage). This reflects both regional sea-level rise and a shift toward more favorable climatic and

environmental conditions during the Santonian transgressive phase, consistent with the global Late Cretaceous green house trend.

The Coniacian and Santonian transition represents a turning point in paleoclimate, marked by a gradual cooling and a reorganization of marine ecosystems. This cooling phase was superimposed on broader global greenhouse conditions of the Late Cretaceous, leading to a regional decrease in biodiversity and a shift from warm, tropical seas during the Coniacian to cooler, stressed environments during the Santonian. These regional responses were driven by global sea-level changes, climatic oscillations, and local paleoceanographic dynamics, reflecting the complex interplay between global greenhouse trends and localized environmental factors.

The Essen and Boukezez sections provide valuable insights into relative sea-level fluctuations along the southern Tethyan margin during the Coniacian and Santonian transition. At Essen, the Coniacian is characterized by low-diversity macrofaunal assemblages dominated by eurytopic oysters (*Pycnodonte*) and spatangoid echinoids, reflecting restricted, shallow-marine settings linked to a global sea-level fall and local tectonic isolation. The absence of black shale and significant facies changes indicates that this area remained well-oxygenated and outside the direct influence of Oceanic Anoxic Event 3 (OAE3). In contrast, the Boukezez section record a complete transgressive–regressive (T–R) cycle. The late Coniacian began under moderately energetic shallow-neritic conditions, followed by a deepening event at the Coniacian–Santonian boundary, marked by the disappearance of benthic fauna and dominance of planktonic foraminifera, representing a Maximum Flooding Surface (MFS). This was followed by an early Santonian regression, evidenced by the return of diverse benthic assemblages and progradational shallow-water facies.

Taken together, both sections highlight the impact of first-order eustatic sea-level changes, with a major transgression around the Coniacian–Santonian boundary followed by a regression in the early Santonian, consistent with global sea-level trends (Haq, 2014; Voigt et al., 2004).

Both sections reflect the impact of first-order eustatic sea-level changes, showing a major transgression that reached its peak around the Coniacian–Santonian boundary, in agreement with global sea-level models. This was followed by a regression in the early Santonian, which facilitated the return of shallow-marine benthic communities and increased habitat diversity. These results emphasize the interaction between global eustatic variations

and local tectonic influences in controlling marine depositional environments along the southern Tethyan margin during the Late Cretaceous.

From paleoenergy perspective and during the Coniacian period, both sedimentary and paleontological data suggest that deposition occurred under conditions of relatively low to moderate marine energy. The prevalence of smooth-shelled ostracods (*Cytherella*, *Spinoleberis*), along with a high abundance of planktic foraminifera and echinoids, implies that deposition took place in environments ranging from the outer shelf to the upper slope, which are characterized by relatively stable yet oxygen-restricted conditions. In contrast, the Santonian period is characterized by a transition towards higher-energy environments, as evidenced by the increased occurrence of inoceramids and other sturdy bivalves that are adapted to more turbulent, shallower water conditions. This shift, along with a decrease in overall faunal diversity and an increase in dominance indices, suggests a more stressed environment influenced by stronger hydrodynamic forces, aligning with shallower neritic conditions.

At Boukezez section record a clear evolution of paleoenergy from the late Coniacian to the Santonian. The lower Coniacian reflects a protected, low- to moderate-energy neritic setting with well-oxygenated bottom waters, dominated by irregular echinoids, small bivalves, and smooth-shelled ostracods, indicating stable, restricted conditions. At the Coniacian–Santonian boundary, a rapid deepening event is marked by the disappearance of ostracods and the rise of planktonic foraminifera, reflecting more open-marine, less oxygenated conditions. During the Santonian, environments shifted back to very shallow, high-energy platform settings, with higher ostracod diversity and well-circulated waters. This evolutionary trend mirrors regional Tethyan patterns, linking faunal turnovers and facies changes to global sea-level fluctuations and mid-Cretaceous climatic cooling.

Overall, the paleoenergy evolution from the Coniacian to the Santonian reflects a regional response to global sea-level fluctuations and mid-Cretaceous climatic cooling. These changes drove faunal turnovers and facies transitions, illustrating the close link between hydrodynamic energy, ecological restructuring, and broader paleoenvironmental dynamics within the southern Tethyan margin.

The Essen and Boukezez sections reveal a clear paleo-salinity evolution from the Coniacian to the Santonian, linked to a regional transgressive trend and progressive reduction

of freshwater influence. At Essen, early Coniacian assemblages reflect stressed mesohaline to polyhaline conditions, marked by low diversity and dominance of euryhaline taxa such as *Agelasina plenodonta* and *Cucullaea*. Up-section, the increasing presence of ammonites, diverse planktonic foraminifera, and normal-marine ostracods indicates a gradual shift toward stable euhaline, fully marine environments by the Santonian. During the Coniacian-Santonian interval of the Essen Formation the paleosalinity reveal a progressive shift from brackish-influenced to fully marine conditions.

Similarly, At Boukezez section, a brackish-influenced (meso-/polyhaline) Lower–Middle Coniacian (salinity-stressed, low diversity) grades upward into more stable, higher salinity conditions in the Upper Coniacian, culminating in fully marine (euhaline) conditions by the Santonian. This pattern fits a transgressive or reduced freshwater-influence trajectory, with substrate consolidation and community stabilization through time. The late Coniacian is dominated by low-diversity, smooth-shelled ostracod assemblages, suggesting restricted polyhaline settings. Across the Coniacian and Santonian transition, a marked faunal turnover and increasing ostracod diversity signal progressive stabilization of salinity and well-ventilated conditions. By the early Santonian, assemblages dominated by robust, ornamented taxa and stenohaline echinoids reflect near-normal marine salinity.

The paleosalinity records of the Essen and Boukezez sections indicate a consistent long-term trend from stressed mesohaline to more stable euhaline conditions across the Coniacian and Santonian interval. In the Essen Formation, early to middle Coniacian assemblages show low diversity, brackish to polyhaline signatures whereas the Upper Coniacian is marked by increasing marine connectivity and the establishment of euhaline conditions, culminating in a fully marine Santonian setting. Similarly, the Boukezez Formation record vertical salinity fluctuations, where the *Cytherella ovata*–*Spinoleberis yotvatensis* Assemblage of the Upper Coniacian reflects mesohaline to polyhaline conditions, while the *Paracypris aff. posteriusacuminatus*–*Ovocytheridea triangularis* Assemblage of the Lower Santonian represents more diverse, euhaline communities. Taken together, both sections document a gradual transition from stressed, brackish-influenced and fluctuating salinity conditions during the early Coniacian toward more stable, near-normal marine environments by the Santonian, reflecting a regional transgressive trajectory and the progressive reduction of freshwater input.

The fossil evidence from both Essen section and Boukezez section indicates that these organisms lived in a warm, shallow neritic environment with mixed substrates (both hard and soft), well-oxygenated waters, and abundant nutrients. This setting reflects a stable and diverse marine ecosystem characteristic of the Cretaceous period. Lagoonal environments characterized by soft substrates, fine-grained sediments, and lowfaunal diversity.

Overall, consistent long-term paleosalinity trend, from fluctuating mesohaline to polyhaline conditions in the early Coniacian to stable, euhaline marine environments in the Santonian. This evolution is closely tied to regional sea-level rise and a progressive reduction of freshwater influence, leading to well-oxygenated, nutrient-rich, and ecologically diverse shallow neritic habitats by the Santonian.

The Coniacian and Santonian transition in both the Essen and Boukezez sections reflects significant paleoenvironmental changes driven by sea-level fluctuations and localized oxygen stress. In the Essen section, the Coniacian shows higher diversity with abundant smooth ostracods and planktonic foraminifera, while the Santonian records lower diversity, higher dominance, and a notable decline in ostracods, suggesting increased environmental stress and slight dysoxia. The absence of black shales indicates that Oceanic Anoxic Event 3 (OAE3) did not strongly affect this shallow, restricted shelf setting. In Boukezez, the disappearance of ostracods and dominance of low-oxygen-tolerant foraminifera such as *Planoheterohelix* and *Gavelinella* near the boundary indicate deeper, more stressed conditions, likely linked to temporary water-column stratification. However, the lack of organic-rich facies suggests only moderate dysoxia rather than full anoxia. Together, both sections indicate that OAE3 was spatially restricted, with local settings in northeastern Algeria experiencing only minor oxygen depletion and driven primarily by regional sea-level changes rather than widespread anoxic events.

The identified fauna shows strong Tethyan affinities, with several cosmopolitan species indicating open marine connections, while regionally restricted taxa such as *Idonearca trigona* and *Meretrix desvauxi* reflect localized environmental controls. Ostracod distributions suggest active faunal exchanges along the southern Tethyan margin, likely facilitated by the Trans-Saharan Seaway and Gibraltar corridor. However, lower similarity compared to the Cenomanian–Turonian indicates a less extensive marine transgression during the Coniacian and Santonian. These patterns reflect a combination of biotic traits and abiotic factors, including sea-level changes, paleobathymetry, and Santonian cooling, which together

shaped faunal dispersal and biogeographic differentiation across North Africa and the Middle East.

During the Turonian–Santonian, extensive shallow-water carbonate platforms developed along the southern Tethyan margin in Tunisia and eastern Algeria. The Essen and Boukezez sections record parallel ecological and stratigraphic changes across the Coniacian–Santonian boundary. Both show a shift from low-diversity, stressed communities in the Coniacian to more diverse assemblages in the Santonian, reflecting sea-level fluctuations and regional paleoenvironmental changes, while remaining largely unaffected by widespread Oceanic Anoxic Event 3 (OAE3).

# *REFERENCES*

## REFERENCES

- Abbass, H. L. 1962. A monograph on the Egyptian Cretaceous pelecypods. Geol. Surv. Miner. Res. Dept., Palaeont. Ser., Mongr. 1, 224, 24 pls., Cairo.
- Abawi, T. S., & Hammoudi, R. A. 1997. Foraminiferal biostratigraphy of the Kometan and Gulneri Formations (Upper Cretaceous) in Kirkuk area, North of Iraq. *Iraqi Geological Journal*, 30, 139–146.
- Abawi, T. S., & Mahmood, S. A. (2005). Biostratigraphy of the Kometan and Gulneri Formations (Upper Cretaceous) in Jambour well no.46, Northern Iraq. *Iraqi Journal of Earth Science*, 5, 1–8.
- Abdel-Gawad, G. I., Orabi, O. H., & Ayoub, W. (2004). Macrofauna and biostratigraphy of the Cretaceous section of Gebel El-Fallig area, northwest Sinai, Egypt. *Egyptian Journal of Paleontology*, 4, 305–333.
- Abdelhady, A. A., & Fürsich, F. T. (2014). Macroinvertebrate palaeo-communities from the Jurassic succession of Gebel Maghara (Sinai, Egypt). *Journal of African Earth Sciences*, 97, 173–193.
- Abdelhady, A. A., & Fürsich, F. T. (2015). Palaeobiogeography of the Bajocian–Oxfordian macrofauna of Gebel Maghara (North Sinai, Egypt): Implications for eustacy and basin topography. *Palaeogeography, Palaeoclimatology, Palaeoecology*, 417, 261–273.
- Abdelhady, A. A., & Mohamed, R. S. 2017. Paucispecific macroinvertebrate communities in the Upper Cretaceous of El Hassana Dome (Abu Roash, Egypt): Environmental controls vs adaptive strategies. *Cretaceous Research*, 74, 120–136.
- Abdelhady, A. A., Khalil, M., Ismail, E., Fan, D., Zhang, S., & Xiao, J. 2019. Water chemistry and substrate type as major determinants for molluscan feeding habit and life-mode in lagoon sediments. *Estuarine, Coastal and Shelf Science*, 220,\* 120–130. [<https://doi.org/10.1016/j.ecss.2019.02.019>](<https://doi.org/10.1016/j.ecss.2019.02.019>)
- Abdelhady, A. A., Mohamed, R., Fathy, D., & Ali, A. 2020. Benthic invertebrate communities as a function of sea-level fluctuations and hydrodynamics: A case from the Cenomanian-Turonian of Wadi Tarfa (Eastern Desert, Egypt). *Journal of African Earth Sciences*, 168, 103870.

Abdelhady, A. A., Farouk, S., Ahmed, F., Alamri, Z., & Al-Kahtani, K. 2021. Impact of the late Cenomanian sea-level rise on the south Tethyan coastal ecosystem in the Middle East (Jordan, Egypt, and Tunisia): A quantitative eco-biostratigraphy approach. \*Palaeogeography, Palaeoclimatology, Palaeoecology, 574(4), 110446.

Abdelhady, A. A., Ayoub-Hannaa, W., Ahmed, M. S., & Hussain, A. M. 2023. Upper Cretaceous (Coniacian-Santonian) low diversity oyster-dominated macrofaunal association in the Eastern Desert of Egypt: Taphonomy versus ecology. *Journal of African Earth Sciences*, 208,105080.[<https://doi.org/10.1016/j.jafrearsci.2023.105080>](<https://doi.org/10.1016/j.jafrearsci.2023.105080>)

Abdo, G. S. (2013). Stratigraphy of the Cenomanian – Early Campanian depositional cycle from selected wells in North Iraq (PhD thesis). University of Mosul. (in Arabic).

Agassiz, L., & Desor, E. (1846–1847). Catalogue raisonné des familles, des genres et des espèces de la classe des Echinodermes. *Annales des Sciences Naturelles*, 3e série, Zoologie, 6, 305–374.

Al-Dulaimi, S. I., & Saeed, A. F. (2017). Biostratigraphy of Al-Khasib Formation at specific wells in Majnoon Oilfield. *International Journal of Science and Research*, 7, 1068–1074.

Alsenz, H., Bornemann, A., Bottini, C., Brassell, S.C., Farnsworth, A., 2017. Cretaceous sea-surface temperature evolution: constraints from TEX86 and planktonic foraminiferal oxygen isotopes. *Earth Sci. Rev.* 172, 224–247.

Al-Shareefi, I. Y., Khalaf, S. K., & Al-Eisa, M. A. (2010). Paleocology of some Upper Cretaceous formations from selected wells northwest and middle Iraq. \*Iraqi Journal of Earth Sciences, 10(2), 67–96.

Almogi-Labin, A., Eshet, Y., Flexer, A., Honigstein, A., Moshkovitz, S., & Rosenfeld, A. (1991). Detailed biostratigraphy of the Santonian/Campanian boundary interval in northern Palestine . *Journal of Micropalaeontology*, 10, 39–50.

Amaglio, G., Petrizzo, M. R., Holbourn, A., Kuhnt, W., & Wolfgring, E. (2023). Benthic foraminiferal response to the Oceanic Anoxic Event 2 (Late Cretaceous) and evidence of bottom water re-oxygenation during the Plenus Cold Event at Clot Chevalier (Vocontian Basin, SE France). *Palaeogeography, Palaeoclimatology, Palaeoecology*, 623, 111598.

Amami-Hamdi, A., & Ben Ismail-Lattrache, K. (2013). Les ostracodes et foraminifères associés des dépôts de l'Eocène moyen et supérieur de la coupe de Jebel Serj (Tunisie centrale): Intérêt biostratigraphique, paléoécologique et paléobiogéographique. *Revue de Micropaléontologie*, 56, 159–174.

Amami-Hamdi, A., Ben Ismail-Lattrache, K., Dhahri, F., & Said-Benzarti, R. 2014. Middle to Upper Eocene ostracofauna of Central Tunisia and Pelagian Shelf: Examples of Jebel Bargou and the Gabes Gulf. *Arabian Journal of Geosciences*, 7, 1587–1603.

Amami-Hamdi, A., Dhahri, F., Jomaa-Salmouna, D., Ben Ismail-Lattrache, K., & Ben Chaabane, N. (2016). Quantitative analysis and paleoecology of middle to upper Eocene ostracods from Jebel Jebil, Central Tunisia. *Revue de Micropaléontologie*, 59, 409–424.

Ameen, F. A., & Gharib, H. (2014). Biostratigraphy of the Tethyan Cretaceous successions from northwestern Zagros fold-thrust belt, Kurdistan region, NE Iraq. *Arabian Journal of Geosciences*, 7, 2689–2710.

Anadón, P., Gliozzi, E., & Mazzini, I. (2002). Paleoenvironmental reconstruction of marginal marine environments from combined paleoecological and geochemical analyses on ostracods. In *The Ostracoda: Applications in Quaternary Research* (Vol. 131, pp. 227–247).

Ando, A., Woodard, S. C., Evans, H. F., Littler, K., Herrmann, S., MacLeod, K. G., et al. (2013). An emerging palaeoceanographic 'missing link': Multidisciplinary study of rarely recovered parts of deep-sea Santonian-Campanian transition from Shatsky Rise. *Journal of the Geological Society, London*, 170, 381–384.

Andreu, B. (1991). Les ostracodes du Crétacé moyen (Barrémien à Turonien), le long d'une transversale Agadir-Nador (Maroc). *Strata*, série 2, 14, 762 pp., 73 pls.

Andreu, B. (1995). Trachyleberididae (ostracodes) du Turonien supérieur (?)-Santonien de la région de Boulmane, Moyen Atlas (Maroc): Systématique et biostratigraphie. *Revista Española de Micropaleontología*, 27(1), 85–142.

Andreu, B. (1996). Nouvelles espèces d'ostracodes du Coniacien (?)-Santonien de la région de Boulmane, Moyen Atlas, Maroc: Systématique, biostratigraphie et paléoécologie, paléobiogéographie. In *Géologie de l'Afrique et de l'Atlantique Sud, Actes Colloque Angers 1994* (pp. 483–509).

Andreu, B. (2002). Cretaceous ostracod biochronology of Morocco. *Eclogae Geologicae Helveticae*, 95(2), 133–152.

Andreu, B., Boutchich, K., & Chbani, B. (1998). Nouvelles espèces d'ostracodes du Coniacien-Santonien et Maastrichtien du Bassin d'Essaouira (Atlas Atlantique, Maroc). *Revue de Micropaléontologie*, 41(2), 91–106.

Andreu, B., Bilotte, M. (2006). Ostracodes du Cénomaniens supérieur et du Turonien de la zone sous-pyrénéenne orientale (Corbières méridionales, SE France): Systématique, biostratigraphie, paléoécologie et paléobiogéographie. *\*Revue de Micropaléontologie*, 49, 55–73.

Andreu, B., Lebedel, V., Wallez, M. J., Lézin, C., & Ettachfini, E. M. (2013). The Upper Cenomanian-Lower Turonian carbonate platform of the Preafrican Trough, Morocco: Biostratigraphy, paleoecological and paleobiogeographic distribution of ostracodes. *Cretaceous Research*, 45, 213–246.

Andreu, B., & Tronchetti, G. (1996). Ostracodes et foraminifères du Crétacé supérieur du synclinal d'El Koubbat, Moyen Atlas, Maroc: Biostratigraphie, paléoenvironnements, paléobiogéographie, systématique des ostracodes. *Geobios*, 29(1), 45–71.

Alsenz, H., Bornemann, A., Bottini, C., Brassell, S.C., Farnsworth, A., 2017. Cretaceous sea-surface temperature evolution: constraints from TEX86 and planktonic foraminiferal oxygen isotopes. *Earth Sci. Rev.* 172, 224–247.

Apostolescu, V. (1961). Contribution à l'étude paléontologique (Ostracodes) et stratigraphique des bassins crétacés et tertiaires de l'Afrique occidentale. *Revue de l'institut Français du Pétrole*, 16, 779–867.

Aref, M., & Ramadan, M. (1990). New record of planktic foraminifera from the Upper Cretaceous rocks of the Esh El Mallaha range, Red Sea, Egypt. *M.E.R.C. Ain Shams University Earth Science Series*, 4, 123–141.

Arthur, M. A., & Schlanger, S. O. (1979). Cretaceous “oceanic anoxic events” as causal factors in development of reef-reservoired giant oil fields. *AAPG Bulletin*, 63, 870–885.

Arthur, M. A., Jenkyns, H. C., Brumsack, H. J., & Schlanger, S. O. (1990). Stratigraphy, geochemistry, and paleoceanography of organic carbon-rich Cretaceous sequences. In R. N. Ginsburg & B. Beaudoin (Eds.), *Cretaceous Resources, Events and Rhythms* (pp. 75–120). Dordrecht: Kluwer Academic Publishers.

Arz, J. A. (1996). Los foraminiferos planctonicos del Campaniense y Maastrichtiense: bioestratigrafia, cronoestratigrafia y eventos paleoecologicos (PhD thesis). Universidad de Zaragoza, 419 p.

Ayyad, S. N., Abed, M. M., & Abu Zied, R. H. (1996). Biostratigraphy and correlation of Cretaceous rocks in Gebel Arif El-Naga, northeastern Sinai, Egypt, based on planktic foraminifera. *Cretaceous Research*, 17, 263–291.

Babazadeh, S.A., Robaszynski, F., Courme, M.D., 2007. New biostratigraphic data from cretaceous planktic foraminifera in Sahlabad province, eastern Iran. *Geobios* 40, 445–454.

Babinot, J.F., Tronchetti, G., 1983. Les microfaunes (foraminifères-ostracodes) du Coniacien-Santonien de Provence (S.E. France): biostratigraphie, paleoecologie. *Geologie Méditerranéenne* 10, 143–154.

Babinot, J.-F., Moullade, M., & Tronchetti, G. (2007). Les Ostracodes du Bédoulien supérieur et du Gargasien inférieur du stratotype de l'Aptien : Systématique et corrélations biostratigraphiques. *Carnets de Géologie / Notebooks on Geology*, 2007(05), 1–46.

Barr, F.T., 1972. Cretaceous biostratigraphy and planktic foraminifera of Libya. *Micropaleontology* 18, 1–46.

Babinot, J.F.P., 1980. Les ostracodes du Crétacé supérieur de Provence: systématique, biostratigraphie, paléoécologie, paléogéographie. PhD. Thesis, Université de Provence.

Babinot, J.F.P., 1987. Les types d'ostracodes du Crétacé supérieur de Provence (collection Babinot): révision synthétique et compléments iconographiques. *Géologie Méditerranéenne*, 14-3, pp. 195-203.

Babinot, J.F., 1995. Patterns of variability in ostracode species and communities from the late Cretaceous carbonate platforms: a report for ecozonal modelling and the study of ambient conditions. *Palaeogeography, Palaeoclimatology, Palaeoecology* 119, 9310

Babinot, J.F. et Colin, J.P., 1988. Paleobiogeography of Tethyan Cretaceous Marine Ostracods. In: T. Hansi, N. Ikeya et K. Ishizaki (Editors), *Evolutionary Biology of Ostracoda*. Elsevier, Amsterdam, 11, pp. 823-839.

Babinot, J.F. et Colin, J.P., 1992. Marine ostracode provincialism in the Late Cretaceous of the Tethyan realm and the Austral Province. *Palaeogeography, Palaeoclimatology, Palaeoecology*, 92, 283-293

Babinot J.-F. and Crumière-Airaud C., 1990. The effect of global events on the evolution of Cenomanian and Turonian marginal Tethyan ostracod faunas in the Mediterranean region. In: Whatley R. and Maybury C. (eds.), *Ostracoda and global events*.- Chapman and Hall, London, p. 25-39.

Bassiouni, M.A.A., 2002. Mid-Cretaceous (Aptian–Early Turonian) ostracoda from Sinai. *Neue Paläontologische Abhandlungen* 5, 1–123.

Bassoullet, J.-P. and Damotte R., 1969. Quelques ostracodes nouveaux du Cénomanién-Turonien de l'Atlas saharien occidental (Algérie). *Revue de Micropaléontologie* 12(3) : 130-144.

Bassiouni, M.A.A., Luger, P., 1990. Maastrichtian to early Eocene Ostracoda from southern Egypt. *Palaeontology, palaeoecology, palaeobiogeography and biostratigraphy*. *Berliner Geowissenschaftliche Abhandlungen Reihe A Geologie Und Palaeontologie* 120, 755–928.

Bassiouni, M.A.A., Morsi, A., Abdel-Mohsen, M., 2000. *Palaeontogr. Abt. A* 257, 27–84.

Bauer, J., Marzouk, A.M., Steuber, T., Kuss, J., 2001. Lithostratigraphy and biostratigraphy of the Cenomanian-Santonian strata of Sinai. *Egypt. Cretaceous Research* 22, 497–526.

Bellier, J.P., 1983. Foraminifères planctoniques du Crétacé de Tunisie septentrionale.

Systematique, biozonation, utilisation stratigraphique de l'Albien au Maastrichtien. PhD thesis,. Universite Pierre et Marie Curie, Paris, p. 250.

Bentahar, F., Defafli, N., Benmansour, S., Fehdi, C., 2023. Investigation of lithobiostratigraphic characteristics and geographical distribution of Coniacian-Santonian formations: a case study in the Aures Mountains, eastern Saharan Atlas, Algeria. *Geomatics, Landmanagement and Landscape* 3, 73–94.

Bekhouch, G., Puckett, M., Khiari, A., Djerrab, R-M., Meguelatti, A., 2023. Optimized event stratigraphy of Cenomanian-Turonian ostracods of North Africa and the Middle East. *Journal of African Earth Sciences*\_208. doi.org/10.1016/j.jafrearsci.2023.105061

Bellion, Y.J., 1972. Etude géologique et hydrogéologique de la terminaison occidentale des Monts de Bellezma (Algérie), Thèse Doct. 3e Cycle Univ. Paris 6:221.

Bellion, Y., Donze, P., Guiraud, R., 1973. Répartition stratigraphique des principaux ostracodes (Cytheracea) dans le Crétacé supérieur du sud-ouest constantinois (Confins Hodna-Aurès, Algérie du Nord). *Publication du Service géologique de l'Algérie (Nlle série)*, 44, 7-44.

Benadla, M., Reolid, M., Marok, A., El Kamali, N., 2018. The Cenomanian–Turonian transition in the carbonate platform facies of the Western Saharan Atlas (Rhoundjaïa Formation, Algeria). *Journal of Iberian Geology* 44: 405-429. <https://doi.org/10.1007/s41513-018-0070-6>

Benmansour S., Andreu B., Yahiaoui A., 2016. The Campaniane Maastrichtian of the Aures Basin, Algeria: Paleobiogeographical distribution of ostracods. *Cretaceous Research* 58: 86 - 107.

Birkelund, T., Hancock, J.M., Hart, M.B., Rawson, P.F., Remane, J., Robaszynski, F., Schmid, F., Surlyk, F., 1984. Cretaceous stage boundaries-proposals. *Bull. Geol. Soc. Den.* 33, 3–20.

Bismuth, H., Keij, A.J., Oertli, H.J., Szczechura, J., 1978. The genus *Loculicytheretta* (Ostracoda). *Bulle. du Centre de Recherches Exploration-Production Elf-Aquitaine* 2, 227–263.

Bodergat, A.M., 1983. Les ostracodes, témoins de leur environnement: approche chimique et écologie en milieu lagunaire et océanique. *Travaux et Documents Des Laboratoires de Géologie de Lyon*, 88(1), 3-246.

Bonnet, L., Andreu B., Rey J., Cubaynes R., Ruget C., N'zaba-Makaya, O., Brunei, F., 1999. Fluctuations of environmental factors as seen by means of statistical analyses in micropaleontological assemblages from a Liassic series. *Micropaleontology*, New York, vol. 45, p. 399-417.

Boomer, I., Horne, D.J., Slipper, Ian. J., 2003. The use of ostracods in palaeoenvironmental studies or what can you do with an Ostracod shell. *The Paleontological Society, Papers*, pp.

Boudinot, F.G., Dildar, N., Leckie, R.M., Parker, A., Jones, M.M., Sageman, B.B., Bralower, T.J., Sepúlveda, J., 2020. Neritic ecosystem response to Oceanic Anoxic Event 2 in the Cretaceous Western Interior Seaway, USA. *Palaeogeography, Palaeoclimatology, Palaeoecology*, 546, p.109673.

Boukhary, M., Eissa, R., Kerdany, M., Bassiouni, M., 1977. Some ostracodespecies from the Galala Formation, Western Coast of the Gulf of Suez, Egypt. *Proceedings of the Egyptian Academy of Science*, Cairo 30, 155–161, pl. 1.

Bryant, R., Leckie, R.M., Bralower, T.J., Jones, M.M. and Sageman, B.B., 2021. Microfossil and geochemical records reveal high-productivity paleoenvironments in the Cretaceous Western Interior Seaway during Oceanic Anoxic Event 2. *Palaeogeography, Palaeoclimatology, Palaeoecology* 584, p.110679.

Bureau, D., 1975. Figures et structures sédimentaires du Crétacé inférieur des Monts du Bellezma (Algérie). *Publ. Serv. Carte géol Algérie, N.S., n° 45*, pp. 93-98.

Carbonel, P., Colin, J.P., 1982. New observations on the morphology of loculate Cenozoic ostracoda. In: Bate, R., Robinson, E., Sheppard, L. (Eds.), *Fossil and Recent Ostracoda*. British Micropalaeontological Society. Ellis Horwood Ltd., Chichester, pp. 439–453.

Caron, M., 1978. Cretaceous planktic foraminifera from DSDP Leg 40, Southeastern Atlantic Ocean. *Initial Reports of the Deep-Sea Drilling Project 40*, 651–678.

Caron, M., 1983. La specification chez les Foraminifères planctoniques: une réponse adaptée aux contraintes de l'environnement. *Zitteliana 10*, 671–676.

Caron, M., 1985. Cretaceous planktic foraminifera. In: Bolli, H.M., Saunders, J.B., Perch-Nielsen, K. (Eds.), *Planktic Stratigraphy*. Cambridge University Press, pp. 17–86.

Caron, M., Homewood, P., 1983. Evolution of early planktic foraminifera. *Mar. Micropaleontol.* 7 (6), 453–462.

Carbonnel, G., 1990. Les traits majeurs de la faune d'ostracodes paléogène (P3A–P14) dans les bassins côtiers de l'Afrique de l'Ouest et du Golfe de Guinée. *Courier Forschungsinstitut Senckenberg*.

Cetean C. G., Setoyama E., Kaminski M. A., Neagu T., Bubík M., Filipescu S., Tyszka J., 2008. Eobigenerina, a cosmopolitan deep-water agglutinated foraminifer, and remarks on late Paleozoic to Mesozoic species formerly assigned to Pseudobolivina and Bigenerina. *Proceedings of the Eighth International Workshop On Agglutinated Foraminifera (Cluj-Napoca, Romania, September 7-13)*.

Colin, J.P., El-Dakkak M.W., 1975. Quelques ostracodes du Cénomaniens du Djebel Nezzazat (Sinai', Egypte). *Rev. Esp. Micropaleontol. Num. Esp.*: 49-60.

Colin, J.P., Hochuli, A., 1992. Biostratigraphie de la Formation de l'Aschia-Tinamou (Crétacé supérieur), Niger oriental : implications paléogéographiques. *Géologie Africaine, Colloque de Géologie de Libreville, recueil des communications*, 6-8 mai 1991, 255- 273.

Cronin, T.M., 2015. Ostracods and sea level. *Handbook of Sea-Level Research*, pp.249-257.

Chacon, B., Martin-Chivelet, J., Grafe, K.U., 2004. Latest Santonian to latest Maastrichtian planktic foraminifera and biostratigraphy of the hemipelagic successions of the Prebetic zone (Murcia and Alicante provinces, south-East Spain). *Cretac. Res.* 25, 585–601.

Coccioni, R., Premoli Silva, I., 2015. Revised Upper Albian–Maastrichtian planktonic foraminiferal biostratigraphy and magnetostratigraphy of the classical Tethyan Gubbio section (Italy). *Newsl. Stratigr.* 48 (1), 47–90.

*Cushman J. A.* (1938). Cretaceous species of *Gümbelina* and related genera. *Contributions from the Cushman laboratory for foraminiferal research.* 14(1): 2-28.

Damotte, R., 1984. Ostracodes barrémiens-cénomaniens en Algérie occidentale (coupe du Djebel Cheguiga, Monts de Daïa, Oranie). *Géologie Méditerranéenne*, 11(1), pp.159-172.

Damotte, R., Fleury, J.J., 1987. Ostracodes maastrichtiens et paléocènes du Djebel Dyr, pros de Tebessa (Algérie orientale). *Géol. Médit.*, Marseille, vol. XIV, n ° 2, p. 87-107.

Damotte, R., Saint-Marc, P., 1972. Contribution à la connaissance des ostracodes crétacés du Liban. *Revista Española de Micropaleontología*, IV, 3, 273-296.

Delicio, M.P., Coimbra J.C. and Carreño, A.L., 2000. Cretaceous marine Ostracoda from the Potiguar Basin, northeastern Brazil.-*Neues Jahrbuch für Geologie und Palaöntologie, Abhandlungen*, Stuttgart, vol. 215, n° 3, p. 321-345.

Dole-Olivier, M.-J., Galassi, D.M., Marmonier, P., Creuzé, M., 2000. The biology and ecology of lotic microcrustaceans. *Freshwater Biology* 44, 63–91

Donze, P., 1973. Corrélations stratigraphiques dans le Berriasien-Valanginien inférieur du Sud-Est de la France, sur la base de nouveaux Trachyleberidinae (Ostracodes). *Remarques paléoécologiques*, 57. Doc. Laboratoires Géol. Fac. Sci. Lyon, pp. 1–13.

Dowsett, H.J., 1984. Documentation of the foraminiferal Santonian-Campanian boundary in the northeastern Gulf of Mexico. *J. Foraminifer. Res.* 14, 129–133.

Dowsett, H.J., 1989. Documentation of the Santonian–Campanian and Austinian–Tayloran stage boundaries in Mississippi and Alabama using calcareous microfossils. *United States Geological Survey Bulletin* 1884, 1–20.

Dimitrova, E., Valchev, B., 2007. Attempt for upper cretaceous planktic foraminiferal zonation of the Srednogorie and Eastern Balkan zones (Bulgaria). *Geologica Balcanica* 36 (1–2), 55–63.

Dubourdieu, G., 1956. Etude geologique de la region d'Ouenza (confins Algero- Tunisiens). These des sciences. Paris. Publications du service de la carte geologique de l'Algerie. *Bulletin* 10 (1), 659.

Durozoy, M.G., 1956. Carte geologique de l'Algerie au 1/50000, feuille 206 Tebessa avec notice explicative detaillee. Publications du Service de la Carte geologique de l'Algerie, Algeria.

Eaton, J.G., 2004. New screen-washing approaches to biostratigraphy and paleoecology of nonmarine rocks, Cretaceous of Utah. *Bulletin of Carnegie Museum of Natural History* 2004(36), 21–30.

Ehrenberg, C.G., 1840. Uber die Bildung der Kreidenfelsen und des Kreidemergels durch unsichtbare Organismen. *Physik. Abh.* (1838), Berlin. 59-147. Gs

El Albani, A., Kuhnt, W., Luderer, F., Herbin, J.P., Caron, M., 1999. Palaeoenvironmentalevolution of the late cretaceous sequence in the Tarfaya Basin (southwest of Morocco). *Geol. Soc. Lond. Spec. Publ.* 153, 223–240. <https://doi.org/10.1144/GSL.SP.1999.153.01.14>.

El Amri, Z., Zaghib-Turki, D., 2005. Caracterisation biostratigraphique du passage Coniacien/Santonien dans les regions d'Elles et El Kef (Tunisie septentrionale). *J. Iber. Geol.* 31 (1), 99–111.

El Amri, A., Zaghib-Turki, D., 2004. Caractérisation biostratigraphique du passage Coniacian/ Santonien dans les régions d'Ellès et El Kef (Tunisie septentrionale). *Journal of Iberian Geology* 3, 99-111.

El Amri, Z., 2008. Etude micropaleontologique, biostratigraphique et paleoecologique des foraminiferes planctoniques du Turonien terminal-Campanien de la Tunisie centrale et septentrionale. These de Doctorat. Universite de Tunis II, Faculte des Sciences de Tunis, p. 253.

ElAmri, Z., Zaghbib-Turki, D., 2014. Santonian-Campanian biostratigraphy of the Kalaat Senan area (West-Central Tunisia). *Turk. J. Earth Sci.* 23, 184–203.

El Amri, Z., Farouk, S., Zaghbib-Turki, D., 2014. Santonian planktic foraminiferal biostratigraphy of northern Tunisia. *Geologica Croatica* 67 (2), 111–126.

El Amri, Z., Abdeslam, R., Zaghbib-Turki, D., 2016. Planktic foraminiferal biostratigraphy and paleoenvironment of the Upper Coniacian-lower Campanian succession in Northern Tunisia. *J. Afr. Earth Sci.* 124, 234–244.

El Baz, Sh.M., Khalil, M.M., 2019. Foraminiferal biostratigraphy and bioevents of the Cenomanian-Turonian succession in southern Sinai, Egypt and relationship to OAE2. *J. Afr. Earth Sci.* 150, 310–318.

El Gammal, R.M.H., Orabi, H., 2019. Coniacian-late Campanian planktic events in the Duwi Formation, Red Sea Region, Egypt. *J. Geol. Geophys.* 8 (1), 1–16.

El Nady, H., Abu Zied, R., Ayyad, S., 2008. Cenomanian - Maastrichtian ostracods from Gabal Arif El-Naga anticline, Eastern Sinai, Egypt. *Revue de Paléobiologie* 27 (2), 533–573.

El-Azabi, M.H., El-Araby, A., 2007. Depositional framework and sequence stratigraphic aspects of the Coniacian and Santonianmixed siliciclastic/carbonate Matulla sediments in Nezzazat and Ekma blocks, Gulf of Suez, Egypt. *Journal of African Earth Sciences*, 47(4-5), pp.179-202.

Elewa, A.M.T., 2004. Quantitative analysis and palaeoecology of Eocene Ostracoda and benthonic foraminifera from Gebel Mokattam, Cairo,. Egypt. *Palaeogeogr. Palaeoclimatol. Palaeoecol.* 211, 309–323.

Elewa, A.M.T., 2005. Paleocology and Paleogeography of Eocene Ostracod Faunas from the Nile Valley between Minia and Maghagha., Upper Egypt. Migration of Organisms, Chapter, pp. 25–69.

Elewa, A.M.T., Abdelhady, A.A., 2020. Migration routes of the genus *Buntonia* Howe, 1935 (Ostracoda, Crustacea) during the late Cretaceous-Paleogene in Africa. *Arab. J. Geosci.* 13, 1182.

Elewa, A.M.T., Morsi, A.-M.M., 2004. Palaeobiotope analysis and palaeoenvironmental reconstruction of the Paleocene-early Eocene ostracodes from east-Central Sinai, Egypt. *Geol. Soc. Lond., Spec. Publ.* 230, 293–308. <https://doi.org/10.1144/GSL.SP.2004.230.01.15>.

Elewa, A.M.T., Omar, A.A., Dakrory, A.M., 1998. Biostratigraphical and paleoenvironmental studies on some Eocene ostracodes and foraminifera from the Fayoum Depression, Western Desert, Egypt. *Egypt. J. Geol.* 42 (2), 439–469.

Fang, P.-Y., Xu, B., Mu, L., Zhu, Y.-H., Luo, H., 2020a. New latest Coniacian to middle Campanian foraminiferal data from the lower Zongshan Formation in the Chaqiela section, Gamba, southern Tibet. *Palaeoworld* 29, 151–160.

Fang, P.-Y., Xu, B., Mu, L., Zhu, Y.-H., Luo, H., 2020b. New latest Coniacian to middle Campanian foraminiferal data from the lower Zongshan Formation in the Chaqiela section, Gamba, southern Tibet. *Palaeoworld* 29, 151–160.

Faris, N., Ram, R., Tardio, J., Bhargava, S., Pownceby, M.I., 2019a. Characterisation of a ferruginous rare earth-bearing lateritic ore and implications for rare earth mineral processing. *Miner. Eng.* 134, 23–36.

Faris, N., Ram, R., Tardio, J., Bhargava, S., Pownceby, M.I., 2019b. Characterisation of a ferruginous rare earth-bearing lateritic ore and implications for rare earth mineral processing. *Miner. Eng.* 134, 23–36.

Farouk, S., 2014a. Maastrichtian carbon cycle changes and planktic foraminiferal bioevents at Gebel Matulla, west-Central Sinai, Egypt. *Cretac. Res.* 50, 238–251.

Farouk, S., 2014b. Maastrichtian carbon cycle changes and planktic foraminiferal bioevents at Gebel Matulla, west-Central Sinai, Egypt. *Cretac. Res.* 50, 238–251.

Farouk, Sh., Faris, M., 2012a. Late cretaceous calcareous nannofossil and planktic foraminiferal bioevents of the shallow-marine carbonate platform in the Mitla Pass, west-Central Sinai, Egypt. *Cretac. Res.* 33, 50–65.

Farouk, Sh., Faris, M., 2012b. Late cretaceous calcareous nannofossil and planktic foraminiferal bioevents of the shallow-marine carbonate platform in the Mitla Pass, west-Central Sinai, Egypt. *Cretac. Res.* 33, 50–65.

Farouk, Sh., Ahmad, F., Powell, J.-H., Marzouk, A.M., 2016a. Integrated microfossil biostratigraphy, facies distribution, and depositional sequences of the upper Turonian to Campanian succession in Northeast Egypt and Jordan. *Facies* 62, 8.

Farouk, Sh., Ahmad, F., Powell, J.-H., Marzouk, A.M., 2016b. Integrated microfossil biostratigraphy, facies distribution, and depositional sequences of the upper Turonian to Campanian succession in Northeast Egypt and Jordan. *Facies* 62, 8.

Farouk, S., Ahmad, F., Powell, J.-H., 2017a. Cenomanian–Turonian stable isotope signatures and depositional sequences in northeast Egypt and central Jordan. *Journal* 134, 207–230.

Farouk, S., Ahmad, F., Powell, J.-H., 2017b. Cenomanian–Turonian stable isotope signatures and depositional sequences in northeast Egypt and central Jordan. *Journal* 134, 207–230.

Fereydoonpour, M., Vaziri-Moghaddam, H., Azizollah, T., 2014a. Biostratigraphy and sequence stratigraphy of the Gurpi Formation at Deh Dasht Area, Zagros Basin, SW Iran. *Acta Geol. Sin.* 88, 1681–1695.

Fereydoonpour, M., Vaziri-Moghaddam, H., Azizollah, T., 2014b. Biostratigraphy and sequence stratigraphy of the Gurpi Formation at Deh Dasht Area, Zagros Basin, SW Iran. *Acta Geol. Sin.* 88, 1681–1695.

Friedrich, O., Norris, R.D., Erbacher, J., 2012a. Evolution of middle to late cretaceous oceans a 55 my record of Earth's temperature and carbon cycle. *Geology* 40, 107–110.

Friedrich, O., Norris, R.D., Erbacher, J., 2012b. Evolution of middle to late cretaceous oceans a 55 my record of Earth's temperature and carbon cycle. *Geology* 40, 107–110.

Gale, A.S., Montgomery, P., Kennedy, W.J., Burnett, J.A., McArthur, J.M., 1995a. Definition and global correlation of the Santonian-Campanian boundary. *Terra Nova* 7, 611–622.

Gale, A.S., Montgomery, P., Kennedy, W.J., Burnett, J.A., McArthur, J.M., 1995b. Definition and global correlation of the Santonian-Campanian boundary. *Terra Nova* 7, 611–622.

Gale, A.S., Kennedy, J.W., Lees, J.A., Petrizzo, M.R., Walaszczyk, I., 2007a. An integrated study (inoceramid bivalves, ammonites, calcareous nannofossils, planktic foraminifera, stable carbon isotopes) of the ten Mile Creek section, Lancaster, Dallas County, North Texas, a candidate Global Boundary Stratotype Section and Point for the base of the Santonian Stage. *Acta Geol. Pol.* 57, 113–160.

Gale, A.S., Kennedy, J.W., Lees, J.A., Petrizzo, M.R., Walaszczyk, I., 2007b. An integrated study (inoceramid bivalves, ammonites, calcareous nannofossils, planktic foraminifera, stable carbon isotopes) of the ten Mile Creek section, Lancaster, Dallas County, North Texas, a candidate Global Boundary Stratotype Section and Point for the base of the Santonian Stage. *Acta Geol. Pol.* 57, 113–160.

Gebhardt, H., 2004a. Planktic foraminifera of the Nkalagu Formation type locality (southern Nigeria, Cenomanian–Coniacian): biostratigraphy and palaeoenvironmental interpretation. *Cretac. Res.* 25, 191–209.

Gebhardt, H., 2004b. Planktic foraminifera of the Nkalagu Formation type locality (southern Nigeria, Cenomanian–Coniacian): biostratigraphy and palaeoenvironmental interpretation. *Cretac. Res.* 25, 191–209.

Gebhardt, H., 2008a. Integrated biostratigraphy of the Cenomanian to Coniacian Nkalagu Formation in the lower Benue Trough, Nigeria. *Berichte der Geologischen Bundesanstalt* 74, 43–44.

Gebhardt, H., 2008b. Integrated biostratigraphy of the Cenomanian to Coniacian Nkalagu Formation in the lower Benue Trough, Nigeria. *Berichte der Geologischen Bundesanstalt* 74, 43–44.

Gebhardt, H., Zorn, I., 2008. Cenomanian ostracodes of the Tarfaya upwelling region (Morocco) as palaeoenvironmental indicators. *Revue de Micropaléontologie* 51, 273–286.

Geiger, W., 1990. The role of oxygen in the disturbance and recovery of the *Cytherissa lacustris* population of Mondsee (Austria). *Bull. Inst. Géol. Bassin Aquitaine* 47, 167–189.

Georgescu, M.D., 2006a. Santonian–Campanian planktic foraminifera in the New Jersey coastal plain and their distribution related to relative sea-level changes. *Can. J. Earth Sci.* 43, 101–120.

Georgescu, M.D., 2006b. Santonian–Campanian planktic foraminifera in the New Jersey coastal plain and their distribution related to relative sea-level changes. *Can. J. Earth Sci.* 43, 101–120.

Glintzboeckel, C.H., Magne, J., 1959. Répartition des microfaunes à plancton et à Ostracodes dans le Crétacé supérieur de la Tunisie et de l'Est algérien. *Revue de Micropaléontologie* 2, 57–67.

Gradstein, F.M., Ogg, J.G., Kranendonk, M., 2008. *The Geologic Time Scale*. Cambridge University Press, p. 150. Group On Planktic Foraminifera, 1984. *Atlas of Late Cretaceous globotruncanids*.

Gradstein F. M., Ogg J. G., Schmitz M. D., Ogg G. M.. 2020. *Geologic time scale*. 2 volumes (xx, 561p.; xii p., p. 563- 1357). Elsevier. <https://lib.ugent.be/catalog/rug01:002969999>.

Grekoff, N., 1951. Quelques ostracodes nouveaux du cenonien supérieur du Caméron. *Revue de l'Institut Français du Pétrole et annales des combustibles liquides* 6, 53–59.

Grekoff, N., 1954. Ostracodes. In: G. Cheylan, J. Magne, J. Sigal et N. g Grosdidier, E., 1973. Associations d'Ostracodes du Cretace d'Iran. Rev. Inst. France Petrol., 28 (2), pp.313-169.

Grekoff, N., Deroo, G., 1956. Quelques ostracodes du crétacé moyen du nord de l'Espagne. Estudios Geologicos, 227–235 (31–32, XII).

Guernet, C., Molina, E., 1997. Les ostracodes et le passage Paléocène-Éocène dans les Cordillères bétiques (Coupe de Caravaca, Espagne). Geobios, 30(1), 31–43.

Guiraud, R., 1973. Evolution post-Triasique de l'Avant pays de la chaîne alpine en Algérie d'après l'étude du Bassin du Hodna et des régions voisines. Thesis, University of Nice, France, 1-270.

Hammer, O., Harper, D.A.T., Ryan, P.D., 2001a. PAST: paleontological statistics software package for education and data analysis. Palaeontol. Electron. 4, 1–9.

Hammer, O., Harper, D.A.T., Ryan, P.D., 2001b. PAST: paleontological statistics software package for education and data analysis. Palaeontol. Electron. 4, 1–9.

Haq, B.U., 2014a. Cretaceous eustasy revisited. Glob. Planet. Chang. 113, 44–58.

Haq, B.U., 2014b. Cretaceous eustasy revisited. Glob. Planet. Chang. 113, 44–58.

Herrig E. 1966. - Ostracoden aus der Weissen Schreibkreide (Unter-Maastricht) der Insel Rugen. Palaontologische Abhandlungen A, 2 (4): 693 - 1024.

Honigstein, A., Almogi-Labin, A., Rosenfeld, A., 1987a. Combined ostracod and planktic foraminiferal biozonation of the Late Coniacian–Early Maastrichtian in Palestine. J. Micropalaeontol. 6, 41–60.

Honigstein, A., Almogi-Labin, A., Rosenfeld, A., 1987b. Combined ostracod and planktic foraminiferal biozonation of the Late Coniacian–Early Maastrichtian in Palestine. J. Micropalaeontol. 6, 41–60. <https://doi.org/10.1144/jm.6.2.41>.

Horne, D. J., Cohen, A. & Martens, K. 2002. Taxonomy, morphology and biology of quaternary and living ostracoda. In: Holmes, J. A. & Chivas, A. R. (eds) *The Ostracoda, Applications in Quaternary Research*. American Geophysical Union, 131, 5–36.

Horne D.J., 2005. Ostracoda. In: Selley R.C., Cocks R.M. and Plimer I.R. (eds.), *Encyclopedia of Geology*. -Elsevier, Oxford, p. 453-463.

Howe H. & LAURENCICH L. 1958. - Introduction to the Study of Cretaceous Ostracoda. Louisiana State University Press editeurs, 536 p.

Huber, B.T., MacLeod, K.G., Watkins, D.K., Coffin, M.F., 2018a. The rise and fall of the cretaceous Hot Greenhouse climate. *Glob. Planet. Chang.* 167, 1–23.

Huber, B.T., MacLeod, K.G., Watkins, D.K., Coffin, M.F., 2018b. The rise and fall of the cretaceous Hot Greenhouse climate. *Glob. Planet. Chang.* 167, 1–23.

Hussain, S.A., Al-Sheikhly, S.S., 2015a. Paleocology of Albian–Santonian succession of Surdash to Shaqlawa area, NE Iraq. *Iraqi J. Sci.* 56, 1076–1097.

Hussain, S.A., Al-Sheikhly, S.S., 2015b. Paleocology of Albian–Santonian succession of Surdash to Shaqlawa area, NE Iraq. *Iraqi J. Sci.* 56, 1076–1097.

Ismail, A.S.A., Ied, I.M., 2005a. Maastrichtian–Lower Eocene ostracodes from Safaga area, Eastern Desert, Egypt. *Egypt. J. Paleontol.* 5, 119–159.

Ismail, A.S.A., Ied, I.M., 2005b. Maastrichtian–Lower Eocene ostracodes from Safaga area, Eastern Desert, Egypt. *Egypt. J. Paleontol.* 5, 119–159.

Jain, S., Alhussein, M., Ahmed, M., Abdelhady, A.A., 2023. Paleoenvironmental reconstruction of the Middle Jurassic rocks in western India using benthic foraminifera. *Facies* 69, 12. <https://doi.org/10.1007/s10347-023-00668-5>.

Jaff, R.B.N., 2015. Late Cretaceous Foraminifera from the Kurdistan Region, NE Iraq: Palaeontological, Biostratigraphical and Palaeoenvironmental Significance. Unpublished Ph.D. Thesis,. University of Leicester, UK.

Jaff, R.B.N., Al-Kahtany, K., 2020. Coniacian/Santonian calcareous nannofossil and planktic foraminifera in the Kurdistan Region, NE Iraq: biostratigraphy and bioevents. *Arab. J. Geosci.* 13, 1–12.

Jaff, R.B.N., Wilkinson, I.P., Lee, S., Zalasiewicz, J., Lawa, F., Williams, M., 2015. Biostratigraphy and palaeoceanography of the early Turonian–early Maastrichtian planktic foraminifera of NE Iraq. *J. Micropalaeontol.* 34, 105–138.

Jenkyns, H.C., 1980. Cretaceous anoxic events: from continents to oceans. *J Geol Soc Lond* 137:171–188.

Jomaa-Salmouna, D., Chaabani, F., Hamdi–Amami, A., Dhahri, F., Mzoughi, M., 2017. Turonian and Coniacian Ostracods from the Gafsa Basin (central-southernAtlas of Tunisia) and the Gulf of Gabes (eastern coast of Tunisia):Biostratigraphic, paleoenvironmental and paleobiogeographic implications. *Revue de micropaléontologie* 60 (2017) 525–547.

Jones, E.J.W., Bigg, G.R., Handoh, I.C., Spathopoulos, F., 2007, Distribution of deep-sea black shales of Cretaceous age in the eastern Equatorial Atlantic from seismic profiling: Palaeogeography, Palaeoclimatology, Palaeoecology, v. 248, 233–246.

Jenkyns, H.C., Gale, A.S., Corfield, R.M., 1994. Carbon-and oxygen-isotope stratigraphy of the English Chalk and Italian Scaglia and its palaeoclimatic significance. *Geol. Mag.* 131, 1–34.

Kalanat, B., Davtalab, E., Vahidinia, M., 2022. The oxic Coniacian-Santonian interval in the Kopet-Dagh Basin (NE Iran): Carbon isotope and benthic-planktic foraminiferal assemblages at the time of the last cretaceous OAE. *Palaeogeogr. Palaeoclimatol. Palaeoecol.* 588, 110817.

Kaiho, K., 1994. Benthic foraminiferal dissolved-oxygen index and dissolved-oxygen levels in the modern ocean. *Geology*, 22(8), pp.719-722.

Kauffman, W., Kennedy, W.J., Wood, Ch.J., 1996. The Coniacian stage and substage boundaries. *Sci. Terre* 66–SUPP, 81–94.

Kochhann, K.G.D., Lopes, F.M., Krahl, G., Aguiar, E., Gerson, F., 2014. Late cretaceous - early Paleogene (Turonian? To early Danian) Planktic Foraminifera from DSDP Site 356: a Biostratigraphic Reappraisal. *Revista Brasileira De Paleontologia* 17 (2), 157–168.

Khalil, M.M., 2020. Biostratigraphy and paleobiogeographic implications of the Cenomanian-Early Turonian ostracods of Egypt. *Annales de Paléontologie*, 106: 102408.

Kruskal, J.B., 1964. Multidimensional scaling by optimizing goodness of fit to a nonmetric hypothesis. *Psychometrika* 29, 1–27.

Laffitte, R., 1939. Etude géologique de l'Aurès. Thesis, Sciences Paris. *Bulletin du Service Géologique de l'Algérie*, série 1, 11, 484, 1 carte au 1/200000.

Lamolda, M.A., Peryt, D., Ion, J., 2007. Planktic foraminiferal bioevents in the Coniacian/Santonian boundary interval at Olazagutia, Navarra province, Spain. *Cretac. Res.* 28, 18–29.

Lamolda, M.A., Paul, C.R.C., Peryt, D., Pons, J.M., 2014. The global boundary stratotype and section point (GSSP) for the base of the Santonian Stage, “Cantera de Margas”, Olazagutia, northern Spain. *Episodes* 37 (1), 2–13.

Luger, P., 2003. Paleobiogeography of late Early Cretaceous to Early Paleocene marine Ostracoda in Arabia and North to Equatorial Africa.- *Palæogeography, Palæoclimatology, Palæoecology*, vol. 196, p. 319-342.

Maddocks, R.F., 1969. Revision of Recent Bairdiidae (Ostracoda). *Bulletin of the United States National Museum*.

Majoran, S., 1989. Mid-Cretaceous ostracoda of northeastern Algeria. *Fossils, and Strata*, Oslo 27, 1-67, 17 pls.

Mansour, A., Wapreid, M., 2022. Earth system changes during the cooling greenhouse phase of the late Cretaceous: Coniacian-Santonian OAE3 subevents and fundamental variations in organic carbon deposition. *Earth-Science Reviews*. Volume 229, June 2022, 104022.

Malchus, N., 1990. Revision der Kreide-Austern (Bivalvia-Pteriomorpha) Ägyptens (Biostratigraphie, Systematik). *Berliner geowissenschaftliche Abhandlungen A125*, 1–231.

Mancini, E.A., Puckett, M., Tew, B.H., 1996. Integrated biostratigraphic and sequence stratigraphic framework for Upper cretaceous strata of the eastern Gulf Coastal Plain, USA. *Cretac. Res.* 17, 645–669.

Manso, C.L., Andrade, E., 2008. Equinóides do Turoniano (Cretáceo Superior) de Sergipe, Brasil. *Geosciences = Geociências* 27 (3), 319–327.

Mansour, A., Wapreid, M., 2022. Earth system changes during the cooling greenhouse phase of the Late Cretaceous: Coniacian-Santonian OAE3 subevents and fundamental variations in organic carbon deposition. *Earth Sci. Rev.* 229, 104022.

Masoli, M., 1966. Sur quelques Ostracodes fossiles mésozoïques (Crétacé) du Bassin côtier de Tarfaya (Maroc méridional). *Colloque International de Micropaléontologie de Dakar*, 1963, 119-134.

Malumián, N.; Masiuk, V., 1977. Foraminíferos de la Formación Cabeza de León (Cretácico Superior, Tierra del Fuego, República Argentina). *Revista de la Asociación Geológica Argentina*. 31(3) [1976]: 180-202.

Martini, R., Cirilli, S., Saurer, C., Abate, B., Ferruzza, G., Lo Cicero, G., 2007. Depositional environment and biofacies characterisation of the triassic (carnian to Rhaetian) carbonate succession of punta bassano (Marettimo Island, Sicily). *Facies* 53, 389–400.

Mendir, S., Salmi: Laouar, S., El Qot, G.M., Ayoub: Hannaa, W., Ferré, B., 2021. Cenomanian (Upper Cretaceous) bivalves from the Hameimat Massifs, north of T´ebessa, Algeria: systematics, biostratigraphy, palaeoecological and taphonomical remarks. *Ann. Paleontol.* 107 (2), 102471.

Meyers, P.A., Bernasconi, S.M., Forster, A., 2006. Origins and accumulation of organic matter in expanded Albian to Santonian black shale sequences on the Demerara Rise, South American margin. *Org. Geochem.* 37 (12), 1816–1830.

Mebarki, K., Sauvagnat, J., Benyoucef, M., Zaoui, D., Benachour, H.B., Adaci, M., Mahboubi, M., Bensalah, M., 2016. Ostracodes cénomano-turonien dans l’Atlas saharien occidental et le Bassin du Guir (sud-ouest de l’Algérie): systématique, biostratigraphie et paléobiogéographie. *Revue de Paléobiologie, Genève* (juin 2016) 35 (1): 249-277.

Moussavou, B.M., 2015. Bivalves (Mollusca) from the Coniacian: Santonian Anguille formation from cap Esterias, northern Gabon, with notes on paleoecology and paleobiogeography. *Geodiversitas* 37 (3), 315: 324.

Moussavou, B.M., 2017. Systematics, palaeoecology and taphonomy of Turonian oysters from the northern Gabon Coastal Basin. *Geodiversitas* 39 (2), 213–224.

Molina, E., 1995. Modelos y causas de la extincion masiva. –*Interdiscipl.*, 20, 2, 83- 89.

Morkhoven F.P.C.M. van., 1963. Post-Paleozoic ostracoda. Their morphology, taxonomy and economic use. - Elsevier Publishing Company, vol. 2, 478 p.

Morsi, A.M., Bauer, J., 2001. Cenomanian ostracod faunas from Sinai Peninsula, Egypt. *Revue de Paléobiologie* 20 (2), 377–414.

Morton, S.G., 1834. Synopsis of the organic remains of the Cretaceous Group of the United States. Philadelphia: Key and Biddle. 88 pp., 19 pls. + Appendix, 8 pp. [The Appendix is titled: Catalogue of the fossil shells of the Tertiary Formations of the United States.].

Murphy, D.P. and Thomas, D.J., 2013. The evolution of Late Cretaceous deep-ocean circulation in the Atlantic basins: Neodymium isotope evidence from South Atlantic drill sites for tectonic controls. *Geochemistry, Geophysics, Geosystems*, 14(12), pp.5323-5340.

Nagm, E., 2019. The late Cenomanian maximum flooding Neolobites bioevent: a case study from the Cretaceous of northeast Egypt. *Mar. Petrol. Geol.* 102, 740–750.

Nagm, E., Boualem, N., 2019. First documentation of the late Albian transgression in northwest Algeria: bivalve stratigraphy and palaeobiogeography. *Cretac. Res.* 93, 197–210.

Naili, H., Belhaj, Z., Robaszynski, F., Caron, M., Depuy, C., 1995. Pr´esence de roche m`ere" Bahloul" au passage C´enomanien-Turonien dans la r´egion de T´ebessa (Alg´erie). *Mem ETAP* 4, 167–168.

Nemouchi, S., Salmi-Laouar, S., Abdelhady, A.A., Ahmed, M.S., Hussain, A.M., Ouelaa, B., Deghaichia, A., 2024. Paucispecific invertebrate assemblages in the Coniacian (Upper cretaceous) Essen Formation (Tebessa Mountains, Northeast Algeria). *J. Afr. Earth Sci.* 220, 105452.

Nemouchi, S., Salmi-Laouar, S., Abdelhady, A., Deghaichia, A., Mohamed, A., Bazeen, B., Hesemann, M., Ahmed, M., Boughdiri, M., 2025. Ostracod and foraminiferal assemblages in Tebessa (Northeast Algeria): Insights into Santonian cooling effects. *Marine Micropaleontology*. 102468.

Neufville, E.M.H., 1973. Ostracoda from the Ezu-Akshale (Turonian, Cretaceous), Nkalagu, Nigeria. *Bulletin of the Geological Institutions of the University of Uppsala, Uppsala, N.S.* 4, 44–51.

Oertli, H.J., 1958. Les Ostracodes de l'Aptien - Albien d'Apt. *Revue Inst. Fr. P´etrole, Paris*, vol. 13, n° 1 1, 1499-1537 ; 9 pl.

Okosun, E.A., 1987. Ostracod biostratigraphy of the Eastern Dahomey Basin, Niger Delta and the Benue Trough of Nigeria. *Geological Survey of Nigeria, Lagos*, vol. 41, 151 p.

Okosun, E.A., 1992. Cretaceous ostracod biostratigraphy from Chad Basin in Nigeria. *Journal of African Earth Sciences*, Oxford, vol. 14, p. 327-339.

Oliveira, J., Manso, C.D.C., Andrade, E.J., Souza-Lima, W., 2013. O gênero *Mecaster* (Echinodermata: Spatangoida) do Cretáceo superior da Formação Jandaíra, Bacia Potiguar, Nordeste do Brasil. *Scientia Plena* 9 (8), 1–17.

Ogg, J.C., Hinnov, L.A., 2012. Cretaceous. In: Gradstein, F.N., Ogg, J.G., Schmitz, M., Ogg, G. (Eds.), *The Geologic Time Scale*. Elsevier, pp. 793–853.

Ogg, J.G., Gabi, M., Gradstein, F.M., 2016. *A Concise Geologic Time Scale*. Elsevier, pp. 1–234.

Ozkan-Altiner, S., Ozcan, E., 1999. Upper cretaceous planktic foraminiferal biostratigraphy from NW Turkey: calibration of the stratigraphic ranges of larger benthic foraminifera. *Geol. J.* 34, 287–301.

Özyurt, M., Kandemir, R., Yıldızoğlu, S., 2023. Geochemistry of the turonian-coniacian strata: new insight into paleoenvironmental conditions of the Tethys, eastern Pontides, NE Türkiye. *J. Asian Earth Sci.* X 10, 100156.

Pardo, A., Keller, G., 2008. Biotic effects of environmental catastrophes at the end of the Cretaceous and early Tertiary: *Guembelitra* and *Heterohelix* blooms. *Cretaceous Research*, 29(5-6), pp.1058-1073.

Péron, A., 1891. *Description des mollusques fossiles des terrains crétacés de la région sud des Hauts-Plateaux de la Tunisie recueillis en 1885 et 1886 par Thomas, M.P.*

Membre de la mission d'Exploration Scientifique de la Tunisie, 1889. Imprimerie Nationale, Paris, p. 405.

Péron., 1896. *Les Ammonites du crétacé supérieur de l'Algérie*. *Mém. S. G. F., Paleontologie*, VI et VII.

Péron, A., Gauthier, V., 1878. Echinides fossiles de l'Algérie. Terrains secondaires. Etage Cénomaniens 4, 1–144.

Perthuisot, V., 1978. Dynamique et pétrogenèse des extrusions triasiques en Tunisie septentrionale. Annexes: Histoires du diapirisme, les dômes de sel. Travaux de Laboratoire de Géologie, Ecole Normale Supérieure, Paris 12, p. 312p. France.

Perthuisot, V., Rouvier, H., 1992. Les diapirs du Magreb central et oriental: des appareils variés, résultats d'une évolution structurales et pétrogénétique complexe. Bulletin Société Géologique France 163, 751–760 (English abs).

Pervinquière, L., 1912. Études de paléontologie tunisienne II. Gastéropodes et Lamellibranches des terrains crétacés. Carte géologique de la Tunisie. J. Lamarre et Cie, Paris, p. 352.

Peryt, D., Dubicka, Z., Wierny, W., 2022. Planktic foraminiferal biostratigraphy of the Upper cretaceous of the central European Basin. *Geosciences* 12, 1–24.

Petrizzo, M.R., 2019. A critical evaluation of planktic foraminiferal biostratigraphy across the Coniacian–Santonian boundary interval in Spain, Texas, and Tanzania. In: Denne, R.A., Kahn, A. (Eds.), *Geologic Problem solving with Microfossils IV* (special Publication), 111. SEPM, pp. 186–198.

Petrizzo, M.R., 2000. Upper Turonian–Lower Campanian planktic foraminifera from southern mid-high latitudes (Exmouth Plateau, NW Australia): biostratigraphy and taxonomic notes. *Cretac. Res.* 21, 479–505.

Petrizzo, M.R., Huber, B.T., Falzoni, F., MacLeod, K.G., 2020. Changes in biogeographic distribution patterns of southern mid-to high latitude planktic foraminifera during the late cretaceous hot to cool greenhouse climate transition. *Cretac. Res.* 104547.

Petrizzo, M.R., MacLeod, K.G., Watkins, D.K., Wolfgring, E., Huber, B.T., 2022. Late Cretaceous paleoceanographic evolution and the onset of cooling in the Santonian at southern

high latitudes (IODP Site U1513, SE Indian Ocean). *Paleoceanography and Paleoclimatology*, 37(1), p.e2021PA004353.

Peypouquet. J.-P., Ducasse, O., Rousselle. L., 1981. Morphogenesis and environment. Theoretical and practical aspect from Hammatocythere: Paleogene Ostracods of the Aquitaine Basin. In : Martinell J. (ed.), *International Symposium on Concepts and Methods in Paleontology*.- Departamento de Paleontologia, Universitat de Barcelona, p. 173-187.

Piovesan, E.K.; Cabral, M.C.; Colin, J.-P.; Fauth, G. and Bergue, C.T., 2014a. Ostracodes from the Upper Cretaceous deposits of the Potiguar Basin, Northeastern Brazil: taxonomy, paleoecology and paleobiogeography, Part 1: Turonian. *Carnets de Géologie*, 14:211–252. doi:10.4267/2042/54003.

Piovesan, E.K., Cabral, M.C., Colin, J.-P., Fauth, G., Trescastro Bergue, C., 2014b. Ostracodes from the Upper Cretaceous deposits of the Potiguar Basin, northeastern Brazil: taxonomy, paleoecology and paleobiogeography. Part 2: Santonien-Campanien. *Carnets de Géologie/Notebooks on Geology* 14, 211–252.

Piovesan, E.K., Fauth, G., Bergue, C.T., 2020. Late Cretaceous ostracods from the central area of the Potiguar Basin, northeastern Brazil. *Revista Brasileira de Paleontologia*, 23(2):81–89. doi:10.4072/rbp.2020.2.01.

Puckett, T.M., 1994. New Ostracoda species from an Upper Cretaceous oyster reef, northern Gulf Coastal Plain, USA. *Journal of Paleontology* 68(6), 1321–1335.

Puckett, T.M. , 2002. Systematics and paleobiogeography of Brachycytherine Ostracoda. *Micropaleontology* 48 (Suppl. 2), 1–87.

Puckett, T.M., Colin, J.P., Mitchell, S., 2012. New species and genera of Ostracoda from the Maastrichtian (Late Cretaceous) of Jamaica. *Micropaleontology*, pp.397-455.

Puckett, T.M., Andreu, B., Colin, J.P., 2016. The evolution of the Brachycytheride Ostracoda in the context of the breakup of Pangea. *Revue de Micropaléontologie* 59, 97–167.

Piovesan, E.K., Cabral, M.C., Colin, J.P., Fauth, G., Trescastro Bergue, C., 2014. Ostracodes from the Upper cretaceous deposits of the Potiguar Basin, northeastern Brazil: taxonomy, paleoecology and paleobiogeography. Part 2: Santonian- Campanian. *Carnets Geol.* 14, 211–252.

Postuma, J.A., 1971. *Manual of Planktic Foraminifera*. Elsevier, Amsterdam.

Prauss, M.L., 2015. Marine palynology of the Oceanic Anoxic Event 3 (OAE3, Coniacian–Santonian) at Tarfaya, Morocco, NW Africa transition from preservation to production controlled accumulation of marine organic carbon. *Cretac. Res.* 53, 19–37.

Premoli Silva, I., Boersma, A., 1977. Upper Cretaceous–Paleocene magnetic stratigraphy at Gubbio, Italy II. *Biostratigraphy*. *GSA Bull.* 88, 371–374.

Premoli Silva, I., Bolli, H.M., 1973. Late cretaceous to Eocene planktic foraminifera and stratigraphy of Leg 15 sites in the Caribbean Sea. *Deep Sea Drilling Project Reports and Publication* 15, 499–547.

Premoli Silva, I., Sliter, W.V., 1999. Cretaceous paleoceanography: Evidence from planktic foraminiferal evolution. In: Barrera, E., Johnson, C.C. (Eds.), *The Evolution of the Cretaceous Ocean-Climate System*, vol. 332. *Geol. Soc. Am. Spec. Pap.*, pp. 301–328.

Premoli Silva, I., Verga, D., 2004. Practical manual of cretaceous planktic foraminifera. In: Verga, D., Rettori, R. (Eds.), *International School on Planktic Foraminifera, 3rd Course: Cretaceous*. Universities of Perugia and Milan, Perugia, Italy, p. 283.

Prauss, M.L., 2012. Potential freshwater dinocysts from marine upper Cenomanian to upper Coniacian strata of Tarfaya, northwest Africa: three new species of *Bosedinia*. *Cretac. Res.* 37, 285–290.

Rajabi, P., 2020. Micro-Paleontology and Lithostratigraphical Study of Ilam Formation in Lorestan Province of Iran (Poshte Jangal Anticline). *Rev. Georaguaia* 10, 70–85.

Rami, A., 1998. Precisions biostratigraphiques et milieu de depot des series du Cretace superieur de la Tunisie centro-septentrionale. These de Doctorat d'Etat. Faculte des Sciences de Tunis, p. 243. 22 pl.

Rami, A., Zaghib-Turki, D., Saadi, M., 2016. Biozonation des foraminiferes planctoniques du Cretace superieur de Tunisie centro-septentrionale. Bol. Geol. Min. 127, 455–468.

Reuss, A.E., 1874. Die Ostracoden des Sachsischen Planers. In: H.B. Geinitz, Das Elbthalgebirge in Sachsen. Palaeontographica 20, 2.

Reyment, R.A., 1960. Studies on Nigerian Upper Cretaceous and Lower Tertiary Ostracoda. Part 1: Senonian and Maestrichtian Ostracoda. Stockholm Contributions in Geol., vol. VII, 238 p., 23 pi.

Reyment, R.A., 1980. Biostratigraphy of the Saharan Cretaceous and Paleocene epicontinental transgression. Cretaceous Research 1, 299–327.

Reyment, R.A. and Elofson, O., 1959. Zur Kenntnis der Ostracodengattung *Buntonia*. Almqvist & Wiksell.

Roemer, F.A., 1841. Die Versteinerungen des norddeutschen Kreidegebirges. Hannover, 16 pls, pp. 1–149.

Roemer, F.A., 1852. Die Kreidebildungen von Texas und ihre organischen Einschlüsse; Mit einem die Beschreibung von Versteinerungen aus paläozoischen und tertiären Schichten enthaltenden Anhang; Adolph Marcus, Bonn; I–VI, 1–95, pls. I–XI.

Rosenfeld, A., Raab, M., 1974. Cenomanian–Turonian ostracods from the Judea Group in Palestine . Bulletin of the Geological Survey of Palestine 62, 1–64, 6 pls.

Richards, F.A., 1957. Oxygen in the ocean. Geol. Soc. Am. Mem. 67, 185–238.

Riedel, L., 1933. Die Oberkreide vom Mungofluß in Kamerun und ihre Fauna. Beiträge zur Geologischen Erforschung der Deutschen Schutzgebiete 16, 1–154.

Roemer, F., 1849. Texas: Mit besondere Rücksicht auf Deutsche Auswanderung und die Physischen Verhältnisse des Landes nach eigener Beobachtung Geschildert: Bonn, p. 464. A. Marcus.

Robaszynski, F., 1998. Planktic foraminifera-upper cretaceous, chart of cretaceous biochronostratigraphy. In: De Graciansky, P.C., Hardenbol, J., Vail, P.R. (Eds.), Mesozoic and Cenozoic Sequence Stratigraphy of European Basins, 60. SEPM Spec. Publ, p. 782.

Robaszynski, F., Caron, M., 1979a. Atlas de foraminifères planctoniques du Crétacé moyen (Mer Boreale et Tethys), première partie. Cah. Micropaleontol. 1, 1–185.

Robaszynski, F., Caron, M., 1979b. Atlas des foraminifères planctoniques du Crétacé supérieur moyen (Mer Boreale et Tethys). Cah. Micropaleontol. 1969. part 1, 1–185, part 2, 1–181.

Robaszynski, F., Caron, M., 1995. Foraminifères planctoniques du Crétacé; commentaire de la zonation Europe-Méditerranée. Bull. Soc. géol. Fr. 166, 681–692.

Robaszynski, F., Caron, M., Dupuis, C., Amedro, F., Gonzales Donoso, J.M., Linares, D., Hardenbol, J., Gartner, S., Calandra, F., Deloffre, R., 1990. A tentative integrated stratigraphy in the Turonian of Central Tunisia: Formations, zones and sequential stratigraphy in the Kalaat Senan area. Bull. Cent. Rech. Explor.-Prod Elf-Aquitaine 14, 213–384.

Robaszynski, F., Donoso, J.G., Linares, D., Amedro, F., Caron, M., Dupuis, C., Dhondt, A.V., Gartner, S., 2000. Le Crétacé supérieur de la région de Kalaat Senan, Tunisie centrale. Litho-biostratigraphie intégrée: zones d'ammonites, de foraminifères planctoniques et de nanofossiles du Turonien supérieur au Maastrichtien. Bull. Cent. Rech. Elf Explor. Prod. 2.

Rodrigues, M.O., Abrantes, N., Goncalves, F.J.M., Nogueira, H., Marques, J.C., Goncalves, A.M.M., 2018. Spatial and temporal distribution of microplastics in water and sediments of a freshwater system (Antua River, Portugal). Sci. Total Environ. 633, 1549–1559.

Roth, P.H., 1973. Calcareous nannofossils—Leg 17, Deep Sea Drilling Project. Initial Rep. Deep Sea Drill. Proj. 17, 695–795.

Roney, R.O., 2013. Paleobiogeographical Variation of Cretaceous *Mecaster Batnensis* and *Mecaster Fourneli* (Echinoidea: Spatangoida).

Ruault-Djerrab, M., Ferré, B., Kechid-Benkherouf, F., Djerrab, A., 2012. Etude micropaléontologique du Cénomano-Turonien dans la région de Tébessa (NE Algérie): implications paléoenvironnementales et recherche de l'empreinte de l'OAE2. *Revue de paléobiologie* 31 (1), 127–144.

Said, R., 1978. Etude stratigraphique et micropaléontologique du passage crétacé-tertiaire du syncinal d'Ellès (région Siliana-Sers), PhD thesis, Pierre and Marie Curie University.

Salaj, J., 1980. Microbiostratigraphie du Crétacé du Paléogène de la Tunisie septentrionale et orientale (hypostratotypes tunisiens). *Inst. Geol. Dionyz Stur Bratislava*. . p. 238, 64 pl.

Salaj, J., 1997. Microbiostratigraphical (foraminifera) division of the Turonian to Santonian in Tunisia (El Kef and Dj. Fguira Salah area). *Geol. Carpath.* 48, 171–178.

Salaj, J., Samuel, O., 1966. Foraminifera der Westkarpaten-Kreide. GUDS, Bratislava, p. 291.  
Salmi-Laouar, S., Ferré, B., Chaabane, K., Laouar, R., Boyce, A.J., Fallick, A.E., 2018. The oceanic anoxic event 2 at Es Souabaa (Tébessa, NE Algeria): bio-events and stable isotope study. *Arabian J. Geosci.* 11, 1–18.

Sari, B., 2006. Upper cretaceous planktic foraminiferal biostratigraphy of the Bey Dağları autochthon in the Korkuteli area, western Taurides, Turkey. *J. Foraminiferal Res.* 36, 241–261.

Sari, B., 2009. Planktic foraminiferal biostratigraphy of the Coniacian-Maastrichtian sequences of the Bey Dağları autochthon, western Taurides, Turkey: thin-section zonation. *Cretac. Res.* 30, 1103–1132.

Sarr, R., 1995. Etude biostratigraphique et paléoenvironnementale des séries d'âge Crétacé terminal à Eocène moyen du Sénégal occidental. *Systématique et migration des ostracodes.*

Systématique et migration des ostracodes [Ph. D. dissertation]: Dakar, Senegal, Université Cheikh Anta Diop de Dakar.

Salel, T., Bruneton, H., Lefèvre, D., 2016. Ostracods and environmental variability in lagoons and deltas along the north-western Mediterranean coast (Gulf of Lions, France and Ebro delta, Spain). *Revue de Micropaléontologie* 59, 425–444.

Santos Filho, M.A.B., Piovesan, E.K., Fauth, G. and Srivastava, N.K., 2015. Paleoenvironmental interpretation through the analysis of ostracodes and carbonate microfacies: study of the Jandaíra Formation, Upper Cretaceous, Potiguar Basin. *Brazilian Journal of Geology*, 45:23–34. doi:10.1590/23174889201500010002.

Sayed, M.M., Abd El-Gaied, I.M., Abdelhady, A.A., Abd El-Aziz, M.A., Wagreich, M., 2022. Ostracods sensitivity to reconstructing water depths and oxygen levels: a case study from the Middle-late Eocene of the Beni Suef area (Egypt). *Mar. Micropaleontol.* 175, 102155.

Sayed, M.M., Abd El-Gaied, I.M., Abdelhady, A.A., Abd El-Aziz, S.M., Wagreich, M., 2022. Ostracods sensitivity to reconstructing water depths and oxygen levels: A case study from the Middle-Late Eocene of the Beni Suef area (Egypt). *Marine Micropaleontology* 175, 102155. <https://doi.org/10.1016/j.marmicro.2022.102155>

Schlanger, S.O., Jenkyns, H., 1976. Cretaceous oceanic anoxic events: causes and consequences. *Geol. Mijnb.* 55, 3–4.

Seeling, J., Bengtson, P., 1999. Cenomanian oysters from the Sergipe basin, Brazil. *Cretac. Res.* 20 (6), 747–765.

Seguenza, G., 1882. Studi geologici e paleontologici sul Cretaceo medio dell'Italia meridionale, 3. Attidella Accademia Nazionale dei Lincei, pp. 65–214.

Seilacher, A., 1984. Constructional morphology of bivalves: evolutionary pathways in primary versus secondary soft-bottom dwellers. *Palaeontology* 27 (2), 207–237.

Sigal, J., 1955. Notes micropaleontologiques nord-africaines. 1. Du Cenomanien au Santonien: zones et limites en facies pelagiques. C. R. Sommaire Seances. Soc. Geol. Fr. 8, 157–160.

Sigal, J., 1977. Essai du zonation du Cretace mediterraneen a l'aide des foraminiferes planctoniques. Geol. Mediterr. 4, 99–108.

Sissingh, W., 1977. Biostratigraphy of cretaceous calcareous nannoplankton. Geol. Mijnb. 56, 37–65.

Shahin, A., 1991. Cenomanian-Turonian ostracods from Gebel Nezzazat, southwestern Sinai, Egypt, with observations on  $\delta^{13}\text{C}$  values and the Cenomanian-Turonian Boundary. Journal Micropalaeontology, 10, 2, 133-150.

Shahin, A., Kora, M., Semiet, A., 1994. Cenomanian ostracodes from west central Sinai, Egypt. Mansoura faculty of Science Bulletin (C. Nat., Sci) 21 (1), 33–102.

Shirazi, B.G., Bakhshandeh, L., Yazdi, A., 2014. Biozonation and Paleo-bathymetry on Foraminifera Upper Cretaceous Deposites of Central Iran Basins (Isfahan, Baharestan Section). Scientific Research- Open Journal of Geology 4, 343–353.

Slami, R., Ferre, B., Benkherouf-Kechid, F., 2022. Cenomanian ostracods (Crustacea) of Djebel Sabaoune (Batna, Algeria): Specific assemblage and significance. Journal of African Earth Sciences 193, 12.

Slipper, I. J., 2005. Ostracod diversity and sea-level changes in the Late Cretaceous of southern England. Palaeogeography, Palaeoclimatology, Palaeoecology 225 (2005) 266–282.

Sokal, R.R., Rohlf, F.J., 1962. The comparison of dendrograms by objective methods. Taxon 11, 33–40.

Sharafi, M., Reolid, M., Bayet-Goll, A., Mohamadi, M., Khanehbad, M., Mahboubi, A., Moussavi-Harami, R., 2022. Differentiate allogenic and autogenic controls on the formation

of parasequences and depositional sequences of a tide- and wavedominated carbonate platform (Lower Cretaceous, Kopet-Dagh Basin, Iran). *Geol. J.* 57 (7), 2828–2853.

Smith, A.B., 1992a. Echinoid distribution in the Cenomanian: an analytical study in biogeography. *Palaeogeogr. Palaeoclimatol. Palaeoecol.* 92 (3–4), 263–276.

Smith, A.B., Bengtson, P., 1991. Cretaceous Echinoids from North-Eastern Brazil. *Idunn*, p. 92.

Slami, R., Ferre, B., Benkherouf-Kechid, F., 2022. Cenomanian ostracods (Crustacea) of Djebel Sabaoune (Batna, Algeria): specific assemblage and significance. *J. Afr. Earth Sci.* 193, 104604.

Sliter, W.V., 1989. Biostratigraphic zonation for cretaceous planktic foraminifera examined in thin section. *J. Foraminiferal Res.* 19, 1–19.

Smith, A.B., 1992b. Echinoid distribution in the Cenomanian: an analytical study in biogeography. *Palaeogeogr. Palaeoclimatol. Palaeoecol.* 92 (3–4), 263–276.

Southward, A., Hiscock, K., Tittley, A., 2004. Effects of changing temperature on benthic marine life in Britain and Ireland. *Aquat. Conserv.* 34 (12), 1052–7613.

Soycan, H., Hakyemez, A., 2018. The first calibration of radiolarian biochronology with late cretaceous (latest Coniacian-Santonian to early Campanian) planktic foraminifera in the volcano-sedimentary sequences of the Eastern Pontides, NE Turkey. *Cretac. Res.* 85, 319–348.

Taylor, M.A., Hendy, I.L., Chappaz, A., 2017. Assessing oxygen depletion in the Northeastern Pacific Ocean during the last deglaciation using I/ca ratios from multiple benthic foraminiferal species. *Paleoceanography* 32, 746–762.

Tchenar, S., Ferre, B., Adaci, M., Zaoui, D., Benyoucef, M., Bensalah, M., and Kentri, T., 2020. Incidences de l'Evenement Anoxique Oceanique II sur l'evolution des ostracodes des

d'épots cenomano-turonien du bassin du Tinrhert (SE Algérie). *Carnets de Geologie* 20, 145–164.

Trabelsi, K., Sames, B., Salmouna, A., Piovesan, E.K., Ben Rouina, S., Houla, Y., Tourir, J., Soussi, M., 2015. Ostracods from the marginal coastal Lower Cretaceous (Aptian) of the Central Tunisian Atlas (North Africa): Paleoenvironment, biostratigraphy and paleobiogeography. *Revue de Micropaleontologie* 58, 309 e 331.

Trabelsi, K., Sames., B, Nasri., A, Piovesan., EK., Elferhi, F., Skanji, A., Houla, Y., Soussi, M., Wagreich, M., 2020. Ostracods as proxies for marginal marine to non-marine intervals in the mid Cretaceous carbonate platform of the Central Tunisian Atlas (North Africa): Response to major short-term sea-level falls, *Cretaceous Research* 117 (2020) 104581.

Vahidinia, M., Youssef, M., Ardestani, M.S., Sadeghi, A., Dochev, D., 2014. Integrated biostratigraphy and stage boundaries of the Abderaz Formation, east of the Kopeh- Dagh sedimentary basin, NE Iran. *J. Afr. Earth Sci.* 90, 87–104.

Vahidinia, M., Haddadi, M., Ardestani, M.Sh., 2016. Investigation of main planktic foraminiferal bio-events in Surgah Formation at Pol-e-Dokhtar area, southwestern Iran. *Open J. Geol.* 6, 774–785.

Van V.J. 1932. - Die Cytherellidae der Maastrichter Tuffkreide und des Kunrader Korralenkalkes von Sud-Limburg. *Geologie en Mijnbouw Genoots Nederlanden, Geological Serie* 10 (9): 317 – 364.

Van den Bold, W.A., 1964. Ostracoden aus der Oberkreide von Abu Rawash, Agypten. *Palaeontographica Abteilung A*, 123, 111-136.

Vila, J.M., 1980. La chaîne alpine d'Algérie orientale et des confins algéro-tunisiens. Thesis, University of Pierreand Marie Curie, Paris 6, France, 1-665.

Vivière J.L., 1985. Les Ostracodes du Crétacé supérieur (Vraconien à Campanien basal) de la région de Tébessa (Algérie du Nord-Est): Stratigraphie, paléoécologie, systématique.- PhD thesis, Université Pierre et Marie Curie, Paris, 261 p.

Viviers, M.C., Koutsoukos, E.A., Silva-Telles, Jr., A.C., Bengtson, P., 2000. Stratigraphy and biogeographic affinities of the late Aptian-Campanian ostracods of the Potiguar and Sergipe basins in north eastern Brazil. *Cretaceous Research* 21, 407–455.

Voigt, S., Gale, A. S., & Flögel, S. 2004. Midlatitude shelf seas in the Cenomanian–Turonian greenhouse world: Temperature evolution and North Atlantic circulation. *Paleoceanography*, 19 (4), PA4020.

Wagreich, M., 1992. Correlation of late cretaceous calcareous nannofossil zones with ammonite zones and planktic foraminifera: the Austrian Gosau sections. *Cretac. Res.* 13, 505–516.

Wagreich, M., 2009. Coniacian-Santonian oceanic red beds and their link to Oceanic Anoxic Event 3. In: Hu, X., Wang, C., Scott, R.W., Wagreich, M., Jansa, L. (Eds.), *Cretaceous Oceanic Red Beds: Stratigraphy, Composition, Origins, and Paleooceanographic and Paleoclimatic Significance*, vol. 91. SEPM Special Publications, pp. 235–242. <https://doi.org/10.2110/sepmssp.091.225>.

Wagreich, M., 2012. “OAE 3”–Regional Atlantic organic carbon burial during the Coniacian-Santonian. *Clim. Past* 8, 1447–1455.

Wagreich, M., Summesberger, H., Kroh, A., 2010. Late Santonian bioevents in the Schattau section, Gosau Group of Austria: implications for the Santonian-Campanian boundary stratigraphy. *Cretac. Res.* 31, 181–191.

Wagreich, M., 2009. *Cretaceous Oceanic Red Beds: Stratigraphy, Composition, Origins, and Paleooceanographic and Paleoclimatic Significance* Special Publication No. 91, Copyright 2009. Society for Sedimentary Geology, ISBN 978-1-56576-135-3, p. 235–242.

Wagreich, M., Mansour, A., 2022. The Coniacian-Santonian Oceanic Anoxic Event OAE3 - global correlation of subevents, EGU General Assembly 2022, Vienna, Austria, 23–27 May 2022, EGU22-11382, <https://doi.org/10.5194/egusphere-egu22-11382>.

Wagner, T., Sinninghe Damsté, J.S., Hofmann, P., Beckmann, B., 2004, Euxinia and primary production in Late Cretaceous equatorial Atlantic surface waters fostered orbitally driven

formation of marine black shales: *Paleoceanography*, v. 19, no. 3, PA3009. doi: 10.1029/2003PA 000898.

Whatley, R. C., 1995. Ostracoda and oceanic palaeoxygen levels.- *Mitteilungen aus dem Hamburgischen Zoologischen Museum und Institut, Hambourg*, vol. 92, p. 337-353.

Whatley, R.C., Pyne, R.S., Wilkinson, I.P., 2003. Ostracoda and palaeo-oxygen levels, with particular reference to the Upper Cretaceous of East Anglia.-*Palæogeography, Palæoclimatology, Palæoecology*, Amsterdam, vol. 194, p. 355-386.

Whatley, R., Boomer, I., & others. 2003. Ostracod palaeoecology and palaeobiogeography in the Cretaceous of the Tethys. *Revue de Micropaléontologie*, 46 (2), 95–114.

Wonders, A.A.H., 1980. Middle and late cretaceous planktic foraminifera of the western Mediterranean area. *Utrecht Micropaleontol. Bull.* 24, 1–158.

Wilson, P. A., & Norris, R. D. 2001. Warm tropical ocean surface and global anoxia during the mid-Cretaceous period. *Nature*, 412, 425–429.

Yahiaoui, A., 1990. La partie inferieure de la seriemarno-calcaire du crétacé supérieur (Cenomanien supérieur a Coniacien inférieur) entre Batna et El kantara (Algerie Orientale).Thèse. Doct.Universite de Nancy I. France.

Yao, N' J. P., Kesse, T-M., Wango, T-E., Goua, T-E., Bamba, K., Digbehi, Z-B., 2018.Evolution of the dissolved oxygen content of water during the Coniacian-Santonian interval from the KM well of Côte d'Ivoire, *Revue Interdisciplinaire Vol 2, N° 2*.

Youssef, M., Ismail, A., El-Sorogy, A., 2017. Paleoecology and paleobiogeography of Paleocene ostracods in Dineigil area, southwestern Desert. *Egypt. J. Afr. Earth Sci.*

Zakharov, Y.D., Smyshlyayeva, O.P., Popov, A.M., Velivetskaya, T.A., Afanasyeva, T.B., Tanabe, K., Shigeta, Y., Maeda, H., 2012. Pole to equator temperature gradient for Coniacian time, Late Cretaceous: oxygen and carbon isotopic data on the Koryak upland and Hokkaido. *Journal of Earth Science*, 23, pp.19-32.

Zapata, E., Padron, V., Madrid, I., Kertznus, V., Truskowski, I., Lorente, M.A., 2003. Biostratigraphic, sedimentologic, and chemostratigraphic study of the La Luna Formation (late Turonian-Campanian) in the San Miguel and Las Hernandez sections, western Venezuela. *Palaios* 18, 367–377.

*APPENDICES*





Appendix C and D-  
Macrofauna Essen data

Sample	Murchie (formid)	Murchie (formid)	Murchie sp. var. albiventris	Murchie sp. var. albiventris	Agrotis pinivorella	Proconotus albivittatus	Proconotus sp.	Agrotis pinivorella	Murchie (formid)	Proconotus albivittatus	Conochilus albivittatus	Conochilus albivittatus	Conochilus albivittatus	Proconotus albivittatus	Murchie (formid)
S1	2														
S2		2													1
S3															
S4			1												
S5														2	
S6															
S7		3												3	3
S8		2												4	2
S9														1	
S10															3
S11														2	4
S12															
S13															
S14															
S15															
S16															
S17															
S18															
S19															
S20															
S21															
S22															
S23															
S24															
S25															
S26															
S27															
S28															
S29															
S30															
S31															
S32															
S33															
S34															
S35															
S36															
S37															
S38															
S39															
S40															
S41															
S42															
S43															
S44															
S45															
S46															
S47															
S48															
S49															
S50															
S51															
S52															
S53															
S54															
S55															
S56															
S57															
S58															
S59															
S60															
S61															
S62															

Appendix E-  
Macrofauna  
Boukezez data

Lithology	sample n°	<i>Hemiaster fourneli</i>	<i>Mecaster fourneli</i>	<i>Phymosoma thevestense</i>	<i>Phymosoma sulcatum</i>	<i>Plicatula ventilabrum</i>	<i>Paraesafaba</i> sp.,	<i>Rachiosoma rectilineatum</i>	<i>Campanile</i> sp.,	<i>Aporrhais</i> sp.	<i>Nerinea</i> s	<i>Cimolithium</i> sp	<i>Inoceramus sicicensis</i>
marls	E71												
marls	E69												
marls	E66												
marls	E64												
marls	E63												
marls	E61		11										
marls	E58												
marls	E56												
marls	E54												
marls	E53												
marls	E45		4										1
marls	E44												
marls	E43												
marls	E42												
marls	E41												
marls	E40												
marls	E39												
marls	E38												
marls	E37												
marls	E36		13										
marls	E29												
marls	E28												
marls	E21												
marls	E16							3	2			1	
marls	E10												
marls	E8												
marls	E5	9		2				1					
marls	E3					3	5				1		
marls	E1	1		3		2	2					1	
		10	28	5		5	7	1	3	2	1	2	1